Mechanism underpinning the immunosuppressive effects of the mycobacterial macrolide mycolactone

Jean-David Morel

Thèse de doctorat

de l'Université Sorbonne Paris Cité

Préparée à l'Université Paris Diderot

Ecole doctorale BioSPC ED562

Unité d'Immunobiologie de l'Infection, Equipe INSERM U1221

Mechanism underpinning the immunosuppressive effects of the mycobacterial macrolide mycolactone

Par Jean-David MOREL

Thèse de doctorat d'Immunologie

Dirigée par Caroline Demangel

Présentée et soutenue publiquement à l'Institut Pasteur, Paris le 26 septembre 2018

Président du jury : Jean-Michel SALLENAVE, Professeur, Université Paris Diderot, INSERM U1152

Rapporteur 1 : Eric CHEVET, DR, Université de Rennes-1, INSERM U1242

Rapporteur 2 : Olivier NEYROLLES, DR, IPBS Université Toulouse 3, CNRS

Examinateur 1 : Stephen HIGH, Professeur, Université de Manchester, Royaume-Uni

Examinateur 2 : Elodie SEGURA, CR, Institut Curie, Paris, INSERM U932

Directeur de thèse : Caroline DEMANGEL, DR, Institut Pasteur, Paris, INSERM U1221

Mechanism underpinning the immunosuppressive effects of the mycobacterial macrolide mycolactone

Abstract: Mycolactone is a diffusible lipid produced by the human pathogen *Mycobacterium ulcerans*, the causative agent of a tropical skin disease called Buruli ulcer. Bacterial production of mycolactone in infected skin causes local tissue necrosis, while inducing immunosuppressive defects at the systemic level. When I started my PhD, the molecular mechanism(s) underpinning these effects were unknown. Over the course of my thesis, I contributed to demonstrate that mycolactone is a novel inhibitor of the Sec61 translocon, a channel regulating the biogenesis of most secreted and membrane proteins in eukaryotic cells. Indeed, a single point mutation in the alpha subunit of Sec61 protected cells from the cytotoxic and immunosuppressive effects of mycolactone. I showed that mycolactone-mediated blockade of the Sec61 translocon efficiently prevents the synthesis of key immune receptors and signaling molecules, impeding the communication between immune cells that is required for the development of anti-mycobacterial immunity. Through a series of large-scale proteomic studies, I demonstrated that mycolactone is a broad-acting inhibitor of Sec61 and identified the Sec61 clients that are primarily downregulated by mycolactone in physiologically-relevant cell types. These analyses also allowed me to describe a unique stress response, encompassing elements of the unfolded protein response and integrated stress response, that is induced upon protein translocation blockade and ultimately causes cell apoptosis. The Sec61 translocon has been proposed to play a role in other cell functions that require the retrograde transport of proteins across membranes, namely Endoplasmic Reticulum-Associated Degradation (ERAD), an essential process in protein quality control, and antigen export to the cytosol during cross-presentation, a pathway essential to the activation of adaptive immunity to intracellular pathogens and cancer. Using mycolactone, I showed that Sec61 blockade does not affect protein export to the cytosol in either of these pathways, arguing against Sec61 operating as a retrotranslocon. Altogether, my work provided a molecular mechanism for the diverse effects of mycolactone in Buruli Ulcer patients, and thus for *M. ulcerans* virulence. Mycolactone representing the most potent Sec61 blocker identified to date, my studies also revealed the key importance of Sec61-mediated protein translocation in the regulation of immune responses and protein homeostasis.

Keywords: Mycolactone, Sec61 translocon, immunosuppression, stress, Buruli ulcer

Mécanisme responsable des effets immunosuppresseurs de la mycolactone, toxine de *M. ulcerans*

Résumé : La mycolactone est un lipide diffusible produit par *Mycobacterium ulcerans*, la bactérie responsable d'une maladie tropicale de la peau appelée ulcère de Buruli. La production de mycolactone dans la peau infectée par *M. ulcerans* provoque une nécrose tissulaire locale, tout en induisant des anomalies immunosuppressives au niveau systémique. Lorsque j'ai commencé mon doctorat, les mécanismes moléculaires à l'origine de ces effets étaient inconnus. Au cours de ma thèse, j'ai contribué à démontrer que la mycolactone est un nouvel inhibiteur du translocon Sec61, le canal régulant la biogenèse de la plupart des protéines sécrétées et membranaires dans les cellules eucaryotes. J'ai démontré qu'une mutation ponctuelle dans la sous-unité alpha de Sec61 protège les cellules des effets cytotoxiques et immunosuppresseurs de la mycolactone. J'ai montré que le blocage du translocon Sec61 par la mycolactone empêche efficacement la synthèse des principaux récepteurs immunitaires et des molécules de signalisation du système immunitaire, blockant la communication entre les cellules immunitaires et inhibant l'immunité anti-mycobactérienne. Par une série d'études protéomiques à grande échelle, j'ai démontré que la mycolactone est un inhibiteur à large action de Sec61 et j'ai identifié les substrats de Sec61 les plus impactés dans différents types cellulaires. Ces analyses m'ont également permis de décrire la réponse au stress induite par le blocage de la translocation des protéines, qui inclut des éléments de la réponse au stress protéostatique (UPR) et de la réponse intégrée au stress (ISR), provoquant finalement l'apoptose cellulaire. Plusieurs études ont impliqué le translocon Sec61 dans des processus qui requièrent le transport rétrograde de protéines à travers les membranes : la Dégradation Associée au Réticulum Endoplasmique (ERAD), processus essentiel du contrôle de la qualité des protéines et la cross-présentation, une voie essentielle à l'activation de l'immunité adaptative aux pathogènes intracellulaires et au cancer. J'ai montré que le blocage de Sec61 par la mycolactone n'affecte pas l'export de protéines vers le cytosol dans ces deux voies, suggérant que Sec61 ne peut pas fonctionner comme un rétrotranslocon. Mes travaux ont permis d'élucider le moléculaire responsable des divers effets de la mycolactone observés chez les patients atteints d'ulcère de Buruli et de révéler l'importance majeure de la translocation des protéines dans la régulation des réponses immunitaires et de l'homéostasie des protéines.

Mots clés : Mycolactone, translocon Sec61, immunosuppression, stress, Ulcère de Buruli

ACKNOWLEDGEMENTS

First and foremost, I wish to thank my advisor, Dr. Caroline Demangel for her unwavering support during my thesis. With each new result, Caroline always had great ideas for going further, always finding great collaborators to combine their expertise with ours and do great research. Caroline has always encouraged me to explore each unforeseen opening, even going into research fields and techniques neither of us knew much about. This freedom has allowed me to learn about a wide variety of techniques and subjects that I never would have ventured into on my own, acquiring a knowledge that will be invaluable to me in future projects. Caroline has provided me not only with a great working environment and support during my thesis but has also helped me in all my future projects with excellent advice, corrections and recommendations.

I am deeply thankful as well to all the members of the Immunobiology of Infection team. Ludivine Baron has worked with me almost since the beginning and has become a great friend over the course of my PhD. Most of what I know about properly designing and documenting experiments, animal experimentation and countless other subjects, I learned from her. I thank Laure Guenin-Macé for accompanying and teaching me a great many things since I started as a Master student in the lab. Laure was always willing to help and offer advice even though she was swamped with work. Veronique Mayau, for teaching me cloning and for always making sure the lab runs so smoothly and for her concern for our safety. From her I learned to be careful during experiments and not to place science above my own health. I also thank her for always livening the mood with her adventurous stories of diving and travel to exotic countries. I thank Reid Oldenburg for the great scientific discussions and for showing me what it means to be a PhD student, as well as his enduring good mood and perspective about life in the United States. I owe much to Thomas Laval for his dedication to science and always smart and accurate opinions on experiments and literature, as well as for his passionate outlook on politics, education and socialism, which made for great discussions around coffee. And more than I can express to Fatoumata Niang for being the first to teach me when I first joined the team, being patient with my clumsiness and encouraging me. Finally, I wish to encourage in turn the younger students I met in the lab, Caroline Isaac, Kemy Ade, Noémie Alphonse and Claire Lescoat and wish them luck for their own PhD, should they choose to pursue one; it is a difficult ride, but also a very rewarding one.

I owe a debt of gratitude to all collaborators that worked with me and taught me throughout my PhD both within the Pasteur Institute, and outside it. There are too many people to list here, but I would like to thank especially Ville Paavilainen at the university of Helsinki for coming to us with the

cotransin-resistant mutants that made a lot of my work possible throughout this PhD, Patrycja Kozick, formerly at Institut Curie, for the great collaboration on the cross-presentation project, Marie-Anne Nicola at the Imagopole for her help with *in vivo* imaging and Francina Langa Vives at the Mouse Genetics Engineering platform for her help in my ill-fated attempt at generating transgenic mice resistant to mycolactone.

I wish to mention all the people who supervised me in my first research internships, and who were patient and encouraging with me when I was more a liability than an asset. I wish to thank Andreas Müller and Phillipe Bousso for first welcoming me at the Pasteur Institute when I was a Bachelor student and giving me a real research project. Luyan Liu and Anne Puel for welcoming me at Necker the next year and letting me take part in their exciting projects on human inborn defects of immunity. Yacine Bounab for taking me under his wing during my first internship in Caroline Demangel's lab. Finally, I thank Robin Schwarzer, who taught me how to use the CRISPR/Cas9 system during my internship in Manolis Pasparakis's lab.

I thank my family for supporting me throughout my PhD. My parents Jean-Michel and Mercedes for providing me with the best possible education and passing down their love of academic research to me. I am very grateful to them for always showing interest in my work and for organizing great family holidays to take my mind off it sometimes. And I thank my sister Mathilde for being a constant source of drama and excitement and for sharing her passionate perspective on the world of theatre, which is so alien to my routine of cells, toxins and bacteria.

The ENS Lyon and the French education system have given me an excellent training and have funded my four years of studies and three years of PhD. These seven years have taught me enormously and I hope to repay them by continuing to contribute to research as much as I can!

I am also grateful to my friend Alexandre Ivagnes for proof-reading this manuscript, providing the fresh insight of an outsider on my convoluted discussions about mycolactone.

Last but not least, I wish to thank Jean-Michel Sallenave, Eric Chevet, Olivier Neyrolles, Stephen High and Elodie Segura for agreeing to take part in my thesis evaluation committee and taking the time to read this manuscript. I hope you find something of interest within.

TABLE OF CONTENTS

ACKNOWLEDGEMENTS **3**

TABLE OF CONTENTS **7**

ABBREVIATIONS **13**

INTRODUCTION **17**

I. BURULI ULCER DISEASE **19**

1. BURULI ULCER, AN EMERGING MYCOBACTERIAL DISEASE 19
2. MYCOLACTONE, THE TOXIN OF *M. ULCERANS* 22

II. MYCOLACTONE: PROPOSED TARGETS AND MECHANISMS **28**

1. HYPERACTIVATION OF THE WISKOTT–ALDRICH SYNDROME PROTEINS WASP AND N-WASP 28
2. ACTIVATION OF THE ANGIOTENSIN 2 RECEPTOR AT2R 29
3. INHIBITION OF PROTEIN TRANSLOCATION AT THE SEC61 COMPLEX 31
4. EFFECTS ON MTOR AND BIM-DEPENDENT APOPTOSIS 32
5. INTERACTION WITH LIPID MEMBRANES 33

III. MECHANISMS OF TRANSLOCATION ACROSS THE ER MEMBRANE, ROLE OF THE SEC61 COMPLEX **34**

1. CANONICAL PATHWAY OF CO-TRANSLATIONAL TRANSLOCATION ACROSS THE ER MEMBRANE 34
2. OTHER PATHWAYS OF TRANSLOCATION ACROSS THE ER MEMBRANE 35
3. KNOWN INHIBITORS OF SEC61-DEPENDENT PROTEIN TRANSLOCATION 36
4. POTENTIAL ROLE OF THE SEC61 TRANSLOCON IN REVERSE TRANSLOCATION EVENTS SUCH AS ERAD AND EXPORT OF ANTIGENS DURING CROSS-PRESENTATION 40
5. ENDOPLASMIC RETICULUM-ASSOCIATED STRESS RESPONSES: THE UNFOLDED PROTEIN RESPONSE AND INTEGRATED STRESS RESPONSE. 42

THESIS OBJECTIVES 45

RESULTS 49

ARTICLE 1: MYCOLACTONE SUBVERTS IMMUNITY BY SELECTIVELY BLOCKING THE SEC61 TRANSLOCON 51

ARTICLE 2: SEC61 BLOCKADE BY MYCOLACTONE INHIBITS ANTIGEN CROSS-PRESENTATION INDEPENDENTLY OF ENDOSOME TO-CYTOSOL EXPORT 69

ARTICLE 3: PROTEOMICS REVEALS SCOPE OF MYCOLACTONE-MEDIATED SEC61 BLOCKADE AND DISTINCTIVE STRESS SIGNATURE 95

DISCUSSION 117

1. STRUCTURAL MECHANISM OF SEC61 BLOCKADE BY MYCOLACTONE 119
2. FROM SEC61 BLOCKADE TO IMMUNE SUPPRESSION, HYPOESTHESIA AND ULCERATION 124
3. TRANSLATIONAL POTENTIAL OF SEC61 BLOCKERS AND MYCOLACTONE IN PARTICULAR 128

CONCLUDING REMARKS 130

BIBLIOGRAPHY 131

Table of Figures

FIGURE 1: DISTRIBUTION OF BURULI ULCER WORLDWIDE, 2016. 20

FIGURE 2: CLINICAL PRESENTATION OF BURULI ULCER. 21

FIGURE 3: STRUCTURE OF M. ULCERANS-DERIVED MYCOLACTONE STEREOISOMERS A/B.. 23

FIGURE 4: SUMMARY OF THE EFFECTS OF MYCOLACTONE ON VARIOUS IMMUNE CELL SUBTYPES..26

FIGURE 5: SCHEMATIC OF N-WASP ACTIVATION AND ACTIN NUCLEATION AND EFFECT OF MYCOLACTONE IN STABILIZING THE ACTIVE OPEN CONFORMATION.. 28

FIGURE 6: MODEL FOR CO-TRANSLATIONAL, SRP/SR-DEPENDENT PROTEIN TRANSLOCATION INTO THE ER.. 35

FIGURE 7: PATHWAYS OF ANTIGEN CROSS-PRESENTATION..... 41

FIGURE 8: PATHWAYS AND INTERACTION BETWEEN THE UNFOLDED PROTEIN RESPONSE AND INTEGRATED STRESS RESPONSE.. 43

FIGURE 9: PATHWAYS OF SEC61 TRANSLOCATION OF NASCENT PROTEINS INTO THE ENDOPLASMIC RETICULUM AFFECTED BY MYCOLACTONE.. 120

FIGURE 10: DIAGRAM ILLUSTRATING THE DIFFERENTIAL EFFECTS OF MYCOLACTONE ON SEC61 CLIENT TRANSLOCATION (*IN VITRO*) AND PRODUCTION IN LIVING CELLS. 122

ABBREVIATIONS

Akt	serine/threonine protein kinase
ARP2/3	Complex of the actin-related proteins ARP2 and ARP3
AT2R	Angiontensin II receptor
ATF4	Activating transcription factor 4
ATF6	Activating Transcription Factor 6
Bim	Bcl-2 Interacting Mediator Of Cell Death, also called Bcl-2l11. A pro-apoptotic protein
BiP	Binding immunoglobulin protein
BU	Buruli ulcer
C57BL/6	Dark brown laboratory mouse strain
CamL	Calcium signal-modulating cyclophilin ligand
Cas9	CRISPR associated protein 9
CD-	Cluster of differentiation (example: CD8)
CD62L	Cluster of differentiation 62, also called L-selectin
CHOP	C/EBP homologous protein
COX-1	Cyclooxygenase-1
CPR	Cytosolic unfolded protein response
Cre/lox system	A system for conditional expression or deletion of genes in mice, comprised of the Cre recombinase and lox recombinatory elements
CRISPR	Clustered Regularly Interspaced Short Palindromic Repeats
Derlin-1	Degradation In Endoplasmic Reticulum Protein-1
DNA	Deoxyribonucleic acid
DRG	dorsal root ganglion
dsRNA	double-stranded ribonuceic acid
eIF2α	eukaryotic translation initiation factor 2 alpha
ER	endoplasmic reticulum
ERAD	Endoplasmic reticulum-associated degradadation
FKBP12	12-kDa FK506-binding protein
FoXO3	Forkhead Box O3
FRET	fluorescence energy transfer
GCN2	General control non-derepressible 2A. A nutrient stress sensor that phosphorylates EiF2alpha. Also called EIF2AK4
HCT-116	Human colon carcinoma -derived cell line
HEK293	Human Embryonic Kidney-derived cell line
Hela	Human cervical cancer-derived cell line
Hrd-1	HMG-CoA Reductase Degradation 1 (E3-ubiquitin ligase)
IFN	Interferon
Il-	Interleukin- (exemple Il-2)
iNOS	inducible nitric oxide synthase
IP10	IFN-gamma-inducible protein-10, also called CXCL10
IRE1	inositol requiring enzyme 1

ISR	integrated stress response
Jurkat	Human T cell leukemia-derived cell line
kb	kilobases (number of nucleotides/1000)
KO	Knock-out
L929	Fibroblast cell line derived from mouse areolar and adipose tissue
LPS	lipopolysaccharide
M. ulcerans	Mycobacterium ulcerans
MIP-1α, MIP-1β	macrophage inflammatory protein-1, alpha or beta
mRNA	messenger ribonucleic acid
mTOR	mechanistic target of rapamycin
MutuDC	Dendritic cell line
N-WASP	Neural-Wiscott-Aldrich syindrome protein
PERK	PKR -like ER kinase
PMA	phorbol 12-myristate 13-acetate
RICTOR	Rapamycin-insensitive companion of mammalian target of rapamycin
RNAse	RNA-cleaving enzyme
Sec61, Sec62, Sec63	Protein of the secretory pathway 61, 62 and 63
SERCA	sarco/endoplasmic reticulum Ca2+-ATPase
Slc3a2	Soluble carrier 3a2, an amino-acid transporter
SRP	Signal recognition particle
SRα, SRβ	SRP receptor subunit alpha, beta
TA	Tail-anchored (protein)
TAP	Transporter associated with antigen processing
TCR	T-cell receptor
TMP	transmembrane protein
TNF	tumor necrosis factor
TRAAK	TWIK-related arachidonic acid activated K+ (channel)
TRAM1	Translocating Chain-Associated Membrane Protein1
TRAP	Translocon-associated protein (complex)
TRC	TA receptor complex
Trc40	TA receptor complex protein 40
TRPV1	Transient receptor potential cation channel subfamily V member 1
UPR	unfolded protein response
VCA	verprolin-cofilin-acidic (domain)
WASP	Wiscott-Aldrich syindrome protein
WHO	World Heath Organization
Wrb	Tryptophan Rich Basic Protein
XBP1	X -box binding protein 1

INTRODUCTION

I. BURULI ULCER DISEASE

1. Buruli ulcer, an emerging mycobacterial disease

1.1 First description of Buruli ulcer

Buruli ulcer (BU) is a necrotizing skin disease caused by infection with *Mycobacterium ulcerans*, the third most prevalent mycobacterial disease after Tuberculosis and Leprosy. The first case of a probable *M. ulcerans* infection was reported in 1864 by Cpt. James Augustus Grant in his account of his quest for the source of the White Nile. In his book "A walk across Africa or domestic scenes from my Nile journal" (Grant, 1864), his description of his own condition closely matches the symptoms of the edematous form of BU. The first clinical description of the disease came 30 years later in 1897, when Sir Albert Cook described cases of chronic disfiguring skin ulcers in Uganda (van der Werf *et al.*, 2005). The name "Buruli ulcer" derives from a region on the southern bank of the Victoria Nile river in Uganda (Clancey *et al.*, 1961). In 1948, MacCallum *et al.* linked these chronic skin ulcers to a germ in six cases in Australia (Mac *et al.*, 1948). Microscopic analyses of biopsies revealed bacilli with the typical acid-fast stain common to all mycobacteria, combined with a unique histopathological pattern distinct from Tuberculosis. This new bacillus was later named *Mycobacterium ulcerans* (Fenner and Leach, 1952). MacCallum's team eventually managed to cultivate the bacterium by culturing it at 32-33°C as the bacteria fail to grow at 37°C (Mac *et al.*, 1948), potentially explaining why the infection only occurs in the skin.

1.2 Epidemiology of Buruli ulcer

Following its first clinical description, BU was identified in an increasing number of countries of Africa, South America and Western Pacific regions, prompting the World Health Organization (WHO) to classify BU as an emerging public health concern in 1998 (Wansbrough-Jones and Phillips, 2006). Today, BU is reported in 33 countries and considered by the WHO as one of the 17 neglected tropical diseases. BU occurs mainly in remote, rural areas of Central and West Africa, but also in Australia and Papua New Guinea as well as scattered foci in Asia and the Americas (WHO, 2018b) (**Figure 1**:). Although its reported annual incidence has decreased from ~5000 to ~2000 cases since 2010, the assessment of the global disease burden is complicated by the remoteness of affected populations and a lack of data on the incidence of BU in several countries, from which cases have been previously reported. Moreover, as BU patients present with diverse symptoms ranging from unspecific

nodules, plaques, or edema to necrotic, ulcerative lesions, differential diagnosis is complex, and BU is often misdiagnosed (Beissner *et al.*, 2010). The disease affects both sexes equally and all age groups, but it is particularly common in children under the age of 15 (WHO, 2018b). Epidemiological and genomic studies have revealed that *M. ulcerans* is associated with lentic environments (reviewed in (Zingue *et al.*, 2018)), and suggest that disease transmission does not occur from human-to-human, but through reservoirs that are not yet fully defined. The primary host of *M. ulcerans* is probably aquatic, and transmission of *M. ulcerans* to humans is believed to result from either insect bites or puncture wounds (Wallace *et al.*, 2017). The study of *M. ulcerans* transmission is further complicated by the large differences in ecosystems between the endemic regions in Africa, Asia and Oceania and the reservoirs, vectors and modes of transmission may be different between these areas.

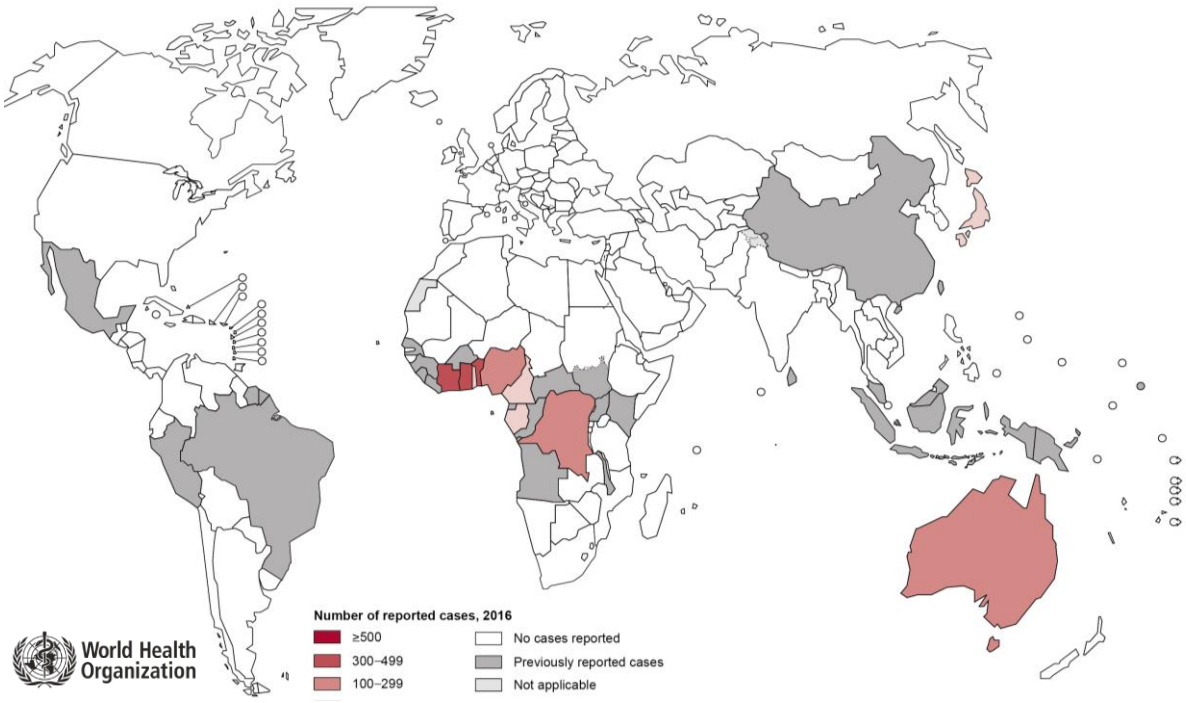

***Figure 1**: Distribution of Buruli ulcer worldwide, 2016, from the WHO website.*

1.3 Clinical manifestations

BU lesions are mainly located in the upper and lower limbs (35% and 55%, respectively) while only 10% occur at other parts of the body (WHO). BU typically starts with a pre-ulcerative stage characterized by painless subcutaneous nodules, edemas or plaques with large areas of indurated skin, gradually expanding over time. After weeks to months, the disease progresses to the ulcerative

stage when the skin splits to reveal indolent, necrotic lesions of the cutaneous and subcutaneous tissues with typically undermined edges ((van der Werf *et al.*, 1999), see **Figure 2**). Generally, extracellular mycobacteria are observed in all (early, pre-ulcerative and ulcerative) stages of disease without being accompanied by granuloma formation (Hayman and McQueen, 1985). The ulcers expand over time and can spread over an entire limb, yet remarkably, ulceration is rarely accompanied by pain and fever. In 5–10% of all cases, *M. ulcerans* invades the bone and causes osteomyelitis leading to severe deformities (Walsh *et al.*, 2008). The core of BU lesions contains large numbers of extracellular bacteria, and typically lacks inflammatory infiltrates, a distinguishing feature of BU (Guarner *et al.*, 2003, Ruf *et al.*, 2017)(**Figure 2**). While BU is rarely fatal, it can lead to permanent disfigurement and long-term disabilities (Ellen *et al.*, 2003, Schunk *et al.*, 2009) and the social and economic burden of BU can be high, particularly in impoverished rural regions.

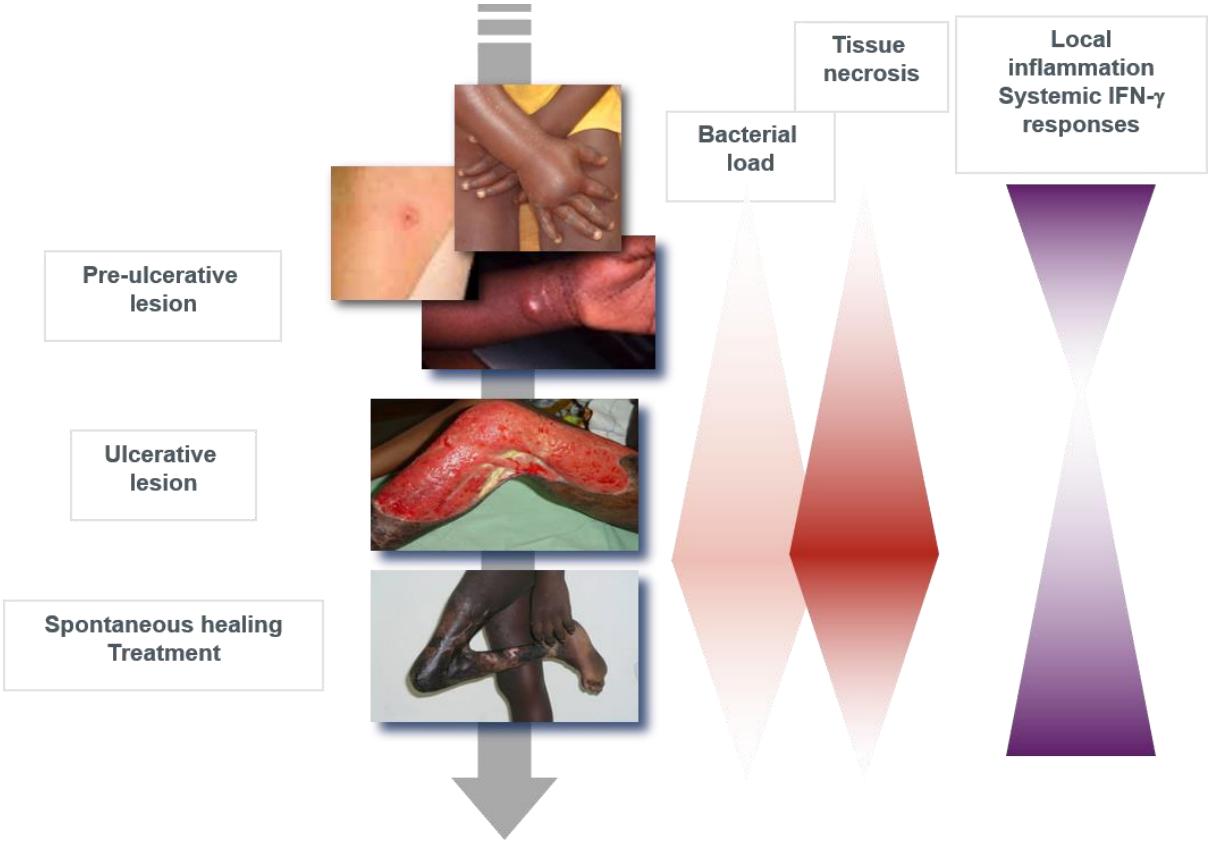

Figure 2: Clinical presentation of Buruli Ulcer. From (Demangel et al., 2009)

1.4 Diagnosis and treatment

The main laboratory methods for BU diagnosis are microscopy, culture, PCR, and histopathology (reviewed in (Sakyi *et al.*, 2016)). The WHO recommends two laboratory tests to confirm BU, and

microscopy and PCR are often used in tandem for diagnosis. PCR targeting the *M. ulcerans*-specific IS2404 is the most accurate metric for distinguishing *M. ulcerans* infections from other necrotizing skin diseases, but culture remains the only method that detects viable bacilli, which is useful for diagnosing relapse as well as monitoring drug resistance.

If left untreated, BU lesions can sometimes self-heal, which is often associated to loss of limbs and contractures. Early treatments of BU involved wide surgical excision of the lesions followed by skin grafting; however, following a successful clinical trial, the WHO changed its recommendation in 2004 to a treatment with streptomycin and rifampicin (Organization, 2004). Today, the mainstay treatment protocol for BU is daily oral rifampicin and intramuscular injection of streptomycin for 56 days, sometimes accompanied by the surgical excision of lesional skin and by skin grafting (Etuaful *et al.*, 2005, Nienhuis *et al.*, 2010).

2. Mycolactone, the toxin of *M. ulcerans*

2.1 Discovery of mycolactone

The existence of a diffusible toxin produced by *M. ulcerans* was first speculated in 1966 by Connor and Lunn (Lunn *et al.*, 1965). Connor and co-workers later confirmed that hypothesis by injecting supernatant filtrates of *M. ulcerans* cultures into mouse footpads and guinea pig skin, triggering the formation of a skin ulcer with very similar characteristics to the one caused by infection with the bacteria (Krieg *et al.*, 1974, Read *et al.*, 1974). The toxin was purified in 1998 by the group of Pamela Small, who isolated a polyketide from *M. ulcerans* lipid extracts by thin layer chromatography and High Performance Lipid Chromatography (HPLC) followed by identification by mass spectrometry, unveiling a 12-membered macrolactone with two polyketide side chains (**Figure 3**:), which they named mycolactone for its mycobacterial origin and lactone structure (George *et al.*, 1998, George *et al.*, 1999). Further Investigation revealed that natural mycolactone is comprised of a 3:2 ratio of two stereoisomers termed mycolactone A and B (**Figure 3**:).

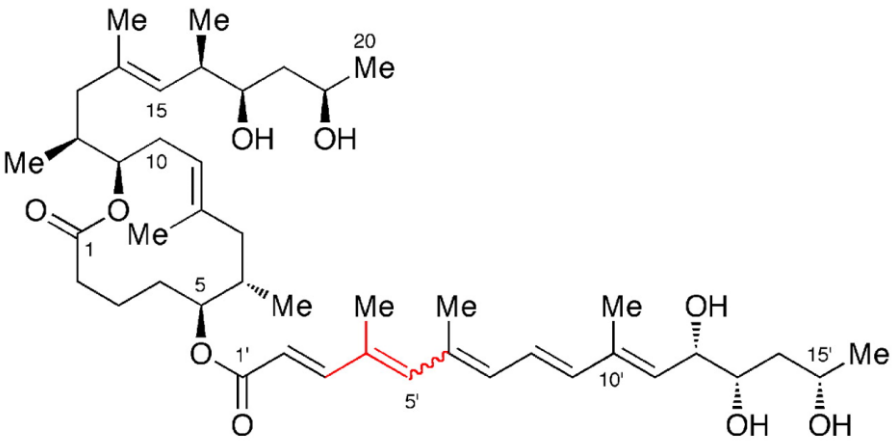

***Figure 3**: Structure of M. ulcerans-derived mycolactone stereoisomers A/B. The red line indicates the region where A and B differ (from (Kishi, 2011)).*

2.2 Mycolactone in Buruli ulcer

Mycolactone is synthesized by a family of enzymes called polyketide synthases, the genes of which are coded on a mega-plasmid (Stinear *et al.*, 2004). *M. ulcerans* strains of different geographical origins, and genetically related mycobacteria, produce variants of the canonical mycolactone structure (reviewed in (Gehringer and Altmann, 2017, Saint-Auret *et al.*, 2017)). Mycolactone is central to the pathogenesis of BU. Its production is required and sufficient for bacterial virulence, as the injection of purified mycolactone in the dermis of rodent models is sufficient to trigger the formation of BU-like lesions, whereas mycolactone-deficient strains trigger no ulceration (George *et al.*, 1999). While *M. ulcerans* bacteria rarely disseminate beyond the skin, mycolactone has a systemic distribution. Its distinctive mass spectrometric signature was detected in peripheral blood cells, spleen, liver and kidneys of mice experimentally infected with *M. ulcerans* (Hong *et al.*, 2008). In patients, intact mycolactone was detected in ulcer exudates, healthy skin around ulcers and serum (Sarfo *et al.*, 2011, Sarfo *et al.*, 2014). Notably, mycolactone could still be detected in perilesional skin several weeks after completion of antibiotic therapy (Sarfo *et al.*, 2011, Sarfo *et al.*, 2014), suggesting that it is relatively stable in tissues and slowly eliminated by infected organisms. Determining the contribution of mycolactone to each manifestation of BU, including skin necrosis associated with a relative lack of inflammatory infiltrates and pain, and defective cellular responses at the systemic level, has been the subject of intensive research over the past decades.

2.3 Cytotoxic effects of mycolactone

The observation that mycolactone was sufficient to trigger skin ulceration in animal models (George *et al.*, 2000) led several groups to study the cytotoxicity of mycolactone *in vitro* in cellular models of skin cell types, such as keratinocytes, fibroblasts, epithelial and endothelial cells. In all skin cells studied, mycolactone treatments of more than 48 hours triggered cell retraction followed by detachment and apoptosis, although the timing and lethal dose varied across cell types (Gama *et al.*, 2014, Bieri *et al.*, 2017, Dangy *et al.*, 2016, George *et al.*, 2000, Guenin-Mace *et al.*, 2013, Snyder and Small, 2003, Ogbechi *et al.*, 2015). The detachment of cells occurred very quickly in Hela cells (4-16h) and was associated with alterations of the actin cytoskeleton, and impaired directed migration in wound-healing assays (Guenin-Mace *et al.*, 2013). The ulceration observed *in vivo* is likely to result from a combination of the cytotoxic effects of mycolactone with other mechanisms, such as the disruption of the structure and junctions of the epidermis (Guenin-Mace *et al.*, 2013). Furthermore, mycolactone triggered a loss of thrombomodulin, a critical regulator of blood coagulation that operates by converting thrombin to an anticoagulant enzyme from a procoagulant enzyme (Sadler, 1997) in human dermal microvascular endothelial cells, thus potentially exacerbating ulceration (Ogbechi *et al.*, 2015). Collectively, these studies suggested that mycolactone provokes ulceration by a combination of cell death, epidermis remodelling and disruption of coagulation control.

2.4 Immunosuppressive effects of mycolactone

The observation that Buruli ulcers lack inflammatory infiltrates despite the extent of the ulcerative lesions has led several research groups to study immune responses in BU patient cells. Interferon gamma (IFN-γ) is a critical cytokine for the control of mycobacterial diseases such as Tuberculosis, and BU is no exception, as IFN-γ knock-out mice were more sensitive to *M. ulcerans* infection (Bieri *et al.*, 2016). Several studies have demonstrated that BU patients present defective production of IFN-γ at the systemic level (Gooding *et al.*, 2001, Prevot *et al.*, 2004, Westenbrink *et al.*, 2005, Yeboah-Manu *et al.*, 2006, Phillips *et al.*, 2009), that eventually reverted after treatment. In addition, blood cells stimulated *ex vivo* showed defective production of IFN-γ in response to both mycobacterial antigens (Gooding *et al.*, 2001, Prevot *et al.*, 2004) and broad acting activators such as phytohemagglutinin (Westenbrink *et al.*, 2005, Yeboah-Manu *et al.*, 2006, Phillips *et al.*, 2006). The immunosuppressive signature of BU extended beyond IFN-γ to a down-modulation of several chemokines and an impaired capacity to produce Th1, Th2, and Th17 cytokines upon stimulation with mitogenic agents (Phillips *et al.*, 2006). Furthermore, patients with BU presented a

downregulation of numerous mediators of inflammation among their serum proteins and this defect persisted weeks after completion of antibiotic therapy (Phillips *et al.*, 2014).

The potential role of mycolactone in this host immune suppression was first suggested by Foxwell and co-workers in 1999, who showed that a "*M. ulcerans* soluble factor" blocks the production of Interleukin-2 (IL-2) by lymphocytes activated with phorbol 12-myristate 13-acetate (PMA) and ionomycin, as well as the production of tumor necrosis factor (TNF) and Interleukin-10 (Pahlevan *et al.*, 1999). Importantly, mycolactone exerted this immunosuppressive activity without impacting cell viability, and inhibition of cytokine production took place after only overnight treatments, whereas mycolactone toxicity typically occurs after 48h (Pahlevan *et al.*, 1999). Later studies showed that mycolactone could exert similar effects on a wide range of immune cell types. In monocytes and macrophages, the production of cytokines (TNF, IL-1β, IL-6, IL-10), chemokines (IFN-gamma-inducible protein-10 (IP10), IL-8), as well as intracellular effector molecules such as cyclooxygenase-2, were powerfully and dose-dependently inhibited by mycolactone, irrespective of the stimulating ligand (Simmonds *et al.*, 2009, Hall *et al.*, 2014). In dendritic cells (DCs), mycolactone blocked the production of cytokines IL-12, macrophage inflammatory protein 1 alpha (MIP1α), MIP-1β, and beta-chemokines at nanomolar concentrations. In addition, peripheral blood-derived DCs treated with mycolactone showed impaired ability to prime T cells, and mouse skin DCs had a reduced ability to migrate into lymph nodes *in vivo* (Coutanceau *et al.*, 2007). In T cells, mycolactone treatment reduced the cell surface expression of L-selectin (CD62L), a critical homing receptor, thus impairing the cell capacity to reach peripheral lymph nodes *in vivo* (Boulkroun *et al.*, 2010). Lymphocytes also showed impaired production of a wide range of cytokines and membrane receptors, including the T Cell Receptor (TCR) (Boulkroun *et al.*, 2010, Guenin-Mace *et al.*, 2011, Guenin-Mace *et al.*, 2015). The suppressive effects of mycolactone on immune cell functions are summarized in **Figure 4** Throughout these studies, several authors noticed that the potent effects of mycolactone on protein expression did not extend to their associated mRNA, which was unaffected and, in some cases, even increased, demonstrating that mycolactone acts at the post-transcriptional level (Boulkroun *et al.*, 2010, Hall *et al.*, 2014). The *in vitro* effects of mycolactone could be verified *in vivo*, as intraperitoneal administration of mycolactone protected mice against PMA-induced skin inflammation and rheumatoid arthritis (Guenin-Mace *et al.*, 2015), demonstrating the ability of mycolactone to exert its immunosuppressive activity remotely from the injection site.

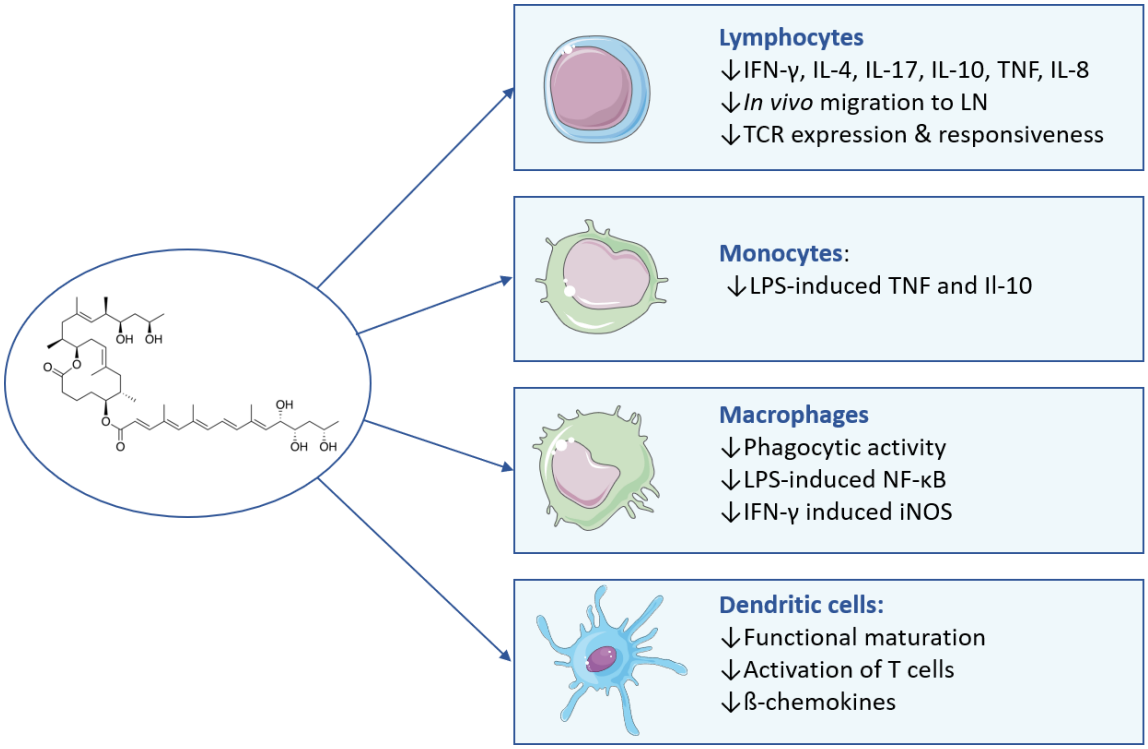

***Figure 4**: Summary of the effects of mycolactone on various immune cell subtypes*

2.5 Analgesic effects of mycolactone

Several research groups have studied the remarkable painlessness of BU lesions. The hypoesthesia in BU was initially attributed to nerve damage, as the histological analysis of late-stage BU lesions typically presents damage to axons and nerve fibers (Zavattaro *et al.*, 2012). Like the cytotoxic and immunosuppressive effects of BU, this unique hypoestesia was attributed to mycolactone, as mice injected with mycolactone or infected by *M. ulcerans*, presented a similar pathology, characterized by extensive damage to nerve tissue and hypoestesia after 28 days in the case of mycolactone injection (Goto *et al.*, 2006, En *et al.*, 2008). Mycolactone is highly toxic on primary sensory neurons, as short-term exposure to mycolactone (24h, 100 nM) causes neurite degeneration in rat and human primary dorsal root ganglion (DRG) neurons (Anand *et al.*, 2016). Longer treatments (>48h) reliably induced cell death of DRG neurons according to two studies (Anand *et al.*, 2016, Isaac *et al.*, 2017), although a third study reported a minimal loss of viability following exposure to mycolactone doses of up to 70µM (Song *et al.*, 2017). Schwann cells and microglia are also killed by nanomolar concentrations of mycolactone after 48h (Isaac, Mauborgne *et al.* 2017).

The role of this cytotoxic effect in the hypoesthesia triggered by mycolactone has since been challenged. Firstly, tropical skin ulcers and conditions that produce extensive ulceration of the skin are generally reported to be very painful (Gupta and Shukla, 2002), despite potential nerve damage. Furthermore, the first signs of nerve damage in mouse footpads injected with mycolactone was only observed after 7 days, and with a high dose of mycolactone (100µg), injected directly into the footpad (En *et al.*, 2008). However, infection with *M. ulcerans*, or injection of low doses (5µg) of mycolactone, induced local hypoesthesia at earlier stages of the disease despite the absence of nerve destruction or ulceration (Marion *et al.*, 2014). Moreover, a systemic administration of mycolactone (2µg) through the intra-peritoneal route partially protected mouse footpads against inflammatory pain, distantly from the injection site (Guenin-Mace *et al.*, 2015). It is therefore reasonable to assume that mycolactone reduces BU-associated pain by multiple mechanisms besides cytotoxicity. In sensory neurons, Schwann cells and microglia, nanomolar concentrations of mycolactone can prevent the activation-induced production of pro-inflammatory cytokines whilst injection of mycolactone in the spinal cord of rats reduces the basal production of inflammatory cytokines (Isaac *et al.*, 2017), which suggests that the immunosuppression triggered by mycolactone may limit the development of inflammatory pain during the course of BU.

II. MYCOLACTONE: PROPOSED TARGETS AND MECHANISMS

Several molecular targets of mycolactone have been described over the years, each of them explaining all or part of its effects on cells and organisms. I will present them here in their order of discovery.

1. Hyperactivation of the Wiskott–Aldrich syndrome proteins WASP and N-WASP

A well-known consequence of mycolactone treatment on adherent cells cultured *in vitro* is their detachment from the culture surface and subsequent cell death. A study performed by our group and collaborators in 2013 demonstrated that this detachment effect was due to alterations in actin dynamics after direct binding of mycolactone to the neural-Wiskott–Aldrich syndrome proteins (N-WASP) (Guenin-Mace *et al.*, 2013). Along with WASP, N-WASP belongs to a family of scaffolding proteins transducing a variety of signals into dynamic remodeling of the actin cytoskeleton, via interaction of their C-terminal verprolin-cofilin-acidic (VCA) domain with the ARP2/3 actin-nucleating complex (Thrasher and Burns, 2010). WASP is mainly expressed in cells of hematopoietic origin, whereas N-WASP is more widely expressed (Snapper *et al.*, 2001).

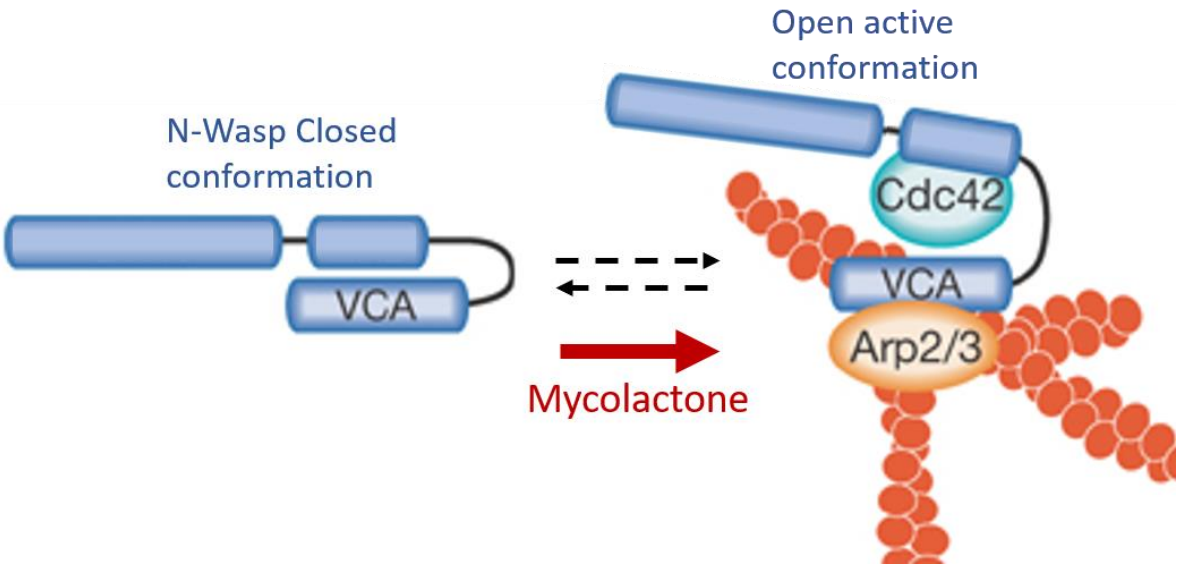

***Figure 5**: Schematic of N-WASP activation and actin nucleation and effect of mycolactone in stabilizing the active open conformation. Adapted from(Brandt and Grosse, 2007).*

In basal conditions, WASP and N-WASP are autoinhibited by intramolecular interactions sequestering the VCA domain from ARP2/3. Binding of activated GTPases or phosphoinositide lipids to N-terminal target sequences triggers conformational changes resulting in release of the VCA, triggering binding to ARP2/3 and subsequent activation ((Padrick and Rosen, 2010), **Figure 5**). Guenin-Macé and colleagues demonstrated that biotinylated mycolactone could bind to both WASP and N-WASP with a dissociation constant in the 20- to 70-nM range. Furthermore, mycolactone significantly accelerated actin polymerization in a cell extract, and this effect could be competed out by adding the recombinantly-expressed binding domain. In Hela cells, the addition of N-WASP inhibitor wiskostatin partially rescued mycolactone-mediated cell detachment and death. Furthermore, coadministration of wiskostatin with the toxin limited mycolactone-induced epidermal thinning and disorganization of the junctions and stratification of keratinocytes *in vivo*. Non-hematopoietic cells, and Hela cells in particular, express only N-WASP. Our group postulated that mycolactone binding to the exclusively hematopoietic WASP could contribute to the immunosuppressive effects of mycolactone in those cells. However, neither WASP silencing nor wiskostatin treatment in relevant cell models modified the inhibitory effect of mycolactone on the cell expression of immune receptors or production of cytokines (Baron *et al.*, 2016). Further, while mycolactone's effect on N-WASP explained some of the actin reorganization and detachment of cells, neither N-WASP silencing nor wiskostatin protected lastingly from mycolactone-induced cell death. These results are consistent with our recent finding that another mechanism, Sec61 blockade ((Baron *et al.*, 2016), see also "Results" section) mediates the immunomodulatory and cytotoxic effects of mycolactone.

2. Activation of the Angiotensin 2 receptor AT2R

As briefly discussed in section I.2.5, BU patients, and animal models infected by *M. ulcerans* or injected with purified mycolactone, display local hypoesthesia. This was initially thought to be the result of direct nerve destruction, however the observation that mycolactone can trigger analgesia quickly, remotely and in the absence of nerve damage strongly suggested that mycolactone-driven analgesia had another cause beside direct nerve damage. Brodin, Marsollier and collaborators shed some light on this matter, by demonstrating in various *in vivo* and *in vitro* systems that direct binding of mycolactone to the angiotensin II receptor AT2R was responsible for locally-induced hypoesthesia (Marion *et al.*, 2014). AT2R is a G-protein-coupled receptor belonging to the renin-angiotensin system that is now recognized as contributing to neuropathic pain in preclinical rodent models (Rice

et al., 2014). While AT1R plays a major role in hypertension, AT2R is expressed in human sensory neurons and, when activated, sensitizes TRPV1 (transient receptor potential cation channel subfamily V member 1) ion channels that mediate thermal pain (Anand *et al.*, 2013).

Brodin and collaborators showed that mycolactone dose-dependently induces hyperpolarization of murine neurons through a direct agonistic binding to AT2R. The hyperpolarization was mediated by AT2R-dependent activation of phospholipase A2, followed by a release of arachidonic acid by Cyclooxygenase-1 (COX-1) and activation of the potassium channel TRAAK (TWIK-related arachidonic acid activated K+ channel) by prostaglandin E2. Furthermore, mice injected with mycolactone or infected by *M. ulcerans* at a pre-ulcerative stage exhibited reduced pain sensitivity as evidenced by a delayed response to pain in a “tail-flick” test. In contrast, AT2R KO mice and mice injected with the AT2R inhibitor piroxicam showed unaltered pain response after mycolactone injection (Marion *et al.*, 2014).

The most controversial point of this study is the high doses required to induce hyperpolarization of neurons *in vitro* using mycolactone. Indeed, mycolactone was able to compete out a known AT2R agonist with an IC50 value of 3 µg/ml (4 µM), which is far beyond the reported cytotoxic concentrations of mycolactone on most cell types (10-100nM), and sensory neurons in particular (Anand *et al.*, 2016, Isaac *et al.*, 2017). Moreover, these concentrations are largely above the estimated concentrations of mycolactone (100nM- 1µM) in BU lesions (Sarfo *et al.*, 2014), questioning their physiological relevance. In response to these criticisms, Brodin and co-workers recently reported that primary dorsal root ganglion (DRG) neurons showed minimal loss of viability following exposure to mycolactone doses of up to 70µM for several days (Song *et al.*, 2017), in opposition with previously reported studies. Another point of debate is the proposed link between AT2R activation and defective pain transmission by neurons, as several AT2R antagonists are currently undergoing clinical trials for their analgesic properties (Rice *et al.*, 2014). Indeed, it remains unclear how both AT2R agonists and antagonists could suppress pain.

3. Inhibition of protein translocation at the Sec61 complex

As mycolactone-mediated inhibition of the Sec61 translocon is the main subject of the articles included in this manuscript, I will only briefly describe the literature on the subject in this section to avoid redundancy. My results and in-depth discussion of my work in relation to the rest of the field will be presented in the next section of this thesis manuscript.

In eukaryotic cells, most secreted, plasma membrane proteins, as well as organelle-resident proteins (Endoplasmic reticulum, Golgi, lysosomal proteins) have to be translocated across or inserted into the endoplasmic reticulum (ER) membrane during their synthesis. This process is facilitated by the translocon, a multi-subunit complex located in the ER membrane. The universally conserved heterotrimeric protein-conducting channel Sec61 forms the core of the translocon and binds to translating ribosomes for co-translational protein transport (Corsi and Schekman, 1996). Simmonds and co-workers were the first to demonstrate that mycolactone can inhibit the translocation of model secretory and membrane proteins into the ER (Hall *et al.*, 2014). In a seminal paper, they showed that the translocation of a number of precursor proteins that use the co-translational signal recognition particle (SRP) pathway for insertion into the ER were efficiently and dose-dependently blocked by mycolactone. Both membrane and secreted proteins were strongly downregulated, but their production could be restored using a proteasome inhibitor, leading to the production of a non-translocated form of the protein, lacking the typical N-glycosylation of ER-translocated proteins (Hall *et al.*, 2014). In a second article McKenna *et al.* showed that mycolactone treatment alters the protease susceptibility of the alpha subunit of Sec61, which is indicative of conformational changes, providing the first evidence that mycolactone could target Sec61α (McKenna *et al.*, 2016).

In my first article as co-first author in JEM (Baron *et al.*, 2016), we demonstrated that mycolactone efficiently displaces the known Sec61 inhibitor cotransin (CT7) from its previously defined binding site on Sec61α, demonstrating direct interaction and pointing to its binding site in this core subunit of the Sec61 translocon. Furthermore, a single amino acid change in Sec61α negated both the immunomodulatory and cytotoxic effects of mycolactone, providing genetic evidence that Sec61 is the host receptor mediating mycolactone biological activity (Baron *et al.*, 2016). During my PhD, I studied the direct and indirect consequences of mycolactone-mediated Sec61 blockade on the cell proteome, and their impact on the cell functions and viability. My findings are described in the following “Results” and “Discussion” sections.

4. Effects on mTOR and Bim-dependent apoptosis.

Since rapamycin shares its macrolide structure and immunosuppressive activity with mycolactone, it was postulated early that mycolactone could inhibit Mechanistic Target of Rapamycin (mTOR) signaling, leading to defects in immunity and impaired survival pathways. However, several studies disproved this hypothesis by showing that mycolactone had no impact on mTOR complex 1 signaling at treatment times that induce immunosuppressive effects *in vitro* (Simmonds *et al.*, 2009, Boulkroun *et al.*, 2010).

Nevertheless, a 2017 study challenged this conclusion by postulating that mycolactone could bind the 12-kDa FK506-binding protein (FKBP12), the same target as rapamycin, triggering a string of downstream events leading to Bcl-2 Interacting Mediator of cell death (Bim)-dependent apoptosis after several days (Bieri *et al.*, 2017). It was proposed that inhibition of the assembly of the Rapamycin-insensitive companion of mammalian target of rapamycin (RICTOR)-containing mTORC2 complex by mycolactone prevents phosphorylation of the serine/threonine protein kinase Akt. The associated inactivation of Akt leads to the dephosphorylation and activation of the Akt-targeted transcription factor FoxO3. Subsequent up-regulation of the Forkhead Box O3 (FoxO3) target Bim drives mycolactone treated mammalian cells into apoptosis. The article provided convincing evidence for the role of Akt and Bim in mycolactone triggered apoptosis in this sytem, as cells with constitutively activated Akt were protected against mycolactone-driven apoptosis and Bim knock-out mice had reduced ulceration upon experimental *M. ulcerans* infection. To demonstrate the direct binding of mycolactone to FKBP12, the authors performed a pull-down experiment using biotinylated mycolactone and a 1000-fold competition assay using the FKBP ligand tacrolimus, which is used as a potent immunosuppressive drug (Bieri *et al.*, 2017). This study provided valuable mechanistic information about the pathway of apoptosis induction in mycolactone-treated cells. However, the proposed mechanism for Akt dephosphorylation, namely FKBP12 binding and defective mTORC2 assembly, is challenged by the demonstration that Sec61 blockade is essential for mycolactone-driven cell death ((Baron *et al.*, 2016, Ogbechi *et al.*, 2018), see also “Results”). Possible mechanisms linking Sec61 blockade and Akt inactivation are provided in the Discussion.

5. Interaction with lipid membranes

The question of whether and how mycolactone can cross lipid membranes is critical to its activity. The observation that bacterially produced, or injected mycolactone can diffuse into distant organs, in particular lymphoid organs (Hong *et al.*, 2008, Sarfo *et al.*, 2011) and can even exert its analgesic and immunosuppressive properties distantly from the injection site (Guenin-Mace *et al.*, 2015) suggests that it has exceptional diffusion capacities *in vivo*. Furthermore, several of the proposed targets of mycolactone are intracellular proteins, which would require mycolactone to incorporate into cellular membranes.

Fluorescent mycolactone, obtained by conjugation with the lipophilic Bodipy moiety, is a powerful tool to study its diffusion although it has a higher mass (965 g/mol instead of 743) and tenfold reduced biological activity (Snyder and Small, 2003). Several studies found that fluorescent mycolactone derivatives quickly entered eukaryotic cells in culture, in a non-saturable and non-competitive manner, which is indicative of a passive diffusion across the plasma membrane (Snyder and Small 2003, Chany, Casarotto *et al.* 2011, Guenin-Mace, Baron *et al.* 2015).

More recently, the interaction of mycolactone with computer simulations of lipid bilayers made up of one or two phospholipids, suggested that mycolactone is mainly localized at the water-membrane interface, with a preference for the glycerol moiety of lipids. Notably, the toxin could “flip” from one side of the membrane to another, which is compatible with crossing the membrane (Lopez *et al.*, 2018). In addition, the addition of mycolactone could destabilize the membrane by acting as a surfactant, suggesting a potential direct activity of mycolactone on lipid membranes. Another study used a model of lipid monolayers at the water/lipid/air interface and confirmed that mycolactone could modify lipid segregation in the monolayer by affecting the formation of ordered microdomains (Nitenberg *et al.*, 2018).

These findings suggest that mycolactone may access its proposed targets, which are primarily membrane proteins such as Sec61 and AT2R or proteins proximal to the membrane such as N-WASP, by localizing, at least transiently, into biological membranes. Our finding that mycolactone targets the lumenal plug of Sec61α, in a region deeply embedded on the luminal side of the ER membrane (Article 1, (Baron *et al.*, 2016)), suggests that modifications in the structure and dynamics of the ER membrane may somehow facilitate mycolactone access to Sec61.

III. MECHANISMS OF TRANSLOCATION ACROSS THE ER MEMBRANE, ROLE OF THE SEC61 COMPLEX

The “Sec” proteins were first described as a group of proteins involved in protein secretion, found in screens for mutants unable to efficiently secrete invertase and acid phosphatase. The Sec61 translocon was identified by Schekman and collaborators in such a screen (Deshaies and Schekman, 1987). Sec61 is a highly conserved protein channel in eukaryotes, which comprises three subunits α, β and γ. The translocon is required for the membrane integration or translocation of almost every newly synthesized polypeptide targeted to organelles of the endo- and exocytotic pathway. The translocon is permanently or transiently associated with several additional proteins and complexes. This translocation complex facilitates the ER targeting of precursor polypeptides, modification of precursor polypeptides in transit through the Sec61 complex, and Sec61 channel gating, namely the regulation of the opening and closing of the pore to control calcium efflux (Lang *et al.*, 2017). Several pathologies are associated with heterozygous defects in the genes comprising the translocon, termed channelopathies (reviewed in (Lang *et al.*, 2017)). Notable examples include common variable immune deficiency (CVID) and tubulo-interstitial kidney disease with anemia in humans in the case of defects in Sec61α (Bolar *et al.*, 2016, Schubert *et al.*, 2018), polycystic liver disease triggered by heterozygous mutations in Sec61β (Besse *et al.*, 2017) and glioblastomas that overexpress Sec61γ to protect against ER stress (Lu *et al.*, 2009).

1. Canonical pathway of co-translational translocation across the ER membrane

1.1 General mechanism of translocation

Precursors of soluble polypeptides and membrane proteins can be targeted to the Sec61 complex via their amino-terminal signal peptides (SP) or transmembrane domains (TMD) either during their synthesis (co-translationally) or after completion of their synthesis (post-translationally). The co-translational translocation pathway involves the recognition of the hydrophobic SP or TMD by the cytosolic signal recognition particle (SRP), which temporarily interrupts translation (Walter and Blobel, 1981, Halic *et al.*, 2004). SRP then docks at the heterodimeric SRP receptor (SRα and SRβ) which is anchored to the ER membrane through the β subunit (Gilmore *et al.*, 1982, Miller *et al.*,

1995). Both SRP and SR hydrolyze their bound GTP and release the nascent polypeptide bound to the ribosome near the Sec61 complex. The ribosome binds to cytosolic loops of the translocon, whereupon the signal sequence mediates pore opening and initiates transfer of the growing polypeptide from the ribosome through the channel. For transmembrane proteins, the lateral gate of the translocon allows TM segments of nascent chains to exit into the lipid bilayer and serve as the signal sequence binding site during the early stages of translocation (Egea and Stroud, 2010). The translocation process involves additional components, notably the ER-lumenal chaperone, Binding immunoglobulin protein (BiP). BiP is involved in gating the Sec61 channel, driving the translocation of precursor polypeptides through the Sec61 complex, and serving as a molecular chaperone for freshly translocated proteins (Tyedmers *et al.*, 2003). Other key components of the translocation machinery include co-chaperones of BiP such as ER DnaJ-like protein 1 (ERj1) and nucleotide exchange factors: The Translocating Chain-Associated Membrane Protein1 (TRAM1), the Translocon-associated protein (TRAP) complex and Sec63. The mechanism of co-translational translocation is illustrated in **Figure 6**. Translocated polypeptides are further processed by the signal peptidase complex for removal of the signal peptide, oligosaccharyl-transferases for glycosylation and/or GPI transamidase for addition of a GPI anchor.

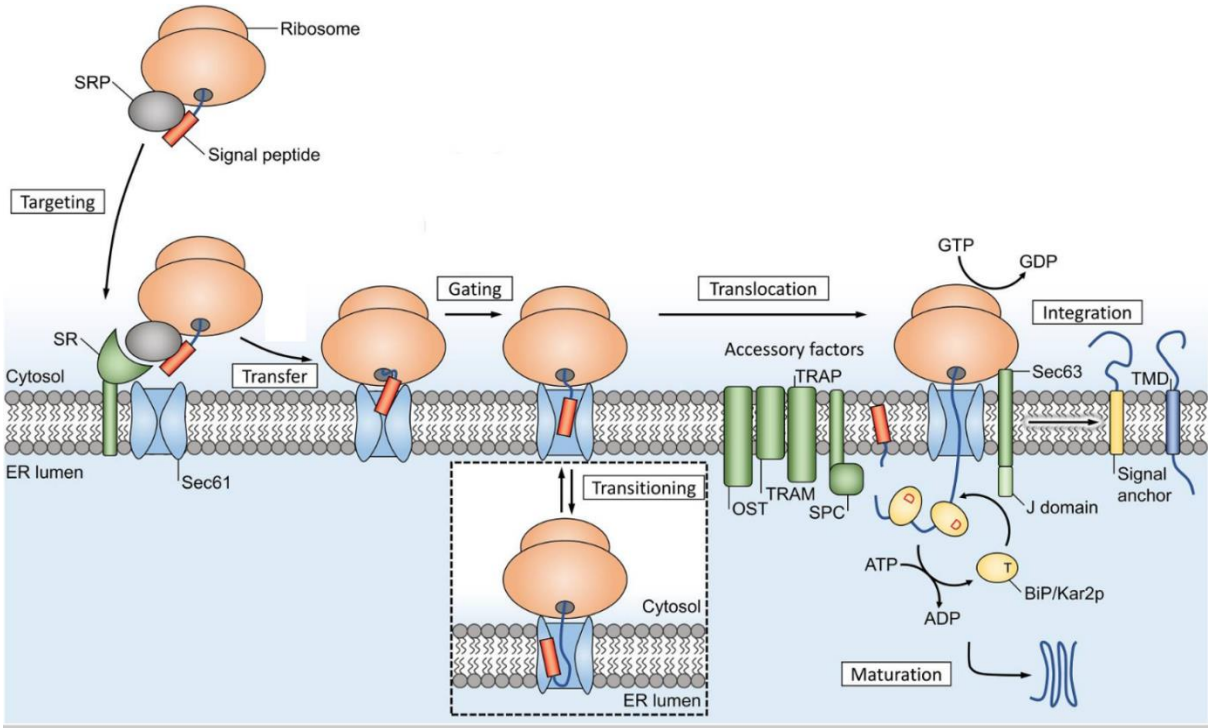

Figure 6: Model for co-translational, SRP/SR-dependent protein translocation into the ER. *Adapted from (Van Puyenbroeck and Vermeire, 2018).*

1.2 Different categories and insertion mechanisms of Sec61 substrates

Sec61 substrates using the SRP pathway can be divided into two categories: “secretory” proteins and transmembrane proteins (TMPs). Secretory proteins are all proteins with a cleavable signal peptide, but no transmembrane domains; this encompasses most secreted proteins such as cytokines, but also ER-, Golgi-, endosome- and lysosome-resident proteins, as well as proteins containing a glycosylphosphatidylinositol-anchoring motif. TMPs include all proteins with one (single-pass) or more than one (multi-pass) transmembrane domain. Single-pass TMPs can be classified as type I, II or III, based on the presence of a signal peptide and the location of the N-terminus after completion of translocation (Goder and Spiess, 2001). Type I TMPs have a signal peptide and an N-terminus in the ER lumen, Type II TMPs have no signal peptide and a cytosolic N-terminus while Type III have no signal peptide and an N-terminus in the ER lumen. The mechanism of translocation differs between these three types, since type I and type II TMPs form a hairpin loop with the SP or TMD, while type III TMPs insert in a “head-first” conformation, without formation of a hairpin loop (Goder and Spiess, 2001). These different categories of Sec61 clients, and modes of translocation, are summarized in **Table 1 of Article 3** (Morel *et al.*, 2018). In my work, I applied the criteria that were used to characterize the different types of single-pass TMPs, e.g. the presence of a signal peptide and final orientation of the N-terminus, to describe the effect of mycolactone on multi-pass TMPs. It should be noted however that membrane insertion of multiple-pass TMPs requires distinct and complex mechanisms, involving proteins of the so-called ER membrane protein complex (EMC) besides Sec61 (Shurtleff *et al.*, 2018).

2. Other pathways of translocation across the ER membrane

In the yeast, about 30% of the secretome was predicted to use SRP-independent pathways, prompting the search for other, possibly redundant pathways (Aviram and Schuldiner, 2014).

2.1 Post-translational translocation of small secretory proteins

A subset of small secretory proteins (SSP) are believed to be inefficiently recognized by SRP, since the signal sequence is exposed only briefly at the ribosomal exit before translation terminates, and the protein dissociates from the ribosome (Muller and Zimmermann, 1987). These proteins utilize a Sec62-dependant pathway in mammals for targeting to the Sec61 translocon (Lakkaraju *et al.*, 2012).

Very short (≤100 amino acids) proteins use this pathway exclusively, while longer (120–160 amino acids) proteins can use either the SRP pathway or the Sec62 pathway (Lakkaraju *et al.*, 2012).

2.2 Translocation of tail-anchored proteins

Tail-anchored (TA) proteins are membrane proteins with no signal peptide and a single TMD near their C-terminus (Borgese and Fasana, 2011). TA proteins only represent about 1% of the human proteome. Notable examples of TA proteins include the β- and γ-subunits of the Sec61 complex. TA proteins do not use SRP nor the Sec61 channel for targeting and insertion into the ER membrane, and instead use a specific system termed the TA receptor complex (TRC) system in mammals (Borgese and Fasana, 2011). TA receptor complex protein 40 (Trc40) recognizes TA proteins in the cytosol and targets them to its receptor, made up of Tryptophan Rich Basic Protein (Wrb) and Calcium signal-modulating cyclophilin ligand (Caml) proteins, which mediates TRC client anchoring in the ER membrane (Vilardi *et al.*, 2014). In 2017, Hegde and collaborators proposed an alternative mechanism for the ER targeting of TA proteins, applying to the 50% of TA proteins with a less hydrophobic TMD. These proteins were shielded in the cytosol by calmodulin and released near the EMC, which mediated the insertion of their transmembrane domain in the ER membrane.

2.3 SND pathway

The finding that knockouts of genes of the TRC system were not lethal, while some TA proteins are essential, prompted a search for redundant systems capable of handling TA proteins. In 2016, Aviram *et al.* described a new targeting system in the yeast termed the SRP-independent (SND) pathway (Aviram *et al.*, 2016). Like the TRC system, the SND system comprises a cytosolic recognition factor, (Snd1) and a heterodimeric receptor at the endoplasmic reticulum membrane, made up of Snd2 and Snd3. Interestingly, this system could provide targeting for both TA proteins and typical SRP-dependent substrates. In humans, the ER-membrane protein transmembrane 208 (TMEM208) was found to be an ortholog of yeast Snd2, and its silencing in Hela cells led to defective protein translocation *in vitro* (Hassdenteufel *et al.*, 2017), suggesting it shares the same function as yeast Snd2. However, no counterpart for Snd1 or Snd3 has been found to date.

2.4 Emerging concept: post-translational triage of membrane proteins

The discovery of a large variety of mechanisms for membrane protein targeting to the ER, but also to the mitochondria, has led to the concept that a triage reaction occurs in the cytosol, which involves chaperones, receptors and targeting proteins, addressing newly synthetized membrane

proteins to different organelles or to the proteasome for degradation (Lang *et al.*, 2017). Hegde and colleagues already described a six-component system for the targeting of a subset of TA proteins (Shao *et al.*, 2017). However, the decision-making mechanisms governing the post-translational triage and destination of membrane proteins remain to be elucidated.

3. Known inhibitors of Sec61-dependent protein translocation

3.1 Cyclodepsipeptides

The fungal macrocycle HUN-7293 was the first described cyclodepsipeptide inhibiting Sec61. HUN-7293 was selected in a screen for small molecules blocking the production of adhesion molecules by cancer lines (Boger *et al.*, 2000). Several derivatives of this molecule were made, among which cotransin, which was extensively characterized and was shown to inhibit the co-translational translocation of several proteins into the ER, in a signal peptide-selective way (Garrison *et al.*, 2005). It was shown that cotransin does not affect SRP targeting of the proteins, but instead traps nascent SPs and TMDs in the cytosolic vestibule of the translocon (Mackinnon *et al.*, 2014). Furthermore, cross-linking experiments showed that cotransin binds to the alpha subunit of the Sec61 channel and single amino-acid mutations of Sec61α were protective against the effects of cotransin (Garrison *et al.*, 2005).

Other natural cyclodepsipeptides have been discovered since, such as the cyanobacterial apratoxin A that was originally discovered in a search for antitumor drugs (Luesch *et al.*, 2001). Like cotransin, apratoxin A binds to the lateral gate of the Sec61 channel, yet at a slightly different site. Unlike cotransin, it does not seem to be substrate-selective as it blocks ER translocation of all tested Sec61 clients with similar potency (Paatero *et al.*, 2016), although a systematic proteomic study would be required to conclude. As a result, apratoxin A is more cytotoxic than cotransin. In 2015, a third natural cyclodepsipeptide, decatransin, was isolated from the fungus *Chaetosphaeria tulasneorum*, and identified in a screen for cytotoxicity in tumor cells (Junne *et al.*, 2015). Like the above described cyclodepsipeptides, decatransin inhibits Sec61 by targeting the lateral gate of Sec61α, but unlike them, decatransin is also effective on yeast Sec61.

3.2 Lipid content of the ER membrane

The membrane lipid composition is very important for the function of the Sec61 channel, and changes in the ER membrane composition can affect Sec61 function in various ways. A 2008 study showed that the phosphatidyl ethanolamine content of the ER membrane can influence the orientation of TMDs during translocation, causing proteins to insert in an inverted conformation (Bogdanov *et al.*, 2008). Although cellular cholesterol is synthesized at the ER membrane, its concentration is typically very low within this organelle. Artificially increasing cholesterol content inhibits Sec61 channel function (Nilsson *et al.*, 2001), but this effect is not specific as cholesterol also inhibits other critical ER machineries, such as the integration of TA proteins and the important sarco/endoplasmic reticulum Ca^{2+} ATPase (SERCA) pump (Yamamoto *et al.*, 2012, Li *et al.*, 2004). The effect of cholesterol may thus result from a general increase in the rigidity of the membrane, rather than a specific interaction.

3.3 Other inhibitors of translocation

Other notable inhibitors of Sec61 are lanthanum ions, which inhibited translocation at millimolar concentrations. Interestingly, the ions cluster at the lateral gate of the translocon, reinforcing the importance of this region for Sec61 blockade (Erdmann *et al.*, 2009). Eeyarestatin 1 was initially described as an inhibitor of ER-associated degradation (ERAD) through a blockade of the ER-associated p97 ATPase (Fiebiger *et al.*, 2004), but more recent data have demonstrated that it also blocks Sec61-dependant translocation into the ER by preventing the transfer of nascent polypeptides from the SRP machinery to the Sec61 translocon (Cross *et al.*, 2009), although its exact molecular target has yet to be identified. There are many other inhibitors of translocation across the ER membrane, but most of them do not act directly on the Sec61 channel, or their mechanism of action is unknown. A comprehensive review of these inhibitors can be found in Kalies and Romisch (2015) and Van Puyenbroeck and Vermeire (2018).

4. Potential role of the Sec61 translocon in reverse translocation events such as ERAD and export of antigens during cross-presentation

4.1 Proposed role of the Sec61 channel in ERAD

Endoplasmic reticulum-associated degradation (ERAD) is the process of degradation of misfolded proteins in the ER. ERAD requires the recognition of terminally misfolded proteins in the ER for export back to the cytosol and degradation by the proteasome (Ruggiano *et al.*, 2014). Being the only known channel capable of transporting entire proteins across the ER membrane, the Sec61 channel was proposed early to be the export channel for the retrograde transport of misfolded proteins into the cytosol (Wiertz *et al.*, 1996). Indeed, Sec61 was found to associate with both ERAD substrates and the proteasome (Scott and Schekman, 2008), and certain yeast Sec61 mutants had defects in degrading model ERAD substrates, even under conditions in which "forward" translocation appeared not to be affected (Plemper *et al.*, 1997). However, the finding that Sec61 colocalizes with ERAD components has lost some significance as Sec61 has been shown to associate with ERAD components during the degradation of proteins that aberrantly or persistently engage the translocon without translocating (Rubenstein *et al.*, 2012). Alternative pathways have also been proposed, including other transmembrane channels such as the multispanning membrane proteins within the E3 ligase complexes, in particular Hrd1 (HMG-CoA Reductase Degradation 1) and Derlin-1 (Degradation In Endoplasmic Reticulum Protein-1) (reviewed in (Ruggiano *et al.*, 2014)) or a more original mechanism involving extraction of proteins through lipid droplets (Ploegh, 2007), but the potential involvement of Sec61 remains debated (Romisch, 2017).

4.2 Proposed role of the Sec61 channel in antigen export during cross-presentation in DCs.

The Major Histocompatibility Complex, Class I (MHC I) molecules are expressed on all the cells of the body and allow the presentation of peptide fragments of degraded cellular proteins to CD8+ lymphocytes. This is a central process of immunity that allows cytotoxic CD8+ T cells to recognize abnormal proteins expressed by the cell, such as viral, bacterial (including mycobacteria such as *M. tuberculosis* and potentially *M. ulcerans*) or cancer-associated proteins, through its T-cell receptor (TCR) and kill them. While most cells are only capable of presenting endogenous antigens (produced within the cell) on their MHC I molecules, some antigen-presenting cells, and DCs in particular, can present exogenous antigens, acquired through phagocytosis, on their MHC I. This process is termed antigen cross-presentation and is critical for priming CD8+ T cells in intracellular infections and cancer (reviewed in (Segura and Amigorena, 2015)). Two main pathways have been described for

cross-presentation: the cytosolic pathway, in which antigen processing occurs in the cytosol, and the vacuolar pathway, in which antigen processing occurs within endocytic compartments. In the cytosolic pathway, exogenous antigens need to be translocated from endosomes into the cytosol for their degradation by the proteasome, and the resulting peptide fragments are then re-imported into endosomes or the endoplasmic reticulum through transporter associated with antigen processing (TAP) channels (Segura and Amigorena, 2015). Several ERAD components have been shown to participate in this process and the Sec61 translocon was proposed to be the export channel responsible for the retrograde transport from endosomes to the cytosol. The two pathways of antigen presentation and proposed role of Sec61 in the cytosolic pathway are depicted on **Figure 7**.

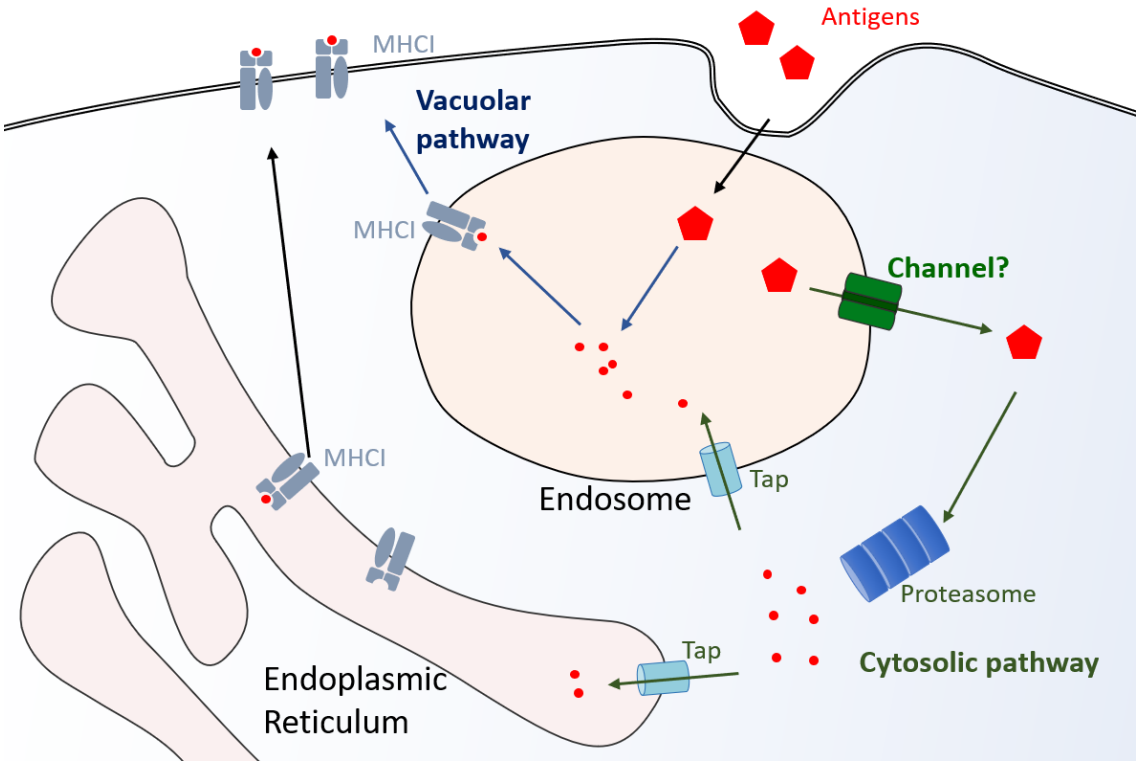

Figure 7: Pathways of antigen cross-presentation*. The vacuolar pathway (blue arrows) and cytosolic pathway are depicted. The endosome-to-cytosol antigen export depicted with an arrow through a green channel represents the potential role of Sec61 in the pathway.*

The Sec61 complex was detected in ER-phagosome fusion compartments (Guermonprez *et al.*, 2003) and the siRNA-mediated knockdown of Sec61α blocked antigen export (Imai *et al.*, 2005), although defects in protein translocation into the ER upon Sec61 knock-down may have confounded the effects. In 2014, Jung and colleagues showed that the *Pseudomonas aeruginosa* Exotoxin A could

bind to the N-terminus of Sec61α and block the passive calcium leak from the translocon and prevent ER export of immunogenic peptides into the cytosol (Schauble *et al.*, 2014). In 2015, Burgdorf and colleagues used a Sec61-specific "intrabody", which reportedly prevents the recruitment of Sec61 into endosomal compartments without impacting its primary functions (Zehner *et al.*, 2015). Expression of this intrabody blocked both antigen export from the endosomes and cross-presentation in a dendritic cell line (Zehner *et al.*, 2015). The role of Sec61 in this export was nevertheless challenged, as the cross-presentation of model peptides was found to be dependent on the ATPase p97, a critical driver of ERAD, but not on Sec61 or Derlin-1 (Menager *et al.*, 2014). The second article I contributed to, as co-first author, took advantage of the Sec61-blocking capability of mycolactone to answer the long-standing question of Sec61's involvement in ERAD and in antigen export during cross-presentation ((Grotzke *et al.*, 2017), see "Results" section).

5. Endoplasmic reticulum-associated stress responses: the unfolded protein response and integrated stress response.

5.1 The Unfolded Protein Response

The Unfolded Protein Response (UPR) is an ER-specific stress pathway that is required for maintaining ER homeostasis. In eukaryotic cells, more than one third of protein folding occurs in the ER, and when the folding capacity of the ER is overwhelmed by misfolded proteins, the UPR is triggered. The UPR helps return to protein homeostasis by increasing the expression of ER chaperones and ERAD components or induces apoptosis if the stress is not resolved (Almanza *et al.*, 2018). Proteostatic stress is sensed in the ER by three main sensors: inositol requiring enzyme 1 (IRE1), PKR -like ER kinase (PERK) and Activating Transcription Factor 6 (ATF6). These sensors are transmembrane proteins embedded in the ER membrane, and they normally associate with the ER chaperone BiP. Upon accumulation of misfolded proteins in the ER, BiP is thought to detach from the sensors to bind misfolded proteins, leading to signaling into the cytosol, although other BiP-independent activating pathways have also been described (Almanza *et al.*, 2018, Carrara *et al.*, 2013). Notably, each of the ER stress sensors activates a distinct signaling pathway, with specialized outcome (See **Figure 8**).

Upon BiP dissociation, IRE1 dimerizes and trans-autophosphorylates, activating its cytosolic RNAse domain, which splices the mRNA of the X -box binding protein 1 (XBP1) protein into its mature form.

The spliced form of XBP1 is an active transcription factor that directs the transcription of a wide range of targets including the expression of chaperones, foldases and components of the ERAD pathway, relieving ER stress and restoring homeostasis. BiP dissociation from AFT6 reveals an ER export motif, which leads to its export to the Golgi apparatus, where it is cleaved by Golgi-resident proteases, releasing its cytosolic domain, which is a functional basic–leucine zipper transcription factor. Active ATF6 binds other basic–leucine zipper such as the transcription factor XBP1, which induces the expression of a range of downstream targets, including XBP1 and C/EBP homologous protein (CHOP) and BiP. Finally, PERK is an eIF2α kinase and activates the integrated stress response (ISR) (Almanza *et al.*, 2018).

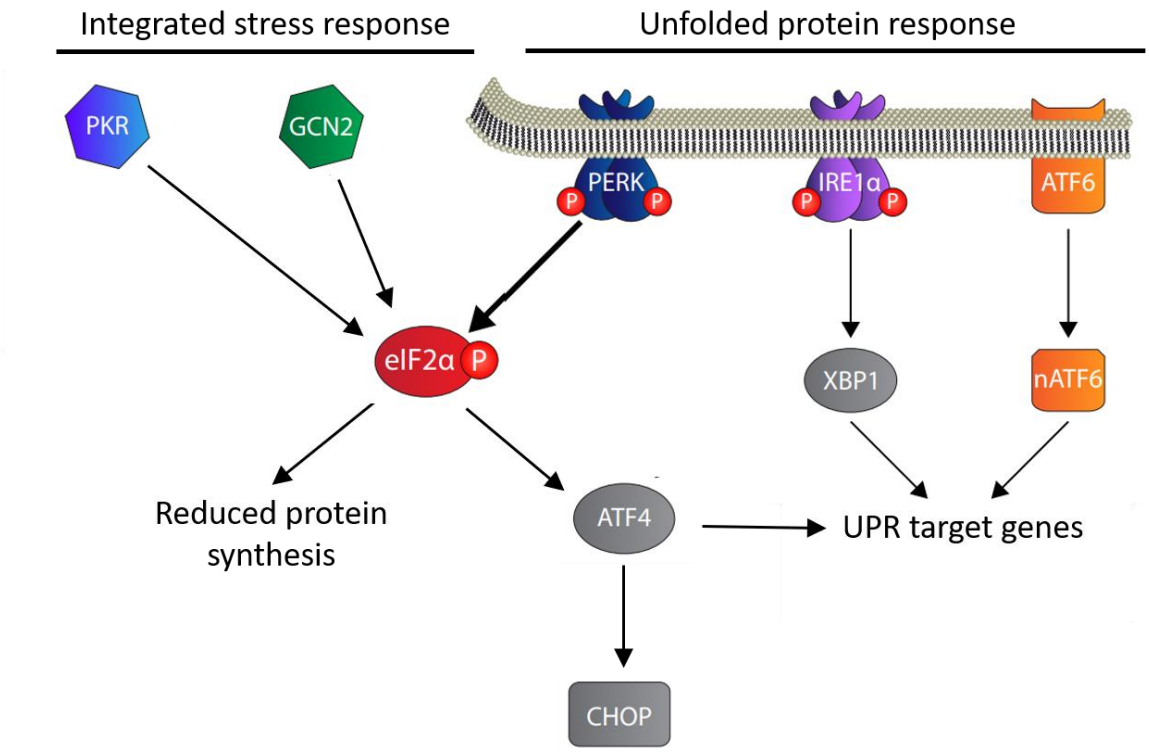

Figure 8: Pathways and interaction between the unfolded protein response and integrated stress response*. Adapted from (Halliday and Mallucci, 2015).*

5.2 The Integrated Stress Response

The ISR is a common cellular stress response in eukaryotic cells, which can respond to a large variety of stimuli. The core event in this pathway is the phosphorylation of eukaryotic translation initiation factor 2 alpha (eIF2α) by one of four members of the eIF2α kinase family, which leads to a decrease in global protein synthesis. Remarkably, some mRNAs can escape the translational blockade by

phosphorylated eIF2α, leading to the selective translation of certain mRNAs, including the transcription factor ATF4 (Activating transcription factor 4) and CHOP (C/EBP homologous protein), which trigger the downstream effectors of the ISR (**Figure 8**). Although the ISR is primarily a pro-survival, homeostatic program, exposure to severe or prolonged stress can drive signaling toward cell death (Pakos-Zebrucka *et al.*, 2016). The four eIF2α kinases PERK, general control non-derepressible 2 (GCN2), protein kinase R (PKR) and heme-regulated eIF2α kinase (HRI) sense a wide variety of different cellular stresses. GCN2 is activated by deacylated transfer RNAs upon amino-acid starvation. PKR is activated by double stranded RNA (dsRNA) during viral infection but can also be activated independently of dsRNA by a variety of stresses, including oxidative stress, ER stress and growth factor deprivation (Pakos-Zebrucka *et al.*, 2016). Finally, HRI is primarily expressed in erythroid stress and senses heme deprivation and other stresses in these cells.

THESIS OBJECTIVES

The principal aim of my PhD project was to elucidate the mechanism by which the *M. ulcerans* toxin mycolactone induces immunosuppressive and cytotoxic effects in patients. As it often happens in science, my specific objectives evolved over time, because my results and those of other teams working in the field opened new questions, and also because the tools that I generated, and the expertise that I acquired in proteomics, bioinformatics and statistics, provided interesting opportunities.

In the introduction, I described the discovery and significance of mycolactone in the pathogenesis of BU, as well as the many mechanisms that were proposed over the years to explain the pleiotropic effects of mycolactone in patients: skin ulceration, local hypoesthesia and systemic immunomodulation. When I joined the Demangel Lab in 2014, the proposed molecular targets and mechanisms of action for mycolactone could not explain its immunomodulatory properties, and more specifically its capacity to block the activation-induced production of cytokines and basal expression of certain membrane receptors by immune cells. Shortly after I joined the team, a breakthrough came from another Lab with the observation that mycolactone inhibits the transport of nascent cytokines into the ER, pointing to defects in Sec61-mediated protein translocation (Hall *et al.*, 2014). Together with Ludivine Baron, post-doc in the Lab, and in collaboration with the team of Ville Paavilainen (University of Helsinki), we showed that mycolactone binds to the alpha subunit of the Sec61 translocon and that this mechanism is responsible for the immunosuppressive effects of mycolactone. We also found that Sec61 blockade is the mechanism underpinning the cytotoxic effects of mycolactone. This work led to a first publication as co-first author in JEM (Article 1, (Baron *et al.*, 2016)). After the completion of this project, I tried different approaches to generate transgenic mice constitutively expressing a mycolactone-resistant mutant of Sec61, to demonstrate the importance of Sec61 blockade in BU pathogenesis and clinical symptoms. However, my attempts were unsuccessful as this mutation turned out to be lethal *in vivo*, and we decided to change priorities for the rest of my thesis.

Indeed, the identification of mycolactone as a novel and highly potent Sec61 blocker opened up new avenues of research. We decided to take advantage of mycolactone to try to answer the long-standing question of the role of the Sec61 translocon in antigen cross-presentation by DCs. As I described in section III.4.2 of the introduction, one of the most critical steps in the process of cross-presentation, the export of antigens internalized in endosomes to the cytosol, had been suggested to be mediated by Sec61, but this concept remained controversial. We used mycolactone as a tool

to determine whether acute Sec61 inhibition in DCs affected antigen export to the cytosol. We later expanded the scope of the work by similarly testing whether Sec61 was the export channel for misfolded proteins during ERAD. This work was performed in collaboration with the teams of Sebastian Amigorena (Curie Institute, Paris) on cross-presentation, and Peter Creswell (Yale School of Medicine, USA) on ERAD. My contribution was to engineer mycolactone-resistant cells for our collaborators, and profile the alterations induced by Sec61 blockade in the proteome of DCs, with a particular focus on the known mediators of ERAD and cross-presentation. Our results supported the concept that Sec61 blockade impairs cross-presentation through indirect effects, and without directly affecting antigen export from the endosomes to cytosol. This work led to a co-first author research publication in PNAS (Article 2, (Grotzke *et al.*, 2017)).

The proteomic analysis that I performed in the frame of Article 2 showed us more than just the indirect effects of mycolactone on cross-presentation. It provided us with a global view of mycolactone-susceptible proteins in the context of a living cell and revealed a set of proteins that were intriguingly upregulated by mycolactone. I decided to conduct an integrated analysis of all proteomic studies that had been realized in the Lab on mycolactone-treated cells, namely Jurkat T cells, MutuDCS and sensory neurons, in order to characterize the conserved and variable features of mycolactone signature across cell types and find a mechanism for the upregulation of certain proteins. This led to a third article, recently published by Molecular & Cellular Proteomics, which I signed as first author (Article 3, (Morel *et al.*, 2018)). In this study, I identified protein features predicting susceptibility or resistance to mycolactone and described an atypical stress response induced by Sec61 blockade.

RESULTS

ARTICLE 1: MYCOLACTONE SUBVERTS IMMUNITY BY SELECTIVELY BLOCKING THE SEC61 TRANSLOCON

As presented in section I.2.4 of the introduction, mycolactone has a strong suppressive effect on immune responses, both in an *in vivo* setting and in numerous *ex vivo* assays of immune cell activation. A common denominator to the observed effects was that mycolactone selectively impacted the activation-induced production of cytokines and membrane receptors in all cell types studied, and that this inhibition was caused by a post-translational mechanism (Boulkroun *et al.*, 2010, Hall *et al.*, 2014) differing from those induced by known immunosuppressors (reviewed in Demangel and High, in press).

The group of Simmonds and colleagues was the first to show that mycolactone can block the translocation of model secretory proteins across the ER membrane, in cell-free systems using ER-derived membrane vesicles (Hall *et al.*, 2014). In a follow-up study, McKenna *et al.* identified the translocation stage that mycolactone inhibits, and highlighted differences in mycolactone-mediated inhibition of cotranslationally versus post-translationally inserted Sec61 secretory substrates (McKenna *et al.*, 2016). They also showed that mycolactone treatment alters the protease susceptibility of Sec61α, indicating that mycolactone induces a conformational change in this subunit of the translocon (McKenna *et al.*, 2016). The breakthrough that allowed us to demonstrate the direct binding of mycolactone to Sec61 was made possible by a collaboration with the group of Ville Paavilainen (University of Helsinki), who contributed to discover the mechanism of action of cotransin. Based on their functional homologies, and despite their structural differences, we postulated that mycolactone may, like cotransin, target Sec61α. Using a variant of cotransin binding Sec61 covalently upon photoactivation, we showed that, mycolactone could indeed efficiently displace cotransin from the translocon.

In a previous study, the group of Ville Paavilainen had used the DNA repair-defective Human colon carcinoma HCT-116 cell to select spontaneous mutants resisting cotransin cytotoxicity. Strikingly, all 11 cotransin-resistant clones had single amino-acid mutations in the Sec61α subunit of the translocon at four positions (M136T, S82P, G80V and R66G/R66I), and overexpressing each mutant in HEK293 cells provided the same level of resistance to cotransin (Mackinnon *et al.*, 2014). Since mycolactone competed with cotransin for binding to Sec61α, we tested cotransin-resistant HEK293

cells for resistance to mycolactone. We found that the M136T mutant provided some level of resistance to mycolactone. In contrast, the S82P and R66G/R66I mutations fully protected the cells from mycolactone cytotoxicity. Together with the above described assays of competition with cotransin, these cellular assays provided definitive proof that mycolactone targets Sec61α and that this interaction mediates the cytotoxicity of mycolactone.

We next performed a proteomic analysis of activated Jurkat T cells, to see if mycolactone was, like cotransin, selective for Sec61 substrates. Consistent with mycolactone blocking Sec61, this analysis showed a selective downregulation of Sec61 clients. In addition, it revealed defects in the levels of certain cytosolic, IFNγ-inducible proteins. T cells present a known IFNγ autocrine loop upon activation (Girdlestone and Wing, 1996), which was disrupted by the rapid, mycolactone-mediated inhibition of IFNγ and IFNγ-receptor, leading to the observed defects of IFNγ-dependent genes in the Jurkat proteome.

I constructed retroviral vectors allowing the over-expression of mycolactone-resistance mutants, in particular Arginine 66 to Glycine (R66G), or wild-type (wt) Sec61α as control, in T cells. Mouse $CD4^+$ T cells transduced with Sec61 mutants were resistant to the inhibitory action of mycolactone on the cell expression of IFN-γ receptor and activation-induced production of IFN-γ. The production of IFNγ by T cells and the IFNγ -triggered activation of inducible nitric oxide synthase (iNOS) in infected macrophages are critical mediators of immunity against mycobacterial infection and *M. ulcerans* in particular (Flynn and Chan, 2001, Bieri *et al.*, 2016). I showed that mycolactone was capable of blocking not only IFNγ production by TCR-activated primary lymphocytes, but also the expression of the IFNγ-receptor and the IFNγ/LPS-induced production of iNOS in bone marrow-derived macrophages. Notably, these effects could be completely abrogated by the overexpression of R66G Sec61. *In vivo,* I showed that the overexpression of R66G Sec61, but not wt Sec61, protected lymphocytes from the homing defects triggered by mycolactone. Consistent with this finding, mutant Sec61 also protected lymphocytes from impaired expression of the homing receptor L-selectin (Article 1, (Baron *et al.*, 2016)).

By demonstrating that Sec61 blockade prevents the generation of cytokines and cytokine receptors, we thus identified Sec61 as a novel key regulator of efficacious immune responses. Therefore, our study not only provided a mechanism for *M. ulcerans* immune evasion, it revealed the potential of inhibiting Sec61 for immune modulation.

Published Online: 7 November, 2016 | Supp Info: http://doi.org/10.1084/jem.20160662

Mycolactone subverts immunity by selectively blocking the Sec61 translocon

Ludivine Baron,[1]* Anja Onerva Paatero,[4]* Jean-David Morel,[1]* Francis Impens,[3] Laure Guenin-Macé,[1] Sarah Saint-Auret,[5] Nicolas Blanchard,[5] Rabea Dillmann,[4] Fatoumata Niang,[1] Sandra Pellegrini,[2] Jack Taunton,[6] Ville O. Paavilainen,[4]** and Caroline Demangel[1]**

[1]Unité d'Immunobiologie de l'Infection and [2]Unité de Signalisation des Cytokines, Institut Pasteur, Institut National de la Santé et de la Recherche Médicale U1221, 75015 Paris, France
[3]Unité des Interactions Bactéries-Cellules, Institut Pasteur, Institut National de la Santé et de la Recherche Médicale U604, Institut National de la Recherche Agronomique, Unité sous-contrat 2020, 75015 Paris, France
[4]Institute of Biotechnology, University of Helsinki, 00014 Helsinki, Finland
[5]Centre National de la Recherche Scientifique, Unité Mixte de Recherche 7509, École européenne de Chimie, Polymères et Matériaux, Université de Strasbourg, 67087 Strasbourg, France
[6]Department of Cellular and Molecular Pharmacology, University of California, San Francisco, San Francisco, CA 94158

Mycolactone, an immunosuppressive macrolide released by the human pathogen *Mycobacterium ulcerans*, was previously shown to impair Sec61-dependent protein translocation, but the underlying molecular mechanism was not identified. In this study, we show that mycolactone directly targets the α subunit of the Sec61 translocon to block the production of secreted and integral membrane proteins with high potency. We identify a single–amino acid mutation conferring resistance to mycolactone, which localizes its interaction site near the lumenal plug of Sec61α. Quantitative proteomics reveals that during T cell activation, mycolactone-mediated Sec61 blockade affects a selective subset of secretory proteins including key signal-transmitting receptors and adhesion molecules. Expression of mutant Sec61α in mycolactone-treated T cells rescued their homing potential and effector functions. Furthermore, when expressed in macrophages, the mycolactone-resistant mutant restored IFN-γ receptor–mediated antimicrobial responses. Thus, our data provide definitive genetic evidence that Sec61 is the host receptor mediating the diverse immunomodulatory effects of mycolactone and identify Sec61 as a novel regulator of immune cell functions.

INTRODUCTION

Mycobacterium ulcerans, the causative agent of Buruli ulcers (BUs), infects and destroys human skin without alerting the host immune system (Demangel et al., 2009). The lack of inflammatory infiltrates in ulcerative lesions is a striking histopathological feature of BU (Guarner et al., 2003). Moreover, BU patients display systemic defects in cellular immune responses, such as a reduced capacity of peripheral blood T cells to produce cytokines upon ex vivo stimulation (Phillips et al., 2009). These defects are independent of the activation stimulus and resolve upon treatment of the disease, showing their association with *M. ulcerans*. Bacterial virulence relies on the production of mycolactone, a polyketide-derived macrolide with ulcerative properties in the skin (George et al., 1999). Although bacteria remain primarily at the site of infection, mycolactone diffuses into mononuclear blood cells, LNs, and spleen (Hong et al., 2008; Sarfo et al., 2011), allowing it to exert immunosuppressive effects at the systemic level. Intraperitoneal delivery of mycolactone protects mice against chemically induced skin inflammation (Guenin-Macé et al., 2015). It prevents peripheral blood lymphocyte homing to draining LNs and expansion upon antigenic stimulation (Guenin-Macé et al., 2011). Finally, *M. ulcerans* strains deficient for mycolactone production do not induce functional defects in peripheral blood T cells of infected mice (Hong et al., 2008). Therefore, mycolactone has the intrinsic capacity to block the development of innate and adaptive immune responses in vivo.

In vitro mycolactone blunts the capacity of immune cells to produce selected cytokines, chemokines, and homing receptors without inducing cellular stress or cytotoxicity (Hall and Simmonds, 2014). Mycolactone operates post-transcriptionally and independently of mammalian target

*L. Baron, A.O. Paatero, and J.-D. Morel contributed equally to this paper.

**V.O. Paavilainen and C. Demangel contributed equally to this paper.

Correspondence to Caroline Demangel: demangel@pasteur.fr; or Ville O. Paavilainen: ville.paavilainen@helsinki.fi

F. Impens's present address is Medical Biotechnology Center, VIB, Ghent University, 9000 Ghent, Belgium.

Abbreviations used: BiP, binding immunoglobulin protein; BU, Buruli ulcer; CRM, canine rough microsome; iNOS, inducible nitric oxide synthase; IO, ionomycin; IRES, internal ribosome entry site; IVT, in vitro translation; LC-MS/MS, liquid chromatography–tandem MS; MS, mass spectrometry; PLN, peripheral LN; SILAC, stable-isotope labeling with amino acids in cell culture; SRP, signal recognition particle; WASP, Wiskott–Aldrich syndrome protein.

The Rockefeller University Press $30.00
J. Exp. Med. 2016
https://doi.org/10.1084/jem.20160662

of rapamycin (mTOR) and, as such, represents a novel type of natural immunosuppressor. Hall et al. (2014) showed that mycolactone blocks the translocation of inflammatory mediators (TNF and Cox2) as well as model secretory proteins into the ER, with subsequent degradation of these proteins by the ubiquitin–proteasome system. Using cell-free systems, McKenna et al. (2016) later identified the translocation stage that mycolactone inhibits and highlighted differences in mycolactone-mediated inhibition of co-translationally versus posttranslationally inserted Sec61 secretory substrates. In eukaryotes, co-translational protein translocation is initiated by recognition of signal peptides or nascent polypeptide anchor domains by the signal recognition particle (SRP). The SRP then targets the ribosome-nascent polypeptide complex to the Sec61 translocon for insertion into the ER lumen (Park and Rapoport, 2012). McKenna et al. (2016) provided biochemical evidence that mycolactone induces a conformational change in the pore-forming subunit of the translocon, Sec61α. Although Sec61, SRP-receptor, and SRP are sufficient for minimal translocation to occur, accessory components such as Sec62/63, translocating chain-associated membrane protein (TRAM), translocon-associated protein (TRAP) complex, and binding immunoglobulin protein (BiP) facilitate the process. What the precise molecular target of mycolactone is and how mycolactone's ability to prevent protein translocation connects with reduced cellular immune responses remained critical open questions.

RESULTS AND DISCUSSION

Mycolactone targets the Sec61 translocon

Among known inhibitors of protein translocation, three have been formally shown to act by directly targeting Sec61α: the cyclic heptadepsipeptide HUN-7293/cotransin/CT8, decadepsipeptide decatransin, and cyanobacterial product apratoxin A (Garrison et al., 2005; Maifeld et al., 2011; MacKinnon et al., 2014; Junne et al., 2015; Paatero et al., 2016). All of these drugs target a partially overlapping site in the pore-forming Sec61α subunit. However, unlike decatransin and apratoxin A, CT8 inhibits Sec61 in a substrate-selective manner. To test the hypothesis that mycolactone and CT8 use similar mechanisms of action, we performed competitive Sec61α-binding assays with a structural variant of CT8 that covalently cross-links to Sec61α upon photoactivation (Fig. S1 A; MacKinnon et al., 2007, 2014). ER microsomes were incubated with CT7 in the presence or absence of increasing amounts of mycolactone and then photolyzed and denatured. The presence of CT7 cross-linked to Sec61α was then quantitatively assessed by click chemistry and in-gel fluorescent scanning. Mycolactone competed dose dependently with CT7 for binding to Sec61α (Fig. 1 A), similarly as the potent cotransin analogue CT9 (Fig. 1 B and Fig. S1 A). Importantly, mycolactone displaced CT7 slightly more efficiently than CT9, indicating that it binds Sec61α with comparable or higher affinity and may share a coinciding binding site on Sec61α.

Mycolactone consists of a lactone ring and two polyketide chains branched in the north and south positions (Fig. S1 A). We reported previously that variant 5b lacking the northern side chain partially retains the immunosuppressive activity of mycolactone, whereas subunits lacking the southern or both side chains (4a and 5a, respectively) are biologically inert (Guenin-Macé et al., 2015). Consistently, 5b competed with CT7 with an ∼10-fold reduced potency, whereas 4a and 5a showed no competitive activity (Fig. 1 C). No difference in ability of mycolactone to compete with CT7 for Sec61α binding was observed after extensive washing of microsomes (Fig. 1 D), indicating that mycolactone binds tightly to the translocon and has a slow dissociation rate.

A previous genetic screen identified several point mutations in Sec61α (R66I, R66G, S82P, and M136T) that reduce CT8 binding without major effects on channel function (MacKinnon et al., 2014). Given that mycolactone and CT8 likely have overlapping binding sites, we tested whether these mutations confer resistance to mycolactone. For this purpose, we treated HEK293-FRT cells overexpressing WT or mutant Sec61α constructs with increasing concentrations of mycolactone. The viability of cells expressing WT Sec61α was potently reduced by mycolactone (IC_{50} = 10 nM; Fig. 1 E). In contrast, cells expressing the R66I-, R66G-, and S82P-mutant alleles were highly desensitized (IC_{50} > 1,000 nM). Interestingly, these mutations cluster near the lumenal plug of Sec61α (Fig. S1 B), suggesting that this region forms the mycolactone interaction site. This finding was fully consistent with the observation by McKenna et al. (2016) that mycolactone alters protease sensitivity of Sec61α in vitro. Focusing on the R66G construct, we investigated whether this single–amino acid mutation confers resistance to mycolactone-mediated blockade of protein secretion. HEK293-FRT cells stably expressing WT or R66G-Sec61α were transfected with a secreted Gaussia luciferase construct and then subjected to a 24-h mycolactone treatment that did not alter cell viability. Although mycolactone efficiently blocked luciferase secretion in cells expressing WT Sec61α (IC_{50} = 3 nM), cells expressing the R66G-Sec61α mutant proved highly resistant (IC_{50} > 1,000 nM; Fig. 1 F). In addition to providing additional evidence that mycolactone binds to Sec61α, these data revealed the critical importance of the Sec61α R66 residue for mycolactone's inhibitory activity on protein translocation.

Mycolactone is a broad-spectrum inhibitor of Sec61

A distinguishing feature of CT8 is its ability to prevent the translocation of only a minor subset of Sec61 clients (Besemer et al., 2005; Garrison et al., 2005; Maifeld et al., 2011). To determine whether mycolactone shares this property, we compared the effects of mycolactone and CT8 on the production of known Sec61 clients by human immune cells (namely TNF production by monocyte-derived macrophages and IFN-γ, IL-2, and L-selectin production by peripheral blood-derived $CD4^+$ T cells). Cotransin showed a highly variable inhibitory activity toward the different substrates (IC_{50} between 20 and

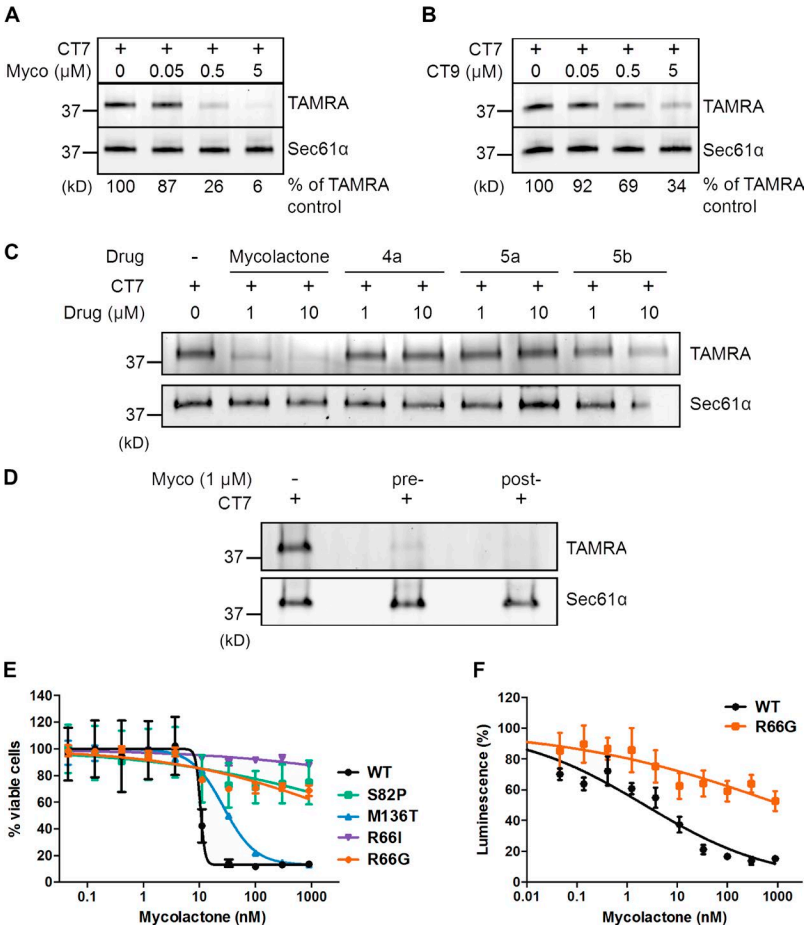

Figure 1. **Mycolactone targets the Sec61 translocon.** (A and B) CRMs were preincubated with increasing concentrations of mycolactone (Myco; A) or CT9 (B) at the indicated concentrations, followed by 100 nM CT7. Covalent CT7/Sec61α adduct was detected using click chemistry between the alkyne group in CT7 and rhodamine-azide (TAMRA). (C) As in A but comparing the competitive activity of mycolactone to that of synthetic subunits of the intact molecule. (D) CRMs were incubated with a saturating concentration of mycolactone (10 μM) either before (pre-) or after (post-) extensive washing. CT7 photo–cross-linking was performed after final CRM pelleting. (E) HEK293-FRT TRex cells stably expressing WT or mutant Sec61α were treated with increasing concentrations of mycolactone for 72 h, and cell viability was analyzed by the Alamar blue assay (Mean ± SEM; $n = 4$). (F) HEK293-FRT TRex cells stably expressing WT Sec61α or R66G-Sec61α were transfected for inducible expression of a secreted Gaussia luciferase and then treated with increasing concentrations of mycolactone for 24 h. Data are luminescence values (mean ± SEM; $n = 2$) measured from culture supernatants. (A–F) Data shown are from one of two independent experiments, which gave similar results.

1,050 nM; not depicted). In contrast, mycolactone prevented the production of all tested proteins with IC_{50} between 4.5 and 12 nM, suggesting that it is a more potent and less selective Sec61 inhibitor. Next, we used global proteome analysis of SILAC (stable-isotope labeling with amino acids in cell culture) T cells to gain a broader view of mycolactone activity and identify the proteins impacted by Sec61 inhibition during T cell activation. Jurkat T cells were grown in light or heavy SILAC medium for five cell divisions and then treated with 40 nM mycolactone or vehicle for 1 h before activation with PMA and ionomycin (IO) for 6 h. These conditions induced full cell activation, bypassing a potential inhibitory effect of mycolactone on TCR expression (Boulkroun et al., 2010). Cells were then lysed, and equal amounts of light- and heavy-labeled protein extracts were mixed. Proteins were trypsin digested, and peptide mixtures were analyzed by liquid chromatography–tandem mass spectrometry (MS; LC-MS/MS). The SILAC analysis was repeated with reversed labeling conditions, allowing the reliable identification and quantification of 6,503 proteins (hereafter referred to as identified proteins). Among these, 4,636 proteins were quantified in both labeling conditions. SILAC analyses were performed on cell extracts, and consequently, most secreted proteins were not detected. Notably, 52 proteins were consistently down-regulated in mycolactone-treated cells (log_2 mycolactone/control ratio <−0.5), whereas only two proteins (putative E3 ubiquitin–protein ligase LRRC58 and Hsp70 chaperone HSPA1A) were up-regulated (log_2 mycolactone/control ratio >0.5; Fig. 2 A and Table S1). Fig. 2 B compares the distribution of mycolactone–down-regulated, identified, and all human proteins across the different subcellular compartments. In contrast to cytoplasmic and nuclear proteins, the incidence of plasma membrane– and ER-located proteins was increased in mycolactone–down-regulated proteins, compared with identified proteins (Fig. 2 B), indicating a selective down-regulation of these proteins by mycolactone. A key word analysis confirmed this observation and revealed an additional enrichment in glycoproteins, immunoglobulin domain–containing proteins, and proteins involved in the immune response among mycolactone–down-regulated proteins (Fig. 2 C).

Consistent with Sec61 inhibition, 42 of the 52 mycolactone–down-regulated proteins contained a signal sequence or transmembrane domain directing newly synthesized proteins to the translocon (Table S1). The mycolactone–down-regulated subset was significantly enriched in single-pass type I/II membrane proteins (Fig. 2 D), indicating that such proteins are particularly

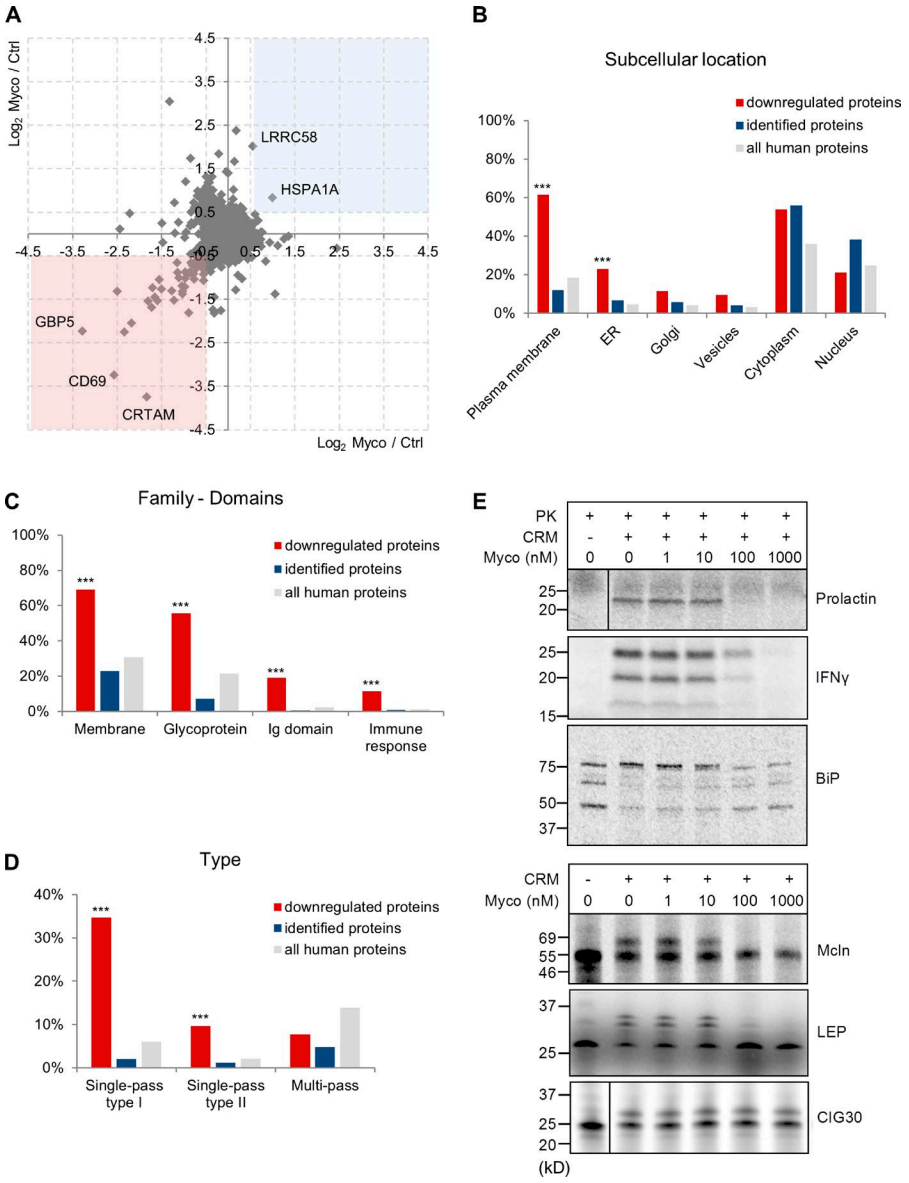

Figure 2. **Mycolactone is a broad-spectrum inhibitor of Sec61.** (A) Scatter plot showing the $\log_2$ SILAC ratios for individual proteins quantified in analysis 1 on the x axis (light condition: 40 nM mycolactone [Myco]; heavy condition: vehicle control [Ctrl]) and analysis 2 on the y axis (reversed conditions). Proteins with a $\log_2$ ratio <−0.5 (pink square) or >0.5 (blue square) in both analyses were considered modulated by mycolactone. CRT AM, cytotoxic and regulatory T cell molecule. (B and C) Gene ontology cellular component (B) and SwissProt Protein Information resource keywords (C) annotation analyses of the proteins that were reproducibly down-regulated in mycolactone-exposed T cells (red; n = 52), compared with identified proteins (blue; n = 6,503) and all human proteins in UniProt (gray; n = 20,204). (D) Distribution of downregulated (red), identified (blue), and all human proteins (gray) over different categories of membrane proteins. (B–D) Statistics were calculated by Fisher exact tests comparing downregulated versus identified proteins. ***, $P < 0.001$. (E) IVT assays of various Sec61 clients in the presence of increasing concentrations of mycolactone. ER translocation of nonglycosylated proteins (prolactin, IFN-γ, and BiP) was assessed by treatment with proteinase K (PK), with resistance to proteinase K indicating correct translocation into the ER lumen. Detergent-treated controls are shown in Fig. S1 C. It should be noted that BiP is largely protease resistant and, upon proteinase K treatment, forms shorter fragments. Translocation of glycosylated proteins (Mcln, LEP, and CIG30) was assessed by analyzing the change in migration in SDS-PAGE and autoradiography. Glycosidase-treated controls are shown in Fig. S1 C. The data shown are from one of two independent experiments, which gave similar results.

susceptible to Sec61 inhibition by mycolactone. In contrast, the incidence of multipass membrane proteins was comparable between down-regulated proteins and identified proteins, suggesting that some multipass membrane proteins may bypass mycolactone-mediated blockade of Sec61. To test this hypothesis, mRNAs for various Sec61 substrates were translated in a reconstituted mammalian translation system in the presence of canine rough microsomes (CRMs), [^{35}S]methionine, and increasing concentrations of mycolactone. In accordance with previously reported in vitro translation (IVT) assays of Sec61-dependent secretory and type II transmembrane protein TNF (Hall et al., 2014; McKenna et al., 2016), ER translocation of secreted prolactin and IFN-γ was efficiently and dose-dependently suppressed by mycolactone (Fig. 2 E and Fig. S1 C). Translocation of ER-resident BiP (also known as HSPA5) was also affected, confirming the SILAC data (Fig. 2 E and Table S1). BiP being a critical mediator of Sec61-dependent translocation, its depletion may contribute indirectly to the defective biogenesis of Sec61 clients in mycolactone-exposed cells. Multipass membrane proteins mucolipin 1 (Mcln) and a synthetic multipass membrane protein derived from *Escherichia coli* leader peptidase (LEP; Lundin et al., 2008) were also susceptible to mycolactone in IVT assays. In contrast, the multipass ER membrane protein CIG30 (Monné et al., 1999) was consistently resistant to mycolactone concentrations up to 1 µM (Fig. 2 E and Fig. S1 C). The SILAC and in vitro assays of protein translocation are thus fully consistent with mycolactone being a broad-acting inhibitor of Sec61 client production, with a more selective activity on multipass membrane proteins.

Sec61 blockade affects IFN-γ signaling in Jurkat T cells

Among the 52 proteins found to be down-regulated by mycolactone in PMA/IO-stimulated Jurkat T cells, 10 did not contain a signal sequence or transmembrane domain identifying them as a Sec61 client (Table S1). They were all encoded by IFN-stimulated genes (nine by IFN-γ and one by IFN-α), leading us to examine the effects of mycolactone on both the production of IFNs and the cell's response to exogenous IFNs. Consistent with a previous study, exposing Jurkat T cells to mycolactone for 1 h before PMA/IO activation efficiently prevented IFN-γ production (Fig. 3 A), despite robust *IFNG* mRNA induction (Fig. 3 B; Phillips et al., 2009). Moreover, mycolactone-treated cells rapidly lost the ability to respond to IFN-γ: T cells exposed to mycolactone for >20 min before 20-min stimulation with IFN-γ showed reduced STAT1 phosphorylation (Fig. 3 C). The IFN-γ receptor (IFNGR) was not detected by our SILAC analysis, likely because protein level was below the detection limit. Yet, using flow cytometry, we found that a 6-h exposure to mycolactone led to a 60% reduction in T cell surface expression of IFNGR1 (Fig. 3 D). Because the level of *IFNGR1* transcripts was not altered in mycolactone-treated cells (Fig. 3 E), the loss of IFNGR1 likely results from Sec61 blockade. We conclude that both the reduced IFN-γ production and the loss of IFNGR1 impair the IFN-γ autocrine loop in PMA/IO-activated T cells exposed to mycolactone. This was further indicated by the reduced accumulation of IFN-γ–inducible GBP2 at the mRNA level (Fig. 3 F) and a Western blot analysis validating our SILAC observation that mycolactone down-regulates GBP2 protein levels in activated Jurkat T cells (Fig. 3 G and Table S1). We also measured T cell responses to IFN-α. In Jurkat T cells exposed for 6 h to mycolactone, the surface level of the type I IFN receptor subunits (IFNAR1 and IFNAR2) was also reduced but to a lesser extent than IFN GR1 (Fig. 3 D). Consistently, phosphorylation of STAT1/3 was barely affected in T cells exposed to mycolactone for 6 h and then pulsed with IFN-α for 20 min. However, after a 24-h exposure, IFN-α signaling declined considerably (Fig. 3 H). Altogether, our SILAC data show that the magnitude and kinetics of mycolactone effects vary between Sec61 substrates, likely reflecting differences in protein turnover rates.

The R66G mutation in Sec61α confers broad resistance to mycolactone

Production of IFN-γ by T cells and IFN-γ–driven expression of inducible nitric oxide synthase (iNOS) in infected macrophages are both essential for control of mycobacterial infection (Flynn and Chan, 2001). *M. ulcerans* is no exception, as shown by the reduced capacity of IFN-γ knockout mice to kill intracellular bacilli during the early intramacrophage growth phase of the bacteria (Bieri et al., 2016). To evaluate the contribution of Sec61 to mycolactone virulence, we examined whether mycolactone-resistant Sec61 mutants rescued the generation of antimycobacterial immune responses. Primary T cells isolated from mouse lymphoid organs were transduced with retroviral vectors for overexpression of WT Sec61α or R66G-Sec61α and fluorescent reporter protein Zsgreen (Fig. 4 A). Nontransduced and WT Sec61α–transduced cells were equally susceptible to mycolactone treatment, as demonstrated by the comparable inhibition of CD4 expression in mycolactone-exposed Zsgreen$^+$ and Zsgreen$^-$ cells (Fig. 4 B). Strikingly, expression of R66G-Sec61α conferred resistance to mycolactone-induced defects in CD4 expression (Fig. 4 B). We reported previously that mycolactone efficiently down-regulates the expression of CD62L at the surface of naive T cells (Guenin-Macé et al., 2011). Similar to CD4, CD62L expression resisted mycolactone treatment in T cells expressing R66G-Sec61α but not WT Sec61α (Fig. 4 C). Further, in T cells transduced with R66G-Sec61α and stimulated with PMA/IO, the production of IFN-γ was unaffected by mycolactone treatment (Fig. 4 D). This demonstrated that defects in cytokine production are also fully corrected by expression of R66G-Sec61α. A similar approach was used to assess the functional impact of Sec61 inhibition in macrophages (Fig. 4 E). Transduction of R66G-Sec61α, but not WT Sec61α, in bone marrow–derived macrophages conferred resistance to mycolactone-mediated inhibition of IFNGR1 expression (Fig. 4 F). This reestablished the bactericidal capacity of macrophages, as LPS + IFN-γ–driven production of iNOS was restored in macrophages expressing R66G-Sec61α but not WT Sec61α (Fig. 4 G). Thus, by inhibiting Sec61 activity, mycolactone prevents both IFN-γ production by T cells and macrophage responsiveness to IFN-γ stimulation.

Mycolactone suppresses Sec61 activity in T cells in vivo

The data in Fig. 4 C show that CD62L expression by mouse primary T cells is highly susceptible to mycolactone-induced inhibition of Sec61. Using this membrane receptor as a readout, we next investigated whether systemically delivered mycolactone impacts Sec61 activity in adoptively transferred T cells. Because mycolactone-induced loss of CD62L impairs T cell capacity to reach peripheral LNs (PLNs; Guenin-Macé et al., 2011), we also examined whether Sec61 blockade results in impaired homing properties. Primary T cells isolated from WT (C57BL/6J and CD45.2$^+$) and congenic CD45.1 mice were transduced with WT Sec61α or R66G-Sec61α (Fig. 5 A). CD45.2$^+$ WT Sec61α–transduced cells were then mixed with CD45.1$^+$ R66G-Sec61α–transduced cells in equal proportions and vice versa. Each mix of cells was then injected intravenously into WT recipient mice. Concomitantly, mice were given an intraperitoneal injection of 1 mg/kg mycolactone, a treatment previously shown to induce antiinflammatory effects in vivo (Guenin-Macé et al., 2015). After 24 h, the mean surface expression of CD62L and the relative proportions of WT Sec61α– and R66G-Sec61α–transduced cells in PLN and spleen were determined by FACS analysis. In mycolactone-injected mice, the expression of CD62L was reduced in WT Sec61α– but not R66G-Sec61α–transduced T cells from the spleen (Fig. 5 B, left). A similar trend was observed in T cells from the PLN (Fig. 5 B,

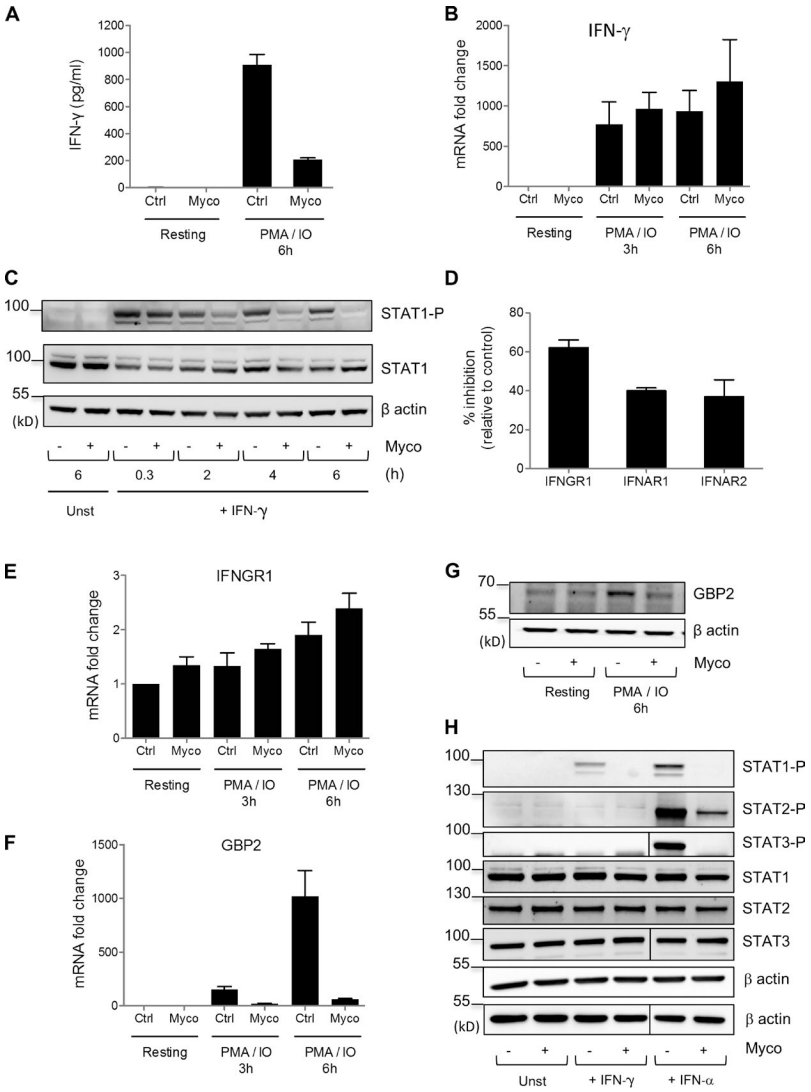

Figure 3. **Mycolactone targets primarily the IFN-γ signaling pathway in Jurkat T cells.** (A) Production of IFN-γ by Jurkat T cells treated with 20 nM mycolactone (Myco) or vehicle (Ctrl) for 6 h (Resting) or for 1 h before 6 h of activation with PMA/IO. (B) Quantitation of *IFNG* mRNAs in Jurkat T cells treated with mycolactone or vehicle for 6 h or for 1 h before 3 or 6 h of activation with PMA/IO. (C) Western blot analysis of tyrosine phosphorylated (STAT1-P) and total STAT1 in Jurkat T cells treated with mycolactone or vehicle for the indicated times before activation with 1 ng/ml IFN-γ for 20 min or left unstimulated (Unst). (D) Flow cytometric analysis of surface expression of IFNGR1, IFNAR1, and IFNAR2 by Jurkat T cells incubated with or without mycolactone for 6 h. (E) Quantification of *IFNGR1* mRNAs in Jurkat T cells treated as in B. (F and G) Quantitation of *GBP2* mRNAs (F) and total GBP2 protein (G) in Jurkat T cells treated as in B. (H) Western blot analysis of phosphorylated (STAT1-P, STAT2-P, and STAT3-P) and total STAT1, STAT2, and STAT3 with β-actin as the loading control in Jurkat T cells treated with mycolactone or vehicle for 24 h before activation with 1 ng/ml IFN-γ or IFN-α for 20 min or left unstimulated (Unst). (A and D) Data are mean IFN-γ levels or mean fluorescence intensity, respectively, ± SEM of one experiment performed in triplicate, relative to vehicle controls. (B, E, and F) Data are mean fold-changes ± SEM of one experiment performed in duplicate, compared with resting controls. Similar results were obtained in independent experiments. (A, C, G, and H) Data are from one of two independent experiments, which gave similar results.

right). This experiment demonstrated that mycolactone modulates T cell expression of CD62L in vivo in a Sec61-dependent manner. Notably, R66G-Sec61α–transduced T cells were recovered from PLNs at significantly higher frequencies than WT Sec61α–transduced T cells (Fig. 5 C, right). These frequencies were instead comparable in the spleen, consistent with CD62L not being critical for T cell homing to this organ (Fig. 5 C, left). Therefore, mycolactone down-regulates both Sec61-dependent expression of CD62L and CD62L-dependent lymphocyte homing in vivo.

In conclusion, we have shown that mycolactone-induced Sec61 blockade is caused by a direct interaction with Sec61α, which determines mycolactone's ability to prevent the generation of innate and adaptive immune responses. These data provide a molecular explanation for the immunological defects of BU patients. More generally, they highlight the critical importance of Sec61 activity for immune cell function, migration, and communication. Compared with CT8, mycolactone was more cytotoxic in human primary dermal fibroblasts and equally poorly cytotoxic in Jurkat T cells (Fig. S2 A). It was more effective than CT8 at inhibiting the production of cytokines and homing receptors by immune cells, and our on-going investigations suggest that mycolactone is also more potent than apratoxin A in these bioassays (not depicted). Among known inhibitors of Sec61, mycolactone is therefore the first produced by a human pathogen and likely the most potent.

Mycolactone was previously reported to bind and activate N–Wiskott–Aldrich syndrome protein (N-WASP) and type 2 angiotensin II receptor (AT2R) to mediate skin ulceration and analgesia, respectively (Guenin-Macé et al., 2013; Marion et al., 2014). Silencing of N-WASP/WASP or AT2R in relevant cell models did not modify the inhibitory effect of mycolactone on the production of secreted and membrane proteins (Fig. S2, B and C), showing that the immunomodulatory properties of mycolactone are independent of these

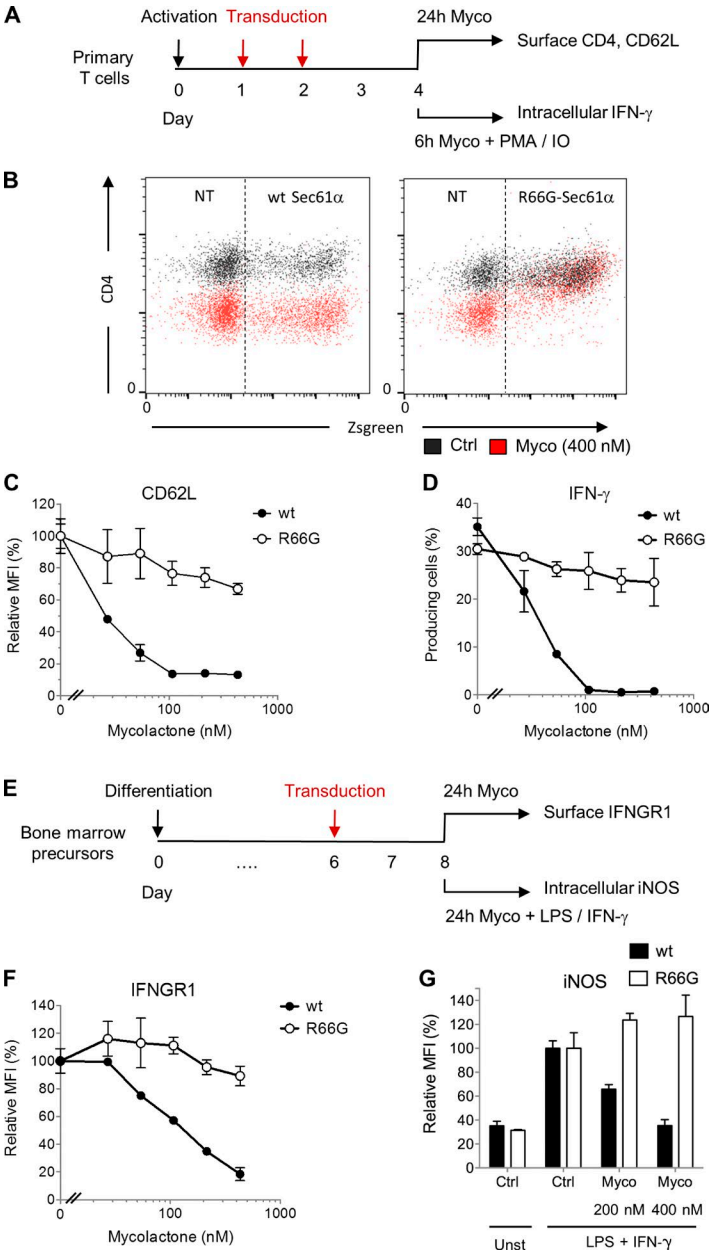

Figure 4. **The R66G mutation in Sec61α confers resistance to mycolactone.** (A) Primary mouse T cells were activated with anti-CD3/CD28 antibodies and then transduced with WT Sec61α or R66G-Sec61α before exposure to mycolactone (Myco) in resting or PMA/IO-stimulated conditions. (B) Differential effect of mycolactone (24 h at 400 nM) on the CD4 surface expression of WT Sec61α– or R66G-Sec61α–transduced (Zsgreen$^+$) cells. Data are mean fluorescence intensity (MFI) from one of two independent experiments, which gave similar results. Ctrl, vehicle control; NT, nontransduced. (C) Dose-dependent effect of mycolactone on the CD62L surface expression of WT Sec61α– or R66G-Sec61α–transduced (Zsgreen$^+$-gated) cells. (D) Effect of a 1-h pretreatment with increasing doses of mycolactone on the PMA/IO-induced production of IFN-γ by primary T cells transduced with WT Sec61α or R66G-Sec61α (Zsgreen$^+$-gated) cells. (E) Bone marrow–derived macrophages were transduced with WT Sec61α or R66G-Sec61α before exposure to mycolactone in resting or LPS + IFN-γ–stimulated conditions. (F) Dose-dependent effect of mycolactone on the IFNGR1 surface expression of WT Sec61α– or R66G-Sec61α–transduced (Zsgreen$^+$-gated) cells. (G) Dose-dependent effect of mycolactone on the LPS + IFN-γ–induced production of iNOS by WT Sec61α– or R66G-Sec61α–transduced (Zsgreen$^+$-gated) cells. (C, D, F, and G) Data are mean fluorescence intensity or mean cell percentages ± SEM of triplicates, relative to vehicle controls. They are from one of two independent experiments, which gave similar results.

proteins. It is nevertheless possible that Sec61 inhibition mediates or at least contributes to the ulcerative and analgesic properties of mycolactone.

Altogether, our data reveal a novel mechanism of immune evasion evolved by pathogenic mycobacteria that targets host cell protein translocation. Inhibition of Sec61 activity efficiently prevented the production of key mediators of innate and adaptive immune responses against intracellular pathogens, as we demonstrated for IFN-γ and IFN-γ receptor. The discovery that mycolactone inhibits Sec61 opens novel perspectives beyond the field of inflammation. Because CT8 was effective at limiting proteostasis of enveloped viruses (Heaton et al., 2016), mycolactone may similarly show broad antiviral activity. It may also prove useful in the treatment of pathologies associated with elevated secretory protein synthesis. Genetically modifying Sec61 demonstrated the specificity of mycolactone binding to the translocon. Because Sec61 clients are expressed in a cell type–specific manner, mycolactone-mediated inhibition of protein translocation into the ER could underpin the variety of its effects in different cell types and the distinctive features of BU.

MATERIALS AND METHODS

Reagents and expression vectors

All experiments using mycolactone were done with natural mycolactone A/B purified from *M. ulcerans* bacteria (strain

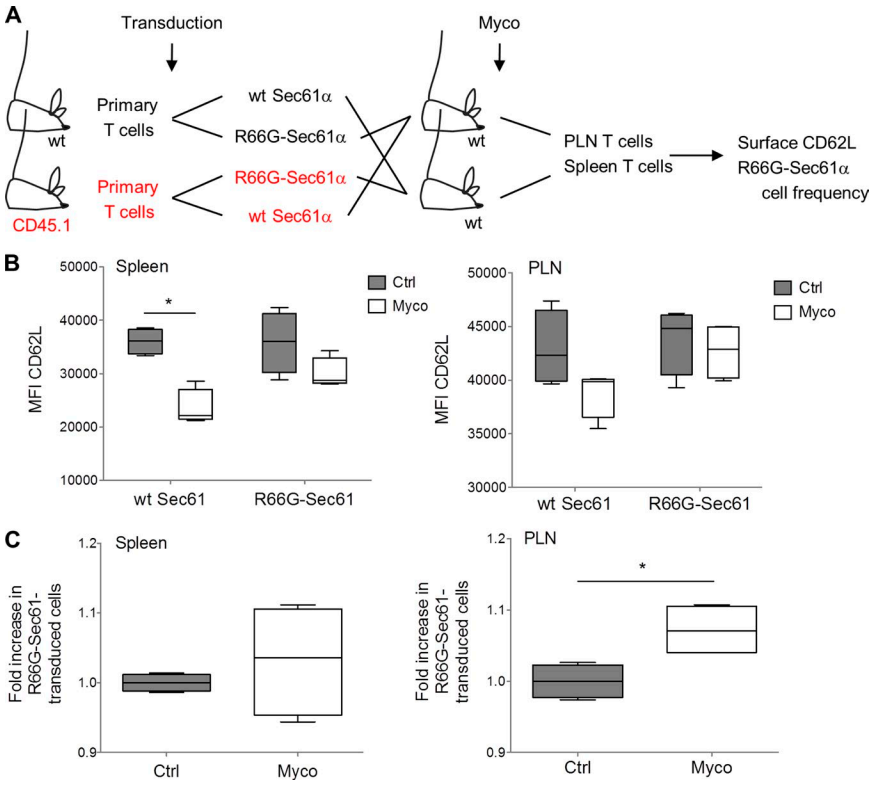

Figure 5. **Mycolactone suppresses Sec61 activity in T cells in vivo.** (A) Primary T cells isolated from WT (C57BL/6J and CD45.2$^+$) and congenic CD45.1 mice were transduced with WT Sec61α or R66G-Sec61α and mixed, as depicted. Each cell mix was injected intravenously into four recipient mice, two of which received concomitantly an intraperitoneal injection of mycolactone (Myco) and, the other two, vehicle as control. (B) CD62L surface expression on WT Sec61α and R66-Sec61α T cells (CD45.1$^+$ or CD45.1$^-$; Zsgreen$^+$ gated) recovered from the spleen and PLN. Ctrl, vehicle control; MFI, mean fluorescence intensity. (C) Relative proportion of R66G-Sec61α cells, compared with WT Sec61α cells, in the spleen and PLN. (B and C) Data are mean fluorescence intensity (B) and mean cell numbers (C) in each experimental group, presented as box and whiskers (*, $P \leq 0.05$, Mann-Whitney test , each box corresponding to four experimental values). They are representative of two independent experiments giving similar results.

1615; 35840; ATCC) and then quantified by spectrophotometry (λ_{max} = 362 nm; log ε = 4.29; Spangenberg and Kishi, 2010). Synthetic modules of mycolactone (4a, 5a, and 5b) were generated as previously described (Chany et al., 2011). Stock solutions were prepared in either ethanol or DMSO and then diluted 1,000× in culture medium for cellular assays or 10× in PBS before injection in mice. CT7, CT8, and CT9 were prepared as previously described (MacKinnon et al., 2007; Maifeld et al., 2011). Sec61 WT or mutant sequences were cloned upstream of an internal ribosome entry site (IRES) of the pRetroX–IRES-Zsgreen retroviral vector (Takara Bio Inc.) for simultaneous translation of Sec61α and Zsgreen in mouse primary T cells and macrophages.

SDS-PAGE, autoradiography, and Western blotting

Cell lysates were resolved on NuPAGE Bis-Tris gels and transferred to nitrocellulose membranes (Thermo Fisher Scientific). For autoradiography, dried Tris-tricine gels were exposed to a storage phosphorus screen (GE Healthcare) and imaged on a Typhoon Trio phosphorimager (GE Healthcare). Protein detections used the following antibodies: WASP F-8 (sc-365859; Santa Cruz Biotechnology, Inc.), N-WASP 30D10 (no. 4848; Cell Signaling Technology), pSTAT1 Y701 (no. 9171L; Cell Signaling Technology), pSTAT2 Y689 (no. 07-224; EMD Millipore), pSTAT3 Y705 (no. 9131L; Cell Signaling Technology), STAT1 (no. 06-501; EMD Millipore), STAT2 (06-502; EMD Millipore), STAT3 (sc-7179; Santa Cruz Biotechnology, Inc.), AT2R (sc-9040; Santa Cruz Biotechnology, Inc.), β-actin (no. 3700; Cell Signaling Technology), GAPDH (no. 2118; Cell Signaling Technology), and Sec61α (NB120-15575; Novus Biologicals). Here, complexes were revealed with ECL Prime detection reagent (GE Healthcare) and chemiluminescence reading on a luminescent image analyzer (LAS-4000; Fujifilm).

Photoaffinity labeling

Protocols for CRM preparation and CT7 photoaffinity labeling and click chemistry were described previously (Walter and Blobel, 1983; MacKinnon et al., 2007). In brief, CRMs equivalent to 100 nM Sec61 were treated with 1 or 10 µM mycolactone or DMSO for 30 min at 0°C, followed by incubation with 100 nM CT7 for 10 min at room temperature. Samples were then photolyzed for 10 min, and cross-linked proteins were detected by click chemistry, SDS-PAGE, and in-gel fluorescence scanning. In Fig. 1 D, 50 µl of photoaffinity-labeling reactions were treated with 10 µM mycolactone on ice before (pre) or after (post-) three rounds of membrane pelleting. A third sample was treated after pelleting with an equal volume DMSO. All the samples were further incubated for 30 min on ice prior to CT7 photoaffinity labeling.

IVT assays

Protein translocation assays were performed as described previously (Sharma et al., 2010): DNA templates encoding the indicated constructs were transcribed with T7 or SP6 polymerase (New England Biolabs, Inc.) for 1–2 h at 37°C and

used in subsequent translation/translocation reactions. The reactions were assembled at 0°C in the presence of mycolactone or an equivalent volume of solvent. Reactions included [^{35}S]methionine (2 µCi per 10 µl translation; PerkinElmer) and CRM. The amount of CRM was optimized to be 0.25 µl per 10 µl reaction volume. Translation was initiated by transferring the reactions to 32°C for 30 or 60 min and stopped by returning reactions onto ice. Translocation of nonglycosylated proteins was assessed by treating the samples with proteinase K for 1 h at 0°C. An aliquot was incubated in the presence of TX-100 to demonstrate protection by CRMs. Proteinase digestion was stopped with PMSF and boiling in the presence of SDS. After TCA precipitation, the remaining, protected proteins/protein fragments were analyzed with SDS-PAGE and autoradiography. The translocation of glycosylated proteins was analyzed by SDS-PAGE and autoradiography. Alternatively, the control samples were first denatured and treated with endoglycosidase H (EndoH) to demonstrate that differences in gel migration are based on glycosylation.

Cell cultures

Jurkat T cells (E6.1 clone; no. 88042803; European Collection of Authenticated Cell Cultures [ECACC]), HeLa cells (no. 93021013; ECACC), human primary dermal fibroblasts (C-013-5C; Thermo Fisher Scientific), and HEK293-FRT TRex cells stably expressing WT or mutant Sec61α were cultured in RPMI GlutaMAX (Jurkat) or DMEM GlutaMAX (other cells) from Thermo Fisher Scientific, supplemented with 10% heat-inactivated FCS (Invitrogen), 100 U/ml penicillin, and 100 µg/ml streptomycin. Human primary T cells were isolated from blood donors by Ficoll density gradient centrifugation and CD4$^+$ T cell purification by negative depletion (Miltenyi Biotec). Human primary macrophages were obtained from peripheral blood–derived monocytes, isolated by adhesion to tissue culture plasticware, and cultured with 10 ng/ml human GM-CSF (PeproTech) for 7–12 d. Mouse CD3$^+$ primary T cells were isolated from spleens and LNs by negative selection using the Pan T cell isolation kit (Miltenyi Biotec) and then placed in RPMI medium supplemented with 10% heat-inactivated FCS, 10 mM Hepes, 1 mM pyruvate, and 25 µM 2-mercaptoethanol. Bone marrow–derived macrophages were obtained by a 7-d differentiation of mouse progenitors in DMEM supplemented with 20% heat-inactivated horse serum (Gibco) and 30% L929-conditioned medium as a source of M-CSF.

SILAC labeling and LC–MS/MS analysis

For SILAC labeling, Jurkat T cells were cultured in DMEM medium without L-lysine, L-arginine, or L-glutamine (Silantes Gmbh) supplemented with 10% heat-inactivated FCS (Invitrogen), 2 mM GlutaMAX, and either natural L-arginine HCl and L-lysine HCl (light labeling; Sigma-Aldrich) or [$^{13}C_6$] [$^{15}N_2$] L-lysine HCl and [$^{13}C_6$]L-arginine HCl (heavy labeling; Silantes Gmbh). L-Lysine HCl was added at its normal concentration in DMEM (146 mg/L), but the concentration of L-arginine HCl was reduced to 30 mg/L (36% of the normal concentration in DMEM) to prevent metabolic conversion of arginine to proline. Cells were kept for at least six population doublings to ensure complete incorporation of the labeled lysine and arginine. Light (L) and heavy (H) SILAC-labeled Jurkat T cells were treated with 40 nM mycolactone or vehicle as control for 1 h and then activated with PMA/IO for 6 h. Two experiments were performed in reverse labeling conditions, yielding four samples. From each condition, 5×10^6 cells were harvested and washed twice with PBS, and cell pellets were frozen at −80°C until further use. Each pellet was resuspended in 500 µl lysis buffer (9 M urea in 20 mM Hepes, pH 8.0), sonicated (three bursts of 15 s at an amplitude of 20%) and centrifuged for 15 min at 16,000 *g* at 4°C to remove insoluble material. The protein concentration in the supernatants was measured using a Bradford assay (Bio-Rad Laboratories), and equal protein amounts of mycolactone-treated and untreated cell lysates were mixed to obtain two replicate samples with reversed SILAC for further analysis, each containing 5.6 mg total protein (sample 1: vehicle [H] + mycolactone [L]; sample 2: vehicle [L] + mycolactone [H]). Proteins in each sample were reduced with 5 mM dithiothreitol and incubation for 30 min at 30°C and then alkylated by addition of 100 mM chloroacetamide for 15 min at room temperature in the dark. Both samples were further diluted with 20 mM Hepes, pH 8.0, to a final urea concentration of 2 M, and proteins were digested with 50 µg trypsin (1/113, wt/wt; Promega) overnight at 37°C. Peptides were then purified on a Sep-Pak C18 cartridge (Waters), and 500 µg of peptides of each sample was redissolved in 10 mM ammonium acetate, pH 5.5, in water/acetonitrile (98/2, vol/vol) and injected on a capillary reversed phase high-performance liquid chromatography column (Zorbax 300SB-C18; 2.1 mm internal diameter and 150 mm length; Agilent Technologies) using a high-performance liquid chromatography system (1200 Series; Agilent Technologies). Peptides were separated by a linear gradient of acetonitrile (from 2% to 70% in 100 min in 10 mM ammonium acetate, pH 5.5), and peptides that eluted between 20 and 92 min were collected in 72 fractions of 1 min each. Fractions with 12-min difference in retention time were pooled to obtain total of 12 fractions for LC-MS/MS per sample. Peptides in each fraction were dried and redissolved in 12 µl of solvent A (0.1% formic acid in water/acetonitrile; 98:2, vol/vol), of which 5 µl was injected for LC-MS/MS analysis on an Ultimate 3000 RSLC-nano system (Thermo Fisher Scientific) in-line connected to a Q Exactive mass spectrometer with a Nanospray Flex Ion source (Thermo Fisher Scientific). Trapping was performed at 10 µl/min for 3 min in solvent A on a PepMap C18 column (0.3 mm inner diameter × 5 mm; Dionex), and after back flushing from the trapping column, the sample was loaded on a reverse-phase column (made in house; 75 µm inner diameter × 500 mm; 1.9 µm beads C18 Reprosil-Pur; Dr. Maisch GmbH). Peptides were eluted by an increase in solvent B (0.08% formic acid in water/acetonitrile; 2:8, vol/vol) in linear gradients from 5% to 20% in 47 min, then from 20% to

40% in 150 min, and finally from 40% to 55% in 30 min, all at a constant flow rate of 300 nl/min. The mass spectrometer was operated in data-dependent mode, automatically switching between MS and MS/MS acquisition for the 15 most abundant ion peaks per MS spectrum. Full-scan MS spectra (300–2,000 m/z) were acquired at a resolution of 70,000 after accumulation to a target value of 1,000,000 with a maximum fill time of 100 ms. The 15 most intense ions above a threshold value of 100,000 were isolated (window of 2.5 Th) for fragmentation by collision-induced dissociation at a normalized collision energy of 27% after filling the trap at a target value of 100,000 for a maximum of 160 ms with an underfill ratio of 0.1%. The S-lens radio frequency level was set at 55, and we excluded precursor ions with single, unassigned, and charge states above six from fragmentation selection.

Data processing and gene ontology terms enrichment analysis

Data analysis was performed with MaxQuant software (version 1.4.1.2; Cox and Mann, 2008) using the Andromeda search engine (Cox et al., 2011) with default search settings including a false discovery rate set at 1% on both the peptide and protein levels. Spectra were searched against the human proteins in the UniProt/SwissProt database (database release version of January 2014 containing 20,272 human protein sequences) with a mass tolerance for precursor and fragment ions of 4.5 and 20 ppm, respectively, during the main search. To enable the identification of SILAC-labeled peptides, the multiplicity was set to two with Lys8 and Arg6 settings in the heavy channel, allowing for a maximum of three labeled amino acids per peptide. Enzyme specificity was set as C-terminal to arginine and lysine, also allowing cleavage at proline bonds and a maximum of two missed cleavages. Variable modifications were set to oxidation of methionine residues and acetylation of protein N termini. Carbamidomethyl formation of cysteine residues was set as a fixed modification. In total, 6,503 proteins were identified in both samples, of which 4,636 proteins were quantified. For each quantified protein, the $\log_2$ values of the normalized mycolactone/untreated ratio in both samples were plotted against each other to generate the scatter plot depicted in Fig. 2 and Table S1. Proteins with $\log_2$ (mycolactone/untreated ratios) <-0.5 in both samples were considered as specific mycolactone targets that are down-regulated upon treatment. Proteomic data were deposited to the ProteomeXchange Consortium via the PRIDE partner repository under accession no. PXD002971. Gene Ontology and SwissProt Protein Information resource terms enrichment analyses were performed using Database for Annotation, Visualization and Integrated Discovery (DAVID) bioinformatics resources (Huang et al., 2009). Information on the topology of membrane proteins were retrieved from the UniProt/SwissProt database.

Flow cytometry

Staining of mouse cells was performed using anti-CD4 (no. 553051; BD), anti-CD62L (L-selectin; no. 553162; BD), anti-CD3 (no. 553064; BD), anti-CD19 (no. 550992; BD), anti-CD45.1 (no. 5061788; BD), anti-IFNGR1 (130-104-988; Miltenyi Biotec), anti–IFN-γ (no. 554412; BD), and anti–IL-2 (no. 554429; BD). For intracellular staining of cytokines, cells were treated with mycolactone for 1 h and then activated with PMA/IO. GolgiStop (BD) was added 2 h later. After 6 h, cells were fixed with 4% (wt/vol) paraformaldehyde during 20 min at room temperature and then stained with PE-conjugated anti–IFN-γ antibodies (BD) in 100 µl PBS + 0.1% BSA + 0.5% saponin for 30 min at room temperature. For intracellular staining of iNOS, macrophages were fixed with Lyse/Fix solution (no. 558049; BD) for 10 min at 37°C and then permeabilized with Perm Buffer III (no. 558050; BD) for 20 min at 4°C. Staining was performed with goat anti-NOS2 (sc-650-G; Santa Cruz Biotechnology, Inc.) followed by an anti–goat secondary antibody (no. 96938; Abcam). Staining of Jurkat was performed using anti-IFNGR1 (no. 558937; BD), IFNAR1 (no. 550331; BD), and IFNAR2 (no. 1080-08; SouthernBiotech). In brief, human cells were stained with IFNAR1 or IFNAR2, washed twice with PBS, incubated with biotin-conjugated rat anti–mouse IgG (no. 415-065-166; Jackson ImmunoResearch Laboratories, Inc.), washed, and then incubated with R-PE–conjugated streptavidin (PNIM0557; Beckman Coulter). All FACS acquisition was performed on a FACS Accuri C6 flow cytometer (BD), and data were analyzed using FlowJo software (Tree Star).

Retroviral transduction

Platinum-E ecotropic packaging cells (plat E; Biolabs) transfected with pRetroX–IRES-Zsgreen plasmids containing Sec61α sequences were used to produce retroviral particles. Immediately after isolation from mouse organs, $CD3^+$ T cells were activated with Dynabeads Mouse T-activator CD3/CD28 (Miltenyi Biotec) with 1 bead/cell in RPMI medium supplemented with 10% heat-inactivated FCS, 10 mM Hepes, 1 mM pyruvate, and 25 µM 2-mercaptoethanol (complete medium). 24 h later, cells were centrifuged at 1,200 rpm, and the supernatant (conditioned medium) was saved. Cells were resuspended at 4×10^6 cells/ml in viral supernatant freshly collected from plat E cells and supplemented with 10 µg/ml polybrene (EMD Millipore) and distributed at 1 ml/well in a 6-well plate and spin infected for 1 h at 2,800 rpm and 32°C. The cell supernatant was then removed and replaced with conditioned medium. After 48 h, spin infection was repeated, and T cells were resuspended in complete medium containing 50% conditioned medium. Bone marrow–derived macrophages were plated in 12- or 24-well plates ($2–4 \times 10^5$ cells/well) for 20 h. Fresh viral supernatant collected from plat E cells and 10 µg/ml polybrene were added before spin infection for 1 h at 2,800 rpm and 32°C. The cell supernatant was then removed and replaced with fresh DMEM supplemented with 20% horse serum.

Bioassays

The cytopathic effect of mycolactone on HEK293-FRT cells was assessed after 72 h of exposure with the Alamar

blue assay (Thermo Fisher Scientific). Its effect on secretory protein production was assessed with the Gaussia Glow-Juice Luciferase kit (PJK GmbH) as follows. HEK293-FRT cell lines expressing WT Sec61α or R66G-Sec61α were grown on a 6-well plate and then transfected with a plasmid encoding a signal sequence-containing Gaussia luciferase using Fugene 6 reagent (Promega). The expression of both the luciferase and Sec61α was induced 5 h later by addition of 1 µg/ml doxycycline. On the next day, 200,000 cells/well were plated in 96-well plates and treated 5 h later with increasing concentrations of mycolactone. Luciferase activity in culture media was measured 24 h later with an EnSpire Multimode plate reader (PerkinElmer). Assays of mycolactone inhibition on cytokine production and homing receptors by mouse and human immune cells have been described previously (Boulkroun et al., 2010; Guenin-Macé et al., 2011, 2015).

WASP/N-WASP and AT2R silencing

siRNAs were ON-Target plus SMARTpools (GE Healthcare) targeting human WASP (L-028294-00-0005), N-WASP (L-006444-00-0005), or AT2R (L-005429-00-005) or were nontargeting SMARTpool (D0018101005) as controls. 10^7 Jurkat T cells were electroporated twice at 48-h interval with 400 nM siRNA using the Gene Pulser Xcell system (Bio-Rad Laboratories) at 300 V and 500 µF. Silencing of WASP/N-WASP expression was optimal 24 h after the second electroporation. HeLa cells were transfected with 10 nM siRNA using Lipofectamine RNAiMAX (Invitrogen). AT2R silencing was optimal 48 h after transfection.

Mouse studies

8-wk-old female mice (C57BL/6NCrl; Charles River) or congenic CD45.1 mice (B6.SJL-*Ptprc*^{a} *Pepc*^{b}/BoyCrlPas; from our animal facilities) were housed under pathogen-free conditions with food and water ad libitum. The described experiments received the approval of the French Ministry of Higher Education and Research. They were performed in compliance with national guidelines and regulations.

Statistical analysis

Two group comparisons used the Mann-Whitney rank test. Statistical analyses were performed with StatView 5 software (SAS Institute, Inc.), and values of $P \leq 0.05$ were considered significant. Prism software (5.0d; GraphPad Software) was used for graphical representation.

Online supplemental material

Fig. S1 shows chemical structures of all mycolactone and cotransin analogues used in this study, mapping of mycolactone-resistance mutations in a three-dimensional model of Sec61α structure, and IVT controls. Fig. S2 shows cytotoxicity of mycolactone and CT8 in human fibroblasts and T lymphocytes and effects of WASP/N-WASP and AT2R silencing on mycolactone-mediated inhibition of secretory protein production. Table S1 shows mycolactone-susceptible proteins in Jurkat T cells, as detected by our SILAC analysis.

ACKNOWLEDGMENTS

We thank T. Chaze and M. Matondo-Bouzanda from the Pasteur Proteomics platform for assistance with proteome analyses. D. Tranter is acknowledged for valuable technical assistance. We are also grateful to P. Cossart and A. Echard for critical reading of the manuscript.

This work was supported by the Fondation pour la Recherche Médicale (FRM 2012 DEQ20120323704 to C. Demangel), the Association Raoul Follereau (C. Demangel), the Région Ile de France (dim130027 to C. Demangel), the Academy of Finland (289737 to V.O. Paavilainen), the Sigrid Juselius Foundation (V.O. Paavilainen), and Biocentrum Helsinki (V.O. Paavilainen). F. Impens received financial support from a Pasteur-Roux Fellowship.

The authors declare no competing financial interests.

Submitted: 6 May 2016
Revised: 26 August 2016
Accepted: 17 October 2016

REFERENCES

Besemer, J., H. Harant, S. Wang, B. Oberhauser, K. Marquardt, C.A. Foster, E.P. Schreiner, J.E. de Vries, C. Dascher-Nadel, and I.J. Lindley. 2005. Selective inhibition of cotranslational translocation of vascular cell adhesion molecule 1. *Nature.* 436:290–293. http://dx.doi.org/10.1038/nature03670

Bieri, R., M. Bolz, M.T. Ruf, and G. Pluschke. 2016. Interferon-γ is a crucial activator of early host immune defense against *Mycobacterium ulcerans* infection in mice. *PLoS Negl. Trop. Dis.* 10:e0004450. http://dx.doi.org/10.1371/journal.pntd.0004450

Boulkroun, S., L. Guenin-Macé, M.I. Thoulouze, M. Monot, A. Merckx, G. Langsley, G. Bismuth, V. Di Bartolo, and C. Demangel. 2010. Mycolactone suppresses T cell responsiveness by altering both early signaling and posttranslational events. *J. Immunol.* 184:1436–1444. http://dx.doi.org/10.4049/jimmunol.0902854

Chany, A.C., V. Casarotto, M. Schmitt, C. Tarnus, L. Guenin-Macé, C. Demangel, O. Mirguet, J. Eustache, and N. Blanchard. 2011. A diverted total synthesis of mycolactone analogues: an insight into Buruli ulcer toxins. *Chemistry.* 17:14413–14419. http://dx.doi.org/10.1002/chem.201102542

Cox, J., and M. Mann. 2008. MaxQuant enables high peptide identification rates, individualized p.p.b.-range mass accuracies and proteome-wide protein quantification. *Nat. Biotechnol.* 26:1367–1372. http://dx.doi.org/10.1038/nbt.1511

Cox, J., N. Neuhauser, A. Michalski, R.A. Scheltema, J.V. Olsen, and M. Mann. 2011. Andromeda: a peptide search engine integrated into the MaxQuant environment. *J. Proteome Res.* 10:1794–1805. http://dx.doi.org/10.1021/pr101065j

Demangel, C., T.P. Stinear, and S.T. Cole. 2009. Buruli ulcer: reductive evolution enhances pathogenicity of *Mycobacterium ulcerans*. *Nat. Rev. Microbiol.* 7:50–60. http://dx.doi.org/10.1038/nrmicro2077

Flynn, J.L., and J. Chan. 2001. Immunology of tuberculosis. *Annu. Rev. Immunol.* 19:93–129. http://dx.doi.org/10.1146/annurev.immunol.19.1.93

Garrison, J.L., E.J. Kunkel, R.S. Hegde, and J. Taunton. 2005. A substrate-specific inhibitor of protein translocation into the endoplasmic reticulum. *Nature.* 436:285–289. http://dx.doi.org/10.1038/nature03821

George, K.M., D. Chatterjee, G. Gunawardana, D. Welty, J. Hayman, R. Lee, and P.L. Small. 1999. Mycolactone: a polyketide toxin from *Mycobacterium ulcerans* required for virulence. *Science.* 283:854–857. http://dx.doi.org/10.1126/science.283.5403.854

Guarner, J., J. Bartlett, E.A. Whitney, P.L. Raghunathan, Y. Stienstra, K. Asamoa, S. Etuaful, E. Klutse, E. Quarshie, T.S. van der Werf, et al. 2003. Histopathologic features of *Mycobacterium ulcerans* infection. *Emerg. Infect. Dis.* 9:651–656. http://dx.doi.org/10.3201/eid0906.020485

Guenin-Macé, L., F. Carrette, F. Asperti-Boursin, A. Le Bon, L. Caleechurn, V. Di Bartolo, A. Fontanet, G. Bismuth, and C. Demangel. 2011. Mycolactone impairs T cell homing by suppressing microRNA control of L-selectin expression. *Proc. Natl. Acad. Sci. USA.* 108:12833–12838. http://dx.doi.org/10.1073/pnas.1016496108

Guenin-Macé, L., R. Veyron-Churlet, M.I. Thoulouze, G. Romet-Lemonne, H. Hong, P.F. Leadlay, A. Danckaert, M.T. Ruf, S. Mostowy, C. Zurzolo, et al. 2013. Mycolactone activation of Wiskott-Aldrich syndrome proteins underpins Buruli ulcer formation. *J. Clin. Invest.* 123:1501–1512. http://dx.doi.org/10.1172/JCI66576

Guenin-Macé, L., L. Baron, A.C. Chany, C. Tresse, S. Saint-Auret, F. Jönsson, F. Le Chevalier, P. Bruhns, G. Bismuth, S. Hidalgo-Lucas, et al. 2015. Shaping mycolactone for therapeutic use against inflammatory disorders. *Sci. Transl. Med.* 7:289ra85. http://dx.doi.org/10.1126/scitranslmed.aab0458

Hall, B., and R. Simmonds. 2014. Pleiotropic molecular effects of the *Mycobacterium ulcerans* virulence factor mycolactone underlying the cell death and immunosuppression seen in Buruli ulcer. *Biochem. Soc. Trans.* 42:177–183. http://dx.doi.org/10.1042/BST20130133

Hall, B.S., K. Hill, M. McKenna, J. Ogbechi, S. High, A.E. Willis, and R.E. Simmonds. 2014. The pathogenic mechanism of the *Mycobacterium ulcerans* virulence factor, mycolactone, depends on blockade of protein translocation into the ER. *PLoS Pathog.* 10:e1004061. http://dx.doi.org/10.1371/journal.ppat.1004061

Heaton, N.S., N. Moshkina, R. Fenouil, T.J. Gardner, S. Aguirre, P.S. Shah, N. Zhao, L. Manganaro, J.F. Hultquist, J. Noel, et al. 2016. Targeting viral proteostasis limits influenza virus, HIV, and Dengue virus infection. *Immunity.* 44:46–58. http://dx.doi.org/10.1016/j.immuni.2015.12.017

Hong, H., E. Coutanceau, M. Leclerc, L. Caleechurn, P.F. Leadlay, and C. Demangel. 2008. Mycolactone diffuses from *Mycobacterium ulcerans*–infected tissues and targets mononuclear cells in peripheral blood and lymphoid organs. *PLoS Negl. Trop. Dis.* 2:e325. http://dx.doi.org/10.1371/journal.pntd.0000325

Huang, W., B.T. Sherman, and R.A. Lempicki. 2009. Systematic and integrative analysis of large gene lists using DAVID bioinformatics resources. *Nat. Protoc.* 4:44–57. http://dx.doi.org/10.1038/nprot.2008.211

Junne, T., J. Wong, C. Studer, T. Aust, B.W. Bauer, M. Beibel, B. Bhullar, R. Bruccoleri, J. Eichenberger, D. Estoppey, et al. 2015. Decatransin, a new natural product inhibiting protein translocation at the Sec61/SecYEG translocon. *J. Cell Sci.* 128:1217–1229. http://dx.doi.org/10.1242/jcs.165746

Lundin, C., H. Kim, I. Nilsson, S.H. White, and G. von Heijne. 2008. Molecular code for protein insertion in the endoplasmic reticulum membrane is similar for N_{in}-C_{out} and N_{out}-C_{in} transmembrane helices. *Proc. Natl. Acad. Sci. USA.* 105:15702–15707. http://dx.doi.org/10.1073/pnas.0804842105

MacKinnon, A.L., J.L. Garrison, R.S. Hegde, and J. Taunton. 2007. Photoleucine incorporation reveals the target of a cyclodepsipeptide inhibitor of cotranslational translocation. *J. Am. Chem. Soc.* 129:14560–14561. http://dx.doi.org/10.1021/ja076250y

MacKinnon, A.L., V.O. Paavilainen, A. Sharma, R.S. Hegde, and J. Taunton. 2014. An allosteric Sec61 inhibitor traps nascent transmembrane helices at the lateral gate. *eLife.* 3:e01483. http://dx.doi.org/10.7554/eLife.01483

Maifeld, S.V., A.L. MacKinnon, J.L. Garrison, A. Sharma, E.J. Kunkel, R.S. Hegde, and J. Taunton. 2011. Secretory protein profiling reveals TNF-α inactivation by selective and promiscuous Sec61 modulators. *Chem. Biol.* 18:1082–1088. http://dx.doi.org/10.1016/j.chembiol.2011.06.015

Marion, E., O.R. Song, T. Christophe, J. Babonneau, D. Fenistein, J. Eyer, F. Letournel, D. Henrion, N. Clere, V. Paille, et al. 2014. Mycobacterial toxin induces analgesia in buruli ulcer by targeting the angiotensin pathways. *Cell.* 157:1565–1576. http://dx.doi.org/10.1016/j.cell.2014.04.040

McKenna, M., R.E. Simmonds, and S. High. 2016. Mechanistic insights into the inhibition of Sec61-dependent co- and post-translational translocation by mycolactone. *J. Cell Sci.* 129:1404–1415. http://dx.doi.org/10.1242/jcs.182352

Monné, M., G. Gafvelin, R. Nilsson, and G. von Heijne. 1999. N-tail translocation in a eukaryotic polytopic membrane protein: synergy between neighboring transmembrane segments. *Eur. J. Biochem.* 263:264–269. http://dx.doi.org/10.1046/j.1432-1327.1999.00498.x

Paatero, A.O., J. Kellosalo, B.M. Dunyak, J. Almaliti, J.E. Gestwicki, W.H. Gerwick, J. Taunton, and V.O. Paavilainen. 2016. Apratoxin kills cells by direct blockade of the Sec61 protein translocation channel. *Cell Chem Biol.* 23:561–566. http://dx.doi.org/10.1016/j.chembiol.2016.04.008

Park, E., and T.A. Rapoport. 2012. Mechanisms of Sec61/SecY-mediated protein translocation across membranes. *Annu. Rev. Biophys.* 41:21–40. http://dx.doi.org/10.1146/annurev-biophys-050511-102312

Phillips, R., F.S. Sarfo, L. Guenin-Macé, J. Decalf, M. Wansbrough-Jones, M.L. Albert, and C. Demangel. 2009. Immunosuppressive signature of cutaneous *Mycobacterium ulcerans* infection in the peripheral blood of patients with buruli ulcer disease. *J. Infect. Dis.* 200:1675–1684. http://dx.doi.org/10.1086/646615

Sarfo, F.S., F. Le Chevalier, N. Aka, R.O. Phillips, Y. Amoako, I.G. Boneca, P. Lenormand, M. Dosso, M. Wansbrough-Jones, R. Veyron-Churlet, et al. 2011. Mycolactone diffuses into the peripheral blood of Buruli ulcer patients - implications for diagnosis and disease monitoring. *PLoS Negl. Trop. Dis.* 5:e1237. http://dx.doi.org/10.1371/journal.pntd.0001237

Sharma, A., M. Mariappan, S. Appathurai, and R.S. Hegde. 2010. In vitro dissection of protein translocation into the mammalian endoplasmic reticulum. *Methods Mol. Biol.* 619:339–363. http://dx.doi.org/10.1007/978-1-60327-412-8_20

Spangenberg, T., and Y. Kishi. 2010. Highly sensitive, operationally simple, cost/time effective detection of the mycolactones from the human pathogen *Mycobacterium ulcerans*. *Chem. Commun. (Camb.).* 46:1410–1412. http://dx.doi.org/10.1039/b924896j

Walter, P., and G. Blobel. 1983. Preparation of microsomal membranes for cotranslational protein translocation. *Methods Enzymol.* 96:84–93. http://dx.doi.org/10.1016/S0076-6879(83)96010-X

The Journal of Experimental Medicine

SUPPLEMENTAL MATERIAL

Baron et al., https://doi.org/10.1084/jem.20160662

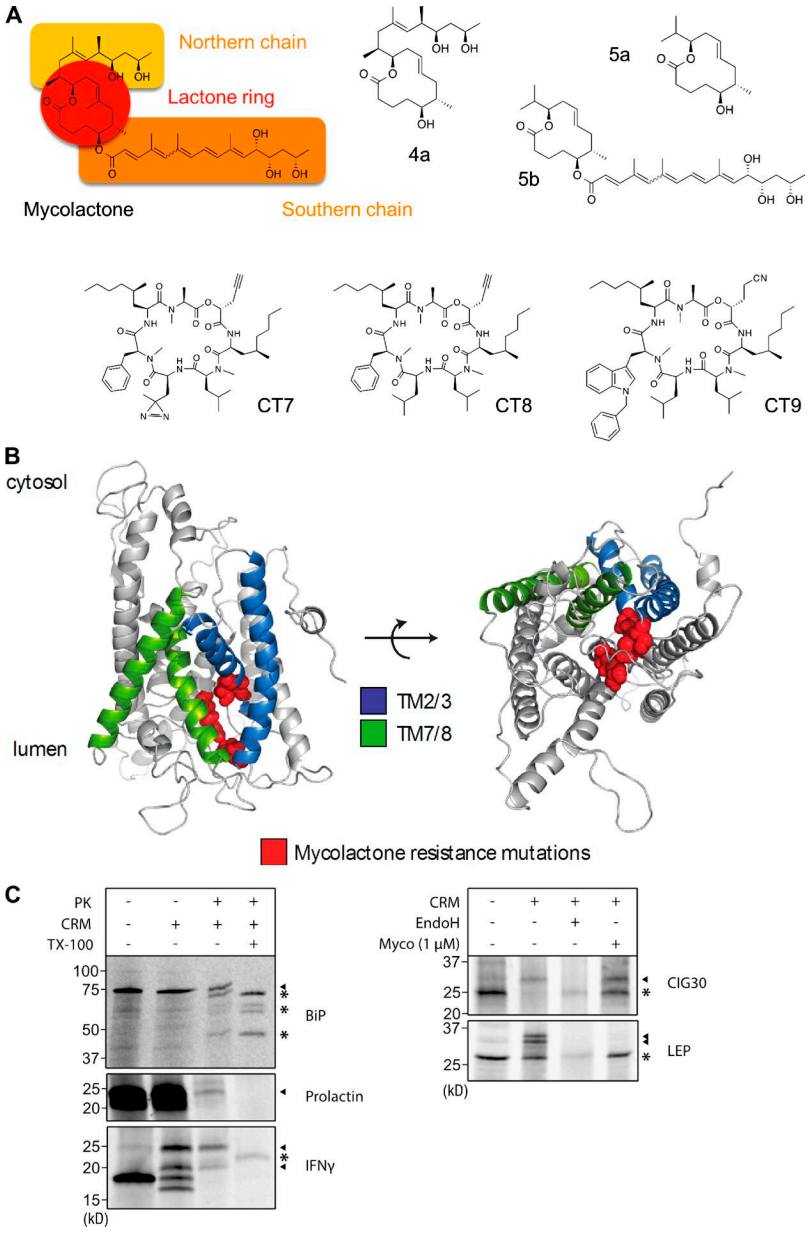

Figure S1. **Mycolactone and cotransin analogs used in this study, localization of mycolactone-resistance mutations in Sec61α and IVT controls.** (A) Chemical structures of natural mycolactone (A/B form; from *M. ulcerans* strain 1615), synthetic subunits of mycolactone, and cotransin variants used in this study. (B) Mutations associated with mycolactone resistance are located near the lumenal plug of Sec61α. A homology model of human Sec61α showing the location of mycolactone-resistance mutations (red) is shown. Lateral gate helices and hydrophobic transmembrane domains TM2/3 and TM7/8 are colored in blue and green, respectively. (C, left) ER translocation of BiP, prolactin, and IFN-γ were confirmed by proteinase K (PK) treatment in the presence and absence of detergent (TX-100). Correctly translocated protein species are indicated with arrowheads. Protease-resistant fragments are indicated with asterisks. ER translocation of these nonglycosylated proteins does not cause a change in band mobility, and resistance to proteinase K was used to indicate the fraction of ER-translocated polypeptide. Treating microsomes with proteinase K and detergent abolished the protected species, indicating correct translocation to the lumen of ER microsomes. (Right) Glycosylation of CIG30 and LEP was assessed by EndoH treatment. Membrane-integrated, glycosylated protein species are indicated with arrowheads and nonintegrated species are indicated with an asterisk. Difference in band mobility indicates that these proteins become glycosylated within the ER lumen upon correct membrane integration. EndoH treatment demonstrates that the altered mobility is caused by protein glycosylation. Myco, mycolactone.

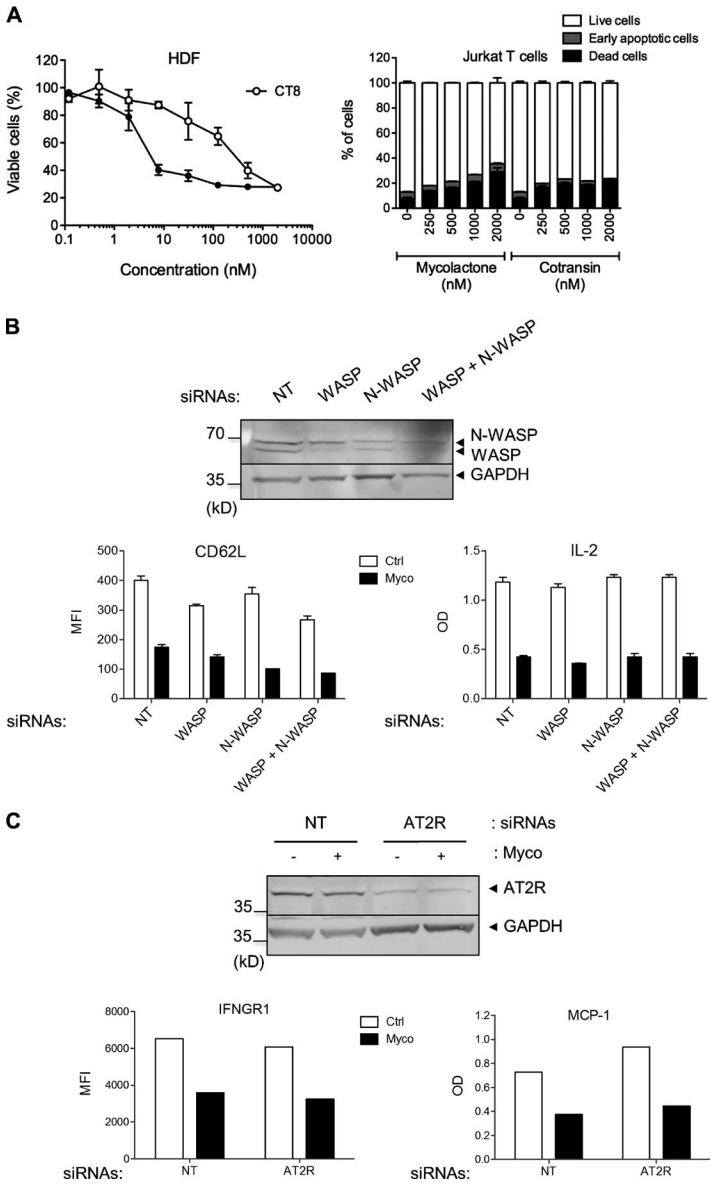

Figure S2. **Cytotoxicity of mycolactone and CT8 and contribution of WASP/N-WASP and AT2R to mycolactone effects on secretory protein production.** (A) Differential cytotoxicity of mycolactone and CT8. (Left) Cell viability, as assessed by methyl-thiazolyl-tetrazolium reduction of human primary dermal fibroblasts (HDF) incubated with mycolactone, CT8, or solvent for 72 h. (Right) Induction of apoptosis in Jurkat T cells incubated with mycolactone, CT8, or solvent for 48 h. Annexin V^+/propidium iodide $(PI)^-$ cells were identified as early apoptotic cells, annexin V^+/PI^+ cells as late apoptotic (dead) cells, and annexin V^-/PI^- cells as live cells. Data are mean percentages ± SD of duplicates relative to solvent and are representative of three independent experiments. (B) Mycolactone (Myco)-mediated inhibition of secreted and membrane protein production is WASP/N-WASP independent. Western blot analysis of total WASP, N-WASP, and GAPDH as loading control in Jurkat T cells transfected with siRNAs targeting WASP, N-WASP, or both proteins or nontargeting (NT) siRNAs as controls for 48 h is shown. (Left) Flow cytometric analysis of CD62L surface expression in siRNA-transfected Jurkat T cells exposed to 25 nM mycolactone or solvent (Ctrl) for 16 h. Mean fluorescent intensities (MFI) ± SD of duplicates are shown. (Right) IL-2 production by siRNA-transfected Jurkat T cells treated with 25 nM mycolactone or solvent for 1 h before activation with PMA/IO for 16 h. Mean OD ± SD of duplicates is shown. Data are representative of two independent experiments. (C) Mycolactone-mediated inhibition of secretory protein production is AT2R independent. Western blot analysis of total AT2R and GAPDH as loading control in HeLa cells transfected with siRNAs targeting AT2R or nontargeting siRNAs as controls for 60 h and then incubated with 50 nM mycolactone or solvent for 16 h is shown. (Left) Flow cytometric analysis of IFNGR1 surface expression in siRNA-transfected HeLa cells exposed to 50 nM mycolactone or solvent for 16 h. Mean fluorescent intensities are shown. (Right) MCP-1 production by siRNA-transfected HeLa cells treated with 50 nM mycolactone or solvent for 16 h. Mean OD ± SD of duplicates is shown. Data are representative of two independent experiments.

Table S1. **Proteomic profiling of mycolactone–exposed Jurkat T cells**

Accession[a]	Gene[a]	Full protein name[a]	Mean[b]	SD[b]	GO_CC[a]	SS or TMD	Protein type	IFN-γ induced[c]
Down-regulated								
Q96PP8	**GBP5**	**Guanylate-binding protein 5**	**−2.76**	**0.75**	**Cytoplasm, membrane**			**+**
Q07108	CD69	Early activation antigen CD69	−2.90	0.47	Plasma membrane	TMD	SP II	–
P13746	**HLA-A**	**HLA class I histocompatibility antigen, A-11 α chain**	**−1.91**	**0.84**	**ER, golgi, plasma membrane**	**SS**	**SP I**	**+**
P32456	**GBP2**	**Interferon-induced guanylate-binding protein 2**	**−2.29**	**0.06**	**Cytoplasm, nucleus, golgi**			**+**
P10321	**HLA-C**	**HLA class I histocompatibility antigen, Cw-7 α chain**	**−2.12**	**0.10**	**ER, golgi, plasma membrane**	**SS**	**SP I**	**+**
O95727	CRTAM	Cytotoxic and regulatory T cell molecule	−2.79	1.35	Plasma membrane	SS	SP I	–
Q92854	SEMA4D	Semaphorin-4D	−1.68	0.19	Plasma membrane	SS	SP I	–
P42224	**STAT1**	**HUMAN signal transducer and activator of transcription 1-α/β**	**−1.70**	**0.03**	**Cytoplasm, nucleus**			**+**
P01850	TRBC1	T cell receptor β-1 chain C region	−1.47	0.34	Plasma membrane	TMD	SP	–
P61769	**B2M**	**β-2-microglobulin**	**−1.55**	**0.14**	**Secreted**	**SS**		**+**
O43736	ITM2A	Integral membrane protein 2A	−1.56	0.05	Membrane	TMD	SP II	–
P09693	CD3G	T cell surface glycoprotein CD3 γ chain	−1.30	0.36	Plasma membrane	SS	SP I	–
P01737	TCRA	T cell receptor α chain V region PY14	−1.39	0.17	Plasma membrane	SS		–
P04234	CD3D	T cell surface glycoprotein CD3 δ chain	−1.29	0.02	Plasma membrane	SS	SP I	–
P32455	**GBP1**	**Interferon-induced guanylate-binding protein 1**	**−1.37**	**0.21**	**Cytoplasm, golgi, secreted**			**+**
P27701	CD82	CD82 antigen	−0.90	0.35	Plasma membrane	TMD	MP	–
O94901	SUN1	SUN domain–containing protein 1	−1.02	0.18	Nucleus membrane	TMD	SP II	–
Q8TDB6	**DTX3L**	**E3 ubiquitin–protein ligase DTX3L**	**−1.06**	**0.08**	**Cytoplasm, nucleus**			**+**
P04439	**HLA-A**	**HLA class I histocompatibility antigen, A-3 α chain**	**−1.12**	**0.11**	**Plasma membrane**	**SS**	**SP I**	**+**
Q8IXQ6	**PARP9**	**Poly [ADP-ribose] polymerase 9**	**−1.17**	**0.20**	**Cytoplasm, nucleus**			**+**
Q03518	TAP1	Antigen peptide transporter 1	−1.20	0.25	ER, membrane	TMD	MP	–
P42892	ECE1	Endothelin-converting enzyme 1	−1.09	0.16	Plasma membrane	TMD	SP II	–
O75787	ATP6AP2	Renin receptor	−0.99	0.03	Plasma membrane	SS	SP I	–
P13598	ICAM2	Intercellular adhesion molecule 2	−0.92	0.06	Plasma membrane	SS	SP I	–
P43489	TNFRSF4	Tumor necrosis factor receptor superfamily member 4	−1.35	0.65	Plasma membrane	SS	SP I	–
P30533	LRPAP1	α-2-macroglobulin receptor-associated protein	−0.89	0.00	ER, cytoplasm	SS		–
Q9BQE5	APOL2	Apolipoprotein L2	−0.88	0.00	Cytoplasm			–
Q15904	ATP6AP1	V-type proton ATPase subunit S1	−0.75	0.13	Membrane, vacuole	SS	SP	–
O14672	ADAM10	Disintegrin and metalloproteinase domain– containing protein 10	−0.87	0.04	Plasma membrane	SS	SP I	–
P11021	HSPA5 (BiP)	78-kD glucose-regulated protein	−0.76	0.07	ER lumen	SS		–
O75976	CPD	Carboxypeptidase D	−0.84	0.10	Membrane	SS	SP I	–
P48723	HSPA13	Heat shock 70-kD protein 13	−0.90	0.19	ER	SS		–
Q460N5	PARP14	Poly [ADP-ribose] polymerase 14	−0.67	0.08	Nucleus, cytoplasm			–
O95399	UTS2	Urotensin 2	−0.74	0.04	Secreted	SS		–
Q96JJ7	TMX3	Protein disulfide-isomerase TMX3	−0.74	0.04	ER	SS	SP	–
P07766	CD3E	T cell surface glycoprotein CD3 ε chain	−0.68	0.02	Plasma membrane	SS	SP I	–
P06127	CD5	T cell surface glycoprotein CD5	−0.71	0.05	Plasma membrane	SS	SP I	–
Q13217	DNAJC3	DnaJ homolog subfamily C member 3	−0.59	0.08	ER	SS		–
Q8NHV1	GIMAP7	GTPase IMAP family member 7	−0.58	0.04	Lipid droplet, cytoplasm			–
Q6PIU2	NCEH1	Neutral cholesterol ester hydrolase 1	−0.64	0.05	Membrane	TMD	SP II	–
Q9UBV2	SEL1L	Protein sel-1 homolog 1	−0.59	0.02	ER	SS	SP I	–
P20645	M6PR	Cation-dependent mannose-6–phosphate receptor	−0.60	0.00	Membrane	SS		–
Q4G148	GXYLT1	Glucoside xylosyltransferase 1	−0.62	0.07	Membrane	TMD	SP II	–
Q99805	TM9SF2	Transmembrane 9 superfamily member 2	−0.57	0.01	Endosome, membrane	SS	MP	–
Q99519	NEU1	Sialidase 1	−0.74	0.26	Membrane	SS	MP	–
Q8NFQ8	TOR1AIP2	Torsin-1A–interacting protein 2	−0.69	0.18	ER	TMD	SP	–
P09326	CD48	CD48 antigen	−0.81	0.36	Plasma membrane	SS		–
P19474	**TRIM21**	**E3 ubiquitin–protein ligase TRIM21**	**−0.62**	**0.10**	**Cytoplasm, nucleus**			**+**
P80303	NUCB2	Nucleobindin 2	−0.54	0.00	Golgi, membrane, ER, nucleus	SS	MP	–
Q13308	PTK7	Inactive tyrosine-protein kinase 7	−0.59	0.07	Membrane	SS	SP I	–
Q03519	TAP2	Antigen peptide transporter 2	−0.58	0.10	ER, membrane	TMD	MP	–
P05107	ITGB2	Integrin β-2	−0.51	0.00	Plasma membrane	SS	SP I	–
Up-regulated								
Q96CX6	LRRC58	Leucine-rich repeat–containing protein 58	1.28	1.04	Unknown			–

Table S1. **Proteomic profiling of mycolactone-exposed Jurkat T cells** *(Continued)*

Accession[a]	Gene[a]	Full protein name[a]	Mean[b]	SD[b]	GO_CC[a]	SS or TMD	Protein type	IFN-γ induced[c]
P08107	HSPA1A	Heat shock 70-kD protein 1A/1B	0.91	0.11	Cytoplasm			–

Proteins that were downregulated or upregulated by mycolactone treatment are shown. Those induced by IFN-γ are bold. GO_CC, gene ontology cellular component; MP, multipass; SP I, single-pass type I; SP II, single-pass type II; SS, signal sequence; TMS, transmembrane domain.

[a]According to the database UniProt.

[b]Mean and SD of $\log_2$ mycolactone/control ratios from two SILAC experiments.

[c]Induced by IFN-γ (+) or not (–), according to the database Interferome.

ARTICLE 2: SEC61 BLOCKADE BY MYCOLACTONE INHIBITS ANTIGEN CROSS-PRESENTATION INDEPENDENTLY OF ENDOSOME TO-CYTOSOL EXPORT

As presented in section III.4.2 of the introduction, the molecular mechanism responsible for antigen exit from endosomes and phagosomes during cross-presentation has been a matter of debate for over 20 years. The hypothesis that Sec61 mediates antigen export to the cytosol was based on the fact that Sec61 could be detected in endosomal compartments (Guermonprez *et al.*, 2003) and that knocking-down Sec61 (Imai *et al.*, 2005), or sequestering Sec61 in the ER (Zehner *et al.*, 2015), inhibited antigen export and cross-presentation. One general caveat of these approaches was that reduced Sec61 activity is also expected to prevent translocation of secreted proteins into the ER, thus impacting numerous cell functions indirectly. Knocking down Sec61 by means of siRNA, or expression of a Sec61-sequestring intrabody, are slow and/or incomplete ways to block Sec61 activity, making it likely for secondary, non-specific effects to occur.

We used mycolactone as a fast-acting Sec61 blocker to examine the direct role of Sec61 in antigen export. In collaboration with the team of Sebastian Amigorena (Institut Curie, Paris), we first examined the effect of mycolactone on antigen export, using a fluorescence energy transfer (FRET) probe that is specifically cleaved upon transfer of phagocytosed β-lactamase to the cytosol. To assess antigen cross-presentation, I engineered a R66G Sec61 mutant, mycolactone-resistant variant of the T cell hybridoma reporter line B3Z, which produces β-galactosidase under the Il-2 promoter upon presentation of OVA peptide by DCs. We found that short-term (5h) treatments with mycolactone had no impact on either antigen cross-presentation or antigen export, while longer treatments (24h), strongly impacted cross-presentation. The effect of prolonged mycolactone treatment was not specific of cross-presentation, as direct presentation of OVA peptide was also affected. Notably, the expression of MHC I and MHC II were both significantly reduced by 24h-long mycolactone treatment. I performed a proteomic analysis of MutuDCs (MutuDCs are described in (Fuertes Marraco *et al.*, 2012)) treated with 100nM mycolactone for 24h, which revealed extensive alterations amongst Sec61 clients. Among the most significantly affected proteins were several chains of MHC-I and MHC-II complexes, as well as several enzymes critical for the lysosomal processing of antigens in the vacuolar pathway, such as Cathepsin S. Together, these results implied that prolonged inhibition of Sec61 decreases the overall capacity of DCs to present antigens by

inhibiting critical mediators of antigen presentation, rather than blocking antigen export from endosomes.

We expanded the scope of the work by similarly testing whether Sec61 could mediate the export of misfolded proteins during Endoplasmic Reticulum-Associated-Degradation (ERAD). The contribution of Sec61 to the export of misfolded proteins during ERAD in mammalian cells has been questioned repeatedly (see section III.4.1 of the introduction), and alternative mechanisms of retro-translocation have been proposed, including other channels such as derlin-1 and Hrd1 or lipid-based models (Grotzke and Cresswell, 2015). To investigate whether and how mycolactone-mediated Sec61 blockade affects ERAD, we collaborated with the team of Peter Cresswell (Yale University School of Medicine, CT, USA). To assess the effect of mycolactone on retro-translocation through ERAD, they used a set of deglycosylation-dependent ERAD substrates that emit fluorescence signals only when exported from the ER to the cytosol. Again, mycolactone inhibited the import, but not the export of model ERAD substrates from the ER. My proteomic analysis showed that long-term mycolactone could impact ERAD indirectly through the downregulation of ERAD mediators.

Together, these results thus suggested that Sec61α is not directly involved in protein export to the cytosol for cross-presentation, nor ERAD.

Sec61 blockade by mycolactone inhibits antigen cross-presentation independently of endosome-to-cytosol export

Jeff E. Grotzke[a,1], Patrycja Kozik[b,1,2], Jean-David Morel[c,d,1], Francis Impens[e,f,g], Natalia Pietrosemoli[h], Peter Cresswell[a,i,3,4], Sebastian Amigorena[b,j,k,3,4], and Caroline Demangel[c,d,3,4]

[a]Department of Immunobiology, Yale University School of Medicine, New Haven, CT 06520; [b]Centre de Recherche, Institut Curie, 75005 Paris, France; [c]Immunobiology of Infection Unit, Institut Pasteur, 75015 Paris, France; [d]INSERM, U1221, 75005 Paris, France; [e]Vlaams Instituut voor Biotechnologie (VIB)-UGent Center for Medical Biotechnology, 9000 Ghent, Belgium; [f]VIB Proteomics Core, 9000 Ghent, Belgium; [g]Department of Biochemistry, Ghent University, 9000 Ghent, Belgium; [h]Center of Bioinformatics, Biostatistics, and Integrative Biology, Institut Pasteur, Unité de Service et de Recherche 3756 Institut Pasteur CNRS, 75015 Paris, France; [i]Department of Cell Biology, Yale University School of Medicine, New Haven, CT 06520; [j]INSERM, U932, 75005 Paris, France; and [k]CBT507 Institut Gustave Roussy-Curie, INSERM Center of Clinical Investigation, 75005 Paris, France

Contributed by Peter Cresswell, June 8, 2017 (sent for review March 29, 2017; reviewed by Jose A. Villadangos and Emmanuel J. Wiertz)

Although antigen cross-presentation in dendritic cells (DCs) is critical to the initiation of most cytotoxic immune responses, the intracellular mechanisms and traffic pathways involved are still unclear. One of the most critical steps in this process, the export of internalized antigen to the cytosol, has been suggested to be mediated by Sec61. Sec61 is the channel that translocates signal peptide-bearing nascent polypeptides into the endoplasmic reticulum (ER), and it was also proposed to mediate protein retrotranslocation during ER-associated degradation (a process called ERAD). Here, we used a newly identified Sec61 blocker, mycolactone, to analyze Sec61's contribution to antigen cross-presentation, ERAD, and transport of internalized antigens into the cytosol. As shown previously in other cell types, mycolactone prevented protein import into the ER of DCs. Mycolactone-mediated Sec61 blockade also potently suppressed both antigen cross-presentation and direct presentation of synthetic peptides to $CD8^+$ T cells. In contrast, it did not affect protein export from the ER lumen or from endosomes into the cytosol, suggesting that the inhibition of cross-presentation was not related to either of these trafficking pathways. Proteomic profiling of mycolactone-exposed DCs showed that expression of mediators of antigen presentation, including MHC class I and β2 microglobulin, were highly susceptible to mycolactone treatment, indicating that Sec61 blockade affects antigen cross-presentation indirectly. Together, our data suggest that the defective translocation and subsequent degradation of Sec61 substrates is the cause of altered antigen cross-presentation in Sec61-blocked DCs.

Sec61 | cross-presentation | ERAD | mycolactone

Dendritic cells (DCs) play a key role in initiation of cytotoxic immune responses against pathogens and tumors (1). To prime relevant T cells, DCs capture antigens released by the surrounding cells and present them in the context of MHC class I (MHC-I) molecules (2). This process is referred to as cross-presentation and, in presence of appropriate costimulatory signals, leads to the activation and proliferation of antigen-specific T cells. Over recent years, extensive research efforts have gone into understanding the molecular mechanism of cross-presentation. The picture that emerged is that efficient cross-presentation requires antigens to be protected from excessive lysosomal degradation and, instead, to be exported into the cytosol for processing by the proteasome (3). Proteasomes generate short peptides that can then be presented on MHC-I. The molecular machinery that controls the step of antigen export from endosomes into the cytosol remains elusive, and the underlying mechanism is controversial. Interestingly, several groups have described that components of endoplasmic reticulum (ER)-associated degradation (ERAD) machinery are recruited to antigen-containing compartments (reviewed in ref. 4). These observations have led to the hypothesis that antigen export might "hijack" a channel used during retrotranslocation of misfolded proteins from the ER during ERAD.

The ERAD process uses a multiprotein complex consisting of lectins, chaperones, disulfide isomerases, E3 ubiquitin ligases, and other accessory factors (5). Once a terminally misfolded protein is recognized by the ERAD machinery, it is targeted to the ERAD membrane complex and ubiquitinated by an E3 ligase, such as Hrd1, during translocation into the cytosol, with the aid of the cytosolic AAA-ATPase p97, and subsequently degraded by the proteasome. Although the function(s) of many ERAD factors are at least partially understood, the precise identity of the pore that mediates cytosolic translocation remains unclear. In addition to its role in co- or posttranslational translocation of secretory proteins, Sec61 has long been proposed to be a potential translocon for dislocation of ERAD substrates from the ER. Experimental evidence supporting this model

Significance

Aside from its undisputed role in the import of newly synthesized proteins into the endoplasmic reticulum (ER), the Sec61 translocon was proposed to ensure the reverse transport of misfolded proteins to the cytosol. Based on this model, Sec61 was also proposed to be the channel exporting internalized antigens from endosomes to the cytosol, for degradation and cross-presentation. Establishing Sec61's contribution to these connected trafficking pathways has nevertheless proven difficult, due to a technical incapacity to blunt its activity acutely. Here, we took advantage of a recently identified Sec61 blocker to determine whether or not Sec61 can mediate retrograde protein transport. Both ER-to-cytosol and endosome-to-cytosol protein export were intact in mycolactone-treated cells, which argues against Sec61 operating as a retrotranslocon.

Author contributions: J.E.G., P.K., J.-D.M., P.C., S.A., and C.D. designed research; J.E.G., P.K., J.-D.M., F.I., and N.P. performed research; P.C. and C.D. contributed new reagents/analytic tools; S.A. analyzed data; J.E.G., P.K., S.A., and C.D. wrote the paper; and P.C. supervised the work performed at Yale University.

Reviewers: J.A.V., The University of Melbourne; and E.J.W., University Medical Center Utrecht.

The authors declare no conflict of interest.

[1]J.E.G., P.K., and J.-D.M. contributed equally to this work.

[2]Present address: Medical Research Council Laboratory of Molecular Biology, CB2 0QH Cambridge, United Kingdom.

[3]P.C., S.A., and C.D. contributed equally to this work.

[4]To whom correspondence may be addressed. Email: peter.cresswell@yale.edu, sebastian.amigorena@curie.fr, or demangel@pasteur.fr.

This article contains supporting information online at www.pnas.org/lookup/suppl/doi:10.1073/pnas.1705242114/-/DCSupplemental.

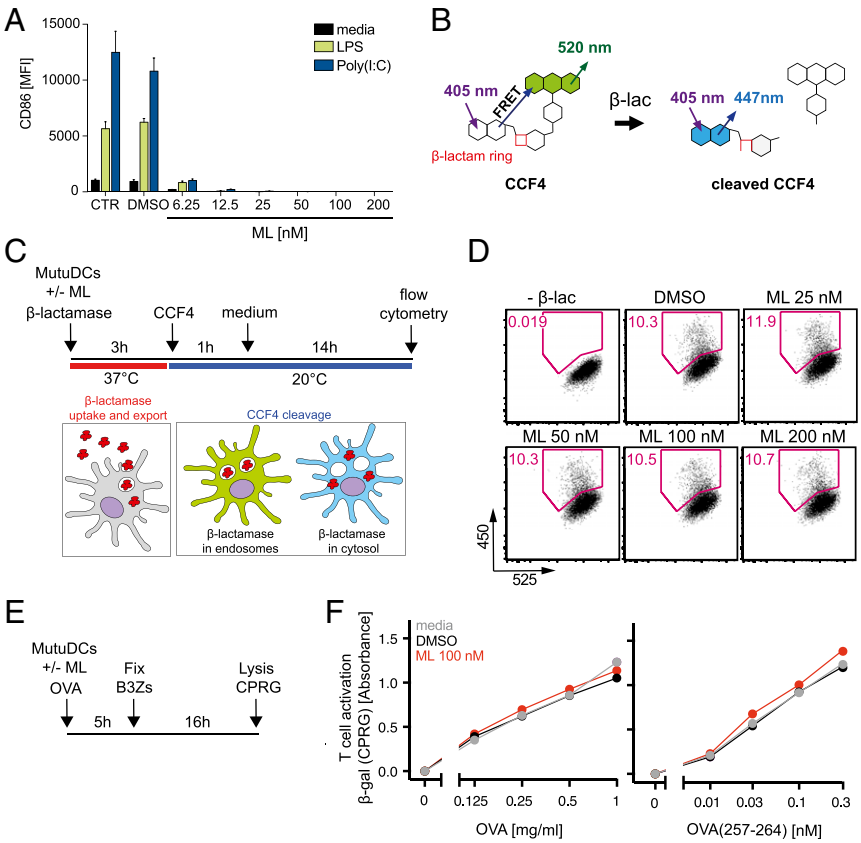

Fig. 1. Acute inhibition of Sec61 with mycolactone (ML) does not inhibit antigen export or cross-presentation. (*A*) ML efficiently prevents the TLR4- or TLR3-induced production of Sec61 substrates in MutuDCs. Cells were activated by 0.5 μg/mL LPS or 5 μg/mL high-molecular-weight poly(I:C) and incubated in the presence of 100 nM ML for 16 h. CTR, control; MFI, mean fluorescence intensity. Up-regulation of CD86 surface expression was monitored by flow cytometry. (*B*) Schematic representation of changes in CCF4 fluorescence upon cleavage of the the β-lactam (β-lac) ring. (*C*) Schematic representation of the antigen export assay. MutuDCs are fed with the β-lactamase and loaded with CCF4 in *B*, and the efficiency of CCF4 cleavage is analyzed by flow cytometry. (*D*) MutuDCs were incubated with β-lac in the presence or absence of increasing concentrations of ML for 3 h and analyzed as described in *C*. (*E*) Schematic representation of the cross-presentation assay. (*F*) MutuDCs were incubated for 5 h with soluble OVA protein or $OVA_{257–264}$ peptide in the presence or absence of increasing concentrations of ML. DCs were then fixed and coincubated with B3Z hybridomas for 16 h. Up-regulation of β-galactosidase (β-gal) expression in B3Zs (driven by the IL-2 promoter) was quantified using a colorimetric substrate, CPRG. For *D* and *F*, representative data from three independent experiments are shown.

was predominantly from yeast Sec61 mutants that are defective in both import of secretory proteins and export of ERAD substrates (6). Furthermore, a Sec61 mutant without defects in protein import but with reduced ability to bind to the 19S proteasome regulatory particle (RP) showed decreased ER export of a 19S proteasome RP-dependent substrate when proteasomes were limiting, providing a functional link between Sec61 and retrotranslocation (7). However, overexpression of the yeast E3 ubiquitin ligase Hrd1p can reduce or abolish the requirement of accessory ERAD factors, and Hrd1p is sufficient for substrate translocation in reconstituted proteoliposomes (8), arguing that Hrd1p is the protein channel for ERAD substrates. Whether these findings using yeast Sec61p and Hrd1p extrapolate to their mammalian counterparts remains to be demonstrated. Based on this model, several groups proposed that Sec61 might also play a role in antigen export from endosomes to the cytosol in DCs (9, 10). In support of this hypothesis, siRNA-mediated depletion of Sec61, or Sec61 exclusion from antigen-containing endosomes with an intrabody, inhibited antigen export into the cytosol, as well as cross-presentation (11, 12). However, these studies did not take into account the contribution of Sec61 to translocation of newly synthesized proteins into the ER, as well as the potential "knock-on" effects.

To investigate direct vs. indirect effects of Sec61 blockade, we used a pharmacological approach. Mycolactone is a polyketide-derived macrolide produced by the human pathogen *Mycobacterium ulcerans*, which was recently identified as a potent Sec61 inhibitor (13–16). Mycolactone diffuses passively across the plasma membrane to target the pore-forming subunit of the translocon (Sec61α) (13), leading to the proteasomal degradation of newly synthesized Sec61 clients blocked in translocation (17). In contrast to previously described Sec61 inhibitors, such as cotransin (18), mycolactone prevents the biogenesis of secretory and transmembrane proteins with minor selectivity toward Sec61 substrates, as well as uniformly high efficacy (13, 16). Single-amino acid mutagenesis localized its binding site on the luminal side of the translocon, near the plug domain that occludes Sec61 in its inactive state (13). Mycolactone allows acute blockade of Sec61, and we used it in the present study to examine the direct contribution of this channel to antigen cross-presentation, endosome-to-cytosol export, and ER-to-cytosol export.

Results

Acute Inhibition of Sec61 Does Not Block Antigen Export and Cross-Presentation. As a DC model, we used a $CD8^+$ cell line called MutuDC that was shown to display the phenotypic and functional features of splenic $CD8^+$ conventional DCs, including cross-presentation (19). We reported previously that mycolactone blocks the activation-induced maturation of peripheral

blood- and bone marrow-derived DCs, as evidenced by the up-regulation of costimulatory molecules (20). In MutuDCs activated with the TLR4 agonist LPS, or with the TLR3 agonist polyinosinic-polycytidylic acid [poly(I:C)], up-regulation of the cell surface expression of CD86 after 24 h was abrogated by coincubation with 6 nM mycolactone, showing that Sec61 blockade is effective in this DC model (Fig. 1*A*). Of note, no cytotoxicity could be detected in MutuDCs treated with up to 400 nM mycolactone for 24 h (Fig. S1*A*). To evaluate the effect of Sec61 blockade on antigen export from endosomes into the cytosol, we used a previously described β-lactamase–based assay that relies on a cytosolic dye (CCF4) consisting of two fluorophores linked by a β-lactam ring (21) (Fig. 1*B*). Upon excitation with a 405-nm laser, CCF4 emits green fluorescence due to the FRET between the two subunits. When β-lactamase is exported into the cytosol, it cleaves the β-lactam ring in CCF4, resulting in loss of FRET and change in fluorescence emission from green to blue (Fig. 1*B*). Here, we fed MutuDCs with β-lactamase in the presence or absence of increasing concentrations of mycolactone for 3 h, and subsequently loaded the cells with CCF4 (Fig. 1*C*). To increase the sensitivity of the assay, following CCF4 loading, we incubated the cells overnight at room temperature. The green-to-blue fluorescence transition was monitored by flow cytometry. No detectable difference in fluorescence could be demonstrated between mycolactone-treated and vehicle control cells, indicating that Sec61 blockade by mycolactone does not affect antigen export (Fig. 1*D* and Fig. S1*B*).

The DCs were then fixed and incubated for 16 h with the T-cell hybridoma B3Z, which expresses T-cell receptor specific for a complex of the MHC-I Kb allele with ovalbumin 257–264 ($OVA_{257–264}$) peptide (Fig. 1*E*). B3Z activation leads to accumulation of β-galactosidase reporter, which is expressed under transcriptional control of the NFAT elements from the IL-2 promoter. β-Galactosidase levels were quantified using a colorimetric substrate, chlorophenol red-β-D-galactopyranoside (CPRG). To ensure that B3Z activation itself was not affected by mycolactone, we used a B3Z line expressing the R66G mycolactone-resistant mutant of Sec61 (Sec61-R66G), generated as described (13). We observed no difference in the efficiency of OVA cross-presentation or in the capacity of DCs to activate T cells when incubated directly with the $OVA_{257–264}$ peptide (Fig. 1*F*). Together, these data thus suggest that acute inhibition of Sec61 does not block antigen export or cross-presentation.

Deglycosylation-Dependent ERAD Substrates Are Differentially Affected by Mycolactone. We next investigated whether mycolactone-mediated Sec61 inhibition affected the export of proteins from the ER into the cytosol during ERAD. To achieve this goal, we used

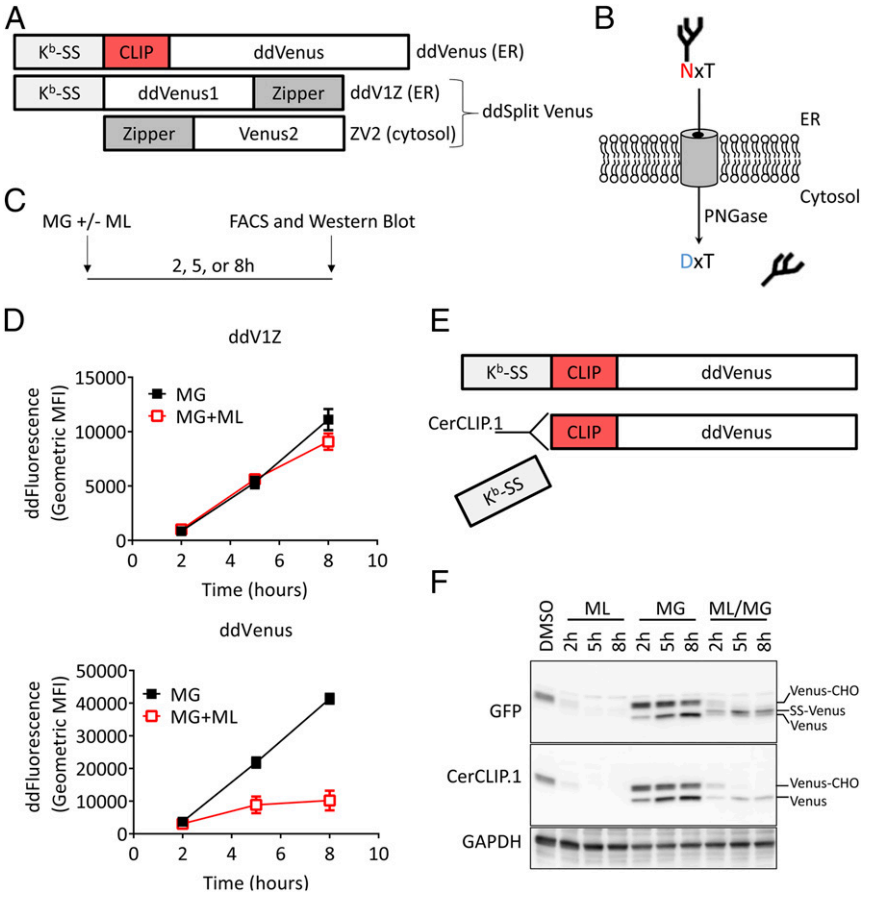

Fig. 2. ERAD dd substrates are differentially affected by ML. (*A*) Constructs used in Fig. 2. The dd substrates are targeted to the ER through fusion to the signal sequence of H2-Kb (Kb-SS). Dimerization of split Venus halves is driven through fusion of both halves to leucine zippers. (*B*) Depiction of dd substrate mechanism. Removal of the N-linked glycan by cytosolic PNGase leads to asparagine deamidation and conversion to an aspartic acid, restoring Venus fluorescence. (*C*) Experimental design. MG, MG-132. (*D*) HEK293T cells stably expressing dd substrates were treated with 4 μM MG ± 100 nM ML for the times indicated. At each time point, cells were harvested and fluorescence was analyzed by flow cytometry. The level of dd fluorescence was quantitated by flow cytometry, as described in *Materials and Methods*. (*E*) Recognition of the CLIP epitope by the monoclonal antibody CerCLIP.1 requires a free N terminus. (*F*) HEK293T cells expressing ddVenus were treated as in *D*, and cell lysates were analyzed by Western blot using antibodies to GFP, which reacts with Venus, and the CLIP epitope. Different forms of Venus are indicated.

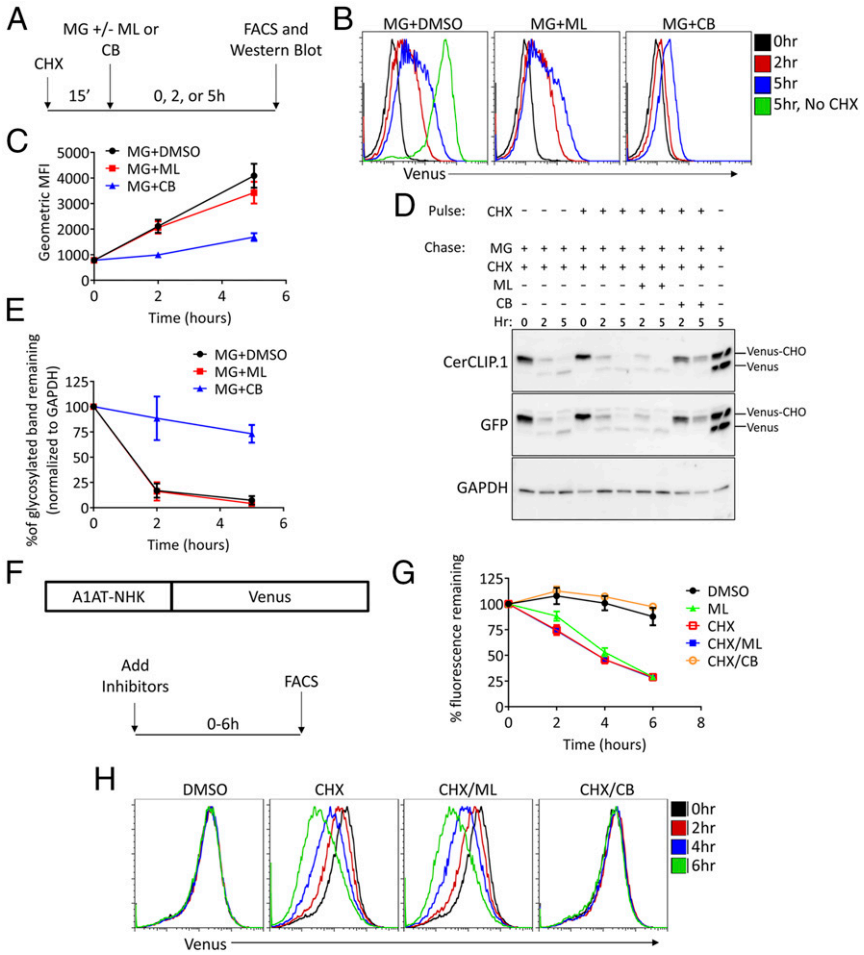

Fig. 3. ML-mediated Sec61 blockade does not inhibit retrotranslocation of ERAD substrates. (*A*) Experimental design for *B*–*E*. (*B*–*E*) HEK293T cells stably expressing ddVenus were pulsed for 15 min with 20 μg/mL cycloheximide (CHX), followed by addition of 4 μM MG ± 100 nM ML or 1 μM CB-5083 (CB). At each time point, cells were harvested and analyzed by flow cytometry (*B* and *C*) or cell lysates were analyzed by Western blot (*D* and *E*). Time 0 (pulse CHX, chase MG+CHX, fourth lane from the left in *D*) was the same for all CHX-pulsed treatments in *D* and *E*. Results in *C* and *E* are the mean ± SEM of at least three independent experiments. (*F*) Construct and experimental design used in *G* and *H*. Wild-type Venus was fused to the N terminus of A1AT-NHK. (*G* and *H*) HEK293T cells stably expressing A1AT-NHK-Venus were treated with 20 μg/mL CHX ± 100 nM ML or 1 μM CB for the indicated times. At each time point, cells were harvested and analyzed by flow cytometry. Results in *H* are the mean ± SEM of at least three independent experiments.

the previously described deglycosylation-dependent (dd) ERAD substrate constructs ddVenus and ddSplit Venus (22) as fluorescent reporters of ERAD activity (Fig. 2*A*). In ddSplit Venus, half of Venus (ddV1Z) is targeted to the ER, whereas the other half (ZV2) is expressed in the cytosol. Both ddVenus and ddSplit Venus were engineered with an N-linked glycosylation site in which an aspartic acid in the wild-type sequence was mutated to an asparagine, resulting in reduced fluorescence. After glycosylation in the ER, substrates that are retrotranslocated to the cytosol are deglycosylated by peptide N′-glycanase (PNGase), resulting in deamidation of the asparagine (red in Fig. 2*B*) and conversion back to the wild-type aspartic acid (blue in Fig. 2*B*), yielding enhanced fluorescence. Cells expressing dd substrates are nonfluorescent at steady state because the substrates are degraded by proteasomes, but cellular fluorescence (ERAD) can be detected after the addition of proteasome inhibitors. This cellular fluorescence requires the ERAD factors Hrd1 and SEL1L, as well as PNGase activity. To determine the effect of mycolactone-mediated Sec61 blockade on ERAD, we used cells stably expressing ddVenus or ddSplit Venus (Fig. 2*A*). Cells were incubated with the proteasome inhibitor MG-132 in the presence or absence of mycolactone for 2–8 h (Fig. 2*C*). When the fluorescence of ddV1Z and ddVenus was quantitated in treated cells, mycolactone, surprisingly, showed different effects on the two substrates. Although fluorescence was largely inhibited for ddVenus, only a slight nonstatistically significant effect was seen at 8 h posttreatment for ddSplit Venus (Fig. 2*D*). With both substrates, fluorescence was decreased by coincubation of the cells with the PNGase inhibitor zVAD-fmk (Fig. S2*A*), showing that it is deglycosylation-dependent. These results suggested that Sec61 blockade differentially affects ERAD of the two substrates.

We tested if mycolactone had different effects on the stability and glycosylation state of ddVenus and ddV1Z by Western blot analysis of cell lysates, as glycosylated (-CHO) and non-glycosylated or deglycosylated species have different molecular weights. Using an anti-GFP antibody cross-reacting with Venus, we found that mycolactone treatment caused a time-dependent depletion of the glycosylated form of ddV1Z (V1Z-CHO; Fig. S2*B*), indicating that ddV1Z translocation into the ER was blocked. Consistent with this finding, mycolactone treatment also caused the appearance of a species that migrated slightly slower than the nonglycosylated or deglycosylated species [labeled signal sequence (SS)-V1Z, compared with V1Z]. This species is likely cytosolically translated ddV1Z with an uncleaved signal sequence (discussed below), and it is stabilized even further in the presence of MG-132. To confirm further that mycolactone was able to block ddV1Z translocation into the ER, we

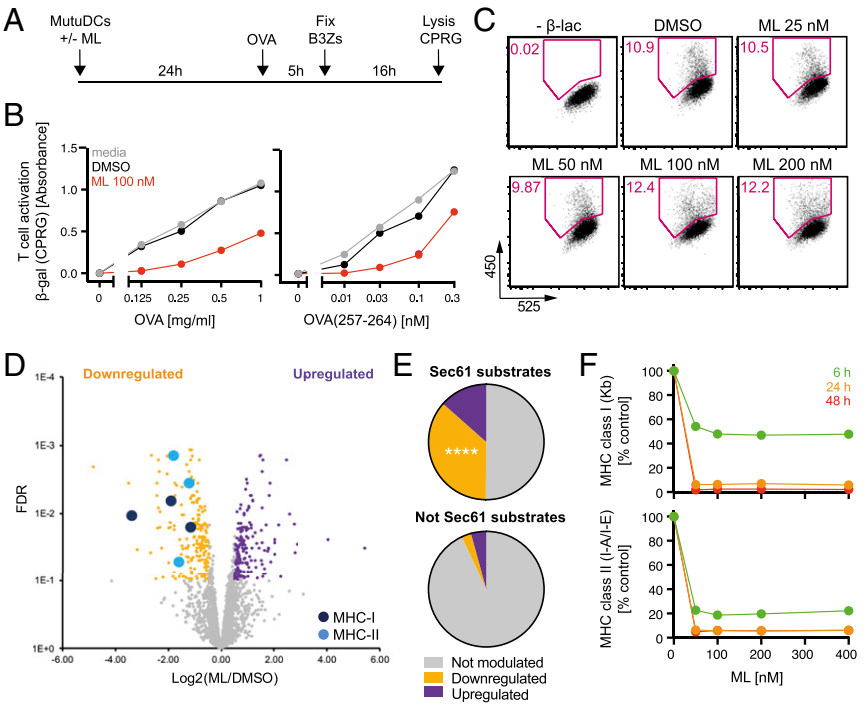

Fig. 4. Prolonged inhibition of Sec61 with ML diminishes T-cell activation capacity of MutuDCs. (*A*) Schematic representation of the assay used in *B*. (*B*) MutuDCs were treated for 24 h with 100 nM ML, reseeded, and incubated with OVA or $OVA_{257–264}$ peptide for 5 h. The efficiency of T-cell activation was quantified as in Fig. 1*F*. (*C*) MutuDCs were treated with ML for 24 h, and the export assay was performed as described in Fig. 1 *B* and *C*. (*D*) Volcano plot showing statistical significance vs. fold change differences for each protein identified in MutuDCs treated with 100 nM ML or vehicle control for 24 h. (*E*) Pie charts depicting the proportion of down-regulated, up-regulated, or not modulated proteins among Sec61 substrates and all other identified proteins (not Sec61 substrates). ****$P < 0.0001$, Fisher exact test comparing the proportion of down-regulation in Sec61 substrates and all other identified proteins. (*F*) FACS analysis of MHC-I and MHC-II surface expression by MutuDCs treated with increasing doses of ML for 6, 24, and 48 h. For *B*, *C*, and *F*, representative data are from three independent experiments.

treated cells with mycolactone or DMSO for 8 h, and glycosylated proteins were depleted from cell lysates using Sepharose beads conjugated to Con A. Although there appeared to be some level of nonspecific binding to Con A beads, Fig. S2*C* clearly shows that mycolactone decreased the glycosylated form of ddV1Z (V1Z-CHO, lanes 1 and 4) and that the mycolactone-induced species was nonglycosylated (SS-V1Z, lane 5). Similarly, mycolactone potently depleted glycosylated HLA-I from treated cells (Fig. S2*C*). Both of these findings are consistent with a lack of ER import. Overall, these data demonstrate that mycolactone blocks the import of ddV1Z into the ER with little to no effect on export and suggest that Sec61 does not play a role in ERAD of this substrate.

In contrast to ddV1Z, ddVenus was rapidly depleted by mycolactone treatment, with little to no protein detectable after 5 h (GFP panel in Fig. 2*F*). To discriminate between signal sequence-cleaved and -uncleaved species, we assessed cell lysates for the presence of ddV1Z proteins containing the CLIP (class II-associated invariant chain peptide) epitope, which is inserted between the signal sequence and ddVenus (Fig. 2*A*). We used the antibody CerCLIP.1, which requires a free amino terminus to bind CLIP, and therefore only detects signal sequence-cleaved ddVenus (Fig. 2*E*). In ddVenus cells cotreated with mycolactone and MG-132, there was an appearance of the same slower migrating species as seen in ddV1Z (SS-Venus; Fig. 2*F*). This band was detected with an antibody to GFP, but not with CerCLIP.1, demonstrating that it represents protein translated in the cytosol with an intact signal sequence. These data suggest that differences in substrate half-life may explain the contrasting effect of mycolactone on ddV1Z vs. ddVenus, but the possibility remained that Sec61 was required for ddVenus export.

Mycolactone-Mediated Sec61 Blockade Does Not Inhibit Retrotranslocation of ERAD Substrates. To distinguish between the role of Sec61 in import and export, we assessed the ability of the preformed ER pool of ddVenus to be retrotranslocated to the cytosol. Cells were pulsed with cycloheximide for 15 min to prevent protein synthesis, and then chased with MG-132 ± mycolactone or CB-5083, a potent p97 inhibitor (23), in the continued presence of cycloheximide (Fig. 3*A*). As shown in Fig. 3 *B* and *D*, cycloheximide markedly reduced both the level of cellular fluorescence and the levels of glycosylated and deglycosylated ddVenus, arguing that the majority of ddVenus fluorescence arises from nascent protein. No significant differences in fluorescence were seen between the cells cotreated with MG-132 and DMSO or mycolactone (Fig. 3 *B* and *C*). Similarly, mycolactone did not stabilize the glycosylated ddVenus band or inhibit the transition of the glycosylated band to the deglycosylated form (Fig. 3 *D* and *E*). CB-5083–mediated inhibition of p97, a protein required for extraction of ERAD substrates from the ER, led to decreased cellular fluorescence, stabilization of glycosylated ddVenus, and lack of deglycosylated ddVenus (Fig. 3 *D* and *E*). Taken together, these results demonstrate that ddVenus fluorescence inhibition by mycolactone is due to decreased levels of nascent substrate and not due to blockade of the ERAD translocon.

Finally, we assessed the ability of mycolactone to block ERAD of an additional substrate, the Null Hong Kong variant of α1-antitrypsin (24) fused to Venus (A1AT-NHK-Venus) (Fig. 3*F*). Unlike the dd substrates, this substrate is fluorescent whether present in the ER or cytosol. We reasoned that if mycolactone blockade of Sec61 prevents export to the cytosol, then it should stabilize the ER pool of A1AT-NHK-Venus when protein synthesis is inhibited. As shown in Fig. 3 *G* and *H*, cycloheximide

Table 1. Effect of mycolactone treatment on known mediators of cross-presentation

FDR	Variation*	Protein name†	Gene name†	Sec61 substrate
3.20E-03	1.89	Protein transport protein Sec61 subunit α1	Sec61a1	Yes
2.58E-02	1.78	Vesicle-associated membrane protein 8	Vamp8	No
1.45E-02	1.65	Heat shock protein (HSP) 90-α	Hsp90aa1	No
6.41E-02	1.52	Ras-related protein Rab-35	Rab35	No
5.43E-02	1.37	HSP 90-β	Hsp90ab1	No
2.21E-01	1.27	Ras-related protein Rab-8B	Rab8b	No
1.61E-01	1.23	AP-3 complex subunit δ1	Ap3d1	No
2.84E-01	1.22	Ras-related protein Rab-10	Rab10	No
4.30E-01	1.20	Proteasome subunit β type 9	Psmb9	No
4.84E-01	1.17	TNF receptor-associated factor 6	Traf6	No
3.85E-01	1.16	Ras-related protein Rab-6A or Rab6b	Rab6a, Rab6b	No
7.59E-01	1.08	Wiskott–Aldrich syndrome protein homolog	Was	No
8.15E-01	1.07	Antigen peptide transporter 1	Tap1	Yes
8.05E-01	1.05	AP-3 complex subunit β1	Ap3b1	No
4.41E-01	1.38	Protein transport protein Sec61 subunit γ	Sec61g	No
8.90E-01	1.03	Synaptosomal-associated protein 23	Snap23	No
9.33E-01	1.01	Large proline-rich protein BAG6	Bag6	No
6.42E-01	1.49	Ras-related protein Rab-5B	Rab5b	No
5.28E-01	0.67	Derlin-1	Derl1	Yes
8.89E-01	0.98	Ras-related protein Rab-11B	Rab11b	No
9.29E-01	0.98	Proteasome subunit β type 8	Psmb8	No
7.04E-01	0.95	Proteasome activator complex subunit 1	Psme1	No
7.69E-01	0.93	Antigen peptide transporter 2	Tap2	Yes
9.35E-01	0.93	H2 MHC-II, E-Q, I-A, E-B, or E-S β chain	H2-Eb1	Yes
1.93E-01	0.86	Transitional ER ATPase	Vcp/p97	No
3.87E-01	0.75	IgG receptor FcRn large subunit p51	Fcgrt	Yes
9.81E-01	0.97	MHC-II, M β1 chain	H2-DMb1	Yes
3.66E-01	0.79	Tapasin	Tapbp	Yes
7.54E-02	0.74	ER aminopeptidase 1	Erap1	Yes
3.27E-02	0.58	γ-IFN–inducible lysosomal thiol reductase	Ifi30	Yes
2.24E-02	0.55	Intercellular adhesion molecule 1	Icam1	Yes
2.88E-02	0.54	Cathepsin S	Ctss	Yes
1.62E-02	0.44	H2 MHC-I, D-B α chain	H2-D1	Yes
3.65E-03	0.42	H2 MHC-II, A or A-U β chain	H2-Ab1	Yes
5.24E-02	0.32	H2 MHC-II γ chain	Cd74	Yes
1.41E-03	0.28	H2 MHC-II, A-B or A-U α chain	H2-Aa	Yes
6.62E-03	0.26	H2 MHC-I, K-B or K-K α chain	H2-K1	Yes
1.07E-02	0.09	β2 microglobulin	B2m	Yes

Proteins that were significantly up-regulated [FDR ≤ 0.1; $\log_2$(variation) > 0.5] or down-regulated [FDR ≤ 0,1; $\log_2$(variation) < −0.5] by mycolactone are highlighted in dark gray and light gray, respectively. FcRn, neonatal Fc receptor.

*Fold change (mycolactone/control).

†According to www.uniprot.org.

caused a gradual loss of A1AT-NHK-Venus over the 6-h course of the experiment. This reduction in fluorescence was mediated by ERAD, because it was inhibited by CB-5083. When cells were cotreated with cycloheximide and mycolactone, no difference was seen in A1AT-NHK-Venus stability compared with when cells were treated with cycloheximide alone. In all, our data using three different ERAD substrates demonstrate that although blockade of Sec61 can mediate apparent decreases in ERAD, these effects are due to depletion of the pool of ERAD substrates without an obvious effect on substrate retrotranslocation.

Sec61 Blockade Affects the Production of Key Mediators of Antigen Cross-Presentation. The observed lack of an effect of Sec61 inhibition on antigen cross-presentation was inconsistent with previous data obtained with Sec61-depleted cells (11, 12). Because acute blockade of Sec61 failed to inhibit substrate export both from the endosomes and from the ER, we hypothesized that prolonged Sec61 inhibition could lead to defects in cross-presentation, similar to siRNA-depleted cells. Indeed, when MutuDCs were pretreated with mycolactone for 24 h (Fig. 4*A*), we observed a strong decrease in cross-presentation efficiency (Fig. 4*B*). However, there was a similar decrease in the efficiency of B3Z activation when mycolactone-treated DCs were incubated directly with the $OVA_{257–264}$ peptide (Fig. 4*B*). Furthermore, this decrease in capacity of DCs to activate T cells did not correlate with inhibition of antigen export into the cytosol (Fig. 4*C*). Together, these data imply that prolonged inhibition of Sec61 decreases the overall capacity of DCs to present antigens in the context of MHC-I molecules, rather than antigen export and cross-presentation specifically.

We hypothesized that the inhibition of Sec61-mediated ER import, rather than retrotranslocation, might contribute to the decrease in the capacity of DCs to present antigens. Therefore, we next monitored the proteome of Sec61-blocked MutuDCs over time, using a label-free quantitative approach. Triplicate cell extracts were prepared from MutuDCs exposed to 100 nM mycolactone or vehicle control for 6 or 24 h. Proteins were trypsin-digested, and peptide mixtures processed were analyzed by LC-tandem MS (MS/MS). The proteomic analysis of cell lysates identified 4,197 proteins, among which 3,206 could be

reproducibly quantified across replicates. With the single exception of Akt2, none of these proteins was significantly modulated after 6 h of mycolactone treatment (data not shown for clarity). However, after 24 h, 204 proteins were down-regulated in mycolactone-treated MutuDCs, whereas 170 proteins were up-regulated (Fig. 4*D* and Table S1). Consistent with Sec61 inhibition, a large proportion of Sec61 substrates (36%) were down-regulated in response to mycolactone, compared with 2% of all other proteins (Fig. 4*E*). We examined in greater detail whether known mediators of antigen cross-presentation were affected, either negatively or positively, by Sec61 blockade. Fig. 4*D* and Table 1 show that the subunits of the MHC-I and MHC-II molecules [heavy chain (H2-Kb and H2-Db) and β_2 microglobulin for MHC-I, α (H2-IAα) and β (H2-Aβ1) chains for MHC-II] were among the most efficiently down-regulated proteins. A flow cytometric analysis of mycolactone-treated MutuDCs confirmed these findings (Fig. 4*F*). Importantly, 24 h of exposure to >50 nM mycolactone caused >90% loss of both MHC-I (H2-Kb) surface expression (orange line in Fig. 4*F*), providing an explanation for the defective capacity of mycolactone-treated MutuDCs to cross-present antigens to $CD8^+$ T cells, as seen in Fig. 4*B*. In contrast, MHC-I expression was only partially affected after 6 h of mycolactone treatment (green line in Fig. 4*F*), which is consistent with the unaltered capacity of MutuDCs to cross-present antigen in the conditions of acute Sec61 inhibition used in Fig. 1*F*. Together, the data in Figs. 1 and 4 are thus fully consistent with Sec61 blockade affecting antigen cross-presentation indirectly.

Discussion

The molecular mechanism responsible for antigen exit from endosomes and phagosomes during cross-presentation has been a matter of debate for over 20 y. Sec61 emerged as a promising candidate for an exit channel after it was detected in phagosomes (25–27) and functionally associated with retrotranslocation of proteins from the ER to the cytosol (28). Indeed, suppression of Sec61 in knockdown experiments reduced antigen export to the cytosol to some extent, and inhibited antigen cross-presentation strongly (11, 12). Reduced Sec61 activity, however, is also expected to prevent translocation of secreted proteins into the ER, and thereby to affect numerous cell functions indirectly. To minimize the indirect effects of Sec61 blockade, we have used a pharmacological approach based on mycolactone, a specific Sec61α binder and potent Sec61 blocker. Acute Sec61 blockade by mycolactone severely inhibited the import of secreted proteins into the ER in DCs, but did not interfere with ERAD or protein export from endocytic compartments. Sustained, but not short-term, Sec61 blockade with mycolactone decreased the efficiency of antigen cross-presentation. Mycolactone also strongly inhibited T-cell activation by synthetic peptides and MHC-I expression, implying a more general effect of the drug on the capacity of DCs to present antigens. These findings are consistent with the extensively characterized function of Sec61 in cotranslational protein translocation into the ER (29). They suggest that Sec61α, the translocon subunit targeted by mycolactone, is not directly involved in antigen export to the cytosol, ERAD, or antigen cross-presentation.

Because mycolactone did not inhibit ERAD, we cannot exclude the possibility that the drug blocks forward (from the cytosol to the lumen), but not retrograde (from the lumen to the cytosol), translocation by Sec61. Recent advances in the structural understanding of the opening and closing of the Sec61 channel do not provide a mechanism for how luminal substrates could drive Sec61 plug displacement, and render the channel permissive to peptides during ERAD or cross-presentation (30). The current view of mycolactone's mode of action is that its binding near the luminal plug of Sec61α maintains the complex in a closed conformation (13, 15), which would be expected to prevent protein transport bilaterally. The contribution of Sec61 to substrate dislocation during ERAD in mammalian cells has been questioned repeatedly. Over the years, other mechanisms for retrotranslocation have been proposed, including novel putative channels (e.g., derlins, Hrd1) or lipid-based models (4). Although Sec61 components other than Sec61α may form part of the dislocation channel, our data support the view that the Sec61 complex is not the retrotranslocon for ERAD.

In contrast to this discrepancy between the effects of mycolactone (this study) and Sec61 knockdown (11, 12) on antigen export to the cytosol, both approaches caused inhibition of antigen cross-presentation. With regard to mycolactone, we show that direct presentation of a synthetic peptide (at low concentrations) is also inhibited upon blockade of Sec61. We also show that this result is due to reduced expression of MHC-I at the cell surface, a parameter that was not analyzed after knocking down Sec61 (12). Likewise, nanobodies used to retain Sec61 in the ER (12) could also inhibit protein translocation into the ER and MHC-I expression, altering antigen cross-presentation independent of antigen export to the cytosol. We note that decreased MHC-I expression is hard to detect using saturating concentrations of peptide.

Our proteomic analysis of mycolactone-exposed DCs also showed that many proteins involved in ERAD are significantly modulated after 24 h of Sec61 blockade (Table S2). Notably, accessory molecules that contribute to ERAD of the substrates used in this study [HERP, AUP1, and FAF2/UbxD8 (22, 25)] were up-regulated. These proteins likely belong to the small subset of Sec61 clients resisting mycolactone inhibitory activity, and their accumulation in treated DCs may reflect a stress response to ER translocation defects (13, 16). Increased levels of these factors are unlikely to confound our results, because we analyzed ERAD within 6 h of mycolactone treatment, a time at which these factors were not modulated in mycolactone-treated T cells or DCs (ref. 13 and this study). In contrast, the Sec61 substrates Endoplasmin, Erdj3, and OS-9 were significantly down-regulated in mycolactone-treated DCs, showing that Sec61 blockade not only limits the availability of ERAD substrates but also the availability of ERAD mediators. In all, the changes shown in Tables S1 and S2 demonstrate the large-scale alterations in the proteome that occur when Sec61 function is perturbed, and reinforce the argument that care must be taken when interpreting results showing functional defects in the face of Sec61 knockdown.

Interestingly, a substrate with a long half-life in the ER was unaffected by Sec61 blockade, whereas substrates with shorter half-lives were. When the export step of ER-localized ERAD substrates was examined, no effect of Sec61 blockade was observed. Hence, reduction of ERAD activity in mycolactone-treated cells was most likely due to reduced substrate import into the ER. Consistent with this finding, we detected the presence of nonglycosylated ERAD substrates with intact signal peptides in mycolactone-treated cells. Interestingly, we also detected the up-regulation of the cytosolic chaperones Hsp90α and HSP90β by proteomics. This result is likely due to the accumulation of ER-targeted proteins in the cytosol that are unable to fold properly in the absence of the ER-oxidizing environment, ER chaperones, and glycosylation machinery, and without membrane insertion to shield hydrophobic patches.

A critical role for Sec61 in protein export to the cytosol is also not fully consistent with the pore size that is required to support the export of functional fully folded proteins, such as β-lactamase or HRP, or heavily glycosylated proteins, such as OVA (31). If Sec61 is not involved, how then do antigens escape endocytic compartments in DCs? Recent studies suggest a role for reactive oxygen species and lipid peroxidation, which could locally destabilize the membrane of endocytic compartments, causing transient "leakage" into the cytosol (32). Local destabilization of the ER membrane through formation of lipid bodies was

suggested a few years ago to mediate ERAD (33). Lipid bodies were also shown to favor antigen cross-presentation (34), suggesting a possible link, independent of Sec61, between ERAD and antigen export of the cytosol. Although the search for the molecular mechanisms of ERAD and antigen export have been the object of sustained efforts for over 20 y, and even though Sec61 appeared to be a good candidate to support both, it is most likely that the search is not over.

Materials and Methods

Reagents and Constructs. Mycolactone A/B was purified from *M. ulcerans* bacteria (strain 1615; American Type Culture Collection 35840) and then quantified by spectrophotometry (λ_{max} = 362 nm, log ε = 4.29) (35). Stock solutions were prepared in DMSO and then diluted 1,000-fold in culture medium for cellular assays. The following inhibitors were used for analysis of the role of mycolactone in ERAD or antigen export: MG-132 (Enzo Life Sciences), cycloheximide (Sigma), CB-5083 (SelleckChem.com), zVAD-fmk (R&D Systems), and Eeyarestatin I (Sigma). Vectors encoding ERAD substrates have been described previously (22). The pRetroX-Sec61-IRES-Zsgreen vector used to transduce B3Z cells was derived from pRetroX-IRES-ZsGreen (Clontech) as described elsewhere (13). Flow cytometry reagents were anti-mouse MHC-I (H2-Kb)-phycoerythrin (PE) (12-5958-80; eBioscience), biotin-conjugated anti-mouse MHC-II (I-A/I-E) (553622; BD Biosciences), allophycocyanin-streptavidin (554067; BD Biosciences), anti-mouse CD86 PE-Cy7 (eBioscience 25-0862-82) and isotype control (eBioscience 25-4321-82). LPS (L4391; Sigma) was used at a final concentration of 0.5 μg/mL. High-molecular-weight poly(I:C) (AV-9030-10; Alpha Diagnostic) was preheated for 10 min at 70 °C and used at a final concentration of 5 μg/mL. DAPI was used at a final concentration of 0.5 μM. Fixable Viability Dye eFluor 780 (65-0865-14; eBioscience) was used at a ratio of 1:2,500 according to the manufacturer's instructions.

Cell Cultures. MutuDCs (kindly provided by Hans-Acha Orbea, University of Lausanne, Lausanne, Switzerland) were cultured in Iscove's modified Dulbecco's medium (12440-053; Gibco), supplemented with 8% (vol/vol) FCS (Biowest), 10 mM Hepes, 100 U/mL penicillin, 100 μg/mL streptomycin, and 50 μM β-mercaptoethanol (all from Life Technologies). B3Z hybridomas with a T-cell receptor specific to the Kb/$OVA_{257–264}$ peptide complex (kindly provided by Nilhab Shastri, University of California, Berkeley, CA) (36) were grown in RPMI, supplemented with 10% FCS, 2 mM GlutaMax, 10 mM Hepes, 1 mM sodium pyruvate, 1× nonessential amino acids, 100 IU/mL penicillin, 100 μg/mL streptomycin, and 50 μM β-mercaptoethanol. Mycolactone-resistant B3Z cells were generated as previously described (13). Briefly, Platinum E (Cell Biolabs) was transfected with the R66G-Sec61-IRES-Zsgreen vector using Fugene HD (Promega) as a transfection reagent. After 24 h, the retroviral supernatant was used to transduce B3Z cells, and R66G-Sec61–expressing cells were selected with mycolactone (200 nM). To generate stable cell lines expressing dd substrates, HEK293T cells were transiently transfected with the indicated ERAD substrates in pcDNA3.1-Zeo using Lipofectamine 2000 (both from Thermo Fisher Scientific) according to the manufacturer's suggestions. After 24–48 h, cells were selected with zeocin (Thermo Fisher Scientific) at 0.25–1 mg/mL to obtain stable integrants. Cells surviving selection were cloned by limiting dilution and screened for fluorescence after treatment with 4–8 μM MG-132 for 6 h. To obtain cells stably expressing A1AT-NHK-Venus, we first modified the retroviral vector pMXs-IRES-Puro (Cell Biolabs, Inc.) by replacing the puromycin resistance cassette with a zeocin resistance cassette, PCR-amplified from pcDNA3.1-Zeo, into the NcoI and SalI restriction sites. A1AT-NHK-Venus was PCR-amplified from pcDNA3.1-Zeo and cloned into the EcoRI site of pMXs-IRES-Zeo using the Gibson Assembly Cloning Kit (New England Biolabs). Retroviral supernatants were generated by cotransfection of pMXs-A1AT-NHK-Venus-IRES-Zeo and the packaging vector pCL-Ampho into HEK293T cells. After 48–72 h, supernatants containing retroviral particles were centrifuged at 500 × *g* for 10 min and filtered through a 0.45-μm filter. HEK293T cells were spinfected in the presence of polybrene (8 μg/mL; EMD Millipore) for 90 min at 32 °C. After 48 h, stable cells were selected with zeocin and cloned as above. Stable clones were maintained in DMEM (Thermo Fisher Scientific) supplemented with 10% FBS (Gemini Bioproducts), 2 mM GlutaMax, 50 U/mL penicillin, 50 μg/mL streptomycin, and 225 μg/mL zeocin (all from Thermo Fisher Scientific).

Analysis of Sec61 Blockade on Cross-Presentation. MutuDCs (100,000 per well) were incubated for 5 h with different concentrations of mycolactone and soluble grade VII OVA (no. A7641; Sigma Aldrich) or $OVA_{257–264}$ peptide. Next, MutuDCs were washed three times in PBS, fixed for 3 min with 0.008% glutaraldehyde solution in PBS (vol/vol), and washed twice with 0.2 M glycine. Finally, 100,000 B3Z hybridoma cells were added per well. After 16 h, the cells were lysed in a buffer containing 0.125% Nonidet P-40 (substitute) (sc-29102; Santa Cruz Biotechnology), 9 mM $MgCl_2$, and a colorimetric CPRG β-galactosidase substrate. The absorbance was measured at 590 nm.

Analysis of Sec61 Blockade on Antigen Export. MutuDCs were seeded at 200,000 cells per well in U-bottom, 96-well plates and incubated in the presence or absence of mycolactone with 10 mg/mL β-lactamase (no. P0389; Sigma) for 3 h at 37 °C. The cells were then washed and loaded with CCF4 for 45–60 min at room temperature (RT) as previously described (21). To increase the sensitivity of the assay, the DCs were then incubated for 16 h at RT in CO_2-independent media supplemented with 8% FCS and 2 mM GlutaMax. Immediately before flow cytometry analysis, the cells were stained with Fixable Viability Dye eFluor 780 (no. 65-0865-14; eBioscience) diluted at a ratio of 1:2,500 in PBS. The percentage of the live cells with a high blue-to-green (V450/V530) fluorescence ratio was used as a measure of the efficiency of antigen export into the cytosol.

Analysis of Sec61 Blockade on ERAD. HEK293T cells expressing ERAD substrates were plated at 50,000 cells per well in 96-well, flat-bottom plates and allowed to adhere overnight at 37 °C. Cells were treated alone or in combination with mycolactone (100 nM), MG-132 (4 μM), cycloheximide (20 μg/mL), CB-5083 (1 μM), and zVAD-fmk (20 μM) for the indicated times at 37 °C. For flow cytometry experiments, cells were harvested using trypsin/EDTA (Thermo Fisher Scientific), pooled into duplicate or triplicate wells, washed in PBS containing 2.5% FBS, and analyzed by means of Venus fluorescence on a BD Accuri C6 with autosampler (BD Biosciences). For Western blot analysis, cells from 96-well plates were washed in PBS and pellets were frozen at −20 °C. After thawing on ice, cells were lysed for 30 min in radioimmunoprecipitation assay buffer [50 mM Tris, 150 mM NaCl, 1% Nonidet P-40, 0.1% SDS, 0.5% sodium deoxycholate, and a Complete Protease Inhibitor tablet (Roche Life Sciences)]. Insoluble material was removed through centrifugation at 18,000 × *g* at 4 °C for 10 min. The soluble material was separated by SDS/PAGE on a 10–20% gradient gel (Thermo Fisher Scientific) and transferred to an Immobilon-P membrane (EMD Millipore). The membrane was blocked in 5% nonfat dry milk in Tris-buffered saline/0.05% Tween-20 (TBS-T) for 60 min, rinsed, and incubated with rabbit anti-GFP (A-6455; Thermo Fisher Scientific), CerCLIP.1 (37), or anti-GAPDH (6C5; Thermo Fisher Scientific) for 60 min of shaking at RT. Membranes were washed in TBS-T and incubated with alkaline phosphatase-conjugated secondary antibodies (Jackson Immunoresearch) for 60 min at RT. After three washes (10 min each wash) in TBS-T, membranes were incubated with ECF substrate (GE Healthcare Life Sciences) for 5 min at RT and imaged with a Typhoon FLA 9500 (GE Healthcare Life Sciences).

Role of Sec61 in Import or Export of ddVenus. HEK293T cells expressing ddVenus were plated in 1 mL of media at 400,000 cells per well in 12-well plates and allowed to adhere overnight. Cells were treated with DMSO or cycloheximide (20 μg/mL) for 15 min at 37 °C, followed by addition of MG-132 (4 μM) in the presence or absence of mycolactone (100 nM) or CB-5083 (1 μM). Note that when added, cycloheximide was present throughout the experiment. At the indicated time points, cells were harvested by pipetting with an aliquot saved for flow cytometry, washed twice in ice cold PBS, and frozen at −20 °C. Cells or cell lysates were analyzed by flow cytometry or Western blot as above.

Proteomic Analysis. MutuDCs (4.10^6 cells) were treated with 100 nM mycolactone or DMSO as a vehicle control for 6 or 24 h, in triplicate. Cells from each condition were harvested and washed twice with PBS, and cell pellets were frozen at −80 °C until further use. Cell pellets were resuspended in 500 μL of lysis buffer [9 M urea, 20 mM Hepes (pH 8.0), phosSTOP tablet (one tablet in 10 mL of buffer; Roche)], sonicated (three bursts of 15 s at an amplitude of 20%), and centrifuged for 15 min at 16,000 × *g* at 4 °C to remove insoluble material. The protein concentration in the supernatants was measured using a Bradford assay (Bio-Rad), and 0.5 mg of total protein in each sample was used to continue the protocol. Proteins in each sample were reduced by addition of 5 mM DTT and incubation for 30 min at 55 °C, and were then alkylated by addition of 100 mM iodoacetamide for 15 min at RT in the dark. Both samples were further diluted with 20 mM Hepes (pH 8.0) to a final urea concentration of 4 M, and proteins were digested with 2 μg of LysC (Wako) (1:250, wt/wt) for 4 h at 37 °C. Samples were again diluted to 2 M urea and digested with 5 μg of trypsin (Promega) (1:100, wt/wt) overnight at 37 °C. The resulting peptide mixture was acidified by

addition of 1% TFA, and after 15 min of incubation on ice, samples were centrifuged for 15 min at 1,780 × *g* at RT to remove insoluble components. Next, peptides were purified on SampliQ C18 cartridges (Agilent). Cartridges were first washed with 1 mL of 100% acetonitrile (ACN) and preequilibrated with 3 mL of solvent A [25 μL of 0.1% TFA in water/ACN (98:2, vol/vol)] before samples were loaded on the cartridge. After peptide binding, the column was washed again with 2 mL of solvent A and peptides were eluted with 700 μL of 0.1% TFA in water/ACN (20:80, vol/vol). Purified peptides were redissolved in solvent A, and 10 μL was injected for LC-MS/MS analysis on an Ultimate 3000 RSLCnano System (Dionex; Thermo Fisher Scientific) connected in-line to a Q Exactive HF mass spectrometer with a Nanospray Flex Ion source (Thermo Fisher Scientific). Trapping was performed at 10 $\mu L \cdot min^{-1}$ for 4 min in solvent A [on a reverse-phase column produced in-house (100-μm i.d. × 20 mm) using 5-μm beads (C18 Reprosil-Pur; Dr. Maisch)], followed by loading the sample on a 40-cm column packed in the needle [produced in-house (75 μm i.d. × 400 mm) using 1.9-μm beads (C18 Reprosil-HD; Dr. Maisch)]. Peptides were eluted by an increase in solvent B [0.1% formic acid in water/ACN (2:8, vol/vol)] in linear gradients from 2 to 30% in 100 min, then from 30 to 56% in 40 min, and finally from 56 to 99% in 5 min, all at a constant flow rate of 250 $nL \cdot min^{-1}$. The mass spectrometer was operated in the data-dependent mode, automatically switching between MS and MS/MS acquisition for the 16 most abundant ion peaks per MS spectrum. Full-scan MS spectra (375–1,500 *m/z*) were acquired at a resolution of 60,000 after accumulation to a target value of 3 million, with a maximum fill time of 60 ms. The 16 most intense ions above a threshold value of 22,000 were isolated [window of 1.5 thomson (Th)] for fragmentation at a normalized collision energy of 32% after filling the trap at a target value of 100,000 for a maximum of 45 ms. The S-lens RF level was set at 55, and we excluded precursor ions with single and unassigned charge states.

Data Processing and Analysis. Data analysis was performed with MaxQuant (version 1.5.3.30) (38) using the Andromeda search engine with default search settings, including a false discovery rate (FDR) set at 1% on both the peptide and protein levels. Spectra were searched against the mouse proteins in the UniProt database (database version of April 2016 containing 16,622 mouse protein sequences; www.uniprot.org) with a mass tolerance for precursor and fragment ions of 4.5 ppm and 20 ppm, respectively, during the main search. Enzyme specificity was set as C-terminal to arginine and lysine, also allowing cleavage at proline bonds and a maximum of two missed cleavages. Variable modifications were set to oxidation of methionine residues and acetylation of protein N termini. Carbamidomethyl formation of cysteine residues was set as a fixed modification. Proteins with at least one unique or razor peptide were retained and then quantified by the MaxLFQ algorithm integrated into the MaxQuant software (39). A minimum ratio count of two unique or razor peptides was required for quantification. Further data analysis was performed with Perseus software (version 1.5.4.1) after loading the protein groups file from MaxQuant. Proteins only identified by site, reverse database hits, and potential contaminants were removed, and replicate samples were grouped. Proteins with less than three valid values in at least one group were removed, and missing values were imputed from a normal distribution around the detection limit. The statistical analysis to determine differentially expressed proteins was performed with R software (version 3.3.2) using the *limma* package. *P* values were corrected for multiple testing using the Benjamini–Hochberg method to obtain an FDR. Proteins with an FDR ≤ 0.1 and a $\log_2$ mycolactone/control LFQ intensity fold change ($\log_2$ FC) > 0.5 were considered up-regulated by mycolactone, whereas proteins with an FDR ≥ 0.1 and a $\log_2$ FC < -0.5 were considered down-regulated. The MS proteomics data have been deposited to the ProteomeXchange Consortium via the PRIDE partner repository (40, 41) with the dataset identifier PXD006103. Gene ontology annotations of proteins were inferred from the UniProt database.

ACKNOWLEDGMENTS. C.D. received funding from the Institut Pasteur, INSERM, and Fondation Raoul Follereau. J.-D.M. is the recipient of a doctoral fellowship from the Ecole Normale Supérieure de Lyon. S.A. received funding from the Institute Curie, INSERM, CNRS, la Ligue Contre le Cancer (Equipe labellisée Ligue, EL2014.LNCC/SA), Association pour la Recherche contre le Cancer, European Research Council (2013-AdG 340046 DCBIOX), Institut National du Cancer PLBIO13-057, Agence Nationale de la Recherche (ANR)-11-LABX-0043, ANR-10-IDEX-0001-02 PSL, ANR-16-CE15001801, and ANR-16-CE18002003. P.K. was supported by European Molecular Biology Organization (ALTF 467-2012) and the Wellcome Trust (101578/Z/13/Z). F.I. was supported by Odysseus Grant G0F8616N from the Research Foundation of Flanders. Work by J.E.G. and P.C. was supported by NIH Grant R01-AI097206.

1. Mellman I (2013) Dendritic cells: Master regulators of the immune response. *Cancer Immunol Res* 1:145–149.
2. Joffre OP, Segura E, Savina A, Amigorena S (2012) Cross-presentation by dendritic cells. *Nat Rev Immunol* 12:557–569.
3. Alloatti A, Kotsias F, Magalhaes JG, Amigorena S (2016) Dendritic cell maturation and cross-presentation: Timing matters! *Immunol Rev* 272:97–108.
4. Grotzke JE, Cresswell P (2015) Are ERAD components involved in cross-presentation? *Mol Immunol* 68:112–115.
5. Vembar SS, Brodsky JL (2008) One step at a time: Endoplasmic reticulum-associated degradation. *Nat Rev Mol Cell Biol* 9:944–957.
6. Tretter T, et al. (2013) ERAD and protein import defects in a sec61 mutant lacking ER-lumenal loop 7. *BMC Cell Biol* 14:56.
7. Kaiser ML, Römisch K (2015) Proteasome 19S RP binding to the Sec61 channel plays a key role in ERAD. *PLoS One* 10:e0117260.
8. Stein A, Ruggiano A, Carvalho P, Rapoport TA (2014) Key steps in ERAD of luminal ER proteins reconstituted with purified components. *Cell* 158:1375–1388.
9. Ackerman AL, Giodini A, Cresswell P (2006) A role for the endoplasmic reticulum protein retrotranslocation machinery during crosspresentation by dendritic cells. *Immunity* 25:607–617.
10. Amigorena S, Savina A (2010) Intracellular mechanisms of antigen cross presentation in dendritic cells. *Curr Opin Immunol* 22:109–117.
11. Imai J, Hasegawa H, Maruya M, Koyasu S, Yahara I (2005) Exogenous antigens are processed through the endoplasmic reticulum-associated degradation (ERAD) in cross-presentation by dendritic cells. *Int Immunol* 17:45–53.
12. Zehner M, et al. (2015) The translocon protein Sec61 mediates antigen transport from endosomes in the cytosol for cross-presentation to CD8(+) T cells. *Immunity* 42:850–863.
13. Baron L, et al. (2016) Mycolactone subverts immunity by selectively blocking the Sec61 translocon. *J Exp Med* 213:2885–2896.
14. George KM, et al. (1999) Mycolactone: A polyketide toxin from *Mycobacterium ulcerans* required for virulence. *Science* 283:854–857.
15. McKenna M, Simmonds RE, High S (2016) Mechanistic insights into the inhibition of Sec61-dependent co- and post-translational translocation by mycolactone. *J Cell Sci* 129:1404–1415.
16. McKenna M, Simmonds RE, High S (2017) Mycolactone reveals the substrate-driven complexity of Sec61-dependent transmembrane protein biogenesis. *J Cell Sci* 130:1307–1320.
17. Hall BS, et al. (2014) The pathogenic mechanism of the *Mycobacterium ulcerans* virulence factor, mycolactone, depends on blockade of protein translocation into the ER. *PLoS Pathog* 10:e1004061.
18. Kalies KU, Römisch K (2015) Inhibitors of protein translocation across the ER membrane. *Traffic* 16:1027–1038.
19. Fuertes Marraco SA, et al. (2012) Novel murine dendritic cell lines: A powerful auxiliary tool for dendritic cell research. *Front Immunol* 3:331.
20. Coutanceau E, et al. (2007) Selective suppression of dendritic cell functions by *Mycobacterium ulcerans* toxin mycolactone. *J Exp Med* 204:1395–1403.
21. Zlokarnik G, et al. (1998) Quantitation of transcription and clonal selection of single living cells with beta-lactamase as reporter. *Science* 279:84–88.
22. Grotzke JE, Lu Q, Cresswell P (2013) Deglycosylation-dependent fluorescent proteins provide unique tools for the study of ER-associated degradation. *Proc Natl Acad Sci USA* 110:3393–3398.
23. Anderson DJ, et al. (2015) Targeting the AAA ATPase p97 as an approach to treat cancer through disruption of protein homeostasis. *Cancer Cell* 28:653–665.
24. Sifers RN, Brashears-Macatee S, Kidd VJ, Muensch H, Woo SL (1988) A frameshift mutation results in a truncated alpha 1-antitrypsin that is retained within the rough endoplasmic reticulum. *J Biol Chem* 263:7330–7335.
25. Ackerman AL, Kyritsis C, Tampé R, Cresswell P (2003) Early phagosomes in dendritic cells form a cellular compartment sufficient for cross presentation of exogenous antigens. *Proc Natl Acad Sci USA* 100:12889–12894.
26. Guermonprez P, et al. (2003) ER-phagosome fusion defines an MHC class I cross-presentation compartment in dendritic cells. *Nature* 425:397–402.
27. Houde M, et al. (2003) Phagosomes are competent organelles for antigen cross-presentation. *Nature* 425:402–406.
28. Wiertz EJ, et al. (1996) Sec61-mediated transfer of a membrane protein from the endoplasmic reticulum to the proteasome for destruction. *Nature* 384:432–438.
29. Park E, Rapoport TA (2012) Mechanisms of Sec61/SecY-mediated protein translocation across membranes. *Annu Rev Biophys* 41:21–40.
30. Voorhees RM, Hegde RS (2016) Structure of the Sec61 channel opened by a signal sequence. *Science* 351:88–91.
31. Voorhees RM, Fernández IS, Scheres SH, Hegde RS (2014) Structure of the mammalian ribosome-Sec61 complex to 3.4 Å resolution. *Cell* 157:1632–1643.
32. Dingjan I, et al. (2016) Lipid peroxidation causes endosomal antigen release for cross-presentation. *Sci Rep* 6:22064.
33. Ploegh HL (2007) A lipid-based model for the creation of an escape hatch from the endoplasmic reticulum. *Nature* 448:435–438.
34. Bougnères L, et al. (2009) A role for lipid bodies in the cross-presentation of phagocytosed antigens by MHC class I in dendritic cells. *Immunity* 31:232–244.
35. Spangenberg T, Kishi Y (2010) Highly sensitive, operationally simple, cost/time effective detection of the mycolactones from the human pathogen *Mycobacterium ulcerans*. *Chem Commun (Camb)* 46:1410–1412.

36. Karttunen J, Sanderson S, Shastri N (1992) Detection of rare antigen-presenting cells by the lacZ T-cell activation assay suggests an expression cloning strategy for T-cell antigens. *Proc Natl Acad Sci USA* 89:6020–6024.
37. Denzin LK, Cresswell P (1995) HLA-DM induces CLIP dissociation from MHC class II alpha beta dimers and facilitates peptide loading. *Cell* 82:155–165.
38. Cox J, Mann M (2008) MaxQuant enables high peptide identification rates, individualized p.p.b.-range mass accuracies and proteome-wide protein quantification. *Nat Biotechnol* 26:1367–1372.
39. Cox J, et al. (2014) Accurate proteome-wide label-free quantification by delayed normalization and maximal peptide ratio extraction, termed MaxLFQ. *Mol Cell Proteomics* 13:2513–2526.
40. Vizcaíno JA, et al. (2016) 2016 update of the PRIDE database and its related tools. *Nucleic Acids Res* 44:D447–D456.
41. Vizcaíno JA, et al. (2014) ProteomeXchange provides globally coordinated proteomics data submission and dissemination. *Nat Biotechnol* 32: 223–226.

Supporting Information

Grotzke et al. 10.1073/pnas.1705242114

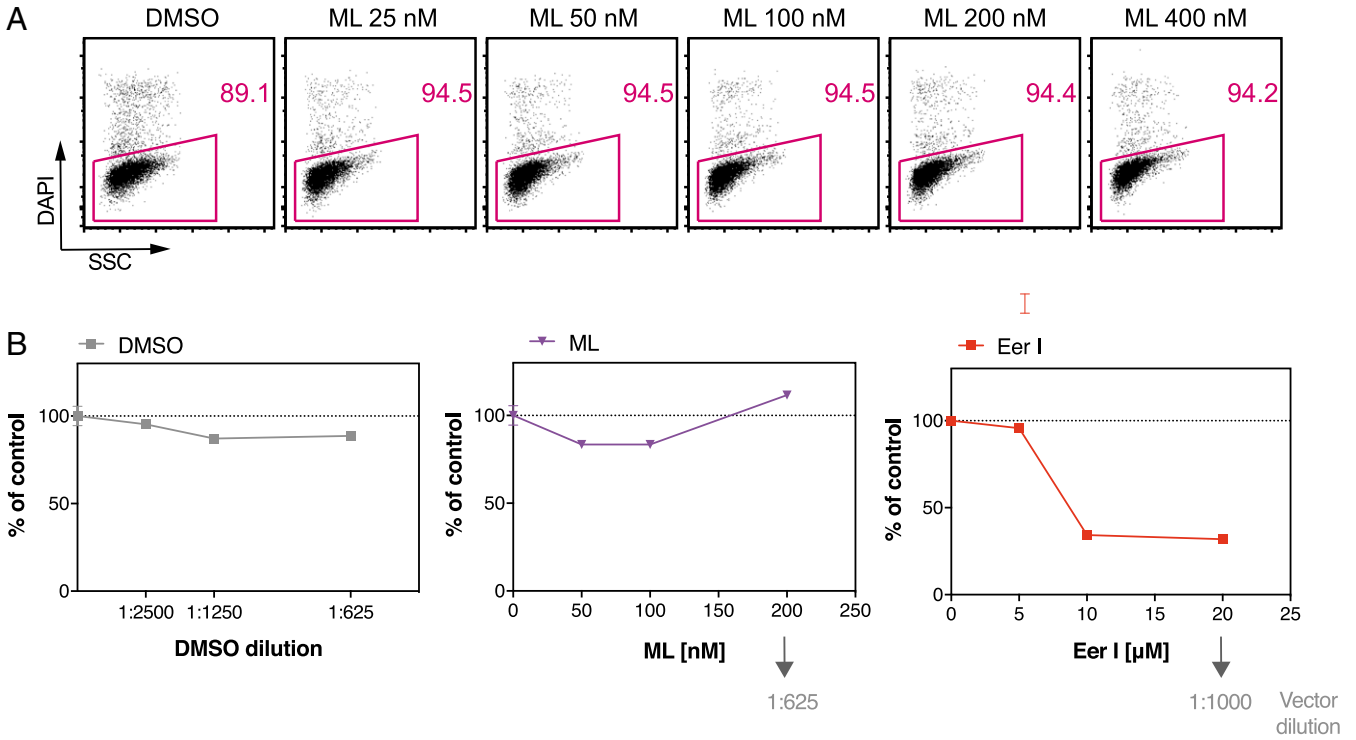

Fig. S1. (*A*) Cytotoxic activity of mycolactone (ML) on MutuDCs. MutuDCs were treated with the indicated concentrations of ML for 24 h and then harvested; cell viability was analyzed by flow cytometry using Fixable Viability Dye eFluor 780. (*B*) In contrast to ML, Eeyarestatin I (Eer I), an inhibitor of p97-associated deubiquitinase enzymes, interferes with antigen export into the cytosol. The β-lactamase assay was performed essentially as described in Fig. 1*C*; however, to exclude an effect of the compounds on antigen uptake, the cells were first fed with β-lactamase for 3 h and subsequently treated with the indicated compounds for 2 h. The percentage of cells with the highest blue-to-green ratio was measured by flow cytometry, and the data are represented relative to untreated cells.

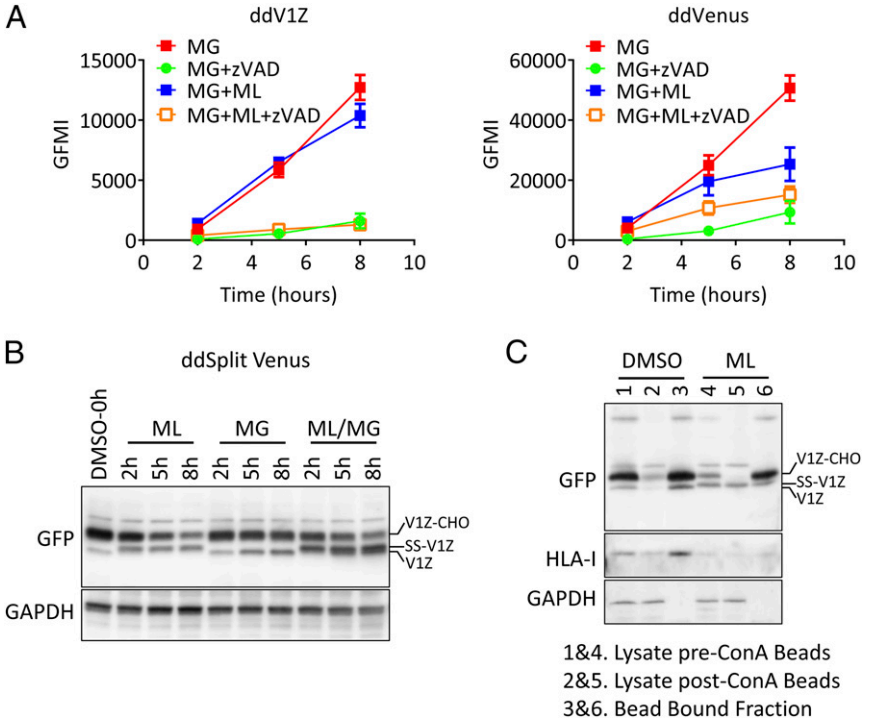

Fig. S2. ML potently blocks translocation of ddV1Z into the ER. (*A*) Stable HEK293T cells were treated with 4 μM MG-132 (MG) ± 100 nM ML and 20 μM zVAD-fmk (zVAD) for the indicated times. At each time point, cells were harvested and fluorescence was analyzed by flow cytometry. To determine dd fluorescence, the geometric mean fluorescence intensity (GMFI) of DMSO- or ML-treated cells was first subtracted from cells treated with MG. Subsequently, the GFMI of zVAD-cotreated cells was subtracted from the GFMI of cells treated with MG or MG/ML only. (*B*) HEK293T cells stably expressing ddV1Z were treated with 4 μM MG ± 100 nM ML for the indicated times. Cell lysates were separated using SDS/PAGE, transferred to a PVDF membrane, and blotted using antibodies to GFP or GAPDH. The different forms of Venus are indicated. (*C*) HEK293T cells stably expressing ddV1Z were treated with DMSO or 100 nM ML for 8 h. Cell lysates were rotated with Con A-Sepharose beads for 90 min, washed, and resuspended in sample buffer. After separation by SDS/PAGE and transfer to a PVDF membrane, samples were blotted using antibodies to GFP, HLA-I (3B10.7), or GAPDH.

Table S1. List of significantly modulated proteins in MutuDCs exposed to mycolactone for 24h. Proteins are sorted on decreasing extent of variation, measured as $\log_2$ fold change (mycolactone/control). Columns from left to right indicate the Uniprot accession number, FDR, variation extent of mycolactone/control, protein name, gene name and an indication of whether the protein is a Sec61 substrate inferred from www.uniprot.org. Upregulated (FDR ≤ 0.1; $\log_2$(Variation) > 0.5); Downregulated (FDR ≤ 0.1; $\log_2$(Variation) < -0.5).

Upregulated proteins					
Uniprot ID	**FDR**	**Variation**	**Protein name**	**Gene name**	**Sec61 substrate**
Q8C2K5	1.91E-04	85.50	RAS protein activator like-3	Rasal3	
Q9JJK5	4.73E-03	9.17	Homocysteine-responsive endoplasmic reticulum-resident ubiquitin-like domain member 1 protein	Herpud1	Yes
Q9EQ06	4.28E-04	2.74	Estradiol 17-beta-dehydrogenase 11	Hsd17b11	Yes
Q64337	3.21E-05	2.67	Sequestosome-1	Sqstm1	
Q9DB25	2.02E-04	2.90	Dolichyl-phosphate beta-glucosyltransferase	Alg5	Yes
P14901	5.20E-06	5.29	Heme oxygenase 1	Hmox1	
P09535	4.58E-03	2.81	Insulin-like growth factor II; Insulin-like growth factor II; Preptin	Igf2	Yes
P61620	1.19E-02	1.89	Protein transport protein Sec61 subunit alpha isoform 1	Sec61a1	Yes
P70295	3.21E-04	1.93	Ancient ubiquitous protein 1	Aup1	Yes
P10852	1.48E-05	3.50	4F2 cell-surface antigen heavy chain	Slc3a2	Yes
P37040	1.09E-03	1.85	NADPH-cytochrome P450 reductase	Por	Yes
Q8CH25	5.09E-05	2.09	SAFB-like transcription modulator	Sltm	
Q9D5T0	3.06E-03	2.12	ATPase family AAA domain-containing protein 1	Atad1	
Q60823	3.93E-05	3.39	RAC-beta serine/threonine-protein kinase	Akt2	
Q9EPL9	8.80E-04	2.21	Peroxisomal acyl-coenzyme A oxidase 3	Acox3	
Q5SS80	1.63E-02	2.22	Dehydrogenase/reductase SDR family member 13	Dhrs13	Yes
Q9Z1E4	2.78E-04	1.62	Glycogen [starch] synthase. muscle	Gys1	
P63037	1.75E-04	2.02	DnaJ homolog subfamily A member 1	Dnaja1	
Q61024	1.51E-05	2.85	Asparagine synthetase [glutamine-hydrolyzing]	Asns	
Q01237	1.52E-01	1.99	3-hydroxy-3-methylglutaryl-coenzyme A reductase	Hmgcr	Yes
Q99K85	5.01E-04	1.60	Phosphoserine aminotransferase	Psat1	
Q8BP47	1.35E-05	1.91	Asparagine--tRNA ligase. cytoplasmic	Nars	
Q8CIS0	9.77E-04	1.49	Caspase recruitment domain-containing protein 11	Card11	
Q62048	4.12E-03	1.75	Astrocytic phosphoprotein PEA-15	Pea15	
P70191	4.05E-03	5.76	TNF receptor-associated factor 5	Traf5	
P26638	1.71E-04	1.78	Serine--tRNA ligase. cytoplasmic	Sars	
P47758	6.03E-02	2.03	Signal recognition particle receptor subunit beta	Srprb	Yes

P07901	1.44E-04	1.65	Heat shock protein HSP 90-alpha	Hsp90aa1	
P63094	3.63E-05	1.54	Guanine nucleotide-binding protein G(s) subunit alpha isoforms short; Guanine nucleotide-binding protein G(s) subunit alpha isoforms XLas	Gnas	
Q8K273	1.92E-04	6.48	Membrane magnesium transporter 1	Mmgt1	Yes
Q61595	2.57E-04	2.13	Kinectin	Ktn1	Yes
Q91VY9	3.05E-04	2.15	Zinc finger protein 622	Znf622	
Q922Q2	7.71E-03	3.11	Serine/threonine-protein kinase RIO1	Riok1	
Q9CR67	5.90E-03	4.31	Transmembrane protein 33	Tmem33	Yes
P28658	2.12E-03	1.78	Ataxin-10	Atxn10	
Q924Z4	5.22E-04	1.87	Ceramide synthase 2	Cers2	Yes
P62331	2.20E-03	1.70	ADP-ribosylation factor 6	Arf6	
P18155	7.34E-04	1.59	Bifunctional methylenetetrahydrofolate dehydrogenase/cyclohydrolase. mitochondrial; NAD-dependent methylenetetrahydrofolate dehydrogenase; Methenyltetrahydrofolate cyclohydrolase	Mthfd2	
P63017	1.04E-04	1.65	Heat shock cognate 71 kDa protein	Hspa8	
Q8BR63	1.21E-02	1.86	Protein FAM177A1	Fam177a1	
O70503	2.02E-04	2.12	Very-long-chain 3-oxoacyl-CoA reductase	Hsd17b12	Yes
Q91YI4	2.44E-04	1.59	Beta-arrestin-2	Arrb2	
Q8K0C4	1.18E-03	1.95	Lanosterol 14-alpha demethylase	Cyp51a1	Yes
A2AN08	6.10E-03	1.51	E3 ubiquitin-protein ligase UBR4	Ubr4	Yes
Q61941	2.88E-04	1.70	NAD(P) transhydrogenase. mitochondrial	Nnt	
Q6WKZ8	1.47E-02	1.89	E3 ubiquitin-protein ligase UBR2	Ubr2	
Q9Z127	1.56E-02	2.76	Large neutral amino acids transporter small subunit 1	Slc7a5	Yes
Q9D0R2	1.98E-02	1.63	Threonine--tRNA ligase. cytoplasmic	Tars	
P59325	1.15E-04	1.63	Eukaryotic translation initiation factor 5	Eif5	
Q91V04	2.24E-04	2.35	Translocating chain-associated membrane protein 1	Tram1	Yes
Q8BMJ2	2.17E-02	1.63	Leucine--tRNA ligase. cytoplasmic	Lars	
Q9DBX6	1.82E-04	1.89	Cytochrome P450 2S1	Cyp2s1	
Q3TBT3	2.77E-04	2.21	Stimulator of interferon genes protein	Tmem173	Yes
Q8VCW4	1.01E-02	1.63	Protein unc-93 homolog B1	Unc93b1	Yes
P62983	1.25E-02	1.47	Ubiquitin-40S ribosomal protein S27a; Ubiquitin;40S ribosomal protein S27a	Rps27a	
Q3U7R1	3.07E-03	1.68	Extended synaptotagmin-1	Esyt1	Yes
Q61699	4.29E-04	1.97	Heat shock protein 105 kDa	Hsph1	
Q9CZB0	3.24E-03	1.56	Succinate dehydrogenase cytochrome b560 subunit. mitochondrial	Sdhc	
Q99LD9	8.81E-04	1.65	Translation initiation factor eIF-2B subunit beta	Eif2b2	
Q9BCZ4	5.56E-05	3.95	Selenoprotein S	Vimp	Yes
P17879	4.62E-03	16.80	Heat shock 70 kDa protein 1B; Heat shock 70 kDa protein 1A	Hspa1b/Hspa1a	
Q6A028	3.17E-03	1.56	Switch-associated protein 70	Swap70	
O70404	1.36E-02	1.78	Vesicle-associated membrane protein 8	Vamp8	

Q9CQV6	4.05E-04	1.66	Microtubule-associated proteins 1A/1B light chain 3B	Map1lc3b	
O88942	2.60E-02	3.93	Nuclear factor of activated T-cells. cytoplasmic 1	Nfatc1	
Q9JM90	8.29E-03	1.73	Signal-transducing adaptor protein 1	Stap1	
O35166	6.95E-04	2.86	Golgi SNAP receptor complex member 2	Gosr2	
Q61335	1.94E-03	2.45	B-cell receptor-associated protein 31	Bcap31	Yes
Q91VK1	8.33E-03	1.59	Basic leucine zipper and W2 domain-containing protein 2	Bzw2	
Q9R0L6	3.43E-04	7.05	Pericentriolar material 1 protein	Pcm1	
P56873	2.17E-03	1.41	Sjoegren syndrome/scleroderma autoantigen 1 homolog	Sssca1	
P47740	4.81E-04	1.81	Fatty aldehyde dehydrogenase	Aldh3a2	
Q3TDN2	1.81E-02	1.70	FAS-associated factor 2	Faf2	
Q8JZR0	1.58E-03	1.48	Long-chain-fatty-acid--CoA ligase 5	Acsl5	Yes
P50396	4.06E-02	1.45	Rab GDP dissociation inhibitor alpha	Gdi1	
Q8VBV3	1.63E-02	1.57	Exosome complex component RRP4	Exosc2	
Q9QYE6	3.29E-03	1.55	Golgin subfamily A member 5	Golga5	
Q5EG47	7.63E-03	1.51	5-AMP-activated protein kinase catalytic subunit alpha-1	Prkaa1	
Q8BKE6	2.02E-02	1.87	Cytochrome P450 20A1	Cyp20a1	Yes
G3X9K3	4.67E-03	2.18	Brefeldin A-inhibited guanine nucleotide-exchange protein 1	Arfgef1	
Q9ER72	1.40E-04	1.84	Cysteine--tRNA ligase. cytoplasmic	Cars	
Q99PL5	1.49E-04	1.72	Ribosome-binding protein 1	Rrbp1	Yes
P70245	7.76E-02	2.59	3-beta-hydroxysteroid-Delta(8). Delta(7)-isomerase	Ebp	Yes
Q3TYS2	1.70E-02	3.32	Uncharacterized protein C17orf62 homolog		Yes
Q3UM18	1.51E-04	43.87	Large subunit GTPase 1 homolog	Lsg1	
Q8VE18	3.83E-02	3.30	Protein SMG8	Smg8	
O55022	1.28E-02	1.43	Membrane-associated progesterone receptor component 1	Pgrmc1	Yes
P20664	2.53E-03	1.47	DNA primase small subunit	Prim1	
Q9Z110	1.56E-03	1.77	Delta-1-pyrroline-5-carboxylate synthase; Glutamate 5-kinase; Gamma-glutamyl phosphate reductase	Aldh18a1	
Q8BH04	2.28E-04	3.03	Phosphoenolpyruvate carboxykinase [GTP]. mitochondrial	Pck2	
Q9CY58	5.64E-03	1.51	Plasminogen activator inhibitor 1 RNA-binding protein	Serbp1	
Q8VCF0	2.04E-02	1.74	Mitochondrial antiviral-signaling protein	Mavs	
Q62465	1.52E-03	3.30	Synaptic vesicle membrane protein VAT-1 homolog	Vat1	
Q9R099	5.67E-03	6.72	Transducin beta-like protein 2	Tbl2	
Q99L48	2.23E-03	1.89	60S ribosomal export protein NMD3	Nmd3	
Q61753	1.85E-04	1.54	D-3-phosphoglycerate dehydrogenase	Phgdh	
E9Q4P1	2.29E-03	1.49	WD repeat and FYVE domain-containing protein 1	Wdfy1	
O70152	6.04E-02	3.92	Dolichol-phosphate mannosyltransferase subunit 1	Dpm1	
Q7TMB8	2.07E-02	1.51	Cytoplasmic FMR1-interacting protein 1	Cyfip1	
Q9CQW9	1.33E-02	1.54	Interferon-induced transmembrane protein 3	Ifitm3	
Q80UU9	1.47E-03	1.55	Membrane-associated progesterone receptor component 2	Pgrmc2	Yes

O35972	1.00E+00	2.05	39S ribosomal protein L23. mitochondrial	Mrpl23	
Q8BP67	1.82E-02	1.52	60S ribosomal protein L24	Rpl24	
Q9DBT5	1.39E-03	1.52	AMP deaminase 2	Ampd2	
P55258	4.70E-02	1.49	Ras-related protein Rab-8A	Rab8a	
Q9WUQ2	1.27E-04	1.82	Prolactin regulatory element-binding protein	Preb	
Q91YR7	2.00E-02	1.58	Pre-mRNA-processing factor 6	Prpf6	
Q8CI04	1.06E-01	1.77	Conserved oligomeric Golgi complex subunit 3	Cog3	
Q8CGC7	2.40E-02	1.46	Bifunctional glutamate/proline--tRNA ligase; Glutamate--tRNA ligase;Proline--tRNA ligase	Eprs	
P46414	2.96E-03	2.76	Cyclin-dependent kinase inhibitor 1B	Cdkn1b	
Q64310	3.68E-03	1.61	Surfeit locus protein 4	Surf4	Yes
Q9QYJ3	2.25E-03	1.46	DnaJ homolog subfamily B member 1	Dnajb1	
Q9JJZ4	1.68E-02	2.13	Ubiquitin-conjugating enzyme E2 J1	Ube2j1	
Q3TEA8	2.42E-02	2.36	Heterochromatin protein 1-binding protein 3	Hp1bp3	
Q5XG71	2.75E-02	3.53	Small subunit processome component 20 homolog	Utp20	
P28867	3.99E-02	1.55	Protein kinase C delta type; Protein kinase C delta type regulatory subunit; Protein kinase C delta type catalytic subunit	Prkcd	
Q9DB43	5.21E-04	1.59	Zinc finger protein-like 1	Zfpl1	Yes
Q8R0X7	1.24E-02	1.84	Sphingosine-1-phosphate lyase 1	Sgpl1	Yes
Q8VEM8	1.37E-02	1.41	Phosphate carrier protein. mitochondrial	Slc25a3	
Q3UPF5	1.29E-03	1.48	Zinc finger CCCH-type antiviral protein 1	Zc3hav1	
Q8C9B9	7.68E-03	1.92	Death-inducer obliterator 1	Dido1	
Q8VEH6	4.00E-03	1.70	COBW domain-containing protein 1	Cbwd1	
O55143	2.55E-03	1.55	Sarcoplasmic/endoplasmic reticulum calcium ATPase 2	Atp2a2	Yes
Q9D898	2.28E-04	1.45	Actin-related protein 2/3 complex subunit 5-like protein	Arpc5l	
Q6KAR6	1.66E-02	2.86	Exocyst complex component 3	Exoc3	
Q9CR57	6.52E-02	1.92	60S ribosomal protein L14	Rpl14	
Q8BGQ7	6.28E-05	1.45	Alanine--tRNA ligase. cytoplasmic	Aars	
Q9CQV1	8.37E-03	1.99	Mitochondrial import inner membrane translocase subunit TIM16	Pam16	
Q3TIR3	8.62E-02	2.40	Synembryn-A	Ric8a	
Q6PHN9	2.89E-02	1.52	Ras-related protein Rab-35	Rab35	
Q3TZZ7	1.53E-02	3.00	Extended synaptotagmin-2	Esyt2	Yes
Q8BVE3	2.87E-03	1.44	V-type proton ATPase subunit H	Atp6v1h	
P04370	6.82E-03	1.55	Myelin basic protein	Mbp	
Q69ZB8	1.70E-02	1.46	Zinc finger CCHC domain-containing protein 2	Zcchc2	
O55142	4.33E-02	1.48	60S ribosomal protein L35a	Rpl35a	
Q9EPE9	9.89E-03	1.63	Manganese-transporting ATPase 13A1	Atp13a1	Yes
O35604	6.65E-02	1.56	Niemann-Pick C1 protein	Npc1	Yes
Q9JIY0	2.22E-02	2.13	Pleckstrin homology domain-containing family O member 1	Plekho1	
Q9JI90	8.13E-02	1.96	E3 ubiquitin-protein ligase RNF14	Rnf14	

Q9JIW9	2.49E-02	1.76	Ras-related protein Ral-B	Ralb	
Q9QY76	3.16E-03	1.61	Vesicle-associated membrane protein-associated protein B	Vapb	
Q4VAC9	3.03E-02	1.43	Pleckstrin homology domain-containing family G member 3	Plekhg3	
Q6ZQH8	1.69E-02	1.60	Nucleoporin NUP188 homolog	Nup188	
Q91YH5	8.46E-03	1.50	Atlastin-3	Atl3	Yes
Q3TKY6	1.61E-02	1.44	Peptidyl-prolyl cis-trans isomerase CWC27 homolog	Cwc27	
Q8BHI7	4.48E-02	3.17	Elongation of very long chain fatty acids protein 5	Elovl5	Yes
Q8VCB1	5.23E-01	3.05	Nucleoporin NDC1	Ndc1	Yes
P35282	2.51E-03	1.60	Ras-related protein Rab-21	Rab21	
P35550	1.46E-02	1.60	rRNA 2-O-methyltransferase fibrillarin	Fbl	
A2AF47	6.85E-02	1.61	Dedicator of cytokinesis protein 11	Dock11	
Q7TMK9	1.34E-02	1.45	Heterogeneous nuclear ribonucleoprotein Q	Syncrip	
Q3TXU5	1.75E-02	1.61	Deoxyhypusine synthase	Dhps	
Q9ERN0	3.36E-03	1.70	Secretory carrier-associated membrane protein 2	Scamp2	Yes
Q6PFQ7	4.76E-02	2.05	Ras GTPase-activating protein 4	Rasa4	
P35821	6.75E-02	1.55	Tyrosine-protein phosphatase non-receptor type 1	Ptpn1	
Q8K2R5	6.64E-01	1.71	Zinc finger protein 668	Znf668	
O35601	3.48E-02	1.44	FYN-binding protein	Fyb	
Q5RL51	5.39E-02	4.78	Glutathione S-transferase C-terminal domain-containing protein	Gstcd	
Q6DFV1	1.80E-02	1.67	Condensin-2 complex subunit G2	Ncapg2	
Q8BGS7	1.00E+00	1.81	Choline/ethanolamine phosphotransferase 1	Cept1	Yes
Q5ND34	7.98E-02	2.98	WD repeat-containing protein 81	Wdr81	
P08103	3.29E-03	1.63	Tyrosine-protein kinase HCK	Hck	
Q9CQU3	1.39E-02	1.48	Protein RER1	Rer1	Yes
Q9DB73	3.33E-03	1.89	NADH-cytochrome b5 reductase 1	Cyb5r1	
Q9CR20	3.36E-03	2.61	Immediate early response 3-interacting protein 1	Ier3ip1	Yes
Q9CPP0	1.16E-01	1.85	Nucleoplasmin-3	Npm3	
P62821	4.34E-02	1.44	Ras-related protein Rab-1A	Rab1A	
Q9CRT8	9.66E-02	1.49	Exportin-T	Xpot	
Q8BM55	4.14E-03	1.57	Transmembrane protein 214	Tmem214	Yes

Downregulated proteins

Uniprot ID	FDR[a]	Variation[b]	Protein name[c]	Gene name[c]	Sec61 substrate
Q9ERR7	1.81E-03	0.52	15 kDa selenoprotein	Sep-15	Yes
Q8BU88	1.36E-02	0.64	39S ribosomal protein L22. mitochondrial	Mrpl22	
Q61112	6.65E-03	0.29	45 kDa calcium-binding protein	Sdf4	Yes
P41105	2.73E-02	0.29	60S ribosomal protein L28	Rpl28	
Q9WV54	2.47E-05	0.46	Acid ceramidase subunit alpha; subunit beta	Asah1	Yes

P51829	1.01E-02	0.33	Adenylate cyclase type 7	Adcy7	Yes
Q8VDL4	1.27E-03	0.67	ADP-dependent glucokinase	Adpgk	Yes
P09242	2.50E-03	0.44	Alkaline phosphatase. tissue-nonspecific isozyme	Alpl	Yes
Q9QWR8	6.38E-03	0.48	Alpha-N-acetylgalactosaminidase	Naga	Yes
P97449	6.99E-03	0.56	Aminopeptidase N	Anpep	Yes
Q80UP5	1.27E-02	0.59	Ankyrin repeat domain-containing protein 13A	Ankrd13a	
P50429	1.22E-01	0.68	Arylsulfatase B	Arsb	Yes
P97450	3.63E-02	0.69	ATP synthase-coupling factor 6. mitochondrial	Atp5j	
Q9JHS4	3.90E-02	0.47	ATP-dependent Clp protease ATP-binding subunit clpX-like. mitochondrial	Clpx	
O70126	6.87E-03	0.26	Aurora kinase B	Aurkb	
Q9CXE2	5.72E-03	0.20	B-cell CLL/lymphoma 7 protein family member A; B-cell CLL/lymphoma 7 protein family member B	Bcl7a; Bcl7b	
O70201	1.29E-03	0.51	Baculoviral IAP repeat-containing protein 5	Birc5	
Q09200	4.76E-03	0.42	Beta-1.4 N-acetylgalactosaminyltransferase 1	B4galnt1	Yes
P01887	1.44E-03	0.09	Beta-2-microglobulin	B2m	Yes
P12265	8.19E-03	0.62	Beta-glucuronidase	Gusb	Yes
P29416	3.89E-04	0.55	Beta-hexosaminidase subunit alpha	Hexa	Yes
P20060	5.22E-03	0.63	Beta-hexosaminidase subunit beta	Hexb	Yes
Q9DAW9	1.64E-01	0.55	Calponin-3	Cnn3	
P14211	1.91E-03	0.61	Calreticulin	Calr	Yes
O35887	1.36E-02	0.54	Calumenin	Calu	Yes
P10605	1.62E-02	0.29	Cathepsin B; Cathepsin B light chain; Cathepsin B heavy chain	Ctsb	Yes
O70370	1.33E-04	0.54	Cathepsin S	Ctss	Yes
P24668	4.49E-03	0.67	Cation-dependent mannose-6-phosphate receptor	M6pr	Yes
Q07113	7.94E-03	0.19	Cation-independent mannose-6-phosphate receptor	Igf2r	Yes
Q61490	6.21E-04	0.40	CD166 antigen	Alcam	Yes
Q62192	4.42E-03	0.66	CD180 antigen	Cd180	Yes
P15379	2.15E-04	0.43	CD44 antigen	Cd44	Yes
P18181	3.34E-04	0.54	CD48 antigen	Cd48	Yes
Q9Z0M6	1.14E-04	0.16	CD97 antigen	Cd97	Yes
Q8R5M8	6.20E-04	0.25	Cell adhesion molecule 1	Cadm1	Yes
Q9JJ66	5.06E-03	0.53	Cell division cycle protein 20 homolog	Cdc20	
Q99M54	1.20E-02	0.57	Cell division cycle-associated protein 3	Cdca3	
Q9CZX2	1.02E-04	0.11	Centrosomal protein of 89 kDa	Cep89	
Q9D0N7	6.67E-03	0.65	Chromatin assembly factor 1 subunit B	Chaf1b	
Q2VPQ9	1.47E-02	0.35	Chromatin modification-related protein MEAF6	Meaf6	
Q6AW69	5.18E-03	0.62	Cingulin-like protein 1	Cgnl1	
Q810U5	9.90E-04	0.52	Coiled-coil domain-containing protein 50	Ccdc50	
Q9CZG3	4.68E-02	0.20	COMM domain-containing protein 8	Commd8	
P61025	8.60E-03	0.61	Cyclin-dependent kinases regulatory subunit 1	Cks1b	

P56390	4.68E-03	0.60	Cyclin-dependent kinases regulatory subunit 2	Cks2	
Q99M07	2.93E-02	0.60	Cytochrome c oxidase assembly factor 5	Coa5	
P56542	8.32E-04	0.39	Deoxyribonuclease-2-alpha	Dnase2	Yes
P97821	4.90E-03	0.64	Dipeptidyl peptidase 1; Dipeptidyl peptidase 1 exclusion domain chain; Dipeptidyl peptidase 1 heavy chain; Dipeptidyl peptidase 1 light chain	Ctsc	Yes
Q99JF5	7.14E-04	0.53	Diphosphomevalonate decarboxylase	Mvd	
O35598	2.09E-02	0.25	Disintegrin and metalloproteinase domain-containing protein 10	Adam10	Yes
Q8K4R9	1.00E+00	0.44	Disks large-associated protein 5	Dlgap5	
O35654	4.96E-02	0.22	DNA polymerase delta subunit 2	Pold2	
Q99KV1	4.35E-03	0.61	DnaJ homolog subfamily B member 11	Dnajb11	Yes
Q91YW3	1.98E-04	0.29	DnaJ homolog subfamily C member 3	Dnajc3	Yes
Q3UVK0	1.93E-02	0.61	Endoplasmic reticulum metallopeptidase 1	Ermp1	Yes
P57759	2.65E-03	0.66	Endoplasmic reticulum resident protein 29	Erp29	Yes
Q9D1Q6	6.36E-04	0.62	Endoplasmic reticulum resident protein 44	Erp44	Yes
P08113	1.26E-03	0.63	Endoplasmin	Hsp90b1	Yes
Q03145	2.95E-03	0.66	Ephrin type-A receptor 2	Epha2	Yes
Q9Z0J0	1.42E-03	0.35	Epididymal secretory protein E1	Npc2	Yes
Q8BFZ9	6.42E-03	0.60	Erlin-2	Erlin2	Yes
Q8R2E9	2.38E-04	0.37	ERO1-like protein beta	Ero1lb	Yes
Q920E5	4.32E-03	0.70	Farnesyl pyrophosphate synthase	Fdps	
Q9Z0R9	9.57E-03	0.47	Fatty acid desaturase 2	Fads2	Yes
P12804	4.60E-03	0.19	Fibroleukin	Fgl2	Yes
Q6ZQ03	3.23E-01	0.53	Formin-binding protein 4	Fnbp4	
Q9ESY9	1.50E-04	0.58	Gamma-interferon-inducible lysosomal thiol reductase	Ifi30	Yes
Q60648	3.18E-03	0.55	Ganglioside GM2 activator	Gm2a	Yes
O08795	3.65E-03	0.58	Glucosidase 2 subunit beta	Prkcsh	Yes
P17439	4.35E-04	0.55	Glucosylceramidase	Gba	Yes
Q9WTK3	1.20E-03	0.45	Glycosylphosphatidylinositol anchor attachment 1 protein	Gpaa1	Yes
Q61543	6.60E-07	0.31	Golgi apparatus protein 1	Glg1	Yes
P28798	1.65E-03	0.48	Granulins; Acrogranin; Granulin-1; Granulin-2; Granulin-3; Granulin-4; Granulin-5; Granulin-6; Granulin-7	Grn	Yes
P01899	4.51E-04	0.44	H-2 class I histocompatibility antigen. D-B alpha chain	H2-D1	Yes
P01901	5.55E-05	0.26	H-2 class I histocompatibility antigen. K-B alpha chain; H-2 class I histocompatibility antigen. K-K alpha chain	H2-K1	Yes
P04441	3.54E-04	0.32	H-2 class II histocompatibility antigen gamma chain	Cd74	Yes
P14483	2.83E-05	0.42	H-2 class II histocompatibility antigen. A beta chain; H-2 class II histocompatibility antigen. A-U beta chain	H2-Ab1	Yes
P14434	1.50E-05	0.28	H-2 class II histocompatibility antigen. A-B alpha chain; H-2 class II histocompatibility antigen. A-U alpha chain	H2-Aa	Yes
P97825	7.64E-04	0.69	Hematological and neurological expressed 1 protein; Hematological and neurological expressed 1 protein. N-terminally processed	Hn1	

Q9DAP7	1.57E-03	0.46	Histone chaperone ASF1B	Asf1b	
Q8JZK9	2.13E-04	0.43	Hydroxymethylglutaryl-CoA synthase. cytoplasmic	Hmgcs1	
Q9JKR6	1.03E-02	0.70	Hypoxia up-regulated protein 1	Hyou1	Yes
P52293	3.93E-05	0.43	Importin subunit alpha-1	Kpna2	
P97287	1.58E-03	0.56	Induced myeloid leukemia cell differentiation protein Mcl-1 homolog	Mcl1	
Q91VM9	8.80E-02	0.34	Inorganic pyrophosphatase 2. mitochondrial	Ppa2	
Q91UZ5	8.09E-05	0.18	Inositol monophosphatase 2	Impa2	
Q00651	2.97E-04	0.19	Integrin alpha-4	Itga4	Yes
P24063	1.94E-03	0.52	Integrin alpha-L	Itgal	Yes
Q9QXH4	5.56E-04	0.59	Integrin alpha-X	Itgax	Yes
P09055	9.01E-04	0.52	Integrin beta-1	Itgb1	Yes
P11835	9.59E-05	0.57	Integrin beta-2	Itgb2	Yes
P26011	3.64E-04	0.26	Integrin beta-7	Itgb7	Yes
P13597	3.50E-03	0.55	Intercellular adhesion molecule 1	Icam1	Yes
P23611	1.32E-05	0.45	Interferon regulatory factor 8	Irf8	
P58044	9.70E-04	0.44	Isopentenyl-diphosphate Delta-isomerase 1	Idi1	
Q9Z2X8	1.43E-03	0.46	Kelch-like ECH-associated protein 1	Keap1	
Q6P9P6	3.06E-04	0.60	Kinesin-like protein KIF11	Kif11	
P97329	3.35E-02	0.52	Kinesin-like protein KIF20A	Kif20a	
Q9CYC5	5.28E-02	0.44	Kinetochore-associated protein DSN1 homolog	Dsn1	
P21956	1.63E-03	0.46	Lactadherin	Mfge8	Yes
O89017	2.46E-03	0.29	Legumain	Lgmn	Yes
Q8K1T1	5.81E-04	0.52	Leucine-rich repeat-containing protein 25	Lrrc25	Yes
Q8C129	1.44E-02	0.66	Leucyl-cystinyl aminopeptidase	Lnpep	Yes
Q8C8U0	6.06E-03	0.67	Liprin-beta-1	Ppfibp1	
O88188	1.68E-04	0.42	Lymphocyte antigen 86	Ly86	Yes
Q9Z0M5	7.28E-03	0.56	Lysosomal acid lipase/cholesteryl ester hydrolase	Lipa	Yes
O09159	1.39E-04	0.55	Lysosomal alpha-mannosidase	Man2b1	Yes
Q7TMR0	5.21E-02	0.39	Lysosomal Pro-X carboxypeptidase	Prcp	Yes
P16675	3.04E-03	0.35	Lysosomal protective protein; Lysosomal protective protein 32 kDa chain; Lysosomal protective protein 20 kDa chain	Ctsa	Yes
P11438	2.09E-03	0.48	Lysosome-associated membrane glycoprotein 1	Lamp1	Yes
P17047	8.34E-02	0.56	Lysosome-associated membrane glycoprotein 2	Lamp2	Yes
A1L314	5.85E-04	0.36	Macrophage-expressed gene 1 protein	Mpeg1	Yes
Q924H2	8.41E-04	0.48	Mediator of RNA polymerase II transcription subunit 15	Med15	
Q8BU85	4.23E-02	0.47	Methionine-R-sulfoxide reductase B3. mitochondrial	Msrb3	Yes
Q9R008	3.01E-02	0.62	Mevalonate kinase	Mvk	
P10404	5.25E-04	0.42	MLV-related proviral Env polyprotein; Surface protein; Transmembrane protein		Yes
Q9CZR2	3.03E-03	0.29	N-acetylated-alpha-linked acidic dipeptidase 2	Naalad2	Yes

Q8BFR4	5.70E-03	0.57	N-acetylglucosamine-6-sulfatase	Gns	Yes
Q9D7V9	6.13E-05	0.24	N-acylethanolamine-hydrolyzing acid amidase; N-acylethanolamine-hydrolyzing acid amidase subunit alpha; N-acylethanolamine-hydrolyzing acid amidase subunit beta	Naaa	Yes
Q9CQZ5	2.52E-04	0.69	NADH dehydrogenase [ubiquinone] 1 alpha subcomplex subunit 6	Ndufa6	
P52503	2.00E-02	0.64	NADH dehydrogenase [ubiquinone] iron-sulfur protein 6. mitochondrial	Ndufs6	
O09043	4.54E-03	0.52	Napsin-A	Napsa	Yes
P61082	1.26E-01	0.18	NEDD8-conjugating enzyme Ubc12	Ube2m	
P97333	6.33E-03	0.40	Neuropilin-1	Nrp1	Yes
P97300	1.26E-03	0.57	Neuroplastin	Nptn	Yes
Q8BHN3	5.11E-04	0.64	Neutral alpha-glucosidase AB	Ganab	Yes
P57716	1.51E-02	0.64	Nicastrin	Ncstn	Yes
Q6GQT9	1.15E-03	0.70	Nodal modulator 1	Nomo1	Yes
Q02819	4.58E-03	0.52	Nucleobindin-1	Nucb1	Yes
P81117	1.22E-02	0.49	Nucleobindin-2; Nesfatin-1	Nucb2	Yes
Q9ERH4	1.49E-02	0.35	Nucleolar and spindle-associated protein 1	Nusap1	
Q9CPT5	1.07E-03	0.26	Nucleolar protein 16	Nop16	
Q99PG2	2.95E-03	0.42	Opioid growth factor receptor	Ogfr	
O88531	1.94E-04	0.45	Palmitoyl-protein thioesterase 1	Ppt1	Yes
P45878	1.07E-03	0.56	Peptidyl-prolyl cis-trans isomerase FKBP2	Fkbp2	Yes
O08807	4.42E-04	0.67	Peroxiredoxin-4	Prdx4	Yes
Q6P8I4	6.56E-03	0.59	PEST proteolytic signal-containing nuclear protein	Pcnp	
Q8VCI0	6.92E-04	0.63	Phospholipase B-like 1; Phospholipase B-like 1 chain A; Phospholipase B-like 1 chain B; Phospholipase B-like 1 chain C	Plbd1	Yes
Q8BG07	3.35E-04	0.67	Phospholipase D4	Pld4	Yes
Q08857	1.36E-05	0.35	Platelet glycoprotein 4	Cd36	Yes
Q9CQF9	5.04E-02	0.41	Prenylcysteine oxidase	Pcyox1	Yes
Q8K297	2.81E-05	0.59	Procollagen galactosyltransferase 1	Colgalt1	Yes
Q9R0E1	4.81E-03	0.60	Procollagen-lysine.2-oxoglutarate 5-dioxygenase 3	Plod3	Yes
Q60715	9.98E-05	0.52	Prolyl 4-hydroxylase subunit alpha-1	P4ha1	Yes
P11680	2.44E-04	0.21	Properdin	Cfp	Yes
Q61207	2.99E-05	0.47	Prosaposin	Psap	Yes
P22437	3.67E-03	0.65	Prostaglandin G/H synthase 1	Ptgs1	Yes
Q9QXT0	4.45E-03	0.53	Protein canopy homolog 2	Cnpy2	Yes
Q9DAU1	3.43E-03	0.54	Protein canopy homolog 3	Cnpy3	Yes
Q8BQ47	2.79E-02	0.57	Protein canopy homolog 4	Cnpy4	Yes
O54972	1.84E-04	0.01	Protein CBFA2T3	Cbfa2t3	
O88668	2.73E-04	0.58	Protein CREG1	Creg1	Yes
P27773	9.37E-04	0.65	Protein disulfide-isomerase A3	Pdia3	Yes

Q922R8	5.41E-03	0.63	Protein disulfide-isomerase A6	Pdia6	Yes
P28574	3.08E-02	0.42	Protein max	Max	
Q8K2C7	1.62E-02	0.35	Protein OS-9	Os9	Yes
Q8C4B4	1.22E-02	0.70	Protein unc-119 homolog B	Unc119b	
P21981	3.58E-03	0.65	Protein-glutamine gamma-glutamyltransferase 2	Tgm2	
Q3TCN2	8.97E-02	0.49	Putative phospholipase B-like 2; Putative phospholipase B-like 2 28 kDa form; Putative phospholipase B-like 2 40 kDa form; Putative phospholipase B-like 2 15 kDa form	Plbd2	Yes
Q05920	2.78E-02	0.24	Pyruvate carboxylase. mitochondrial	Pc	
P35486	5.12E-02	0.65	Pyruvate dehydrogenase E1 component subunit alpha. somatic form. mitochondrial	Pdha1	
Q9WVM1	3.85E-02	0.63	Rac GTPase-activating protein 1	Racgap1	
P18052	5.77E-03	0.38	Receptor-type tyrosine-protein phosphatase alpha	Ptpra	Yes
P06800	3.30E-05	0.55	Receptor-type tyrosine-protein phosphatase C	Ptprc	Yes
Q8BP92	2.60E-02	0.61	Reticulocalbin-2	Rcn2	Yes
P11370	1.48E-03	0.03	Retrovirus-related Env polyprotein from Fv-4 locus	Fv4	
P11157	1.76E-03	0.54	Ribonucleoside-diphosphate reductase subunit M2	Rrm2	
Q99KG3	2.65E-02	0.59	RNA-binding protein 10	Rbm10	
Q6NZN0	1.48E-01	0.61	RNA-binding protein 26	Rbm26	
O09126	4.99E-03	0.20	Semaphorin-4D	Sema4d	Yes
Q8BTI7	6.01E-02	0.58	Serine/threonine-protein phosphatase 6 regulatory ankyrin repeat subunit C	Ankrd52	
Q920G3	8.96E-02	0.31	Sialic acid-binding Ig-like lectin 5	Siglec5	Yes
Q8VDN2	9.57E-04	0.59	Sodium/potassium-transporting ATPase subunit alpha1	Atp1a1	Yes
P97370	5.53E-04	0.45	Sodium/potassium-transporting ATPase subunit beta-3	Atp1b3	Yes
O70492	8.39E-03	0.59	Sorting nexin-3	Snx3	
Q3TXT3	5.61E-03	0.55	SOSS complex subunit C	Inip	
Q9ESP1	1.70E-02	0.58	Stromal cell-derived factor 2-like protein 1	Sdf2l1	Yes
Q8R0F3	3.19E-04	0.45	Sulfatase-modifying factor 1	Sumf1	Yes
Q8BJS4	1.98E-04	0.34	SUN domain-containing protein 2	Sun2	Yes
Q5SV85	5.84E-02	0.51	Synergin gamma	Synrg	
O08992	8.09E-05	0.64	Syntenin-1	Sdcbp	
A2APB8	4.20E-01	0.29	Targeting protein for Xklp2	Tpx2	
Q9CQU0	4.96E-03	0.48	Thioredoxin domain-containing protein 12	Txndc12	Yes
Q91W90	7.34E-04	0.56	Thioredoxin domain-containing protein 5	Txndc5	Yes
Q9QZ06	3.21E-02	0.40	Toll-interacting protein	Tollip	
Q6QNU9	3.36E-03	0.18	Toll-like receptor 12	Tlr12	Yes
Q99MB1	1.31E-02	0.68	Toll-like receptor 3	Tlr3	Yes
Q80V24	6.78E-02	0.54	Transcription cofactor vestigial-like protein 4	Vgll4	
P62869	7.20E-03	0.66	Transcription elongation factor B polypeptide 2	Tceb2	
Q04207	2.93E-02	0.69	Transcription factor p65	Rela	
Q62351	1.20E-03	0.49	Transferrin receptor protein 1	Tfrc	Yes

Q6PFR5	8.88E-03	0.69	Transformer-2 protein homolog alpha	Tra2a	
Q9JJ11	6.05E-03	0.51	Transforming acidic coiled-coil-containing protein 3	Tacc3	
P58021	1.83E-03	0.45	Transmembrane 9 superfamily member 2	Tm9sf2	Yes
Q9ET30	2.45E-05	0.65	Transmembrane 9 superfamily member 3	Tm9sf3	Yes
Q9CXE7	7.63E-02	0.38	Transmembrane emp24 domain-containing protein 5	Tmed5	Yes
Q9DBS1	1.88E-03	0.60	Transmembrane protein 43	Tmem43	Yes
Q8C7V3	1.41E-01	0.46	U3 small nucleolar RNA-associated protein 15 homolog	Utp15	
P62313	6.36E-04	0.16	U6 snRNA-associated Sm-like protein LSm6	Lsm6	
Q9CQQ8	4.64E-03	0.09	U6 snRNA-associated Sm-like protein LSm7	Lsm7	
Q9D1C1	5.84E-05	0.52	Ubiquitin-conjugating enzyme E2 C	Ube2c	
Q6P5E4	6.77E-04	0.68	UDP-glucose:glycoprotein glucosyltransferase 1	Uggt1	Yes
P23949	7.78E-01	0.63	Zinc finger protein 36. C3H1 type-like 2	Zfp36l2	
A2AKY4	3.81E-04	0.55	Zinc finger protein 804A	Znf804a	

Table S2. Effect of mycolactone treatment on potential mediators of ERAD. PNGase, Golgi mannosidase I, EDEM1, EDEM2, EDEM3, Derlin-2, Derlin-3, Erdj5, ER mannosidase I, XTP3-B, Gp78, Sec61α2 and Sec61β were not detected. Proteins found significantly upregulated (FDR ≤ 0.1; $\log_2$(Variation) > 0.5) or downregulated (FDR ≤ 0.1; $\log_2$(Variation) < -0.5) by mycolactone are highlighted in dark and light gray. respectively.

FDR	Variation[a]	Protein name[b]	Gene name[b]	Sec61 substrate
4.73E-03	9.17	Homocysteine-responsive ER-resident ubiquitin-like domain member 1 protein	Herpud1	Yes
2.45E-02	3.95	Selenoprotein S	Vimp	Yes
3.65E-03	1.93	Ancient ubiquitous protein 1	Aup1	Yes
1.68E-02	2.13	Ubiquitin-conjugating enzyme E2 J1	Ube2j1	No
3.20E-03	1.89	Protein transport protein Sec61 subunit α1	Sec61a1	Yes
3.02E-02	1.70	FAS-associated factor 2	Faf2/ubxD8	No
1.45E-02	1.65	Heat shock protein (HSP 90)-α	Hsp90aa1	No
5.43E-02	1.37	HSP 90-β	Hsp90ab1	No
3.94E-01	1.29	E3 ubiquitin-protein ligase synoviolin	Syvn1/ hrd1	Yes
4.41E-01	1.38	Protein transport protein Sec61 subunit γ	Sec61g	No
9.32E-01	1.06	Protein sel-1 homolog 1	Sel1l	Yes
5.28E-01	0.67	Derlin-1	Derl1	Yes
8.31E-01	0.94	Ubiquitin fusion degradation protein 1 homolog	Ufd1l	No
4.64E-01	0.89	UV excision repair protein RAD23 homolog B	Rad23b/hr23b	No
1.93E-01	0.86	Transitional endoplasmic reticulum ATPase	Vcp/p97	No
2.92E-01	0.83	Nuclear protein localization protein 4 homolog	Nploc4/NPL4	No
1.00E-01	0.73	78 kDa glucose-regulated protein	Hspa5/BiP/Grp78	Yes
3.83E-02	0.63	Endoplasmin	Hsp90b1	Yes
2.24E-02	0.61	DnaJ homolog subfamily B member 11	Dnajb11/erdj3	Yes
5.41E-02	0.35	OS-9	OS-9	Yes

[a] Fold change (mycolactone/control)

[b] According to www.uniprot.org

ARTICLE 3: PROTEOMICS REVEALS SCOPE OF MYCOLACTONE-MEDIATED SEC61 BLOCKADE AND DISTINCTIVE STRESS SIGNATURE

As explained in paragraph III.1.2 of the introduction and illustrated on table 1 of Article 3, Sec61 substrates can be divided into secretory proteins and type I, type II and type III TMPs, based on the presence of a SP and the final cytosolic or luminal orientation of their N-terminal domain. We had performed our first proteome on Jurkat T cells that were pre-treated with mycolactone for 1h, then activated using PMA and ionomycin for 6h (Article 1(Baron *et al.*, 2016)). Only 51 proteins were found downregulated by mycolactone in this experiment, likely due to the short treatment time. Yet, mycolactone downregulated multiple Type I and Type II TMPs suggesting that mycolactone has a broader spectrum of activity than cotransin. Meanwhile, McKenna *et al.* reported that secretory proteins, Type I and Type II TMPs are generally susceptible to mycolactone-mediated Sec61 blockade (McKenna *et al.*, 2017). In contrast, mycolactone had no effect on Type III TMP integration. Since Type III proteins differ from other Sec61 substrates in the way they insert into Sec61 and were the only examples of mycolactone-resistant Sec61 substrates in biochemical assays of protein translocation, the authors suggested that protein resistance to mycolactone depends on how the protein initially engage the translocon.

Our second proteomic study performed in MutuDCs brought additional information regarding the differential susceptibility of the various types of Sec61 clients. While initially meant to ascertain the effects of mycolactone on mediators of antigen cross-presentation and ERAD, it quickly grew into a powerful resource for further analyzing the substrate selectivity of mycolactone blockade of Sec61. I completed these datasets by adding a third proteome, acquired on the MED17.11 dorsal root ganglion cell line, a model of sensory neuron. With these three independent proteomic datasets, I decided to conduct an integrated analysis aiming at (i) examining the relevance of the McKenna model of Sec61 substrate susceptibility to mycolactone in a biological setting, (ii) delineating the impact of mycolactone on the proteome of sensory neurons and (iii) characterizing the secondary effects of Sec61 blockade in living cells.

In all cell lines studied, mycolactone treatment impacted the cell proteome by downregulating a subset of proteins composed of 81%, 62% and 79% of Sec61 substrates in Jurkat T cells, MutuDC and MED17.11 respectively. Consistent with mycolactone targeting Sec61, no mitochondrial

membrane protein and only a single tail-anchored (TA) protein was affected. Among Sec61 substrates, we found that secretory proteins (65%) were the most uniformly downregulated proteins, followed by Type I (44%), Type II (22%) and Type III (0%) TMPs. Type III transmembrane proteins are rarer, representing about 5% of membrane proteins in humans, yet none of the 28 type III TMPs detected in MutuDC were downregulated by mycolactone, supporting McKenna's prediction that Type III TMPs resist mycolactone inhibition (McKenna *et al.*, 2017). Type II TMPs displayed an intermediate phenotype, with a relatively low incidence of mycolactone-downregulated proteins compared with secretory proteins and Type I TMPs, and the presence of mycolactone-upregulated proteins, leaving open the question of whether they contain mycolactone resistant elements. In general, proteins with a signal peptide (secretory, type I) and to a lesser extent, all those that enter using a hairpin loop conformation (secretory, type I and type II) were susceptible to mycolactone-mediated inhibition, whereas proteins entering in a headfirst conformation (type III) were resistant. Multi-pass TMPs behaved very similarly to single-pass proteins, although the higher proportion of type II and type III among multi-pass TMPs results in them being more resistant to mycolactone overall.

Interestingly, I found little overlap between mycolactone-altered proteins across Jurkat T cells, MutuDCs and MED17.11 neurons, suggesting that Sec61 blockade affects total proteomes in a cell-type specific manner, because of differences in Sec61 client expression and turnover rates. Differences in the duration of mycolactone treatments may also account for variations its inhibitory effects across experiments. Notably, beta-2 microglobulin (β2m, a component of the class I major histocompatibility complex) and cation-dependent mannose-6-phosphate receptor (M6PR) were downregulated by mycolactone in all cell types, probably due to their ubiquitous expression and high sensitivity to mycolactone.

I was surprised to find that 170 proteins were upregulated in response to mycolactone in the MutuDC proteome, and among them a significant amount of Sec61 substrates, mostly type II and III TMPs. I investigated one of the upregulated type II TMPs, the amino acid transporter Slc3a2 (Soluble carrier 3a2) and confirmed its upregulation by flow cytometry analysis. Moreover, I found that Slc3a2 mRNA levels were greatly induced by mycolactone treatment. However, Slc3a2 was not resistant to mycolactone blockade of translocation in a cell-free translocation assay, indicating that sufficient induction of mRNA can compensate for mycolactone-blockade of Sec61 in some cases.

Slc3a2 is a known target of the transcription factor ATF4, and other targets of the ATF4 transcription factor were greatly enriched among mycolactone targets. An unbiased gene ontology analysis revealed that mycolactone-upregulated proteins were significantly enriched in mediators of the UPR, protein exit from the ER, and to a lesser extent with proteins involved in tRNA aminoacylation for protein translation and positive regulation of tyrosine kinase activity, suggesting that mycolactone-mediated Sec61 blockade activates stress responses.

Meanwhile, Ogbechi *et al.* reported that mycolactone induces the ISR in RAW264.7 and HeLa cells without activating ER stress sensors, driving cytotoxicity via the ATF4/CHOP/Bcl-2/Bim route (Ogbechi *et al.*, 2018). Our studies in DCs led to comparable conclusions with regard to mycolactone stimulating ATF4/CHOP signaling, however we detected ER stress-specific activation signals within hours of treatment. Mycolactone-driven ER stress nevertheless differed from conventional UPR by the downregulation of BiP, a master regulator of the UPR that is normally induced by canonical ER stress. While mycolactone-driven ATF4 induction results primarily from ISR or UPR may thus depend on the cell type, both studies support the view that mycolactone-mediated cytotoxicity is a late consequence of Sec61 blockade, resulting from the induction of chronic stress triggering apoptosis via the ATF4/CHOP/Bim signaling pathway.

Research Article

Proteomics Reveals Scope of Mycolactone-mediated Sec61 Blockade and Distinctive Stress Signature*[S]

Jean-David Morel‡§, Anja O. Paatero¶, Jiajie Wei‖, Jonathan W. Yewdell‖, Laure Guenin-Macé‡§, Delphi Van Haver‡‡§§, Francis Impens**‡‡§§, Natalia Pietrosemoli¶¶, Ville O. Paavilainen¶, and Caroline Demangel‡§‖‖**

Mycolactone is a bacteria-derived macrolide that blocks the biogenesis of a large array of secretory and integral transmembrane proteins (TMP) through potent inhibition of the Sec61 translocon. Here, we used quantitative proteomics to delineate the direct and indirect effects of mycolactone-mediated Sec61 blockade in living cells. In T lymphocytes, dendritic cells and sensory neurons, Sec61 substrates downregulated by mycolactone were in order of incidence: secretory proteins (with a signal peptide but no transmembrane domain), TMPs with a signal peptide (Type I) and TMPs without signal peptide and a cytosolic N terminus (Type II). TMPs without a signal peptide and the opposite N terminus topology (Type III) were refractory to mycolactone inhibition. This rule applied comparably to single- and multi-pass TMPs, and extended to exogenous viral proteins. Parallel to its broad-spectrum inhibition of Sec61-mediated protein translocation, mycolactone rapidly induced cytosolic chaperones Hsp70/Hsp90. Moreover, it activated an atypical endoplasmic reticulum stress response, differing from conventional unfolded protein response by the down-regulation of Bip. In addition to refining our mechanistic understanding of Sec61 inhibition by mycolactone, our findings thus reveal that Sec61 blockade induces proteostatic stress in the cytosol and the endoplasmic reticulum. ***Molecular & Cellular Proteomics 16: 1–16, 2018. DOI: 10.1074/mcp.RA118.000824.***

Mycolactone is a polyketide synthase-derived macrolide produced by *Mycobacterium ulcerans*, the skin pathogen causing Buruli ulcer disease (1). In addition to inducing local skin tissue destruction and analgesia, mycolactone diffuses in infected hosts to dampen immune responses at the systemic level (2). Recent findings demonstrate that mycolactone targets the central subunit of the Sec61 translocon, preventing import of newly synthesized Sec61 substrates into the endoplasmic reticulum (ER)[1], and resulting in their cytosolic degradation by the ubiquitin-proteasome system (3, 4). Contrary to the Sec61 inhibitor cotransin, mycolactone is broadly active toward Sec61 substrates. *In vitro* assays of protein translocation (IVT) nevertheless identified several single- and multi-pass transmembrane proteins (TMPs) resisting its inhibitory action (3, 5, 6). The factors governing Sec61 substrate susceptibility or resistance to mycolactone are only partially understood.

Sec61 substrates include secretory and integral transmembrane proteins (TMPs), which can be divided into Type I, II or III, according to the presence of a signal peptide (SP) and the orientation of the protein N terminus at the ER membrane (7) (Table I and Fig. 6). We classified as secretory all Sec61 substrates with a SP and without transmembrane domain (TMD). This encompasses secreted proteins and most ER-, Golgi-, endosome- and lysosome-resident proteins, as well as proteins containing a glycosylphosphatidylinisotol-anchoring motif. Type I TMPs contain a SP and at least one downstream TMD for initial insertion in the ER membrane, whereas Type II and Type III TMPs do not contain a SP. In Type I and Type III TMPs, the first N-terminal TMD is in a N-lumenal/C-cytosolic orientation at the ER membrane. In Type II TMPs, the N terminus of the initial TMD is on the lumenal side of the ER membrane. By testing the effects of mycolactone on the translocation of TMPs representing each category of Sec61 substrates in cell-free systems, McKenna *et al.* found that secretory proteins, Type I and Type II TMPs are generally susceptible to mycolactone-mediated Sec61 blockade (5, 6). Partial resistance to mycolactone was observed for some Type I TMPs, depending on their TMD hydrophobicity and

From the ‡Immunobiology of Infection Unit, Institut Pasteur, 75015 Paris, France; §INSERM, U1221, 75005 Paris, France; ¶Institute of Biotechnology, University of Helsinki, 00014 Helsinki, Finland; ‖Laboratory of Viral Diseases, National Institute of Allergy and Infectious Diseases, National Institutes of Health, Bethesda, Maryland 20892; **VIB-UGent Center for Medical Biotechnology, 9000 Ghent, Belgium; ‡‡VIB Proteomics Core, 9000 Ghent, Belgium; §§Department of Biochemistry, Ghent University, 9000 Ghent, Belgium; ¶¶Bioinformatics and Biostatistics Hub, Center of Bioinformatics, Biostatistics, and Integrative Biology, Institut Pasteur, Unité de Service et de Recherche 3756 Institut Pasteur CNRS, 75015 Paris, France

Received for publication, September 26, 2017, and in revised form, June 17, 2018
Published, MCP Papers in Press, June 18, 2018, DOI 10.1074/mcp.RA118.000824

TABLE I

Sec61 substrate classification used in this study. The four types of Sec61 substrates are shown, with characteristic topogenic determinants and mode of insertion in Sec61: Signal peptide (SP, blue segment), final orientation (FO) of the first N-terminal transmembrane domain (TMD, pink). The differential susceptibility of each type of Sec61 sustrates to mycolactone-mediated Sec61 blockade, as proposed by McKenna et al. (6), is indicated (Myco)

Type	SP	FO	Myco[a]	Insertion mode
Sec[b]	Yes	No TMD	S	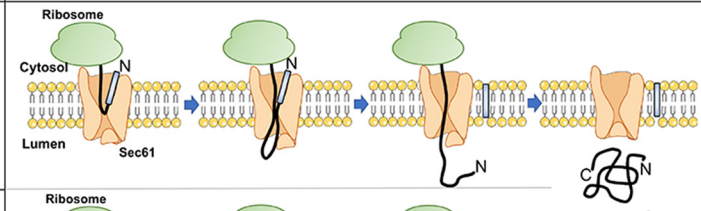
I	Yes	Lumenal	S[c]	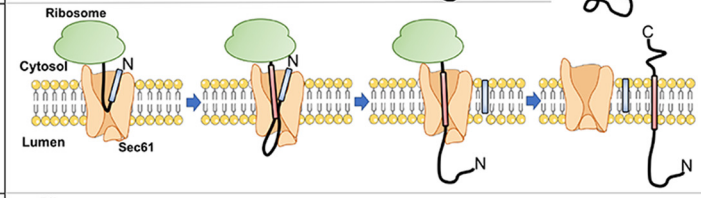
II	No	Cytosolic	S[d]	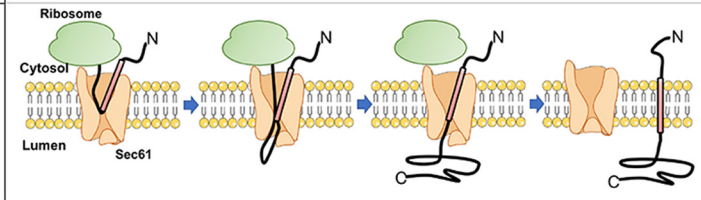
III	No	Lumenal	R	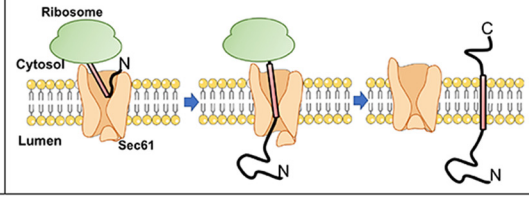

[a]S: Susceptible; R: Resistant.
[b]Secretory.
[c]Partial resistance possible, depending on TMD hydrophobicity and lumenal domain size.
[d]Type II TMPs with a short N-terminal domain may be trapped by mycolactone in an inverted orientation.

lumenal domain size. In contrast, mycolactone had no effect on Type III TMP integration. Because Type III proteins differ from other Sec61 substrates in the way they insert into Sec61 (Table I), and were the only examples of mycolactone-resistant Sec61 substrates in IVT, the authors suggested that protein resistance to mycolactone essentially depends on how the protein initially engage the translocon. Whether this model applies to multi-pass TMPs, and explains all biological effects of mycolactone remained to be addressed.

In addition to inducing skin necrosis at the site of infection, bacterial production of mycolactone during infection has been associated with defective induction of pain and immune responses in infected hosts (3, 8–14). By profiling mycolactone-downregulated proteins in dendritic cells and Jurkat T cells exposed to mycolactone *in vitro* (3, 15), we were able to connect Sec61 blockade with alterations in immune cell functions such as cytokine production, cytokine signaling, antigen

[1] The abbreviations used are: ER, endoplasmic reticulum; AGTR2, type 2 angiotensin II receptors; bFGF, basic fibroblast growth factor; β_2M, beta 2 microglobulin; cAMP, cyclic adenosine monophosphate; DMSO, dimethyl sulfoxide; DMEM, Dulbecco's Modified Eagle's medium; DTT, 1,4-dithiothreitol; ECM, Extracellular Matrix; FCS, fetal calf serum; FDR, false discovery rate; GOT, Gene Ontology Terms; Hepes, 4-(2-hydroxyethyl)-1-piperazineethanesulfonic acid; Hsp, heat shock protein; IMDM, Iscove's Modified Dulbecco's medium; IAV, Influenza A virus; LC-MS, liquid chromatography-mass spectrometry; ISR, integrated stress response; IVT, *in vitro* protein translocation assay; MHC, major histocompatibility complex; mTOR, mammalian target of rapamycin; PBS, phosphate-buffered saline; PCR, polymerase chain reaction; RPMI, Roswell Park Memorial Institute medium; SDS-PAGE, sodium dodecyl sulfate polyacrylamide gel electrophoresis; SEM, standard error of the mean; SP, signal peptide; SRM, sheep rough microsomes; TMD, transmembrane domain; TMP, transmembrane protein; UPR, unfolded protein response; wt, wild type.

TABLE II
Experimental conditions and result of proteomic studies

Cell line	Mycolactone treatment	Cell activation	Sample size (n)[b]	Proteomic approach	Total quantified proteins[c]	Ref
Jurkat (T cell)	40 nM, 7h	PMA/IO[a], 6h (1h post mycolactone)	n=2 (Mycolactone/DMSO) pairs labelled in mirror conditions	SILAC LC-MS/MS	4585 (51/2)	(3)
MutuDC (dendritic cell)	100 nM, 24h	-	Mycolactone-treated (n=3) DMSO vehicle control (n=3)	Label-Free LC-MS/MS	3206 (208/170)	(15)
MED17.11 (sensory neuron)	25 nM, 16h	No activation	Mycolactone-treated (n=2) DMSO vehicle control (n=3)	Label-Free LC-MS/MS	3562 (45/8)	This study
		LPS, 15h30 (30 min post mycolactone)	Mycolactone-treated (n=3) DMSO vehicle control (n=3)		3562 (27/3)	

[a]Phorbol myristate acetate/ionomycin.
[b]Biological replicates.
[c]Total number (mycolactone-downregulated/mycolactone-upregulated).

presentation and cell migration. With regard to analgesia, mycolactone was shown to activate type 2 angiotensin II receptors (AGTR2) expressed by sensory neurons, leading to cell hyperpolarization and defective pain transmission (12). Our observations that mycolactone prevents the release of inflammatory mediators by nervous cells *in vitro*, and development of inflammatory pain *in vivo*, indicated that mycolactone-mediated Sec61 blockade likely contributes to the analgesic properties of mycolactone (10, 16). Further, these data suggested that Sec61 blockade may alter the functional biology of sensory neurons beyond inflammation, and interfere with AGTR2 expression and signaling.

In the present study, we have analyzed the structure and content of mycolactone-susceptible proteomes in dendritic cells, T cells and sensory neurons. Our objectives were to (1) examine the relevance of the McKenna model in a biological setting, (2) delineate the impact of mycolactone on the proteome of sensory neurons and (3) characterize the secondary effects of Sec61 blockade in living cells.

EXPERIMENTAL PROCEDURES

Experimental Design—Table II outlines the conditions used to generate each proteomic dataset, with sample size (number of biological replicates), number and type of controls, and number of proteins that were reliably quantified and modulated by mycolactone. The proteomics data corresponding to Jurkat T cells (3) and dendritic cells (15) were generated previously. Detailed information on the materials and methods used to profile mycolactone-modulated proteins in these cells can be found in the cited references. In the present study, we performed an additional proteomic analysis to characterize the effects of mycolactone on sensory neurons. We used the mouse dorsal root ganglion cell line MED17.11 as it provides a convenient model for nociceptor cell biology (17), and exposed MED17.11 neurons to mycolactone in resting or LPS-activated conditions (supplemental Table S1). In T cells, dendritic cells and MED17.11 neurons, the mycolactone treatment conditions (dose, duration) were optimized prior to proteomic analyses to achieve maximal Sec61 inhibition without inducing cytotoxicity. Statistical methods for analysis are detailed in the *Data Processing and Analysis* paragraph.

Mycolactone—Natural mycolactone A/B was purified from *M. ulcerans* bacteria (strain 1615) (18), then quantified by spectrophotometry (λmax = 362 nm; log ε = 4.29) as previously described (19). Stock solutions were prepared in DMSO, and diluted 1000 x in culture medium immediately before use in cellular assays.

DNA Constructs—The DNA transcription template for IVT analysis of human SLC3A2 was PCR amplified from a plasmid using 5′-primers containing a T7 promoter, a Kozak sequence and a region complementary to the 5′-end of the gene (SLC3A2 in pENTR221, Genome Biology Unit cloning service, Biocenter Finland, University of Helsinki). The 3′-primers contained a stop-codon and a region complementary to the 3′-end of the gene. The PCR products were purified with a PCR Clean-up kit (Macherey-Nagel) before *in vitro* transcription. The pBABE-puro vector was kindly donated by Jay Morgenstern and Hartmut Land and distributed through Addgene (Cambridge, MA) (plasmid n°1764, (20)). Sec61 wt or mutant sequences were cloned into the pBABE-puro retroviral vector, for simultaneous translation of Sec61 and puromycin resistance gene in mouse lymphoma B cells.

Cell Cultures, Flow Cytometric Studies and Viral Infection—MutuDCs (provided by Hans-Acha Orbea, University of Lausanne) were cultured in IMDM (Gibco), supplemented with 8% (v/v) FCS (Biowest-Biosera), 10 mM HEPES, 100 U/ml penicillin, 100 μg/ml streptomycin and 50 μM β-mercaptoethanol (all from Life Technologies). Flow cytometric studies of MutuDCs used anti-mouse MHC I (H2-K^b)-PE (eBioscience 12–5958-80), biotin-conjugated anti-mouse MHC II (I-A/I-E) (BD 553622) with APC-streptavidin (BD 554067), and anti-CD98 (Biolegend 128207). Flow cytometric acquisitions were conducted on an Accuri C6 (BD Biosciences) and analyzed by FlowJo software (TreeStar, Ashland, OR). To induce the UPR response, we used Tunicamycin 1 μM (Sigma T7765), Thapsigargin 1 μM (Sigma T9033) or 1 μM MG132 (Selleckchem S2619). MED17.11 (kindly provided by Mohammed Nassar, University of Sheffield) were cultured in DMEM/F12 Glutamax (Gibco), supplemented with 10% FCS (Bio-

west-Biosera), 10 ng/ml bFGF (Peprotech), 0.5 mM di-butryl cAMP (Sigma), 25 μM Forskolin (ApexBio Technology), 5 μg/ml Y-27632 (Focus Biomolecules), 100 ng/ml NGF (R&D Systems), 10 ng/ml GDNF (Peprotech) and 100 U/ml penicillin, 100 μg/ml streptomycin (Life Technologies). For Influenza A virus (IAV) infection assays, we used HEK293-K^b cells maintained in DMEM with 7.5% FBS in a 9% CO_2 incubator. Recombinant IAV PR8 (A/Puerto Rico/8/34 H1N1) was grown in 10-day embryonated chicken eggs, and used as infectious allantoic fluid. HEK293 cells were resuspended in FCS-free acidified RPMI 1640 medium, infected with IAV at a multiplicity of infection of 10 at 37 °C for 1h, and then subcultured in the presence or absence of 125 nM mycolactone. At the indicated time points, an aliquot of 10^6 cells was removed, stained with antibodies and analyzed by flow cytometry using the following monoclonal antibodies: NA2–1C1 (anti-NA), H36–26 (anti-HA), O19 (anti-M2), BBM.1 (anti-beta 2 microglobulin), and HB54 (anti-HLA-A2). These antibodies were labeled with Pacific Orange, Alexa Fluor 647 or Alexa Fluor 488, using protein labeling kits from Life Technologies following the manufacturer's recommended protocols. Flow cytometric acquisitions were conducted on an LSR Fortessa X-20 flow cytometer (BD Biosciences) and analyzed by FlowJo software (TreeStar, Ashland, OR). Mouse v-Abl lymphoma B cells were kindly donated by Ludovic Deriano (Institut Pasteur, Paris). They were transduced with retroviruses prepared with the pBABE-Sec61-puro wt or R66G vectors as described in (3), and selected with 2 μg/ml puromycin over 1 week.

Quantitative Real-Time PCR (qPCR)—Total RNA was extracted from MutuDC using Qiazol lysis reagent (Qiagen), then purified using Qiagen RNeasy Mini Kit and digested with RNase-Free DNase set (Qiagen 79254) for 15 min at room temperature. First-strand cDNA was synthesized from 1 μg of total RNA with the high capacity cDNA reverse transcription kit (Applied Biosystems 4368814). Expression was quantified using Power SybR Green PCR Master Mix (Applied Biosystems 4367659) and gene-specific primers (supplemental Table S2). Amplification was performed in duplicate, from 5 ng of cDNA template in a final volume of 20 μl in a 96-well PCR plate. Amplification conditions were 2 min at 50 °C, 10 min at 95 °C, followed by 40 cycles of 15 s at 95 °C and 1 min at 60 °C on a StepOnePlus Real-time PCR System (Applied Biosystems). Results were normalized with the $2^{-\Delta\Delta Ct}$ method by using Rpl-19 as an endogenous control.

IVT Assay—Protein translocation assays were performed as described in (21). DNA templates were transcribed with T7 Polymerase (New England Biolabs) for 1–2 h at 37 °C and used used without purification in subsequent translation/translocation reactions. The reactions were assembled at 0 °C in the presence of mycolactone or an equivalent volume of DMSO. Reactions included ^{35}S-Methionine (Perkin Elmer, 2 μCi per 10 μl translation), RNasin (NEB, #M0314S) 10 U per 10 μl, and Sheep Rough Microsomes (SRM) (22). The amount of SRM was optimized to be 0.25 μl per 10 μl reaction. Translation was initiated by transferring the reactions to 32 °C for 60 min after which they were returned on ice. Reactions were then mixed with an equal volume of 2x High-Salt Buffer (50 mM Hepes, pH 7.8, 1 M KAc, 10 mM $MgAc_2$). The samples were centrifuged at 49,000 rpm for 10 min at 4 °C in a S100-AT3 rotor (Thermo Scientific) through a sucrose cushion in 1 × High Salt Buffer (50 mM Hepes, pH 7.8, 0.5 M KAc, 5 mM $MgAc_2$, 0.5 M sucrose) and the pelleted SRMs with associated translated nascent polypeptides were retrieved. The control reaction without SRMs was analyzed without pelleting. Endoglycosidase H treatment (500 U/reaction, 37 °C, overnight, NEB #P0702S) was performed with the manufacturer's buffer system, to demonstrate that differences in CD98 gel migration are based on glycosylation. After trichloroacetic acid precipitation, the synthesized polypeptides were analyzed by SDS-PAGE and autoradiography. SDS-PAGE analysis was performed either with 12% Tris/Tricine polyacrylamide gels containing 0.5% trichloroethanol (25) for stain-free total protein detection or TGX stain-free gradient gels (Bio-Rad). The dried gels were exposed on a storage phosphorus screen (GE Healthcare) and imaged on a Typhoon Trio phosphorimager (GE Healthcare).

Proteomic Analysis—MED17.11 cells (10^7 cells, $n = 3$) were treated with 25 nM mycolactone or DMSO vehicle for 16h, with or without activation with 10 nM LPS after 30 min of exposure to mycolactone. Cells in each condition were harvested and washed twice with PBS. The resulting cell pellets were re-suspended in 4 ml lysis buffer (1 mg/ml amphipol A8–35 (Anatrace) in 50 mM ammonium bicarbonate pH 8.0) and further processed as described in (23). Briefly, lysates were sonicated (three bursts of 15 s at an amplitude of 20%) and centrifuged for 15 min at 20,000 × *g* at 4 °C to remove insoluble material. The protein concentration in the supernatants was measured using a Bradford assay (Bio-Rad) and 1 ml of each sample containing ~1 mg of total protein was used to continue the protocol. Proteins in each sample were reduced by addition of 20 mM DTT and incubation for 30 min at 55 °C, and then alkylated by addition of 40 mM iodoacetamide and incubation for 15 min at room temperature in the dark. Samples were acidified with 5% formic acid to pH 3.0 and precipitated proteins and amphipol were pelleted by centrifugation for 10 min at 20,000 × *g* at room temperature. The resulting protein pellet was washed once with 500 μl water and redissolved in 1 ml 50 mM ammonium bicarbonate pH 8.0. Proteins were digested with 4 μg LysC (Wako) (1/250, w/w) for 4h at 37 °C and then digested with 4 μg trypsin (Promega) (1/250, w/w) overnight at 37 °C. The resulting peptide mixture was acidified by addition of 10% trifluoroacetic acid (TFA) to pH 3.0 and samples were centrifuged for 10 min at 20,000 × *g* at room temperature to remove amphipol. Purified peptides were dried completely by vacuum drying, re-dissolved in loading solvent A (0.1% TFA in water/acetonitrile (98:2, v/v)) and 3 μg was injected for LC-MS/MS analysis on an Ultimate 3000 RSLCnano System (Thermo) in-line connected to a Q Exactive HF mass spectrometer equipped with a Nanospray Flex Ion source (Thermo). Trapping was performed at 10 μl/min for 4 min in solvent A (on a reverse-phase column produced in-house, 100 μm I.D. x 20 mm, 5 μm beads C18 Reprosil-Pur, Dr. Maisch) followed by loading the sample on a 40 cm column packed in the needle (produced in-house, 75 μm I.D. × 400 mm, 1.9 μm beads C18 Reprosil-HD, Dr. Maisch). Peptides were eluted by an increase in solvent B (0.1% formic acid in water/acetonitrile (2:8, v/v)) in linear gradients from 2% to 30% in 100 min, then from 30% to 56% in 40 min and finally from 56% to 99% in 5 min, all at a constant flow rate of 250 nl/min. The column temperature was kept constant at 50 °C (CoControl 3.3.05, Sonation). The mass spectrometer was operated in data-dependent mode, automatically switching between MS and MS/MS acquisition for the 16 most abundant ion peaks per MS spectrum. Full-scan MS spectra (375–1500 m/z) were acquired at a resolution of 60,000 after accumulation to a target value of 3,000,000 with a maximum fill time of 60 ms. The 16 most intense ions above a threshold value of 13,000 were isolated (window of 1.5 Thomson) for fragmentation at a normalized collision energy of 28% after filling the trap at a target value of 100,000 for maximum 80 ms. The S-lens RF level was set at 55 and we excluded precursor ions with single and unassigned charge states.

Data Processing and Analysis—Data analysis was performed with MaxQuant (version 1.6.0.16) (24) using the Andromeda search engine with default search settings including a false discovery rate set at 1% on both the peptide and protein level. Spectra were searched against the mouse proteins in the Uniprot/Swiss-Prot database (September 2017 version, www.uniprot.org, containing 16,840 entries) with a mass tolerance for precursor and fragment ions of 4.5 and 20 ppm, respectively, during the main search. Enzyme specificity was set as C-terminal to arginine and lysine, also allowing cleavage at proline bonds and a maximum of two missed cleavages. Variable modifica-

tions were set to oxidation of methionine residues and acetylation of protein N termini. Carbamidomethyl formation of cysteine residues was set as a fixed modification. Proteins with at least one unique or razor peptide were retained, then quantified by the MaxLFQ algorithm integrated in the MaxQuant software (25). A minimum ratio count of two unique or razor peptides was required for quantification. Further data analysis was performed with the Perseus software (version 1.5.4.1) after loading the protein groups file from MaxQuant. Proteins only identified by site, reverse database hits and potential contaminants were removed and replicate samples were grouped. Proteins with less than three valid values in at least one group were removed and missing values were imputed from a normal distribution around the detection limit. The statistical analysis to determine differentially expressed proteins was performed in R software (version 3.3.2) using the *limma* package. *p* values were corrected for multiple testing using the Benjamini-Hochberg method to obtain a False Discovery Rate (FDR). Proteins with a FDR $\leq$ 0,1 and a $\log_2$ mycolactone/control LFQ intensity fold change ($\log_2$ FC) $>$ 0.5 were considered upregulated by mycolactone, whereas proteins with a FDR $\leq$ 0.1 and a $\log_2$ FC $<$ -0.5 were considered downregulated.

Protein Annotation and Gene Ontology Analysis—Annotations of SP and TMD positions were downloaded from the Uniprot/Swiss-Prot database. Proteins with a single TMD located less than 20 amino acid residues from the C terminus were labeled as C-tail anchored proteins, and all proteins annotated with a mitochondrial localization were labeled as mitochondrial proteins. Other proteins with a SP and/or at least one TMD were considered Sec61 substrates and classified as secretory protein, Type I, II, or III TMP according to the criteria described in Table I. Proteins missing information needed for classification were excluded from the analysis. Gene ontology analysis was performed using the GoStats package on R software (version 3.3.2). A hypergeometric test was used to rank gene ontology terms (GOT) pertaining to biological processes, then redundant terms were removed using the REVIGO online software (26) and the four most significant terms were retained (Table III).

Statistics—The Graphpad Prism software (6.0; La Jolla, CA) was used for statistical comparisons and graphical representations. Values of $p \leq 0.05$ were considered significant.

RESULTS

Conserved and Variable Features of Mycolactone-induced Proteomic Alterations—In previous studies using activated Jurkat T cells and MutuDCs, mycolactone-mediated Sec61 blockade impacted the cell proteome by downregulating a subset of proteins primarily composed of Sec61 substrates (3, 15). As shown in Fig. 1*A*, Sec61 substrates constituted 81 and 62% of mycolactone-downregulated proteins in Jurkat T cells and MutuDCs respectively, whereas their incidence in "all quantified" proteins was close to 10%. This distinctive alteration of the proteome was conserved in mycolactone-exposed MED17.11 neurons, in both resting and LPS-stimulated conditions (Figs. 1*A* and supplemental Fig. S1, supplemental Table S1). At the same time, we detected proteins that were significantly upregulated by mycolactone in each proteome. Although limited to 2 and 8 proteins, respectively, in Jurkat T cells and MED17.11 neurons exposed to mycolactone, 170 proteins were upregulated by mycolactone in MutuDCs, with a clear preference for Sec61 substrates (Fig. 1*A*). We next sought to compare mycolactone-upregulated and -downregulated proteins across cell types, by matching the genes of all proteins detected in Jurkat T cells with their mouse orthologs, which was possible for 2032 of 4585. We observed little overlap between mycolactone-altered proteins across Jurkat T cells, MutuDCs and MED17.11 neurons (Fig. 1*B*). Among proteins that were detected and conserved across species, those modulated by mycolactone in only one cell type were not modulated in others (supplemental Table S3). Together, our data in Figs. 1*A* and 1*B* thus support the view that mycolactone-mediated Sec61 blockade affect total proteomes in a cell-type specific manner, because of differences in Sec61 client turnover rates. Differences in the duration of mycolactone treatments may also account for variations in the magnitude of its inhibitory effects across experiments. Of note, beta-2 microglobulin (β2m, a component of the class I major histocompatibility complex) and cation-dependent mannose-6-phosphate receptor (M6PR) were downregulated by mycolactone in all cell types, thus representing potential markers of its activity.

Primary Determinants of Sec61 Substrate Susceptibility or Resistance to Mycolactone—We initially analyzed the relative incidence of each category of Sec61 substrates (as defined in Table I) among mycolactone-downregulated proteins. Proteomic analyses were performed on cell extracts, and consequently secreted proteins could not be analyzed. Yet, $>$100 secretory, organelle-resident proteins were reliably quantified in MutuDCs, allowing statistical comparisons in the protein datasets from this cell type. The highest proportion of mycolactone-downregulated proteins was found in secretory proteins (65%), followed by Type I (44%), Type II (22%) and Type III (0%) TMPs (Fig. 2*A*). In all three studied cell types, presence of a SP in a Sec61 substrate was highly predictive of its down-regulation by mycolactone (Fig. 2*B*). The near complete absence of mycolactone-upregulated proteins in secretory proteins and Type I TMPs was consistent with SP-bearing Sec61 substrates being globally susceptible to mycolactone inhibition. At the opposite end of the spectrum, no Type III TMPs were downregulated by mycolactone. In this regard, Type III TMPs resembled C-terminal tail-anchored proteins and mitochondrial membrane proteins (Fig. 2*A*), which are not Sec61 substrates. This result supported McKenna's prediction that Type III TMPs resist mycolactone inhibition (6). Type II TMPs displayed an intermediate phenotype, with a relatively low incidence of mycolactone-downregulated proteins compared with secretory proteins and Type I TMPs, and the presence of mycolactone-upregulated proteins (Fig. 2*A*), leaving open the question of whether they contain mycolactone-resistant elements.

The relative incidence of mycolactone-downregulated proteins in Type I/II/III TMPs was comparable in single-pass and multi-pass TMPs (Fig. 2*C*). Similarly, to single-pass TMPs, multi-pass TMPs with a SP included a higher proportion of mycolactone-downregulated proteins than multi-pass TMPs without SP and did not contain any mycolactone-upregulated proteins (Fig. 2*D*). This observation suggested that Sec61

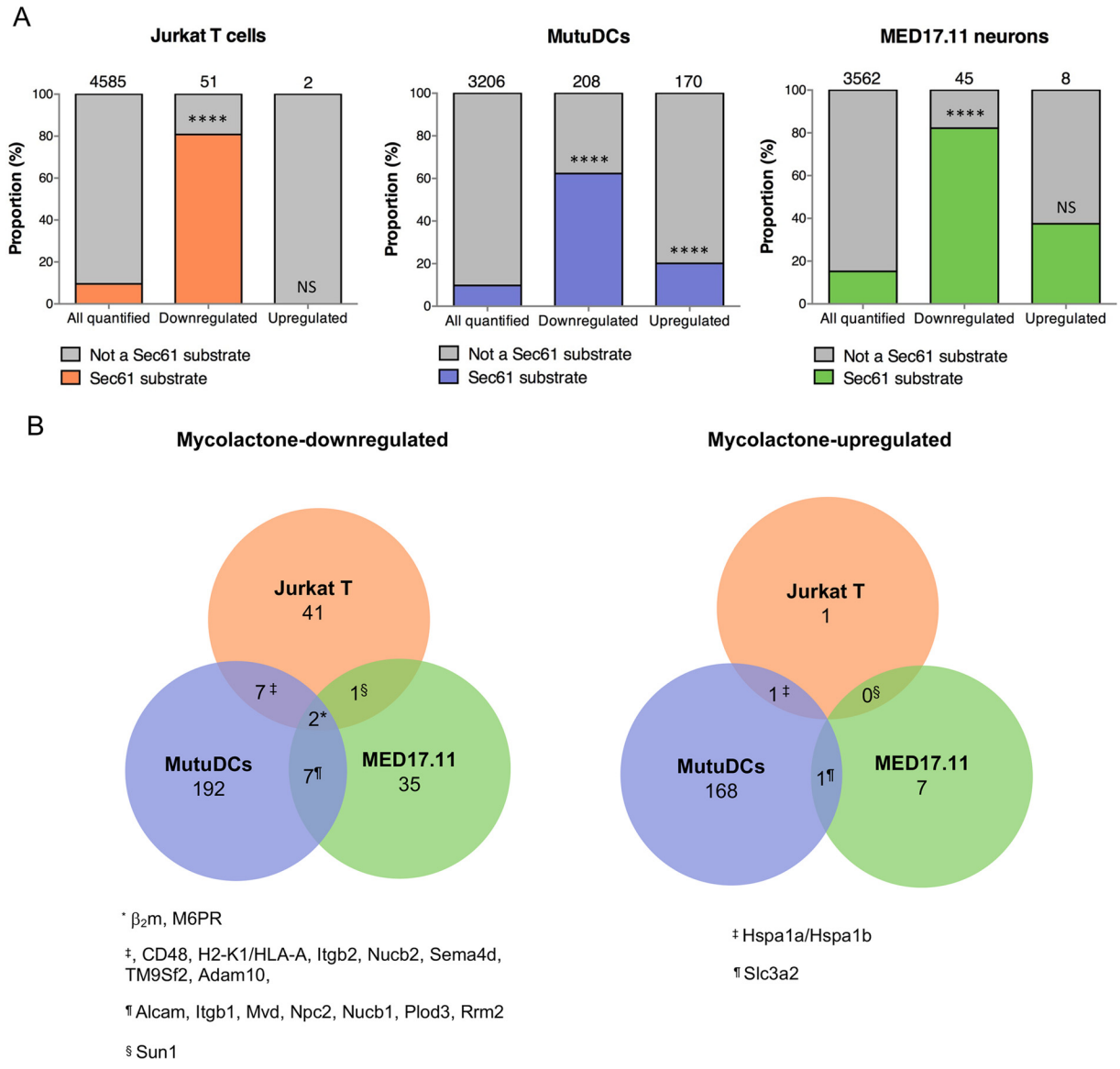

FIG. 1. **Conserved and variable features of mycolactone-induced proteomic alterations.** *A*, The proportion of Sec61 substrates in "all quantified" proteins is compared with that in "mycolactone downregulated" or "mycolactone-upregulated" proteins, in each cell type studied. Jurkat T cells (left), MutuDCs (middle) and MED17.11 cells (right) were treated with mycolactone or vehicle as control in the conditions outlined in Table II. Number of identified proteins in each subset are indicated on the top of each bar, **** p value < 0.0001, ns: not significant, Fisher exact test. *B*, Venn diagrams representing the overlap between mycolactone downregulated (left) or mycolactone-upregulated (right) proteins across cell types. Human proteins (Jurkat T cells) were matched to their mouse orthologues (MutuDCs and MED17.11 neurons). Proteins that were found downregulated or upregulated by mycolactone in 2 cell types or more are listed.

substrate susceptibility to mycolactone is primarily determined by the initial interaction between SP or first TMD of nascent polypeptides with the translocon, irrespective of the number of TMDs.

Interestingly, Type I TMPs were differentially downregulated by mycolactone. We found that the length of their N-terminal domain discriminated significantly mycolactone-downregulated proteins from the non-regulated ones (Fig. 2*E*). In line with McKenna *et al.* 's findings using genetically modified Type I TMPs (6) (Table I), this result indicated that Type I TMPs with a long N-terminal lumenal domain in the ER are relatively more sensitive to mycolactone. In contrast, N-terminal domain length did not affect Type II TMP's modulation by mycolactone (Fig. 2*F*).

Mycolactone-mediated Sec61 Blockade Prevents the Production of Viral Type I/II but not Type III TMPs—Having described the effects of mycolactone on the biogenesis of endogenous Sec61 substrates, we used influenza A virus (IAV) as a convenient model to study mycolactone's impact on production of virus-derived Sec61 substrates in infected cells. The IAV envelope contains three viral proteins, with Type I (HA), Type II (NA), and Type III (M2) topology. Mycolactone

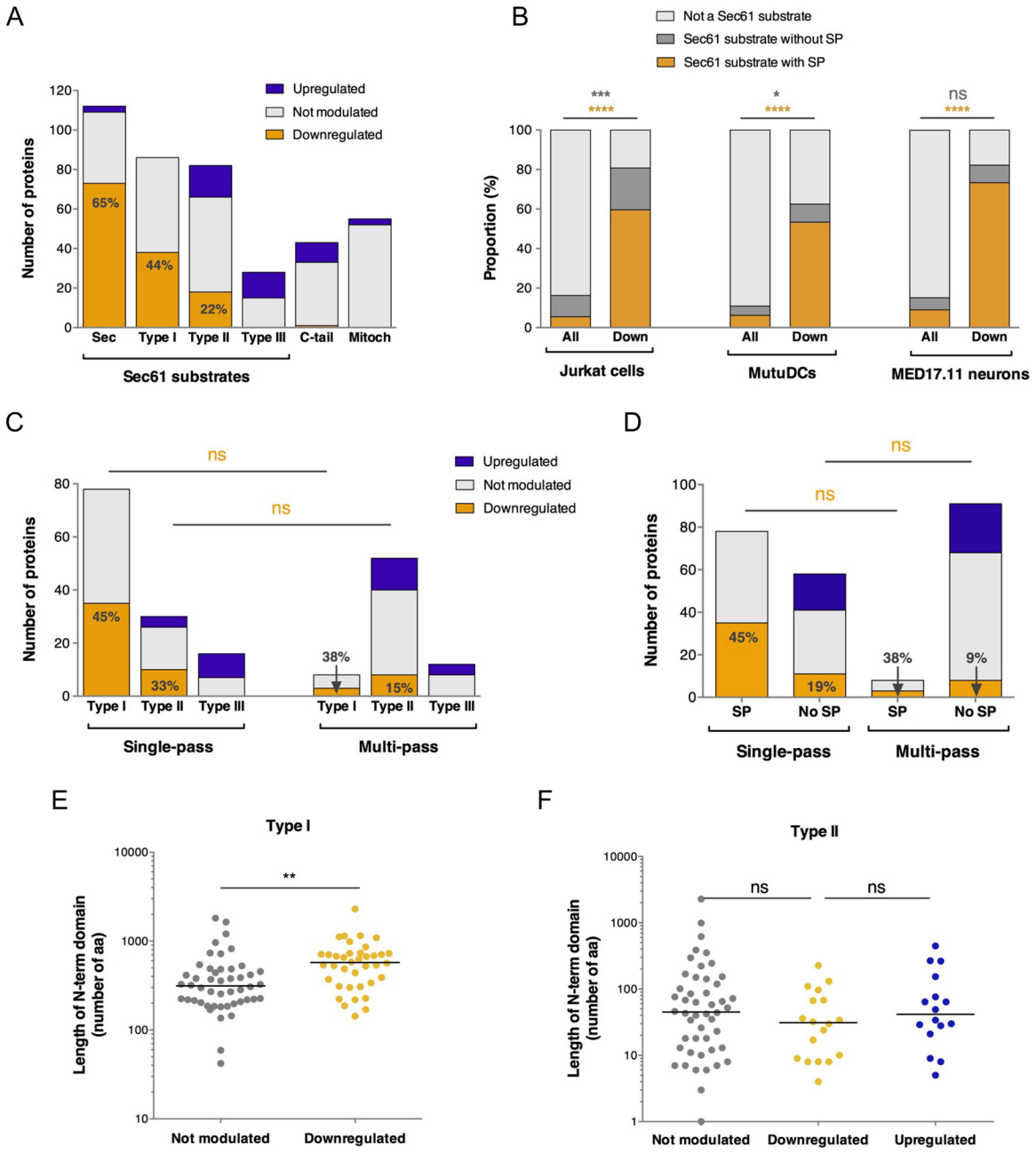

FIG. 2. **Primary determinants of Sec61 substrate susceptibility or resistance to mycolactone.** *A*, Bar plot depicting the number of proteins that were upregulated, downregulated or not significantly modulated by mycolactone in MutuDCs. Sec: secretory proteins; C-tail: C-terminal tail-anchored proteins, depending on the Guided Entry of Tail-anchor (GET) pathway for insertion into the ER membrane; Mitoch: mitochondrial membrane proteins, depending on the TIM/TOM complexes for mitochondrial membrane insertion. *B*, The proportion of Sec61 substrates with a SP (secretory + Type I TMP) or without a SP (Type II/III TMPs) in ≪ all detected ≫ proteins (All) or downregulated proteins (Down) is shown for each cell type studied. Fisher exact tests comparing the proportions of Sec61 substrates with SP (orange) or without SP (gray) to all other proteins. *$p < 0.05$; *** $p < 0.001$; **** $p < 0.0001$. *C*, The proportions of mycolactone-downregulated proteins in each class of single-pass TMPs is shown compared with those in multi-pass TMPs. *D*, The proportion of mycolactone-downregulated proteins in single-pass TMPs with or without an SP is shown compared with those in multi-pass TMPs. Fisher exact test comparing the proportion of mycolactone-downregulated proteins in each subset. ns: not significant. *E*, *F*, Scatter dot plot representing the length (in amino acid residues) of the N-terminal domain before the first TMD in Type I (*E*) and Type II (*F*) TMPs of MutuDCs. A Mann-Whitney test was used to compare mean lengths in mycolactone-downregulated proteins and proteins not modulated by mycolactone. **$p < 0.01$; ns: no significant difference.

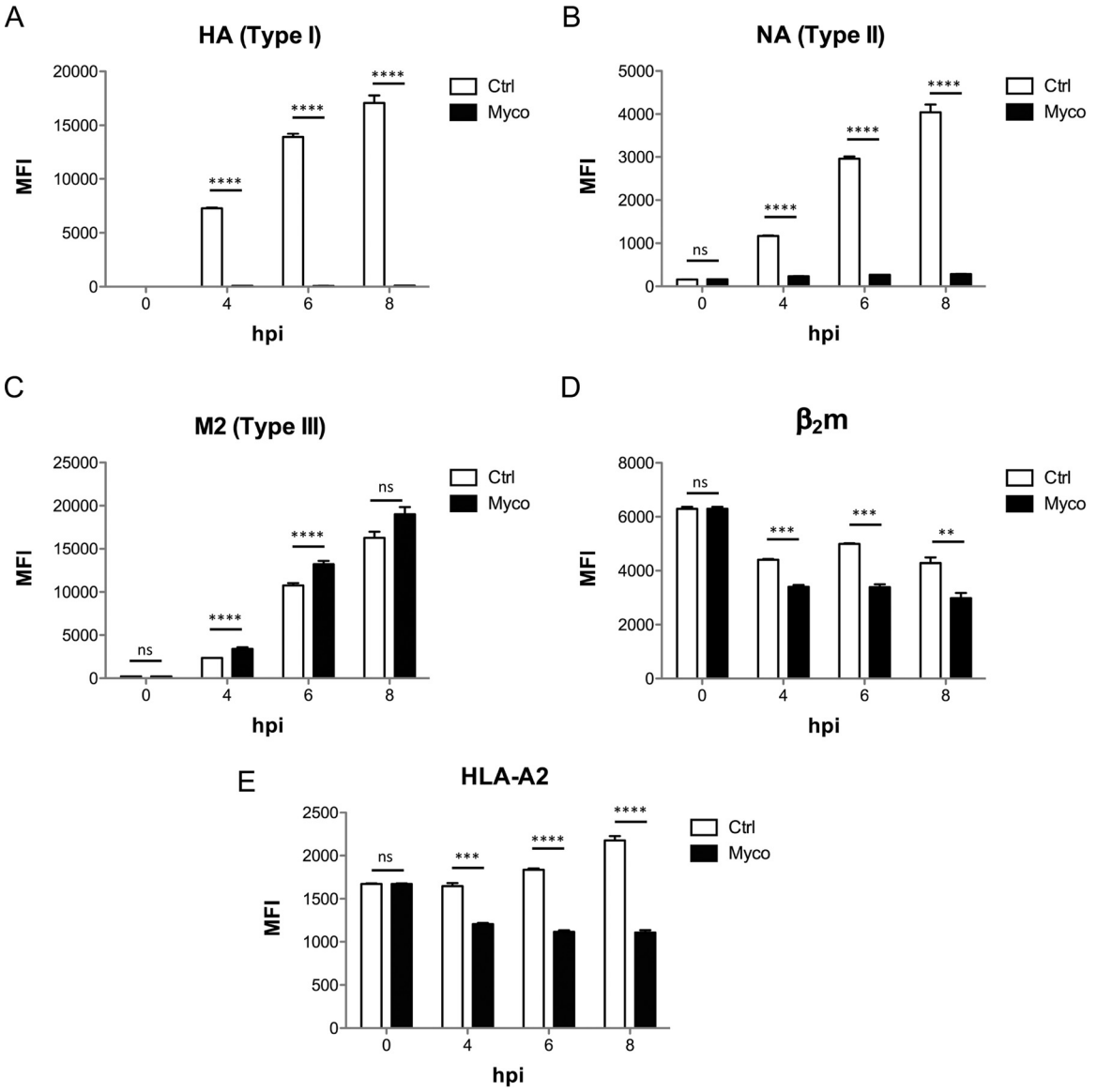

FIG. 3. **Mycolactone-mediated Sec61 blockade prevents the production of viral Type I/II but not Type III TMPs.** Surface expression of viral envelope proteins HA (*A*), NA (*B*) and M2 (*C*) as well as HLA components B2M (*D*) and HLA-A2b (*E*), in HEK293 cells infected with IAV for 1h prior to incubation with Mycolactone, or vehicle as control. MFI: mean fluorescence intensity; hpi: hours post infection. Data shown are MFI ± S.E. ($n = 3$) from one of two independent experiments, which gave similar results. MFIs of mycolactone-treated cells were compared with vehicle controls using a *t* test with Holm-Sidak correction for multiple testing. *$p < 0.05$; **$p < 0.01$; ***$p < 0.001$; ***$p < 0.001$; ns: no significant difference.

added to HEK293-K^b cells 1h post-infection with IAV efficiently prevented the cell surface expression of HA and NA, but not M2 protein (Figs. 3*A*–3*C*). In fact, the cell production of M2 was slightly elevated in mycolactone-treated cells, compared with controls (Fig. 3*C*), suggesting that inhibition of Type I/II TMP translocation may promote that of mycolactone-resistant Type III TMPs. Mycolactone treatment decreased concomitantly the cell surface expression of MHC Class I molecules, measured with antibodies specific for β_2m or HLA-A2, which are constitutively synthesized by HEK293-K^b cells (Fig. 3*D*–3*E*). These data are consistent with previous findings, showing that MHC class I heavy chains and β_2m are Sec61 substrates that are among the most susceptible to mycolactone inhibition (3, 15) (Fig. 1*B*).

Low Doses of Mycolactone Upregulate the Transcription of Selected Sec61 Substrates—We were surprised to see in MutuDCs, but also in MED17.11 cells to a limited extent, the presence of mycolactone-upregulated Sec61 substrates (Fig. 1). In MutuDCs, most mycolactone-upregulated Sec61 substrates belonged to Type II or Type III subtypes of TMPs (Fig. 2*A*). CD98 (Slc3a2/Slc7a5) is a heterodimeric receptor contributing to amino acid transport and integrin signaling (27), of

which both chains were significantly upregulated by mycolactone in MutuDCs (15). Notably, Slc3a2 was also upregulated in mycolactone-exposed MED17.11 neurons, in both resting and LPS-activated conditions (Fig. 1*B*, supplemental Table S1). Flow cytometric analysis of mycolactone-exposed MutuDCs revealed that the Slc3a2 dose-response curve displayed an unusual "bell" shape, with mycolactone doses <100 nM leading to increased surface expression of the receptor after 24 h (Fig. 4*A*). In comparison, (Type I) MHC class II expression was consistently suppressed by mycolactone, and fully abrogated by 100 nM mycolactone (Fig. 4*A*).

In biochemical assays, 100 nM mycolactone fully blocked Slc3a2 membrane integration (Fig. 4*B*), demonstrating Slc3a2 susceptibility to mycolactone-mediated Sec61 blockade. Intriguingly, the increased expression of Slc3a2 by MutuDCs exposed to 25 nM mycolactone correlated with an acute upregulation of slc3a2 gene expression (Fig. 4*C*). This was a selective effect, as the same mycolactone treatment did not modify the levels of β_2m transcripts (Fig. 4*C*). Low doses of mycolactone (<10 nM) triggered a comparable increase in slc3a2 gene and protein expression in a B-lymphoma cell line over-expressing wild-type (wt) Sec61 (Fig. 4*D*–4*E*). These effects were largely attenuated in B cells transduced with the mycolactone-resistant R66G mutant of Sec61 (Fig. 4*D*–4*E*), demonstrating the essential participation of Sec61 in Slc3a2 upregulation. Notably, transcription of Slc3a2 (Type II TMP), Herpud1 (Type II TMP), Hmox1 (not a Sec61 substrate) and Vimp (Type III TMP), all proteins upregulated by mycolactone in our proteomic analysis of MutuDCs, was increased in MutuDCs exposed to 25 nM mycolactone for only 3 h (Fig. 4*F*). From these data, we propose that mycolactone triggers a transcriptional stress response to ER translocation blockade encompassing the above described genes. Partial Sec61 inhibition by low mycolactone doses may explain the increased production of stress-induced Sec61 clients, despite their biochemical susceptibility to mycolactone.

Mycolactone-upregulated Proteins Outline Distinctive Stress Responses—The data presented in Figs. 1 and 4 show that mycolactone triggered proteome-wide alterations, beyond Sec61 substrates. Hsp70 (Hspa1a/b), the stress-induced form of the Hsc70 molecular chaperone critical for nascent protein folding, was upregulated by mycolactone in both Jurkat T cells and MutuDCs (Fig. 1). Hsp90 (Hsp90aa/b1), which forms with Hsp70 a multichaperone machinery regulating proteostasis, was also upregulated by mycolactone in MutuDCs. In order to identify additional stress markers, we next analyzed in further detail all proteins upregulated by mycolactone in MutuDCs. Fig. 5*A* compares the distribution of mycolactone-upgulated, mycolactone-downregulated and non-modulated proteins in the different subcellular compartments of MutuDCs. Notably, mycolactone-upregulated proteins were most prevalent in the ER, but some were present in every cell compartment. A GOT analysis revealed that mycolactone-upregulated proteins were selectively enriched in markers of the ≪ unfolded protein response ≫ (UPR) and ≪ protein exit from the ER ≫, and to a lower extent with proteins involved in ≪ tRNA aminoacylation for protein translation≫ and ≪ positive regulation of tyrosine kinase activity ≫ (Table III). Together, these data suggested that Sec61 blockade triggers ER stress propagating to diverse physiological processes through the UPR (reviewed in (28)).

ER-resident stress sensors IRE1α, PERK and ATF6 were not detected in our proteomic analyses, however as Type I (IRE1α and PERK) or Type II (ATF6) TMPs, they are predicted to be susceptible to mycolactone inhibition. When activated by ER stress, IRE1α splices Xbp1 mRNA, which can be monitored by quantitative real time PCR (29). We detected enhanced splicing of Xbp1 mRNA in MutuDCs exposed to mycolactone for 4h, indicating that the IRE1-α pathway was activated (Fig. 5*B*). Thapsigargin, tunicamycin, and MG132 are potent inducers of ER stress, which operate through inhibition of sarco-endoplasmic reticulum Ca^{2+} ATPases, protein glycosylation, and proteasome, respectively. Although less potent than thapsigargin (1 μM), mycolactone used at 25 nM was comparable to tunicamycin (1 μM) and superior to MG132 (1 μM) in capacity to induce Xbp-1 mRNA splicing (supplemental Fig. S3). ER stress-activated PERK phosphorylates eIF2α, which stimulates the translation of the ATF4 transcription factor. Together with activated ATF6, activated ATF4 induces the transcriptional upregulation of the C/EBP Homologous protein (Chop). Although less potent than canonical ER stressors in the conditions tested, mycolactone induced significant expression of Chop in MutuDCs after 2 h (Fig. 5*C*). Moreover, we identified 27 targets of the ATF4 and/or Chop transcription factors (30) within the 170 proteins upregulated by mycolactone in MutuDCs (Table IV), a significant enrichment compared with controls (p value<0.0001, Fisher exact test). ATF4/Chop targets upregulated by mycolactone included both chains of CD98 (Slc3a2/Slc7a5), Herpud1 and Hmox1. Fig. 5*D* shows that mycolactone was comparable to tunicamycin and MG132 for stimulation of Slc3a2 expression. In MED17.11 neurons, 2 of the 8 proteins upregulated by mycolactone were ATF4 targets (Table IV). Altogether, these data indicated that mycolactone robustly activates the ATF4/Chop branch of UPR. Importantly, although thapsigargin, tunicamycin, and MG132 all upregulated the expression of Bip, a master regulator of the UPR, mycolactone showed the opposite effect (Fig. 5*D*). Significant reduction in Bip transcript levels was reproducibly observed in MutuDCs exposed to mycolactone for longer than 4 h. We conclude that mycolactone triggers an atypical ER stress response, differing from conventional UPR by the down-regulation of Bip.

DISCUSSION

The present work outlines distinctive proteomic alterations induced by mycolactone, resulting from primary and secondary effects on protein translocation blockade (summarized in Fig. 6). Regarding the direct consequences of Sec61 block-

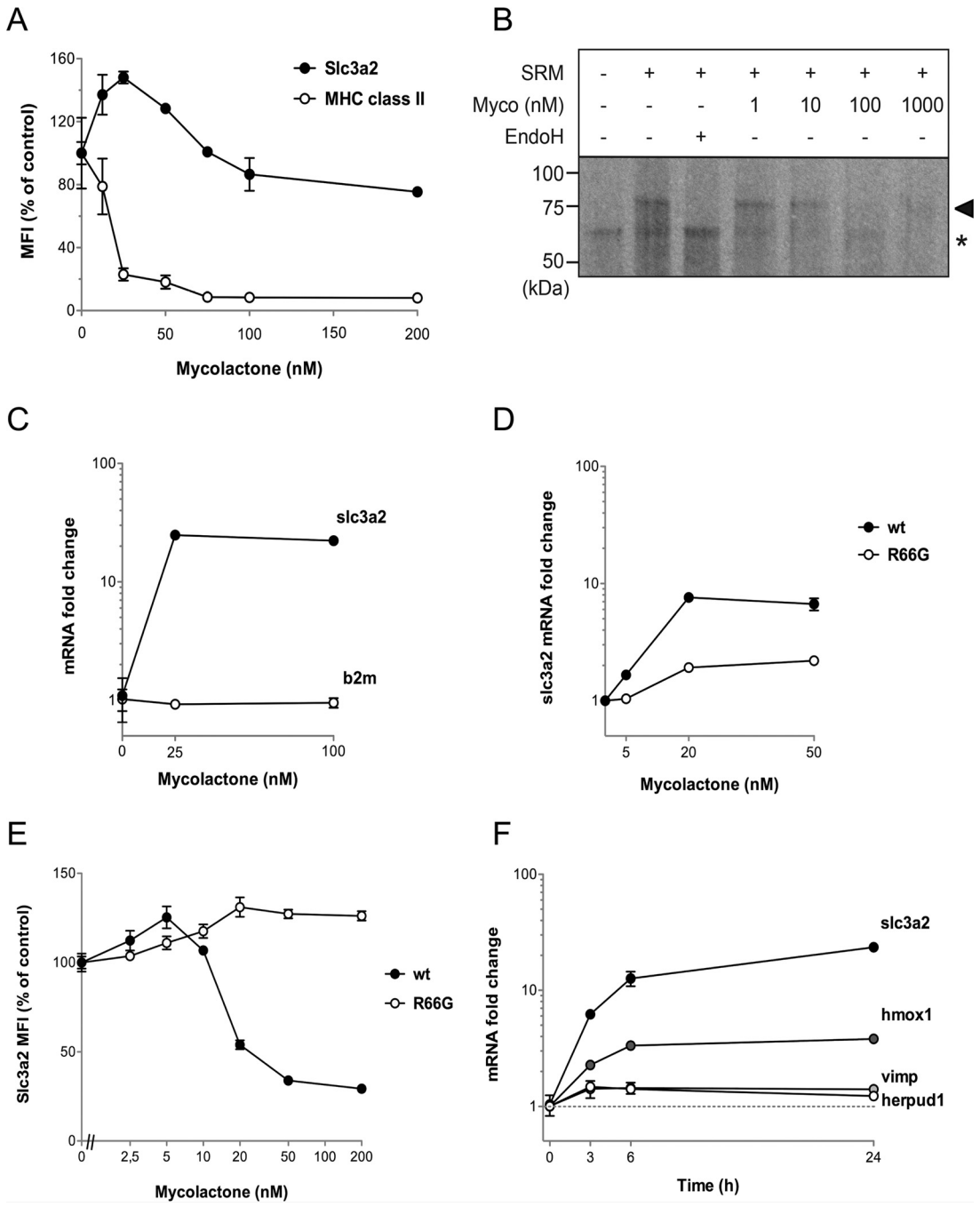

FIG. 4. **Low doses of mycolactone-upregulate the transcription of selected Sec61 substrates.** *A*, Surface expression of Slc3a2 and MHC class II (I-A/I-E) in MutuDCs treated with the indicated doses of mycolactone for 24 h. *B*, Assay of Slc3a2 insertion in SRM, in the presence of increasing amounts of mycolactone (Myco). Membrane integration was assessed by analyzing the change in SDS-PAGE mobility and autoradiography. Correctly integrated, glycosylated SLC3A2 species are indicated with arrowheads and non-translocated, unglycosylated protein species with an asterisk. Endoglycosidase H (EndoH) treatment demonstrates that the change in SDS-PAGE migration is because of glycosylation. *C*, qRT-PCR comparing the expression slc3a2 and b2m in MutuDCs treated with 25 or 100 nM mycolactone for 24 h. *D*, qRT-PCR comparing the expression of slc3a2 in wt or R66G Sec61-expressing lymphoma B cells following a 24h treatment with 25 or 100 nM mycolactone. *E*, Effect of mycolactone on CD98 surface expression by lymphoma B cells overexpressing wild-type (wt) Sec61 or the mycolactone-resistant R66G Sec61 mutant. Cells were treated with the indicated doses of mycolactone for 24h, prior to flow cytometric analysis. *F*, Kinetic effects of mycolactone on transcript levels of slc3a2, hmox1, vimp and herpud1, as measured by qPCR in MutuDCs treated with 25 nM mycolactone for the indicated times. Data are mean ± S.E. ($n = 3$) from one of two independent experiments, which gave similar results.

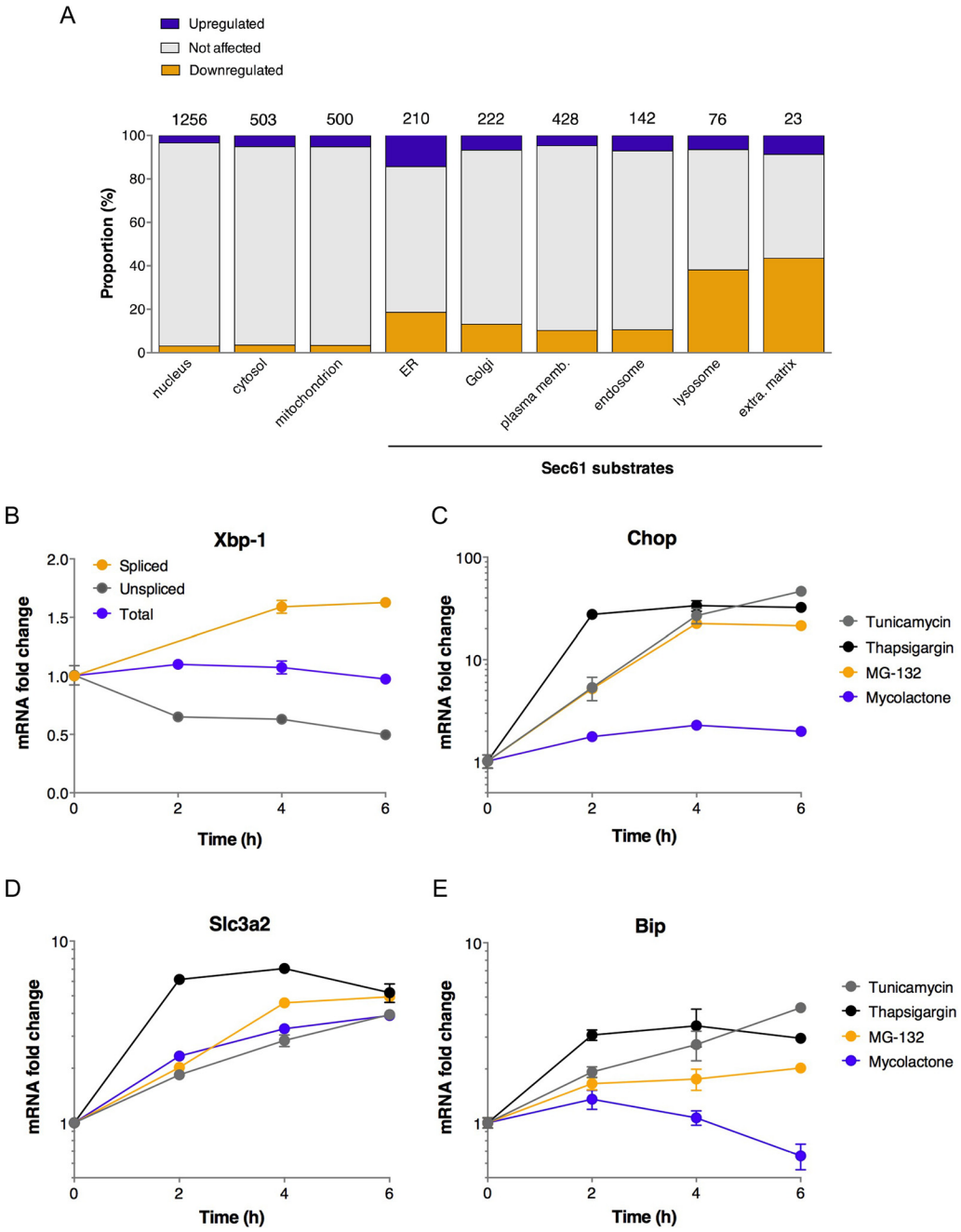

FIG. 5. **Mycolactone-upregulated proteins outline an atypical stress response.** *A*, Proportion of mycolactone-downregulated or -up-regulated Sec61 substrates across cell compartments in MutuDCs. Compartements primarily composed of Sec61 substrates are indicated. The numbers above the bars indicate the number of proteins in each category. *B*, Kinetics of mycolactone effects (25 nM) on MutuDC expression of total, spliced and unspliced Xbp-1. *C–E*, Differential effects of Tunicamycin (1 μM), Thapsigargin (1 μM), MG132 (1 μM) and mycolactone (25 nM) on expression of Chop, Slc3a2 and Bip in MutuDCs. Data are mean ± S.E. from biological triplicates.

ade, our integrated analysis of mycolactone's signature across cell types confirmed the predictions of McKenna's model *e.g.* (1) susceptibility of secretory proteins, (2) susceptibility of Type I TMPs, modulated by the size of their N-terminal TMD, and (3) resistance of Type III TMPs (Fig. 6). It remains to be determined whether a fraction of Type II TMPs may resist mycolactone inhibition. We detected mycolactone-upregulated Sec61 substrates within Type II TMPs, which supports this possibility. CD98 characterization nevertheless revealed that Type II TMPs upregulated by mycolactone are not necessarily resistant to mycolactone-mediated Sec61 blockade. Interestingly, a positive correlation was observed between the hydrophobicity of the sequences flanking the first N-terminal TMD in Type II TMPs and their susceptibility to

TABLE III

Biological process analysis of MutuDC proteins upregulated by mycolactone. The biological processes that were most significantly enriched in "mycolactone-upregulated" proteins, compared to "all quantified" proteins, are listed. Proteins significantly upregulated by mycolactone in each category are shown with Uniprot accession number, FDR, variation extent of mycolactone/control, gene name and an indication of whether the protein is a Sec61 substrate inferred from www.uniprot.org. Upregulated (FDR ≤ 0.1; log2(Variation) > 0.5)

Uniprot ID	FDR[a]	Variation[b]	Protein name[c]	Gene name[c]	Sec61 substrate
			Response to unfolded protein****[d]**		
P17879	9.42E-03	16.8	Heat shock 70 kDa protein 1A;1B	Hspa1b;Hspa1a	
Q9JJK5	7.45E-05	9.17	Homocysteine-responsive endoplasmic reticulum-resident ubiquitin-like domain member 1 protein	Herpud1	Yes
Q9R099	2.05E-02	6.72	Transducin beta-like protein 2	Tbl2	
Q9BCZ4	7.86E-03	3.95	Selenoprotein S	Vimp	Yes
Q61699	7.70E-03	1.97	Heat shock protein 105 kDa	Hsph1	
Q3TDN2	2.03E-02	1.7	FAS-associated factor 2	Faf2	
P07901	4.20E-03	1.65	Heat shock protein HSP 90-alpha	Hsp90aa1	
Q9QY76	3.70E-02	1.61	Vesicle-associated membrane protein-associated protein B	Vapb	
P35821	5.61E-02	1.55	Tyrosine-protein phosphatase non-receptor type 1	Ptpn1	
Q8BGQ7	2.79E-02	1.45	Alanine–tRNA ligase, cytoplasmic	Aars	
			Protein exit from endoplasmic reticulum***[d]**		
Q9BCZ4	7.86E-03	3.95	Selenoprotein S	Vimp	Yes
O35166	1.75E-02	2.86	Golgi SNAP receptor complex member 2	Gosr2	
P70295	1.52E-03	1.93	Ancient ubiquitous protein 1	Aup1	Yes
P61620	1.35E-02	1.89	Protein transport protein Sec61 subunit alpha isoform 1	Sec61a1	Yes
Q8CI04	3.28E-02	1.77	Conserved oligomeric Golgi complex subunit 3	Cog3	
Q3TDN2	2.03E-02	1.7	FAS-associated factor 2	Faf2	
P07901	4.20E-03	1.65	Heat shock protein HSP 90-alpha	Hsp90aa1	
Q9CQU3	5.68E-02	1.48	Protein RER1	Rer1	Yes
			tRNA aminoacylation for protein translation**[d]**		
Q8BP47	2.57E-03	1.91	Asparagine–tRNA ligase, cytoplasmic	Nars	
P26638	3.02E-03	1.78	Serine–tRNA ligase, cytoplasmic	Sars	
Q9ER72	1.25E-02	1.84	Cysteine–tRNA ligase, cytoplasmic	Cars	
Q9D0R2	1.32E-02	1.63	Threonine–tRNA ligase, cytoplasmic	Tars	
Q8BMJ2	2.57E-02	1.63	Leucine–tRNA ligase, cytoplasmic	Lars	
Q8BGQ7	2.79E-02	1.45	Alanine–tRNA ligase, cytoplasmic	Aars	
Q8CGC7	3.73E-02	1.46	Bifunctional glutamate/proline–tRNA ligase	Eprs	
			Positive regulation of tyrosine kinase activity**[d]**		
Q60823	8.73E-03	3.39	RAC-beta serine/threonine-protein kinase	Akt2	
P09535	7.12E-04	2.81	Insulin-like growth factor II;Preptin	Igf2	Yes
Q61699	7.70E-03	1.97	Heat shock protein 105 kDa	Hsph1	
Q8R0X7	8.57E-02	1.84	Sphingosine-1-phosphate lyase 1	Sgpl1	Yes
Q9JM90	1.20E-02	1.73	Signal-transducing adaptor protein 1	Stap1	
P08103	8.74E-02	1.63	Tyrosine-protein kinase HCK	Hck	
Q91YI4	5.71E-03	1.59	Beta-arrestin-2	Arrb2	
P35821	6.75E-02	1.55	Tyrosine-protein phosphatase non-receptor type 1	Ptpn1	
P28867	5.61E-02	1.55	Protein kinase C delta type	Prkcd	
O55143	3.28E-02	1.55	Sarcoplasmic/ER calcium ATPase 2	Atp2a2	Yes

[a]False Discovery Rate.

[b](mycolactone/control) ratio of relative LFQ intensities.

[c]According to www.uniprot.org.

[d]Hypergeometric test comparing the incidence of GOT between "upregulated" and "all quantified" proteins in MutuDCs ******, $p < 10^{-6}$; *****, $p < 10^{-5}$; ****, $p < 10^{-4}$.

mycolactone (supplemental Fig. S2). How hydrophobic signals in nascent polypeptides trigger Sec61 opening is not fully understood. In an inactive translocon, the Sec61 channel is occluded by a plug helix that must be displaced for protein translocation. The recent structure of an active, signal-engaged Sec61 suggests that ribosome binding triggers dynamic conformational changes in Sec61 that allow the insertion of hydrophobic signals in the central pore, while destabilizing the plug (30). Notably, amino acid substitutions conferring resistance to mycolactone all localize to the plug or

TABLE IV

Mycolactone upregulated proteins are enriched in targets of the ATF4 and CHOP transcription factor targets. Mycolactone upregulated proteins (FDR ≤ 0.1; log2(Variation) > 0.5) of MutuDCs and MED17.11 neurons that are known targets of the ATF4 and CHOP transcription factors (37) are listed with Uniprot accession number, FDR, variation extent of mycolactone/control, gene name, presence of an ATF4 and/or CHOP binding site on their promoter region and type of Sec61 substrate type

MutuDCs						
Uniprot ID	FDR[a]	Variation[b]	Protein name[c]	Gene name	CHOP/ATF4	Sec61 substrate
Q3UM18	7.50E-02	43.87	Large subunit GTPase 1 homolog	Lsg1	ATF4 Only	No
Q9JJK5	7.45E-05	9.17	Homocysteine-responsive endoplasmic reticulum-resident ubiquitin-like domain member 1 protein	Herpud1	ATF4 Only	Type II TMP
P14901	2.11E-04	5.29	Heme oxygenase 1	Hmox1	ATF4 Only	No
P10852	5.85E-04	3.50	4F2 cell-surface antigen heavy chain	Slc3a2	ATF4 Only	Type II TMP
Q8BH04	1.36E-02	3.03	Phosphoenolpyruvate carboxykinase [GTP], mitochondrial	Pck2	ATF4 Only	No
Q61024	1.66E-03	2.85	Asparagine synthetase [glutamine-hydrolyzing]	Asns	ATF4 Only	No
Q9Z127	7.67E-03	2.76	Large neutral amino acids transporter small subunit 1	Slc7a5	Both	Type II TMP
Q64337	1.41E-04	2.67	Sequestosome-1	Sqstm1	Both	No
P53995	7.62E-02	2.42	Anaphase-promoting complex subunit 1	Anapc1	ATF4 Only	No
Q8CH25	1.56E-03	2.09	SAFB-like transcription modulator	Sltm	ATF4 Only	No
Q8BP47	2.57E-03	1.91	Asparagine–tRNA ligase, cytoplasmic	Nars	Both	No
Q6WKZ8	1.58E-02	1.89	E3 ubiquitin-protein ligase UBR2	Ubr2	Both	No
Q9ER72	1.25E-02	1.84	Cysteine–tRNA ligase, cytoplasmic	Cars	ATF4 Only	No
P26638	3.02E-03	1.78	Serine–tRNA ligase, cytoplasmic	Sars	Both	No
Q9Z110	1.41E-02	1.77	Delta-1-pyrroline-5-carboxylate synthase;Glutamate 5-kinase;Gamma-glutamyl phosphate reductase	Aldh18a1	Both	No
Q9D0R2	1.32E-02	1.63	Threonine–tRNA ligase, cytoplasmic	Tars	ATF4 Only	No
P59325	7.67E-03	1.63	Eukaryotic translation initiation factor 5	Eif5	Both	No
Q8BMJ2	2.57E-02	1.63	Leucine–tRNA ligase, cytoplasmic	Lars	Both	No
Q99K85	2.16E-03	1.60	Phosphoserine aminotransferase	Psat1	ATF4 Only	No
P18155	5.51E-03	1.59	Bifunctional methylenetetrahydrofolate dehydrogenase/cyclohydrolase	Mthfd2	Both	No
Q64131	7.39E-02	1.57	Runt-related transcription factor 3	Runx3	ATF4 Only	No
Q61753	1.96E-02	1.54	D-3-phosphoglycerate dehydrogenase	Phgdh	ATF4 Only	No
A2AN08	1.26E-02	1.51	E3 ubiquitin-protein ligase UBR4	Ubr4	ATF4 Only	Type II or III TMP
Q3UPF5	2.33E-02	1.48	Zinc finger CCCH-type antiviral protein 1	Zc3hav1	Both	No
Q8CGC7	3.73E-02	1.46	Bifunctional glutamate/proline–tRNA ligase; Glutamate–tRNA ligase;Proline–tRNA ligase	Eprs	Both	No
Q9D898	3.66E-02	1.45	Actin-related protein 2/3 complex subunit 5-like protein	Arpc5l	ATF4 Only	No
Q8BGQ7	2.79E-02	1.45	Alanine–tRNA ligase, cytoplasmic	Aars	Both	No
MED17.11 sensory neurons						
P10852	1.43E-02	1.709	4F2 cell-surface antigen heavy chain	Slc3a2	ATF4 Only	Type II SP
Q9DB73	3.56E-02	1.556	NADH-cytochrome b5 reductase 1	Cyb5r1	Both	Type II or III SP

[a]False Discovery Rate.
[b](mycolactone/control) ratio of relative LFQ intensities.
[c]According to www.uniprot.org.

lateral gate junction (3). The data in supplemental Fig. S2 thus suggest that mycolactone may operate by strengthening the molecular contacts between plug and lateral gate, thus increasing the hydrophobic threshold that is required for channel opening.

In accordance with the tissue-specific effects of mycolactone in patients with Buruli ulcer disease, the host proteins that were downregulated by mycolactone varied across cell types. Notably, β_2m and M6PR were downregulated by mycolactone in T cells, dendritic cells and neurons, highlighting their potential interest as indicators of mycolactone activity. Virus envelope proteins were not different from endogenous TMPs in regard of their susceptibility to mycolactone-mediated Sec61 inhibition. Blocking Sec61 with mycolactone in Zika virus-infected cells efficiently prevented the cytopathic formation of ER-derived vacuoles (31). In the present work, mycolactone treatment of IAV-infected cells prevented production of Type I/II virus envelope glycoproteins, further illustrating the interest of mycolactone as a research tool to investigate Sec61 contribution to viral life cycles.

AGTR2 was not detected in our proteomic analysis of MED17.11 neurons (supplemental Table S1). However, as a Type III multi-pass TMP, AGTR2 is predicted to resist mycolactone-mediated Sec61 blockade. Only 8 proteins were upregulated by mycolactone in the conditions tested, suggesting that mycolactone induction of neuronal stress was minimal (Table II). Yet, we identified 45 proteins that were significantly downregulated by mycolactone (supplemental Table S1). Interestingly, a GOT analysis revealed that mycolactone-downregulated proteins were enriched in Sec61 clients mediating interactions between neurons and the extra-

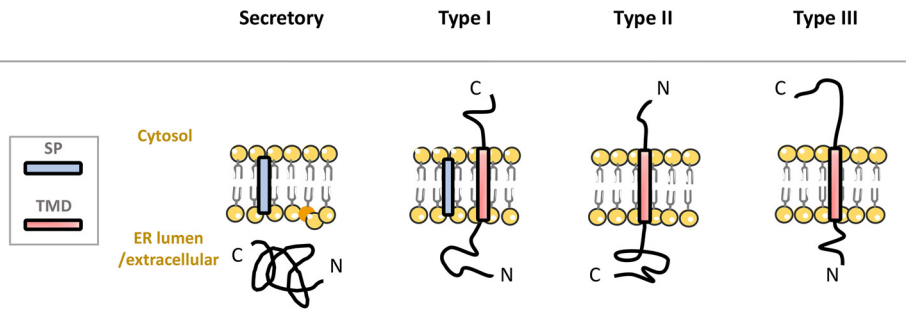

	Secretory	Type I	Type II	Type III
Translocation (*in vitro*)	Blocked	Largely inhibited	Largely inhibited	Unaffected
Production (in cells)	Decreased [a] or unchanged	Unchanged or decreased [b]	Unchanged or decreased or augmented [c]	Unchanged or augmented [d]
Examples	[a] IFN-γ, B2M	[b] HLA-A	[c] SLC3A2	[d] VIMP
Correlates of susceptibility (S) or resistance (R) to mycolactone (in cells)	• Presence of a SP and absence of TMD (S)	• Presence of a SP (S) • Large N-terminal domain (S)	• Absence of SP (R) • Hydrophobicity of the sequences flanking the first N-terminal TMD (S)	• Absence of SP (R) • "Headfirst" mode of insertion (R)

FIG. 6. **Diagram illustrating the differential effects of mycolactone on Sec61 client translocation (*in vitro*) and production in living cells.**

cellular matrix (ECM): Col1a1, Col3a1, Col5a1, Fn1, Itga6, Itgb1, Lamb1, Lamc1, and Sdc4 ($p < 10^{-6}$; hypergeometric test comparing the incidence of GOT between "downregulated" and "all quantified" proteins). Given the importance of the ECM in neuronal structure and functions, alterations in ECM receptor activation may represent additional mechanisms by which Sec61 inhibition impairs pain signal integration and transmission by neurons (32).

A major new finding in this work was the description of a stress response to mycolactone-mediated Sec61 blockade manifesting through the transcriptional induction of several proteins, including Sec61 substrates. Despite the low number of mycolactone-upregulated proteins in Jurkat T cells and MED17.11 neurons under the conditions employed, Slc3a2 was upregulated in both MutuDCs and MED17.11 neurons, and Hsp90 in both MutuDCs and Jurkat T cells, suggesting that these proteins represent conserved markers of Sec61 blockade-driven stress response. Upregulation of Hsp70/Hsp90 in mycolactone-treated MutuDCs likely results from the cytosolic accumulation of mycolactone-susceptible Sec61 substrates blocked in translocation, which are unable to fold properly outside the oxidizing environment of the ER and without membrane insertion. Notably, a significant proportion of mycolactone-upregulated proteins were targets of the ATF4 and/or Chop transcription factors. These findings are consistent with those of Ogbechi *et al.*, who reported recently that mycolactone-mediated Sec61 blockade drives ATF4 expression (33). However, in contrast to this study, we detected mycolactone-induced Xbp-1 splicing, indicative of ER stress. Our observation that mycolactone decreases Bip expression nevertheless highlighted a major difference between mycolactone-driven ER stress response and conventional UPR (Fig. 5*E*). Although the underlying mechanism is unclear, the 6h time to onset of Bip decrease suggests that it may result from secondary effects. Bip representing a major survival arm of the UPR, mycolactone-driven decline in Bip levels is likely to increase the cell susceptibility to ER stress-induced apoptosis. Mycolactone was recently proposed to promote BIM-dependent cell apoptosis through the mTORC2-Akt-FoxO3 axis (34). By transducing cells with a mycolactone-resistant Sec61 mutant, we were able to show that mycolactone cytotoxicity strictly depends on Sec61 inhibition (3). With mycolactone promoting a decrease in anti-apoptotic Bip and an increase in pro-apoptotic Chop, the data presented here thus support an additional scenario for mycolactone-induced toxicity, where mycolactone-mediated Sec61 blockade causes UPR-mediated apoptosis.

DATA AVAILABILITY

Proteomics data were deposited to the ProteomeXchange Consortium via the PRIDE partner repository (35, 36). The data sets corresponding to Jurkat T cells, MutuDCs and MED17.11 neurons are available under the identifiers PXD002971, PXD006103 and PXD007770. Annotated spectra were deposited in MS viewer with the following identifier keys: Jurkat: nnkr7jkmbl and xyczcpn2y0, MutuDCs: dmbpnhmpqb, MED17.11 neurons: lijxc0lue5. The proteomic analysis of mycolactone's effect on MutuDCs was performed with two time points (6 h and 24 h). Because only one protein was

modulated after 6 h of mycolactone treatment, we only analyzed the 24 h time point (15).

* This work was supported by Institut Pasteur, Institut National de la Santé et de la Recherche Médicale (INSERM) and Fondation Raoul Follereau (C.D.). J.D.M. is the recipient of a doctoral fellowship from the Ecole Normale Supérieure de Lyon. F.I. is supported by Odysseus grant G0F8616N from the Research Foundation Flanders (FWO). J.W. and J.W.Y. are supported by the Division of Intramural Research, NIAID. V.O.P. is supported by the Academy of Finland (grant 289737), and the Sigrid Juselius Foundation.

S This article contains supplemental Figures and Tables. The authors declare that they have no competing interests.

|||| To whom correspondence should be addressed: To whom correspondence should be addressed. Institut Pasteur, Immunobiology of Infection Unit, 75015 Paris, France. Tel.: +33 (0)1 4061 3066; E-mail: demangel@pasteur.fr.

Author contribution: J.-D.M. and C.D. designed the research, J.-D.M., A.P., J.W., L.G.-M., and F.I. performed the experiments, J.-D.M., A.P., J.W., J.W.Y., L.G.-M., N.P., V.O.P. and C.D. analyzed the data; J.-D.M. and C.D. wrote the manuscript.

REFERENCES

1. Demangel, C., Stinear, T. P., and Cole, S. T. (2009) Buruli ulcer: reductive evolution enhances pathogenicity of Mycobacterium ulcerans. *Nat. Rev. Microbiol*. **7,** 50–60
2. Sarfo, F. S., Phillips, R., Wansbrough-Jones, M., and Simmonds, R. E. (2016) Recent advances: role of mycolactone in the pathogenesis and monitoring of Mycobacterium ulcerans infection/Buruli ulcer disease. *Cell Microbiol.* **18,** 17–29
3. Baron, L., Paatero, A. O., Morel, J. D., Impens, F., Guenin-Mace, L., Saint-Auret, S., Blanchard, N., Dillmann, R., Niang, F., Pellegrini, S., Taunton, J., Paavilainen, V. O., and Demangel, C. (2016) Mycolactone subverts immunity by selectively blocking the Sec61 translocon. *J. Exp. Med.* **213,** 2885–2896
4. Hall, B. S., Hill, K., McKenna, M., Ogbechi, J., High, S., Willis, A. E., and Simmonds, R. E. (2014) The pathogenic mechanism of the Mycobacterium ulcerans virulence factor, mycolactone, depends on blockade of protein translocation into the ER. *PLoS Pathog.* **10,** e1004061
5. McKenna, M., Simmonds, R. E., and High, S. (2016) Mechanistic insights into the inhibition of Sec61-dependent co- and post-translational translocation by mycolactone. *J. Cell Sci.*
6. McKenna, M., Simmonds, R. E., and High, S. (2017) Mycolactone reveals the substrate-driven complexity of Sec61-dependent transmembrane protein biogenesis. *J. Cell Sci.* **130,** 1307–1320
7. Goder, V., and Spiess, M. (2001) Topogenesis of membrane proteins: determinants and dynamics. *FEBS letters* **504,** 87–93
8. Boulkroun, S., Guenin-Mace, L., Thoulouze, M. I., Monot, M., Merckx, A., Langsley, G., Bismuth, G., Di Bartolo, V., and Demangel, C. (2010) Mycolactone suppresses T cell responsiveness by altering both early signaling and posttranslational events. *J. Immunol.* **184,** 1436–1444
9. Coutanceau, E., Decalf, J., Martino, A., Babon, A., Winter, N., Cole, S. T., Albert, M. L., and Demangel, C. (2007) Selective suppression of dendritic cell functions by Mycobacterium ulcerans toxin mycolactone. *J. Exp. Med.* **204,** 1395–1403
10. Guenin-Mace, L., Baron, L., Chany, A. C., Tresse, C., Saint-Auret, S., Jonsson, F., Le Chevalier, F., Bruhns, P., Bismuth, G., Hidalgo-Lucas, S., Bisson, J. F., Blanchard, N., and Demangel, C. (2015) Shaping mycolactone for therapeutic use against inflammatory disorders. *Sci. Transl. Med.* **7,** 289ra285
11. Guenin-Mace, L., Carrette, F., Asperti-Boursin, F., Le Bon, A., Caleechurn, L., Di Bartolo, V., Fontanet, A., Bismuth, G., and Demangel, C. (2011) Mycolactone impairs T cell homing by suppressing microRNA control of L-selectin expression. *Proc. Natl. Acad. Sci. U.S.A.* **108,** 12833–12838
12. Marion, E., Song, O. R., Christophe, T., Babonneau, J., Fenistein, D., Eyer, J., Letournel, F., Henrion, D., Clere, N., Paille, V., Guerineau, N. C., Saint Andre, J. P., Gersbach, P., Altmann, K. H., Stinear, T. P., Comoglio, Y., Sandoz, G., Preisser, L., Delneste, Y., Yeramian, E., Marsollier, L., and Brodin, P. (2014) Mycobacterial toxin induces analgesia in buruli ulcer by targeting the Angiotensin pathways. *Cell* **157,** 1565–1576
13. Pahlevan, A. A., Wright, D. J., Andrews, C., George, K. M., Small, P. L., and Foxwell, B. M. (1999) The inhibitory action of Mycobacterium ulcerans soluble factor on monocyte/T cell cytokine production and NF-kappa B function. *J. Immunol.* **163,** 3928–3935
14. Phillips, R., Sarfo, F. S., Guenin-Mace, L., Decalf, J., Wansbrough-Jones, M., Albert, M. L., and Demangel, C. (2009) Immunosuppressive signature of cutaneous Mycobacterium ulcerans infection in the peripheral blood of patients with Buruli Ulcer Disease. *J. Infect Dis.*
15. Grotzke, J. E., Kozik, P., Morel, J. D., Impens, F., Pietrosemoli, N., Cresswell, P., Amigorena, S., and Demangel, C. (2017) Sec61 blockade by mycolactone inhibits antigen cross-presentation independently of endosome-to-cytosol export. *Proc. Natl. Acad. Sci. U.S.A.* **114,** E5910–E5919
16. Isaac, C., Mauborgne, A., Grimaldi, A., Ade, K., Pohl, M., Limatola, C., Boucher, Y., Demangel, C., and Guenin-Mace, L. (2017) Mycolactone displays anti-inflammatory effects on the nervous system. *PLoS Negl. Trop. Dis.* **11,** e0006058
17. Doran, C., Chetrit, J., Holley, M. C., Grundy, D., and Nassar, M. A. (2015) Mouse DRG Cell Line with Properties of Nociceptors. *Plos One* **10,** e0128670
18. George, K. M., Chatterjee, D., Gunawardana, G., Welty, D., Hayman, J., Lee, R., and Small, P. L. (1999) Mycolactone: a polyketide toxin from Mycobacterium ulcerans required for virulence. *Science* **283,** 854–857
19. Spangenberg, T., and Kishi, Y. (2010) Highly sensitive, operationally simple, cost/time effective detection of the mycolactones from the human pathogen Mycobacterium ulcerans. *Chem. Commun.* **46,** 1410–1412
20. Morgenstern, J. P., and Land, H. (1990) Advanced mammalian gene transfer: high titre retroviral vectors with multiple drug selection markers and a complementary helper-free packaging cell line. *Nucleic Acids Res.* **18,** 3587–3596
21. Sharma, A., Mariappan, M., Appathurai, S., and Hegde, R. S. (2010) In vitro dissection of protein translocation into the mammalian endoplasmic reticulum. *Methods Mol. Biol.* **619,** 339–363
22. Vermeire, K., Allan, S., Provinciael, B., Hartmann, E., and Kalies, K. U. (2015) Ribonuclease-neutralized pancreatic microsomal membranes from livestock for in vitro co-translational protein translocation. *Anal. Biochem.* **484,** 102–104
23. Ning, Z., Seebun, D., Hawley, B., Chiang, C. K., and Figeys, D. (2013) From cells to peptides: "one-stop" integrated proteomic processing using amphipols. *J. Proteome Res.* **12,** 1512–1519
24. Cox, J., and Mann, M. (2008) MaxQuant enables high peptide identification rates, individualized p.p.b.-range mass accuracies and proteome-wide protein quantification. *Nat. Biotechnol.* **26,** 1367–1372
25. Cox, J., Hein, M. Y., Luber, C. A., Paron, I., Nagaraj, N., and Mann, M. (2014) Accurate proteome-wide label-free quantification by delayed normalization and maximal peptide ratio extraction, termed MaxLFQ. *Mol. Cell. Proteomics* **13,** 2513–2526
26. Supek, F., Bosnjak, M., Skunca, N., and Smuc, T. (2011) REVIGO Summarizes and Visualizes Long Lists of Gene Ontology Terms. *Plos One* **6,** 7
27. Nguyen, H. T., and Merlin, D. (2012) Homeostatic and innate immune responses: role of the transmembrane glycoprotein CD98. *Cell Mol. Life Sci.* **69,** 3015–3026
28. Arensdorf, A. M., Diedrichs, D., and Rutkowski, D. T. (2013) Regulation of the transcriptome by ER stress: non-canonical mechanisms and physiological consequences. *Front Genet*. **4,** 256
29. Oslowski, C. M., and Urano, F. (2011) Measuring ER stress and the unfolded protein response using mammalian tissue culture system. *Methods Enzymol.* **490,** 71–92
30. Voorhees, R. M., and Hegde, R. S. (2016) Structure of the Sec61 channel opened by a signal sequence. *Science* **351,** 88–91
31. Monel, B., Compton, A. A., Bruel, T., Amraoui, S., Burlaud-Gaillard, J., Roy, N., Guivel-Benhassine, F., Porrot, F., Genin, P., Meertens, L., Sinigaglia, L., Jouvenet, N., Weil, R., Casartelli, N., Demangel, C., Simon-Loriere, E., Moris, A., Roingeard, P., Amara, A., and Schwartz, O. (2017) Zika virus induces massive cytoplasmic vacuolization and paraptosis-like death in infected cells. *EMBO J.*
32. Kerrisk, M. E., Cingolani, L. A., and Koleske, A. J. (2014) ECM receptors in neuronal structure, synaptic plasticity, and behavior. *Progress Brain Res.* **214,** 101–131

33. Ogbechi, J., Hall, B. S., Sbarrato, T., Taunton, J., Willis, A. E., Wek, R. C., and Simmonds, R. E. (2018) Inhibition of Sec61-dependent translocation by mycolactone uncouples the integrated stress response from ER stress, driving cytotoxicity via translational activation of ATF4. *Cell Death Dis.* **9,** 397
34. Bieri, R., Scherr, N., Ruf, M. T., Dangy, J. P., Gersbach, P., Gehringer, M., Altmann, K. H., and Pluschke, G. (2017) The Macrolide Toxin Mycolactone Promotes Bim-Dependent Apoptosis in Buruli Ulcer through Inhibition of mTOR. *ACS Chem. Biol.* **12,** 1297–1307
35. Vizcaino, J. A., Csordas, A., del-Toro, N., Dianes, J. A., Griss, J., Lavidas, I., Mayer, G., Perez-Riverol, Y., Reisinger, F., Ternent, T., Xu, Q. W., Wang, R., and Hermjakob, H. (2016) 2016 update of the PRIDE database and its related tools. *Nucleic acids research* **44,** D447–D456
36. Vizcaino, J. A., Deutsch, E. W., Wang, R., Csordas, A., Reisinger, F., Rios, D., Dianes, J. A., Sun, Z., Farrah, T., Bandeira, N., Binz, P. A., Xenarios, I., Eisenacher, M., Mayer, G., Gatto, L., Campos, A., Chalkley, R. J., Kraus, H. J., Albar, J. P., Martinez-Bartolome, S., Apweiler, R., Omenn, G. S., Martens, L., Jones, A. R., and Hermjakob, H. (2014) ProteomeXchange provides globally coordinated proteomics data submission and dissemination. *Nat. Biotechnol.* **32,** 223–226
37. Han, J., Back, S. H., Hur, J., Lin, Y. H., Gildersleeve, R., Shan, J., Yuan, C. L., Krokowski, D., Wang, S., Hatzoglou, M., Kilberg, M. S., Sartor, M. A., and Kaufman, R. J. (2013) ER-stress-induced transcriptional regulation increases protein synthesis leading to cell death. *Nat. Cell Biol.* **15,** 481–490

Supplemental material *Molecular & Cellular Proteomics 16.?*

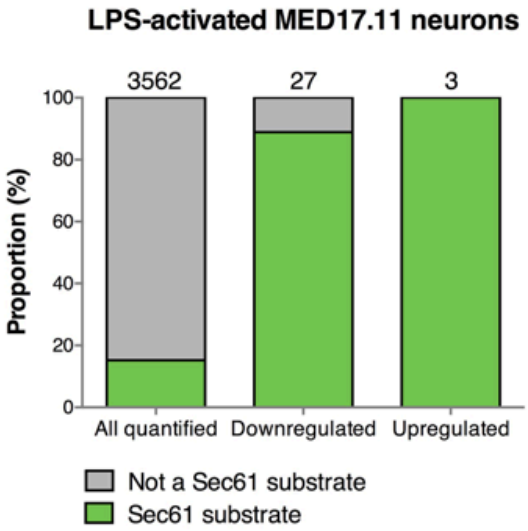

Figure S1: The proportion of Sec61 substrates in "all quantified" proteins is compared to that in "mycolactone-downregulated" or "mycolactone-upregulated" proteins, in MED17.11 cells exposed to mycolactone or not for 30 min, prior to activation with 10 nM LPS. The number of identified proteins in each subset is indicated on the top of each bar.

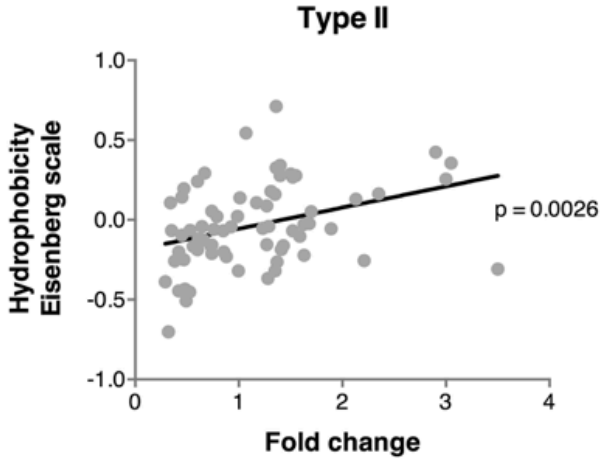

Figure S2: Average hydrophobicity of the 20-aminoacid long segments flanking the first N-terminal TMD, as a function of protein level variation (mycolactone/control relative LFQ intensity factor), in Type II TMPs of mycolactone-exposed MutuDCs. Linear regression line and p-value from Pearson's correlation test are shown.

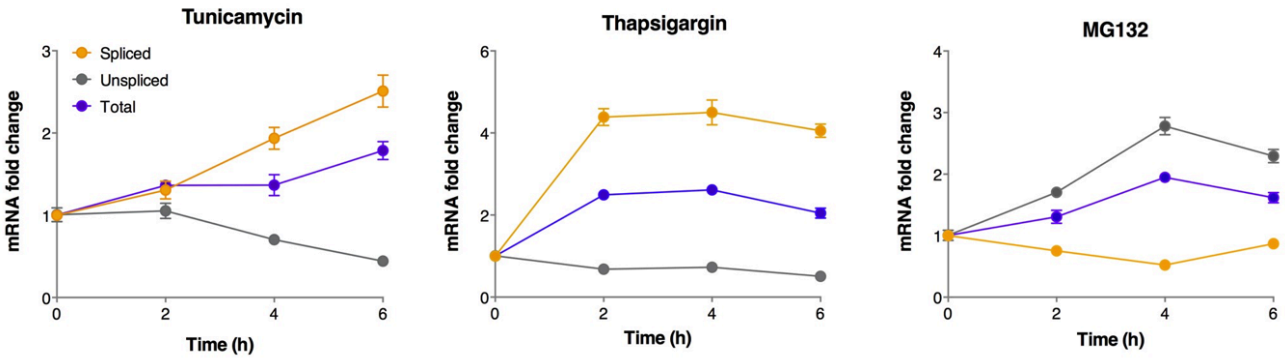

Figure S3: Differential effects of canonical ER stressors on Xbp-1 splicing. The kinetic effects of Tunicamycin (1µM), Thapsigargin (1µM) and MG132 (1 µM) on MutuDC expression of total, spliced and unspliced Xbp-1 are shown.

Table S1. MED17.11 proteins modulated by mycolactone. Excel file with three tabs: [Differentially expressed tab]: List of all proteins found differential expressed in response to mycolactone in both non-activated and LPS activated conditions. [All quantified tab] List all the proteins that were quantified in the analysis. Proteins in each category are shown with Uniprot accession number, FDR, variation extent of mycolactone/control, gene name and an indication of whether the protein is a Sec61 substrate inferred according to www.uniprot.org. Upregulated: significantly upregulated by mycolactone (FDR≤0.1, log2 mycolactone/control ratio>0.5). Downregulated: significantly downregulated by mycolactone (FDR≤0.1, log2 mycolactone/control ratio<-0.5). [Statistics tab] Statistics on Sec61 substrates in each category, as shown in Figures 1 and 2. http://www.mcponline.org/content/early/2018/06/18/mcp.RA118.000824/suppl/DC1

Table S2: qPCR primers used in this study

Genebank	Name	Primer-Forward	Primer-Reverse
NM_009078	Rpl-19	TACTGCCAATGCTCGG	AACACATTCCCTTTGACC
NM_022331.1	Herpud1	ACTCCTCGCTGAGCAGATTT	CTCTGTCTGAACGGAAACCA
NM_024439	Vimp/Selenos	GCAGGAAGATCTAAATGCCC	CATGCTGTCCCACATTTCAA
NM_010442.2	Hmox1 (Heme oxygenase 1)	AGGTACACATCCAAGCCGAGA	CATCACCAGCTTAAAGCCTTCT
NM_009735	Beta2 microglobulin	TTCTGGTGCTTGTCTCACTGA	CAGTATGTTCGGCTTCCCATTC
NM_001161413	SLC3a2 /CD98hc	TGATGAATGCACCCTTGTACTTG	TCCCCAGTGAAAGTGGA
NM_001271730	Spliced Xbp1	CTGAGTCCGAATCAGGTGCAG	GTCCATGGGAAGATGTTCTGG
NM_001271730	Unspliced Xbp1	CAGCACTCAGACTATGTGCA	GTCCATGGGAAGATGTTCTGG
NM_001271730	Total Xbp1	TGGCCGGGTCTGCTGAGTCCG	GTCCATGGGAAGATGTTCTGG
NM_001290183	Chop	CCACCACACCTGAAAGCAGAA	AGGTGAAAGGCAGGGACTCA
NM_001163434	Bip	TTCAGCCAATTATCAGCAAACTCT	TTTTCTGATGTATCCTCTTCACCAGT

Table S3: Comparison of mycolactone-modulated proteins across datasets. All human proteins found in the Jurkat cell dataset were mapped to their mouse orthologs when available. Human genes for which no mouse ortholog was found were not included. The numbers in the table correspond to the number of genes that were found upregulated/downregulated/not modulated in multiple datasets; the percentagesrepresent the proportion of these genes to the total above. Note that the total numbers of detected genes are slightly lower than the numbers of detected proteins presented in other figures, due to missing or redundant protein to gene mapping.

		Total	MutuDCs			MED17.11 neurons		
			Not modulated	Upregulated	Downregulated	Not modulated	Upregulated	Downregulated
Total			2806	169	206	3473	8	45
Jurkat T cells	Not modulated	2002	1018 (36.3%)	51 (30.2%)	51 (24.8%)	1137 (32.7%)	1 (12.7%)	3 (6.5%)
	Upregulated	1	0 (0%)	1 (0.6%)	0 (0%)	1 (0.03%)	0 (0%)	0 (0%)
	Downregulated	29	6 (0.2%)	0 (0%)	9 (4.4%)	10 (0.3%)	0 (0%)	3 (6.5%)
MutuDCs	Not modulated	2806				2094 (60.3%)	2 (25%)	4 (8.7%)
	Upregulated	169				123 (3.5%)	1 (12.5%)	0 (0%)
	Downregulated	206				131 (3.8%)	0 (0%)	9 (19.6%)

Table S4. Detailed information on MED17.11 neuron peptide and protein identifications: http://www.mcponline.org/content/early/2018/06/18/mcp.RA118.000824/suppl/DC1

DISCUSSION

1. Structural mechanism of Sec61 blockade by mycolactone

1.1 Binding of mycolactone to the α subunit of the translocon

The translocon is comprised of a central subunit, Sec61α, and two TA proteins named Sec61β and Sec61γ. In the inactive Sec61α, the central pore of the translocon is occluded by a short "'plug"' that must be displaced to allow translocation. Engagement of hydrophobic signals in the channel triggers the opening of a "lateral gate" in the channel, and the insertion of nascent polypeptides in the lipid bilayer (Reithinger *et al.*, 2014). In our 2016 study, we showed that mycolactone competes with cotransin for binding to Sec61α, and that cotransin-resistant Sec61α mutants R66G and S82P in the lateral gate region protected against the effects of mycolactone on membrane and secreted proteins synthesis (Article 1, (Baron *et al.*, 2016)). A recent study reported a similar mutant screen in HCT-116 cells, where 8 out of 9 resistant clones carried a Sec61α mutation (Ogbechi *et al.*, 2018). The mutations were R66K, confirming the importance of the arginine 66 for mycolactone activity, and D60G, a new mutation. While we cannot exclude indirect effects, these data strongly suggest that the region containing these mutations, near the lumenal plug of Sec61α, forms the mycolactone interaction site.

Notably, the lateral gate of the translocon seems to be a shared binding site of many Sec61 blockers, including cyclodepsipeptides such as cotransin, apratoxin and decatransin ((Mackinnon *et al.*, 2014, Paatero *et al.*, 2016, Junne *et al.*, 2015), see also III.3.2 of the introduction), but also lanthanum ions (Erdmann *et al.*, 2009). Endogenous ligands may exist for this binding site, such as perhaps phosphatidyl ethanolamines, which also disrupt Sec61 channel activity (Bogdanov *et al.*, 2008).

In 2016, High and co-workers were able to identify the precise step at which the translocation of precursor proteins is blocked by mycolactone, by using truncated proteins lacking a STOP codon, allowing the stabilization of various stages of translocation and cross-linking of the nascent polypeptide to the channel (McKenna *et al.*, 2016). They found that the SRP-mediated targeting and initial binding to the translocon were unaffected, yet the nascent polypeptide failed to engage within the channel (See stage 4, **Figure 9**). We observed a positive correlation between the hydrophobicity of the sequences flanking the first N-terminal transmembrane domain in Type II TMPs and their susceptibility to mycolactone (Article 3, (Morel *et al.*, 2018)). This suggests that mycolactone may operate by strengthening the molecular contacts between plug and lateral gate, thus increasing the hydrophobic threshold that is required for channel opening.

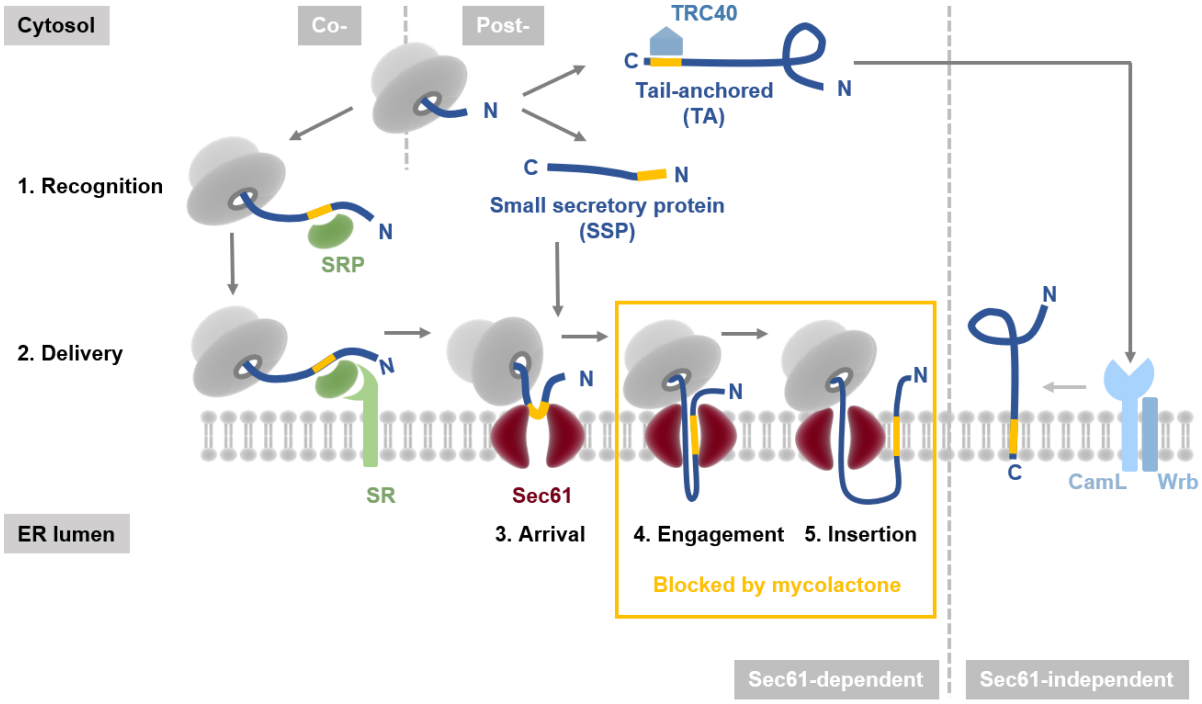

Figure 9: Pathways of Sec61 translocation of nascent proteins into the endoplasmic reticulum affected by mycolactone. *The classical SRP-dependent co-translation pathway as well as the post-translational translocation of small secretory proteins (SSP) are blocked by mycolactone at the Sec61 translocon, while the translocation of tail-anchored proteins through TRC40, CamL and Wrb is not impacted. Adapted from (Demangel and High, (In review)).*

1.2 Spectrum of activity of mycolactone

Short secretory proteins (SSPs) are a class of Sec61 substrates that are too short (<120 amino acids) to be recognized by SRP before they complete translation and are targeted to the translocon through a post-translational, SRP-independent mechanism (see introduction section III.2.1). McKenna *et al.* found that, although mycolactone strongly inhibits the co-translational translocation of typical secretory proteins, it was less effective at blocking the translocation of SSPs ((McKenna *et al.*, 2016), see **Figure 9**).

The finding that some Sec61 substrates can partially resist mycolactone inhibition prompted both the group of S. High and ours to further examine the substrate selectivity of mycolactone. We used different, complementary approaches, but arrived at remarkably similar conclusions (**Figure 10**). As

explained in paragraph III.1.2 of the introduction, Sec61 substrates can be divided into secretory proteins and type I, type II and type III TMPs. McKenna *et al.* used *in vitro* translocation of model Sec61 substrates in each category, as well as engineered variants of these substrates to gain insights into the determinants of protein resistance or susceptibility to mycolactone (McKenna *et al.*, 2017). Their findings suggested that the translocation of secretory proteins, and type I and type II membrane proteins is strongly inhibited by mycolactone, while in contrast that of type III TMPs resists mycolactone inhibition (McKenna *et al.*, 2017). They observed partial resistance to mycolactone was observed for some Type I TMPs, depending on the hydrophobicity of their TMD and when their lumenal N-terminal domain was short (<20 aminoacids). Since type I TMPs have the same final orientation as type III TMPs, it was postulated that when the N-terminal domain is short, the first TMD could act as a signal-anchor, bypassing the SP and inserting like a type III TMP. Similarly, some type II TMPs could escape mycolactone inhibition by inserting headfirst into the translocon like a type III TMP, leading to a fully integrated protein where the cytosolic and luminal domains are inverted (McKenna *et al.*, 2017).

Our proteomic study of T cells, DCs and sensory neurons exposed to mycolactone supported the conclusions of Mckenna *et al.* (Article 3, (Morel *et al.*, 2018)). We found that secretory proteins were the most often downregulated by mycolactone, followed by type I, type II TMPs, while type III TMPs were never downregulated in mycolactone-treated cells. Interestingly, we found that the criteria of type I, type II and type III TMPs applied equally well for multi-pass TMPs as single-pass TMPs, suggesting that the insertion of the first transmembrane domain is the limiting step for Sec61 blockade of multi-pass TMPs. In contrast to McKenna's study, we found that type II TMPs displayed an intermediate phenotype, with a large number of both downregulated and upregulated proteins, suggesting that some type II TMPs may at least partially resist mycolactone. However, we found little correlation between upregulated proteins and sequence properties, such as the length of the N-terminal domain or the hydrophobicity of the TMDs. Upon testing one of the upregulated type II proteins, Slc3a2, in an *in vitro* translocation assay, we found that it was not in fact resistant to mycolactone and that its upregulation was the result of a strong transcriptional activation (Article 3, (Morel *et al.*, 2018)), leaving open the question of whether type II TMPs can resist mycolactone blockade of Sec61. The effects of mycolactone on the different subsets of Sec61 substrates are summarized on **Figure 10**.

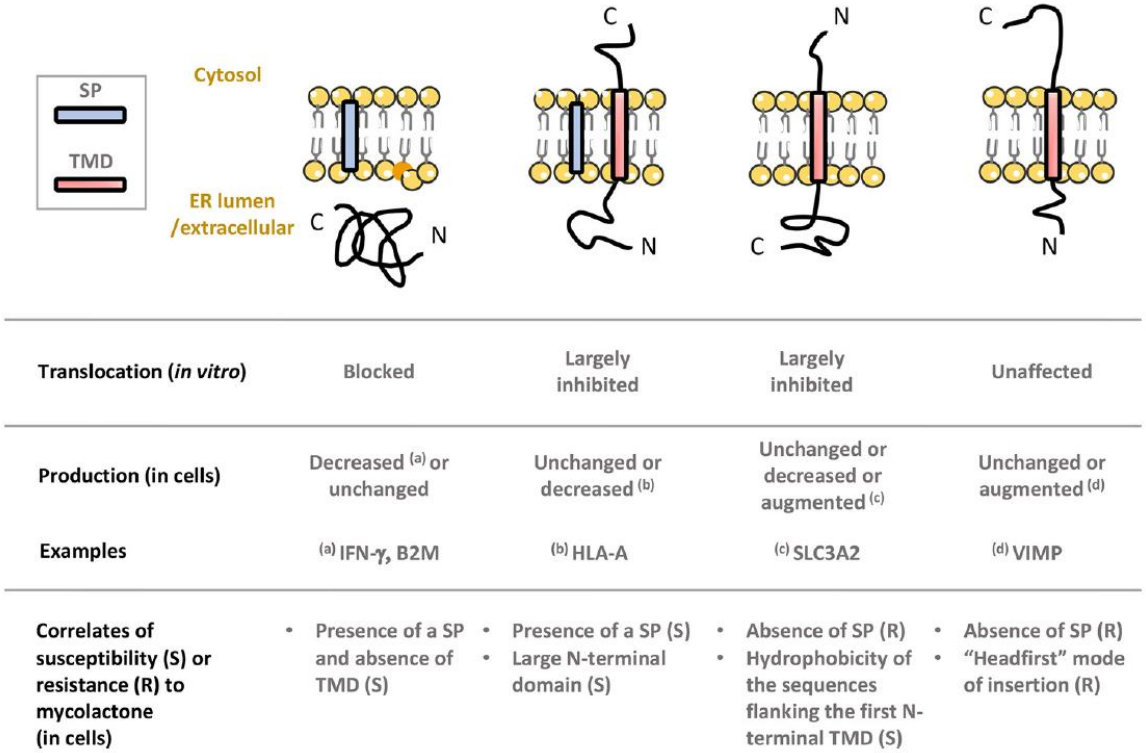

	Secretory	Type I	Type II	Type III
Translocation (*in vitro*)	Blocked	Largely inhibited	Largely inhibited	Unaffected
Production (in cells)	Decreased [a] or unchanged	Unchanged or decreased [b]	Unchanged or decreased or augmented [c]	Unchanged or augmented [d]
Examples	[a] IFN-γ, B2M	[b] HLA-A	[c] SLC3A2	[d] VIMP
Correlates of susceptibility (S) or resistance (R) to mycolactone (in cells)	• Presence of a SP and absence of TMD (S)	• Presence of a SP (S) • Large N-terminal domain (S)	• Absence of SP (R) • Hydrophobicity of the sequences flanking the first N-terminal TMD (S)	• Absence of SP (R) • "Headfirst" mode of insertion (R)

Figure 10: Diagram illustrating the differential effects of mycolactone on Sec61 client translocation (in vitro) and production in living cells*. From article 3 in the results section (Morel et al., 2018) and duplicated here for reading convenience.*

1.3 The SND system, an alternative targeting system to Sec61, and how it could play a role in resistance to mycolactone inhibition

The SND system is a newly discovered targeting system for membrane proteins that was initially described in yeast in 2016 and extended to mammals in 2017 (see Introduction section III.2.3). This system is capable of recognizing proteins with a TMD post-translationally and addressing them either to the Sec61 translocon or the Wrb/CamL complex in the case of TA proteins. Interestingly, SND-targets proteins partially overlap with mycolactone-resistant proteins, as SND was reported to deliver SP-devoid (type II and type III) proteins to Sec61. This led us to hypothesize that proteins targeted through the SND system could resist mycolactone-mediated inhibition, providing a potential mechanism for resistance to Sec61 blockade. To address this hypothesis, I generated HEK293 cells deficient for the human snd2/tmem208 gene using the CRISPR/Cas9 approach. Wild-

type (wt) and knock-out (KO) cells were treated with mycolactone or not, then subjected to proteomic analysis. The results are very preliminary, but early analysis does not support the hypothesis that snd2 KO reverses the resistance of type II and III TMPs to mycolactone (data not shown). Yet, this analysis revealed significant differences in the proteomes of wt and KO cells, irrespective of mycolactone treatment, which will help further characterize the function of SND2.

1.4 Role of Sec61 in ERAD and cross-presentation

In our PNAS paper, we showed that short term treatments with mycolactone did not impact retrograde transport of proteins during either ERAD or cross-presentation. Longer treatments with mycolactone inhibited the direct translocation of mediators of ERAD and cross-presentation into the ER, impacting those processes indirectly (Article 2, (Grotzke *et al.*, 2017)). These results suggested that Sec61α is not directly involved in the retrograde transport of proteins to the cytosol, and that previous findings using Sec61 knock-downs or anti-Sec61 intrabodies may have suffered from similar confounding effects (Imai *et al.*, 2005, Zehner *et al.*, 2015). Additionally, the evidence provided by Zehner *et al.* that Sec61 is in the endosome was weak. Since the ER forms close contacts with most organelles, co-localisation by immune-electron microscopy is not convincing.

We cannot exclude the possibility that mycolactone blocks forward (from the cytosol to the lumen), but not retrograde (from the lumen to the cytosol) transport. The findings of McKenna *et al.* in 2017, and our own in 2018, suggested a mechanism of action wherein mycolactone blocks the engagement step of the hairpin loop conformation that is common to secretory proteins, type I, type II TMPs (McKenna *et al.*, 2017, Morel *et al.*, 2018). In contrast, mycolactone did not interfere with the engagement of type III TMPs, which cross the translocon in a head-first manner. If mycolactone acts by preventing plug displacement, then it would be expected to inhibit both forward and reverse transport. If instead mycolactone works by keeping the lateral gate of Sec61 shut, then forward transport would certainly be inhibited, but reverse transport might be spared if it does not rely on lateral gate opening.

That said, our results reinforce the growing evidence that Sec61α is not the export channel for ERAD and cross-presentation. Additionally, given that the cytosolic side of Sec61 binds ribosomes with nanomolar affinity, it is hard to understand how endosomal Sec61 would avoid binding ribosomes and retain the proton gradient across the endosome during protein export. Moreover, there is no

mechanism for how lumenal substrates could drive Sec61 plug displacement to allow retrograde transport (Voorhees and Hegde, 2016).

2. From Sec61 blockade to immune suppression, hypoesthesia and ulceration

2.1 The immunosuppression by mycolactone is caused by Sec61 channel blockade

The first objective of my PhD, as reflected in my title, was to find how mycolactone exerted its immunosuppressive activity on cells and organisms. We discovered that mycolactone is a Sec61 blocker and that this mechanism enabled it to block IFNγ signaling at the level of T cells and macrophages (Article 1, (Baron *et al.*, 2016)), as well as block antigen presentation in dendritic cells (Article 2, (Grotzke *et al.*, 2017)).

To fully demonstrate that Sec61 blockade is the mechanism responsible for the immunosuppressive activity of mycolactone *in vivo*, an animal model would be preferable. To address this question, I attempted to introduce the R66G mutation in the mouse Sec61α gene using the CRISPR/Cas9 system together with a homology directed repair (HDR) template carrying the mutation. Over 30 embryos of C57BL/6 mice were injected with the construct, but only one female mouse was heterozygous for the desired R66G mutation. Upon breeding this founder mouse with a C57BL/6 male she produced 14 pups over 3 litters, among which 4 carried the R66G mutation, but died at birth, suggesting that R66G Sec61 may be detrimental to development. Another attempt was made to transfer bone marrow stem cells overexpressing R66G Sec61 into an irradiated receiver mouse to obtain a mycolactone-resistant immune system. Although the graft was successful, the cells rapidly eliminated the construct-carrying cells, again suggesting the R66G mutation may be detrimental *in vivo*. There was no apparent defect in either the viability or the production of Sec61 substrates in R66G Sec61-overexpressing cells *in vitro,* however the mutation could impact other functions of the channel, such as facilitating calcium leak from the ER or being excessively permissive to proteins not normally meant to translocate. Despite these setbacks, efforts continue by another member of the lab to generate mycolactone-resistant mice with two potential approaches: finding another mycolactone-resistance mutation that is not so detrimental *in vivo*, with S82P or D60G Sec61 as potential candidates, or expressing a Sec61 mutant under an inducible and/or tissue specific promoter by using the Cre/lox system.

2.3 From Sec61 blockade to stress responses and cell death

By transducing cells with the mycolactone-resistant R66G mutant of Sec61, we showed that mycolactone's toxicity is strictly dependent on its action on the Sec61 channel (Article 1, (Baron *et al.*, 2016)). How does one go from Sec61 blockade to cell death? Many Sec61 substrates are essential to cell survival, such as nutrient transporters, growth factor receptors, ER enzymes for lipid synthesis, lysosomal proteases, adhesion molecules and many more. The prolonged loss of any one of them could be responsible for cell death. Indeed, the duration of mycolactone treatment and lethal dose that is required to induce apoptosis varies across cell types. Certain cell types, such as naïve T cells or Jurkat cells resist >72h long treatments with micromolar concentrations of mycolactone despite being sensitive to the blockade of cytokine production at nanomolar concentrations. Other cells, such as HEK or Hela cells loose viability after 48h of exposure to 20nM mycolactone (Gama *et al.*, 2014, Bieri *et al.*, 2017, Dangy *et al.*, 2016, George *et al.*, 2000, Guenin-Mace *et al.*, 2013, Snyder and Small, 2003, Ogbechi *et al.*, 2015). For this reason, care should be taken when examining potential mechanisms of mycolactone-triggered cell death, as the exact mechanism may vary depending on which Sec61 substrate is most essential in a given cell type, and which types of cellular stress it is more sensitive to.

It was shown early that mycolactone kills cells by apoptosis, which could be prevented by the addition of the pan-caspase inhibitor Boc-Asp-(Ome)-fluoromethylketone (B-D-FMK) (George *et al.*, 2000). However, the authors noted that B-D-FMK did not prevent the cell-cycle arrest triggered by mycolactone and the cells eventually died by necrosis. As presented in section II.4 of the introduction, a 2017 study showed that mycolactone could trigger Bim-dependent apoptosis by inhibiting the assembly of the RICTOR-containing mTORC2 complex leading to a defect in Akt phosphorylation and subsequent activation of FoxO3 in L929 fibroblasts (Bieri *et al.*, 2017).

In 2018, Ogbechi *et al.* connected this pathway with the inhibition of Sec61, when they showed that Sec61-inhibition induces the integrated stress response (ISR) through the ER stress sensor protein PERK and to a lesser extent through the cytosolic nutrient sensor GCN2 and the stress and dsRNA sensor PKR, leading to Bim-dependant apoptosis (Ogbechi *et al.*, 2018) (see Section III.5 of the introduction for a presentation of the ISR and UPR). Interestingly, they found that PERK activation occurred without triggering the other sensors of the UPR: ATF6 and IRE1, as evidenced by an absence of IRE1-dependant XBP1 splicing or ATF6 cleavage (Ogbechi *et al.*, 2018).

While our study in MutuDCs also concluded that mycolactone triggered the ATF4/CHOP arm of the UPR, our results differed on the induction of ER stress. Indeed, our proteomic analysis found that many mycolactone-upregulated genes were targets of the ATF4 transcription factor, but also more broadly, mediators of the UPR and ERAD. When we assessed the activation of XBP1 splicing, an ER stress-specific marker, we found it quickly and dose dependently increased by mycolactone treatment, suggesting that mycolactone activates at least the IRE-1 and PERK sensors of the UPR (Article 3, (Morel *et al.*, 2018)). In practice, whether mycolactone-driven ATF4 induction results from the ISR, the UPR, or a combination of these stress responses, may well depend on cell type. Notably, we described that mycolactone-induced ER stress differs from conventional UPR by the fact that BiP is downregulated at both the mRNA and protein level (Article 3, (Morel *et al.*, 2018)). Decrease in "secretory" protein BiP likely reflects inhibition of the protein translocation by mycolactone at the level of Sec61. Likewise, ATF6 is a type II TMP, IRE1 and PERK are type I TMPs, all predicted to be efficiently blocked in translocation by mycolactone. Consistently, mycolactone caused depletion of ATF6, IRE1 and PERK after extended exposure times (Ogbechi *et al.*, 2018), and BiP was found significantly downregulated in one of our proteomic analyses. BiP being a target gene of ATF6 (Szegezdi *et al.*, 2006), decreased expression of BiP may result from mycolactone-driven downregulation of ATF6.

How Sec61 blockade by mycolactone initially triggers ER stress remains unclear. Downregulation of BiP expression and of other ER chaperones may cause the accumulation of misfolded, mycolactone-resistant proteins in the ER, thus triggering the UPR (Eletto *et al.*, 2012). Alternatively, some stress pathways may be triggered directly by the blockade of the Sec61 translocon, as proteins that aberrantly or persistently engage the translocon without translocating can recruit ERAD components to the translocon (Rubenstein *et al.*, 2012). The cytosolic unfolded protein response (CPR) may also play a role; while it is not yet very well defined, it is known to have significant cross-talk with the UPR (Liu *et al.*, 2012).

2.4 Possible role of Sec61 in hypoesthesia

Mycolactone was shown to activate Type 2 angiotensin II receptors (AT2R) in neurons, leading to a hyperpolarization of neurons, that was deemed responsible for the analgesic properties of mycolactone ((Marion *et al.*, 2014), see section II.2 of the introduction). However, a direct effect of Sec61 blockade by mycolactone on hypoesthesia cannot be ruled out. AT2R is a type III, multi-pass

transmembrane protein which may resist mycolactone inhibition of Sec61. We showed that mycolactone-mediated Sec61 blockade prevents the release of inflammatory mediators by neurons and microglia *in vitro* (Isaac *et al.*, 2017), and the development of inflammatory pain *in vivo* (Guenin-Mace *et al.*, 2015), which strongly suggests that the anti-inflammatory effects of mycolactone contribute to its analgesic properties. Moreover, our proteomic analysis of the DRG neuronal cell line MED17.11 exposed to mycolactone revealed 45 significantly downregulated proteins. A gene ontology analysis showed that mycolactone-downregulated proteins were significantly enriched in proteins involved in the adhesion of neurons to the extracellular matrix. Given the importance of the matrix in neuronal structure and functions, their loss may represent an additional mechanism by which Sec61 inhibition impairs pain signal transmission by neurons.

2.5 Sec61 blockade as a virulence mechanism for *M. ulcerans*

Although Sec61 blockers have been found to be produced by a wide variety of organisms, including fungi and cyanobacteria, mycolactone is the first Sec61 blocker to be produced by a human pathogen. *M. ulcerans* has the exceptional feature of seemingly relying on a single toxin for virulence. Mycolactone blocked IFNγ production by lymphocytes and IFNγ signaling in macrophages, which are known to play a critical role in immunity against mycobacteria. Mycolactone also impaired direct and cross-presentation in DCs and is thus likely to alter T cell priming against mycobacterial antigens. Finally, we showed that mycolactone impairs the trafficking of DCs (Coutanceau *et al.*, 2007) and T cells (Boulkroun *et al.*, 2010) *in vivo*. Therefore, bacterial production of mycolactone in infected hosts is likely to prevent the development of protective immune responses at many levels.

A variety of animals around the world e.g., rodents, shrews, possums, horses, dogs, alpacas, koalas and even Indian flap-shelled turtles have been recorded as being infected with *M. ulcerans* (Singh *et al.*, 2018). Sec61 is extremely well conserved across life and mammals in particular (100% identity in most mammals, including mice and humans), suggesting that mycolactone-mediated Sec61 blockade operates in all these hosts. Since aquatic insects have been proposed as a potential vector for transmission of Buruli ulcer (Marsollier *et al.*, 2002), it would be interesting to test whether insect Sec61 is resistant to mycolactone-mediated inhibition. Mycolactone had no antimicrobial activity against either gram-positive or gram-negative bacteria (Scherr *et al.*, 2013), suggesting that it cannot interfere with the SecY translocon, the bacterial homolog of Sec61. This is consistent with the finding that Buruli ulcers can be co-infected with bacteria (Yeboah-Manu *et al.*, 2013).

Despite its usefulness, the production of mycolactone requires a huge investment on the part of the bacteria, as the megaplasmid required for mycolactone synthesis is 174kb long and encodes to produce four giant modular polyketide synthases of 1.8 MDa, 1.8 MDa, 1.2 MDa and 0.26 MDa respectively (Stinear *et al.*, 2004). Our lab has observed that *M. ulcerans* bacteria frequently eliminate the plasmid after prolonged culture, further suggesting that the maintenance of this plasmid is very costly. This complexity and difficulty of synthesis is shared also for laboratory production of mycolactone and other Sec61 blockers, that can only be synthesized in small amounts and with limited efficiency (Song *et al.*, 2007, Coin *et al.*, 2008). This high synthesis cost may explain why Sec61 blockade is not a more widespread mechanism of immune escape by human pathogens. In addition, the potential for resistance mutations in Sec61α may lead to animals acquiring resistance to such a blockade over time, although my finding that the R66G mutation is lethal in mice, even in heterozygous form and the conservation of Sec61 across species make that unlikely.

3. Translational potential of Sec61 blockers and mycolactone in particular

3.1 Mycolactone as an anti-inflammatory drug

The discovery that mycolactone could inhibit immune responses at the systemic level without toxicity opens the possibility of using mycolactone as an immunosuppressive drug. Systemic administration of mycolactone protected mice against PMA-induced skin inflammation and rheumatoid arthritis, providing a proof-of-concept of the immunosuppressive potential of mycolactone (Guenin-Mace *et al.*, 2015). Today, we know that mycolactone-mediated immunosuppressive and cytotoxic effects rely on the same molecular mechanism, Sec61 blockade. Exploiting mycolactone therapeutically will therefore require dissociating the early (immunosuppressive) effects from the late (cytotoxic) ones. For this, detailed investigations of the pharmacokinetics of the molecule, currently lacking, will be needed.

3.2 Sec61 blockers as anti-cancer drugs

The Sec61 inhibitors cotransin, apratoxin A and decatransin were all identified through screens for anti-cancer drugs (Luesch *et al.*, 2001, Junne *et al.*, 2015), suggesting that protein transport into the ER is essential for cancer cell viability and/or growth. Mycolactone was more active than cotransin and apratoxin A at killing epithelial and fibroblast cell lines (data not shown), suggesting that it has the best potential. While Sec61 blockers may not be efficient against every type of tumor, they could be extremely toxic in those relying heavily on the endosomal pathway. One example of such a cancer

is multiple myeloma (MM), which is a malignancy of differentiated plasma cells, the main producers of antibodies (Kumar *et al.*, 2017). Indeed, as plasma cells are antibody-producing cells, they have a high basal induction of the UPR to accommodate for intense antibody production, and, as such, MM are highly sensitive to therapies that increase stress on proteostasis, such as proteasome inhibition. For this reason, proteasome inhibitors such as bortezomib have become the staple of treatment for MM (Kumar *et al.*, 2017). However, MM can acquire resistance to bortezomib over time, in particular by increasing the expression of proteasome subunits. These resistance mechanisms, together with the high toxicity of proteasome inhibitors, make it a high priority to find alternative treatments in MM. Sec61 inhibition by mycolactone may also achieve a lethal activation of the UPR in those cells by preventing the ER import of antibody chains, causing untranslocated antibodies to accumulate in the cytosol.

3.3 Sec61 blockers as anti-viral drugs

Cotransin has been shown to block the production of key proteins of influenza virus, HIV and dengue virus, greatly impairing viral replication (Heaton *et al.*, 2016). In our own study, we found that mycolactone efficiently prevented the cell surface expression of two essential influenza proteins (Article 3, (Morel *et al.*, 2018)). While Sec61 blockers can efficiently prevent viral replication (Heaton *et al.*, 2016), the inhibitory effects of mycolactone on Type I IFN production and signaling (Article 1(Baron *et al.*, 2016)), suggests that they may be difficult to exploit in this context.

CONCLUDING REMARKS

The macrolide mycolactone, the virulence factor of the human pathogen *Mycobacterium ulcerans,* has a wide variety of effects: ulcerative, immunosuppressive, analgesic. When I first started this PhD project, mycolactone had as many reported targets as it had effects. Over the last three years however, several teams, including ours, have provided evidence to support the concept that Sec61 blockade is the major, if not only mechanism mediating all the biological effects of mycolactone, and therefore the virulence of *M. ulcerans* and pathogenesis of BU (reviewed in Demangel and High, in press). Generating animal model expressing mycolactone-resistant, yet functional Sec61 would allow to address this hypothesis. In particular, such an animal model would help answer the question of the role of Sec61 in the hypoesthesia observed in BU patients.

The diffusion capacity of mycolactone, and high potency at inhibiting Sec61 allow acute Sec61 blockade in living cells, something that was not technically possible before with the available tools and techniques. Mycolactone thus provides researchers with a powerful mean to investigate the biology of the translocon. It already allowed us to question the involvement of Sec61 in the retrotransport of proteins in ERAD and cross-presentation. Because Sec61 mediates the biogenesis of viral proteins, mycolactone treatment of influenza A virus-infected cells prevented the production of Type I/II virus envelope glycoproteins, illustrating the interest of mycolactone as a research tool to investigate Sec61 contribution to viral life cycles.

The anti-inflammatory effects of mycolactone have brought to light the importance of Sec61 in the regulation of inflammation, and the translational potential of Sec61 blockers as novel drug candidates in the treatment of inflammatory disorders. Since mycolactone promotes ER stress by dirsupting protein homeostasis, it may also have an interest as single or adjunctive chemotherapy, in cancers with high susceptibility to proteotoxic stress such as multiple myeloma.

BIBLIOGRAPHY

Grant. A. J. 1864. A walk across Africa or Domestic scenes from my Nile journal. *Edinburgh, London: W. Blackwood and sons*.

ALMANZA, A., CARLESSO, A., CHINTHA, C., CREEDICAN, S., DOULTSINOS, D., LEUZZI, B., LUIS, A., MCCARTHY, N., MONTIBELLER, L., MORE, S., PAPAIOANNOU, A., PUSCHEL, F., SASSANO, M. L., SKOKO, J., AGOSTINIS, P., DE BELLEROCHE, J., ERIKSSON, L. A., FULDA, S., GORMAN, A. M., HEALY, S., KOZLOV, A., MUNOZ-PINEDO, C., REHM, M., CHEVET, E. & SAMALI, A. 2018. Endoplasmic Reticulum Stress signalling - from basic mechanisms to clinical applications. *FEBS J*.

ANAND, U., FACER, P., YIANGOU, Y., SINISI, M., FOX, M., MCCARTHY, T., BOUNTRA, C., KORCHEV, Y. E. & ANAND, P. 2013. Angiotensin II type 2 receptor (AT2 R) localization and antagonist-mediated inhibition of capsaicin responses and neurite outgrowth in human and rat sensory neurons. *Eur J Pain,* 17**,** 1012-26.

ANAND, U., SINISI, M., FOX, M., MACQUILLAN, A., QUICK, T., KORCHEV, Y., BOUNTRA, C., MCCARTHY, T. & ANAND, P. 2016. Mycolactone-mediated neurite degeneration and functional effects in cultured human and rat DRG neurons: Mechanisms underlying hypoalgesia in Buruli ulcer. *Mol Pain,* 12.

AVIRAM, N., AST, T., COSTA, E. A., ARAKEL, E. C., CHUARTZMAN, S. G., JAN, C. H., HASSDENTEUFEL, S., DUDEK, J., JUNG, M., SCHORR, S., ZIMMERMANN, R., SCHWAPPACH, B., WEISSMAN, J. S. & SCHULDINER, M. 2016. The SND proteins constitute an alternative targeting route to the endoplasmic reticulum. *Nature,* 540**,** 134-138.

AVIRAM, N. & SCHULDINER, M. 2014. Embracing the void--how much do we really know about targeting and translocation to the endoplasmic reticulum? *Curr Opin Cell Biol,* 29**,** 8-17.

BARON, L., PAATERO, A. O., MOREL, J. D., IMPENS, F., GUENIN-MACE, L., SAINT-AURET, S., BLANCHARD, N., DILLMANN, R., NIANG, F., PELLEGRINI, S., TAUNTON, J., PAAVILAINEN, V. O. & DEMANGEL, C. 2016. Mycolactone subverts immunity by selectively blocking the Sec61 translocon. *J Exp Med*.

BEISSNER, M., HERBINGER, K. H. & BRETZEL, G. 2010. Laboratory diagnosis of Buruli ulcer disease. *Future Microbiol,* 5**,** 363-70.

BESSE, W., DONG, K., CHOI, J., PUNIA, S., FEDELES, S. V., CHOI, M., GALLAGHER, A. R., HUANG, E. B., GULATI, A., KNIGHT, J., MANE, S., TAHVANAINEN, E., TAHVANAINEN, P., SANNA-CHERCHI, S., LIFTON, R. P., WATNICK, T., PEI, Y. P., TORRES, V. E. & SOMLO, S. 2017. Isolated polycystic liver disease genes define effectors of polycystin-1 function. *J Clin Invest,* 127**,** 1772-1785.

BIERI, R., BOLZ, M., RUF, M. T. & PLUSCHKE, G. 2016. Interferon-gamma Is a Crucial Activator of Early Host Immune Defense against Mycobacterium ulcerans Infection in Mice. *PLoS Negl Trop Dis,* 10**,** e0004450.

BIERI, R., SCHERR, N., RUF, M. T., DANGY, J. P., GERSBACH, P., GEHRINGER, M., ALTMANN, K. H. & PLUSCHKE, G. 2017. The Macrolide Toxin Mycolactone Promotes Bim-Dependent Apoptosis in Buruli Ulcer through Inhibition of mTOR. *ACS Chem Biol,* 12**,** 1297-1307.

BOGDANOV, M., XIE, J., HEACOCK, P. & DOWHAN, W. 2008. To flip or not to flip: lipid-protein charge interactions are a determinant of final membrane protein topology. *J Cell Biol,* 182**,** 925-35.

BOGER, D. L., CHEN, Y. & FOSTER, C. A. 2000. Synthesis and evaluation of aza HUN-7293. *Bioorg Med Chem Lett,* 10**,** 1741-4.

BOLAR, N. A., GOLZIO, C., ZIVNA, M., HAYOT, G., VAN HEMELRIJK, C., SCHEPERS, D., VANDEWEYER, G., HOISCHEN, A., HUYGHE, J. R., RAES, A., MATTHYS, E., SYS, E., AZOU, M., GUBLER, M. C., PRAET, M., VAN CAMP, G., MCFADDEN, K., PEDIADITAKIS, I., PRISTOUPILOVA, A., HODANOVA, K., VYLETAL, P., HARTMANNOVA, H., STRANECKY, V., HULKOVA, H., BARESOVA, V., JEDLICKOVA, I., SOVOVA, J., HNIZDA, A., KIDD, K., BLEYER, A. J., SPONG, R. S., VANDE WALLE, J., MORTIER, G., BRUNNER, H., VAN LAER, L., KMOCH, S., KATSANIS, N. & LOEYS, B. L. 2016. Heterozygous Loss-of-Function SEC61A1 Mutations Cause Autosomal-Dominant Tubulo-Interstitial and Glomerulocystic Kidney Disease with Anemia. *Am J Hum Genet,* 99**,** 174-87.

BORGESE, N. & FASANA, E. 2011. Targeting pathways of C-tail-anchored proteins. *Biochim Biophys Acta,* 1808**,** 937-46.

BOULKROUN, S., GUENIN-MACE, L., THOULOUZE, M. I., MONOT, M., MERCKX, A., LANGSLEY, G., BISMUTH, G., DI BARTOLO, V. & DEMANGEL, C. 2010. Mycolactone suppresses T cell responsiveness by altering both early signaling and posttranslational events. *J Immunol,* 184**,** 1436-44.

BRANDT, D. T. & GROSSE, R. 2007. Get to grips: steering local actin dynamics with IQGAPs. *EMBO Rep,* 8**,** 1019-23.

CARRARA, M., PRISCHI, F. & ALI, M. M. 2013. UPR Signal Activation by Luminal Sensor Domains. *Int J Mol Sci,* 14**,** 6454-66.

CLANCEY, J. K., DODGE, O. G., LUNN, H. F. & ODUORI, M. L. 1961. Mycobacterial skin ulcers in Uganda. *Lancet,* 2**,** 951-4.

COIN, I., BEERBAUM, M., SCHMIEDER, P., BIENERT, M. & BEYERMANN, M. 2008. Solid-phase synthesis of a cyclodepsipeptide: cotransin. *Org Lett,* 10**,** 3857-60.

CORSI, A. K. & SCHEKMAN, R. 1996. Mechanism of polypeptide translocation into the endoplasmic reticulum. *J Biol Chem,* 271**,** 30299-302.

COUTANCEAU, E., DECALF, J., MARTINO, A., BABON, A., WINTER, N., COLE, S. T., ALBERT, M. L. & DEMANGEL, C. 2007. Selective suppression of dendritic cell functions by Mycobacterium ulcerans toxin mycolactone. *J Exp Med,* 204**,** 1395-403.

CROSS, B. C., MCKIBBIN, C., CALLAN, A. C., ROBOTI, P., PIACENTI, M., RABU, C., WILSON, C. M., WHITEHEAD, R., FLITSCH, S. L., POOL, M. R., HIGH, S. & SWANTON, E. 2009. Eeyarestatin I inhibits Sec61-mediated protein translocation at the endoplasmic reticulum. *J Cell Sci,* 122**,** 4393-400.

DANGY, J. P., SCHERR, N., GERSBACH, P., HUG, M. N., BIERI, R., BOMIO, C., LI, J., HUBER, S., ALTMANN, K. H. & PLUSCHKE, G. 2016. Antibody-Mediated Neutralization of the Exotoxin Mycolactone, the Main Virulence Factor Produced by Mycobacterium ulcerans. *PLoS Negl Trop Dis,* 10**,** e0004808.

DEMANGEL, C. & HIGH, S. (In review). Sec61 blockade by mycolactone: a central mechanism in Buruli ulcer disease

DEMANGEL, C., STINEAR, T. P. & COLE, S. T. 2009. Buruli ulcer: reductive evolution enhances pathogenicity of Mycobacterium ulcerans. *Nat Rev Microbiol,* 7**,** 50-60.

DESHAIES, R. J. & SCHEKMAN, R. 1987. A yeast mutant defective at an early stage in import of secretory protein precursors into the endoplasmic reticulum. *J Cell Biol,* 105**,** 633-45.

EGEA, P. F. & STROUD, R. M. 2010. Lateral opening of a translocon upon entry of protein suggests the mechanism of insertion into membranes. *Proc Natl Acad Sci U S A,* 107**,** 17182-7.

ELETTO, D., MAGANTY, A., ELETTO, D., DERSH, D., MAKAREWICH, C., BISWAS, C., PATON, J. C., PATON, A. W., DOROUDGAR, S., GLEMBOTSKI, C. C. & ARGON, Y. 2012. Limitation of individual folding resources in the ER leads to outcomes distinct from the unfolded protein response. *J Cell Sci,* 125**,** 4865-75.

ELLEN, D. E., STIENSTRA, Y., TEELKEN, M. A., DIJKSTRA, P. U., VAN DER GRAAF, W. T. & VAN DER WERF, T. S. 2003. Assessment of functional limitations caused by Mycobacterium ulcerans infection: towards a Buruli ulcer functional limitation score. *Trop Med Int Health,* 8**,** 90-6.

EN, J., GOTO, M., NAKANAGA, K., HIGASHI, M., ISHII, N., SAITO, H., YONEZAWA, S., HAMADA, H. & SMALL, P. L. 2008. Mycolactone is responsible for the painlessness of Mycobacterium ulcerans infection (buruli ulcer) in a murine study. *Infect Immun,* 76**,** 2002-7.

ERDMANN, F., JUNG, M., EYRISCH, S., LANG, S., HELMS, V., WAGNER, R. & ZIMMERMANN, R. 2009. Lanthanum ions inhibit the mammalian Sec61 complex in its channel dynamics and protein transport activity. *FEBS Lett,* 583**,** 2359-64.

ETUAFUL, S., CARBONNELLE, B., GROSSET, J., LUCAS, S., HORSFIELD, C., PHILLIPS, R., EVANS, M., OFORI-ADJEI, D., KLUSTSE, E., OWUSU-BOATENG, J., AMEDOFU, G. K., AWUAH, P., AMPADU, E., AMOFAH, G., ASIEDU, K. & WANSBROUGH-JONES, M. 2005. Efficacy of the combination rifampin-streptomycin in preventing growth of Mycobacterium ulcerans in early lesions of Buruli ulcer in humans. *Antimicrob Agents Chemother,* 49**,** 3182-6.

FENNER, F. & LEACH, R. H. 1952. Studies on Mycobacterium ulcerans. I. Serological relationship to other mycobacteria. *Aust J Exp Biol Med Sci,* 30**,** 1-10.

FIEBIGER, E., HIRSCH, C., VYAS, J. M., GORDON, E., PLOEGH, H. L. & TORTORELLA, D. 2004. Dissection of the dislocation pathway for type I membrane proteins with a new small molecule inhibitor, eeyarestatin. *Mol Biol Cell,* 15**,** 1635-46.

FLYNN, J. L. & CHAN, J. 2001. Immunology of tuberculosis. *Annu Rev Immunol,* 19**,** 93-129.

FUERTES MARRACO, S. A., GROSJEAN, F., DUVAL, A., ROSA, M., LAVANCHY, C., ASHOK, D., HALLER, S., OTTEN, L. A., STEINER, Q. G., DESCOMBES, P., LUBER, C. A., MEISSNER, F., MANN, M., SZELES, L., REITH, W. & ACHA-ORBEA, H. 2012. Novel murine dendritic cell lines: a powerful auxiliary tool for dendritic cell research. *Front Immunol,* 3**,** 331.

GAMA, J. B., OHLMEIER, S., MARTINS, T. G., FRAGA, A. G., SAMPAIO-MARQUES, B., CARVALHO, M. A., PROENCA, F., SILVA, M. T., PEDROSA, J. & LUDOVICO, P. 2014. Proteomic analysis of the action of the Mycobacterium ulcerans toxin mycolactone: targeting host cells cytoskeleton and collagen. *PLoS Negl Trop Dis,* 8**,** e3066.

GARRISON, J. L., KUNKEL, E. J., HEGDE, R. S. & TAUNTON, J. 2005. A substrate-specific inhibitor of protein translocation into the endoplasmic reticulum. *Nature,* 436**,** 285-9.

GEHRINGER, M. & ALTMANN, K. H. 2017. The chemistry and biology of mycolactones. *Beilstein J Org Chem,* 13**,** 1596-1660.

GEORGE, K. M., BARKER, L. P., WELTY, D. M. & SMALL, P. L. 1998. Partial purification and characterization of biological effects of a lipid toxin produced by Mycobacterium ulcerans. *Infect Immun,* 66**,** 587-93.

GEORGE, K. M., CHATTERJEE, D., GUNAWARDANA, G., WELTY, D., HAYMAN, J., LEE, R. & SMALL, P. L. 1999. Mycolactone: a polyketide toxin from Mycobacterium ulcerans required for virulence. *Science,* 283**,** 854-7.

GEORGE, K. M., PASCOPELLA, L., WELTY, D. M. & SMALL, P. L. 2000. A Mycobacterium ulcerans toxin, mycolactone, causes apoptosis in guinea pig ulcers and tissue culture cells. *Infect Immun,* 68**,** 877-83.

GILMORE, R., BLOBEL, G. & WALTER, P. 1982. Protein translocation across the endoplasmic reticulum. I. Detection in the microsomal membrane of a receptor for the signal recognition particle. *J Cell Biol,* 95**,** 463-9.

GIRDLESTONE, J. & WING, M. 1996. Autocrine activation by interferon-gamma of STAT factors following T cell activation. *Eur J Immunol,* 26**,** 704-9.

GODER, V. & SPIESS, M. 2001. Topogenesis of membrane proteins: determinants and dynamics. *FEBS Lett,* 504**,** 87-93.

GOODING, T. M., JOHNSON, P. D., CAMPBELL, D. E., HAYMAN, J. A., HARTLAND, E. L., KEMP, A. S. & ROBINS-BROWNE, R. M. 2001. Immune response to infection with Mycobacterium ulcerans. *Infect Immun,* 69**,** 1704-7.

GOTO, M., NAKANAGA, K., AUNG, T., HAMADA, T., YAMADA, N., NOMOTO, M., KITAJIMA, S., ISHII, N., YONEZAWA, S. & SAITO, H. 2006. Nerve damage in Mycobacterium ulcerans-infected mice - Probable cause of painlessness in Buruli ulcer. *American Journal of Pathology,* 168**,** 805-811.

GROTZKE, J. E. & CRESSWELL, P. 2015. Are ERAD components involved in cross-presentation? *Mol Immunol,* 68**,** 112-5.

GROTZKE, J. E., KOZIK, P., MOREL, J. D., IMPENS, F., PIETROSEMOLI, N., CRESSWELL, P., AMIGORENA, S. & DEMANGEL, C. 2017. Sec61 blockade by mycolactone inhibits antigen cross-presentation independently of endosome-to-cytosol export. *Proc Natl Acad Sci U S A,* 114**,** E5910-E5919.

GUARNER, J., BARTLETT, J., WHITNEY, E. A., RAGHUNATHAN, P. L., STIENSTRA, Y., ASAMOA, K., ETUAFUL, S., KLUTSE, E., QUARSHIE, E., VAN DER WERF, T. S., VAN DER GRAAF, W. T., KING, C. H. & ASHFORD, D. A. 2003. Histopathologic features of Mycobacterium ulcerans infection. *Emerg Infect Dis,* 9**,** 651-656.

GUENIN-MACE, L., BARON, L., CHANY, A. C., TRESSE, C., SAINT-AURET, S., JONSSON, F., LE CHEVALIER, F., BRUHNS, P., BISMUTH, G., HIDALGO-LUCAS, S., BISSON, J. F., BLANCHARD, N.

& DEMANGEL, C. 2015. Shaping mycolactone for therapeutic use against inflammatory disorders. *Sci Transl Med,* 7**,** 289ra85.

GUENIN-MACE, L., CARRETTE, F., ASPERTI-BOURSIN, F., LE BON, A., CALEECHURN, L., DI BARTOLO, V., FONTANET, A., BISMUTH, G. & DEMANGEL, C. 2011. Mycolactone impairs T cell homing by suppressing microRNA control of L-selectin expression. *Proc Natl Acad Sci U S A,* 108**,** 12833-8.

GUENIN-MACE, L., VEYRON-CHURLET, R., THOULOUZE, M. I., ROMET-LEMONNE, G., HONG, H., LEADLAY, P. F., DANCKAERT, A., RUF, M. T., MOSTOWY, S., ZURZOLO, C., BOUSSO, P., CHRETIEN, F., CARLIER, M. F. & DEMANGEL, C. 2013. Mycolactone activation of Wiskott-Aldrich syndrome proteins underpins Buruli ulcer formation. *J Clin Invest*.

GUERMONPREZ, P., SAVEANU, L., KLEIJMEER, M., DAVOUST, J., VAN ENDERT, P. & AMIGORENA, S. 2003. ER-phagosome fusion defines an MHC class I cross-presentation compartment in dendritic cells. *Nature,* 425**,** 397-402.

GUPTA, S. K. & SHUKLA, V. K. 2002. Leg ulcers in the tropics. *Int J Low Extrem Wounds,* 1**,** 58-61.

HALIC, M., BECKER, T., POOL, M. R., SPAHN, C. M., GRASSUCCI, R. A., FRANK, J. & BECKMANN, R. 2004. Structure of the signal recognition particle interacting with the elongation-arrested ribosome. *Nature,* 427**,** 808-14.

HALL, B. S., HILL, K., MCKENNA, M., OGBECHI, J., HIGH, S., WILLIS, A. E. & SIMMONDS, R. E. 2014. The pathogenic mechanism of the Mycobacterium ulcerans virulence factor, mycolactone, depends on blockade of protein translocation into the ER. *PLoS Pathog,* 10**,** e1004061.

HALLIDAY, M. & MALLUCCI, G. R. 2015. Review: Modulating the unfolded protein response to prevent neurodegeneration and enhance memory. *Neuropathol Appl Neurobiol,* 41**,** 414-27.

HASSDENTEUFEL, S., SICKING, M., SCHORR, S., AVIRAM, N., FECHER-TROST, C., SCHULDINER, M., JUNG, M., ZIMMERMANN, R. & LANG, S. 2017. hSnd2 protein represents an alternative targeting factor to the endoplasmic reticulum in human cells. *FEBS Lett,* 591**,** 3211-3224.

HAYMAN, J. & MCQUEEN, A. 1985. The pathology of Mycobacterium ulcerans infection. *Pathology,* 17**,** 594-600.

HEATON, N. S., MOSHKINA, N., FENOUIL, R., GARDNER, T. J., AGUIRRE, S., SHAH, P. S., ZHAO, N., MANGANARO, L., HULTQUIST, J. F., NOEL, J., SACHS, D., HAMILTON, J., LEON, P. E., CHAWDURY, A., TRIPATHI, S., MELEGARI, C., CAMPISI, L., HAI, R., METREVELI, G., GAMARNIK, A. V., GARCIA-SASTRE, A., GREENBAUM, B., SIMON, V., FERNANDEZ-SESMA, A., KROGAN, N. J., MULDER, L. C., VAN BAKEL, H., TORTORELLA, D., TAUNTON, J., PALESE, P. & MARAZZI, I. 2016. Targeting Viral Proteostasis Limits Influenza Virus, HIV, and Dengue Virus Infection. *Immunity,* 44**,** 46-58.

HONG, H., COUTANCEAU, E., LECLERC, M., CALEECHURN, L., LEADLAY, P. F. & DEMANGEL, C. 2008. Mycolactone Diffuses from Mycobacterium ulcerans-Infected Tissues and Targets Mononuclear Cells in Peripheral Blood and Lymphoid Organs. *PLoS Negl Trop Dis,* 2**,** e325.

IMAI, J., HASEGAWA, H., MARUYA, M., KOYASU, S. & YAHARA, I. 2005. Exogenous antigens are processed through the endoplasmic reticulum-associated degradation (ERAD) in cross-presentation by dendritic cells. *Int Immunol,* 17**,** 45-53.

ISAAC, C., MAUBORGNE, A., GRIMALDI, A., ADE, K., POHL, M., LIMATOLA, C., BOUCHER, Y., DEMANGEL, C. & GUENIN-MACE, L. 2017. Mycolactone displays anti-inflammatory effects on the nervous system. *PLoS Negl Trop Dis,* 11**,** e0006058.

JUNNE, T., WONG, J., STUDER, C., AUST, T., BAUER, B. W., BEIBEL, M., BHULLAR, B., BRUCCOLERI, R., EICHENBERGER, J., ESTOPPEY, D., HARTMANN, N., KNAPP, B., KRASTEL, P., MELIN, N., OAKELEY, E. J., OBERER, L., RIEDL, R., ROMA, G., SCHUIERER, S., PETERSEN, F., TALLARICO, J. A., RAPOPORT, T. A., SPIESS, M. & HOEPFNER, D. 2015. Decatransin, a new natural product inhibiting protein translocation at the Sec61/SecYEG translocon. *J Cell Sci,* 128**,** 1217-29.

KALIES, K. U. & ROMISCH, K. 2015. Inhibitors of Protein Translocation Across the ER Membrane. *Traffic,* 16**,** 1027-38.

KRIEG, R. E., HOCKMEYER, W. T. & CONNOR, D. H. 1974. Toxin of Mycobacterium ulcerans. Production and effects in guinea pig skin. *Arch Dermatol,* 110**,** 783-8.

KUMAR, S. K., RAJKUMAR, V., KYLE, R. A., VAN DUIN, M., SONNEVELD, P., MATEOS, M. V., GAY, F. & ANDERSON, K. C. 2017. Multiple myeloma. *Nat Rev Dis Primers,* 3**,** 17046.

LAKKARAJU, A. K., THANKAPPAN, R., MARY, C., GARRISON, J. L., TAUNTON, J. & STRUB, K. 2012. Efficient secretion of small proteins in mammalian cells relies on Sec62-dependent posttranslational translocation. *Mol Biol Cell,* 23**,** 2712-22.

LANG, S., PFEFFER, S., LEE, P. H., CAVALIE, A., HELMS, V., FORSTER, F. & ZIMMERMANN, R. 2017. An Update on Sec61 Channel Functions, Mechanisms, and Related Diseases. *Front Physiol,* 8**,** 887.

LI, Y., GE, M., CIANI, L., KURIAKOSE, G., WESTOVER, E. J., DURA, M., COVEY, D. F., FREED, J. H., MAXFIELD, F. R., LYTTON, J. & TABAS, I. 2004. Enrichment of endoplasmic reticulum with cholesterol inhibits sarcoplasmic-endoplasmic reticulum calcium ATPase-2b activity in parallel with increased order of membrane lipids: implications for depletion of endoplasmic reticulum calcium stores and apoptosis in cholesterol-loaded macrophages. *J Biol Chem,* 279**,** 37030-9.

LIU, X. D., KO, S., XU, Y., FATTAH, E. A., XIANG, Q., JAGANNATH, C., ISHII, T., KOMATSU, M. & EISSA, N. T. 2012. Transient aggregation of ubiquitinated proteins is a cytosolic unfolded protein response to inflammation and endoplasmic reticulum stress. *J Biol Chem,* 287**,** 19687-98.

LOPEZ, C. A., UNKEFER, C. J., SWANSON, B. I., SWANSON, J. M. J. & GNANAKARAN, S. 2018. Membrane perturbing properties of toxin mycolactone from Mycobacterium ulcerans. *PLoS Comput Biol,* 14**,** e1005972.

LU, Z., ZHOU, L., KILLELA, P., RASHEED, A. B., DI, C., POE, W. E., MCLENDON, R. E., BIGNER, D. D., NICCHITTA, C. & YAN, H. 2009. Glioblastoma proto-oncogene SEC61gamma is required for tumor cell survival and response to endoplasmic reticulum stress. *Cancer Res,* 69**,** 9105-11.

LUESCH, H., YOSHIDA, W. Y., MOORE, R. E., PAUL, V. J. & CORBETT, T. H. 2001. Total structure determination of apratoxin A, a potent novel cytotoxin from the marine cyanobacterium Lyngbya majuscula. *J Am Chem Soc,* 123**,** 5418-23.

LUNN, H. F., CONNOR, D. H., WILKS, N. E., BARNLEY, G. R., KAMUNVI, F., CLANCEY, J. K. & BEE, J. D. 1965. Buruli (Mycobacterial) Ulceration in Uganda. (a New Focus of Buruli Ulcer in Madi District, Uganda): Report of a Field Study. *East Afr Med J,* 42**,** 275-88.

MAC, C. P., TOLHURST, J. C. & *ET AL.* 1948. A new mycobacterial infection in man. *J Pathol Bacteriol,* 60**,** 93-122.

MACKINNON, A. L., PAAVILAINEN, V. O., SHARMA, A., HEGDE, R. S. & TAUNTON, J. 2014. An allosteric Sec61 inhibitor traps nascent transmembrane helices at the lateral gate. *Elife,* 3**,** e01483.

MARION, E., SONG, O. R., CHRISTOPHE, T., BABONNEAU, J., FENISTEIN, D., EYER, J., LETOURNEL, F., HENRION, D., CLERE, N., PAILLE, V., GUERINEAU, N. C., SAINT ANDRE, J. P., GERSBACH, P., ALTMANN, K. H., STINEAR, T. P., COMOGLIO, Y., SANDOZ, G., PREISSER, L., DELNESTE, Y., YERAMIAN, E., MARSOLLIER, L. & BRODIN, P. 2014. Mycobacterial toxin induces analgesia in buruli ulcer by targeting the Angiotensin pathways. *Cell,* 157**,** 1565-76.

MARSOLLIER, L., ROBERT, R., AUBRY, J., SAINT ANDRE, J. P., KOUAKOU, H., LEGRAS, P., MANCEAU, A. L., MAHAZA, C. & CARBONNELLE, B. 2002. Aquatic insects as a vector for Mycobacterium ulcerans. *Appl Environ Microbiol,* 68**,** 4623-8.

MCKENNA, M., SIMMONDS, R. E. & HIGH, S. 2016. Mechanistic insights into the inhibition of Sec61-dependent co- and post-translational translocation by mycolactone. *J Cell Sci*.

MCKENNA, M., SIMMONDS, R. E. & HIGH, S. 2017. Mycolactone reveals the substrate-driven complexity of Sec61-dependent transmembrane protein biogenesis. *J Cell Sci,* 130**,** 1307-1320.

MENAGER, J., EBSTEIN, F., OGER, R., HULIN, P., NEDELLEC, S., DUVERGER, E., LEHMANN, A., KLOETZEL, P. M., JOTEREAU, F. & GUILLOUX, Y. 2014. Cross-presentation of synthetic long peptides by human dendritic cells: a process dependent on ERAD component p97/VCP but Not sec61 and/or Derlin-1. *PLoS One,* 9**,** e89897.

MILLER, J. D., TAJIMA, S., LAUFFER, L. & WALTER, P. 1995. The beta subunit of the signal recognition particle receptor is a transmembrane GTPase that anchors the alpha subunit, a peripheral membrane GTPase, to the endoplasmic reticulum membrane. *J Cell Biol,* 128**,** 273-82.

MOREL, J. D., PAATERO, A. O., WEI, J., YEWDELL, J. W., GUENIN-MACE, L., VAN HAVER, D., IMPENS, F., PIETROSEMOLI, N., PAAVILAINEN, V. O. & DEMANGEL, C. 2018. Proteomics reveals scope of mycolactone-mediated Sec61 blockade and distinctive stress signature. *Mol Cell Proteomics*.

MULLER, G. & ZIMMERMANN, R. 1987. Import of honeybee prepromelittin into the endoplasmic reticulum: structural basis for independence of SRP and docking protein. *EMBO J,* 6**,** 2099-107.

NIENHUIS, W. A., STIENSTRA, Y., THOMPSON, W. A., AWUAH, P. C., ABASS, K. M., TUAH, W., AWUA-BOATENG, N. Y., AMPADU, E. O., SIEGMUND, V., SCHOUTEN, J. P., ADJEI, O., BRETZEL, G. & VAN DER WERF, T. S. 2010. Antimicrobial treatment for early, limited Mycobacterium ulcerans infection: a randomised controlled trial. *Lancet,* 375**,** 664-72.

NILSSON, I., OHVO-REKILA, H., SLOTTE, J. P., JOHNSON, A. E. & VON HEIJNE, G. 2001. Inhibition of protein translocation across the endoplasmic reticulum membrane by sterols. *J Biol Chem,* 276**,** 41748-54.

NITENBERG, M., BENAROUCHE, A., MANITI, O., MARION, E., MARSOLLIER, L., GEAN, J., DUFOURC, E. J., CAVALIER, J. F., CANAAN, S. & GIRARD-EGROT, A. P. 2018. The potent effect of mycolactone on lipid membranes. *PLoS Pathog,* 14**,** e1006814.

OGBECHI, J., HALL, B. S., SBARRATO, T., TAUNTON, J., WILLIS, A. E., WEK, R. C. & SIMMONDS, R. E. 2018. Inhibition of Sec61-dependent translocation by mycolactone uncouples the integrated stress response from ER stress, driving cytotoxicity via translational activation of ATF4. *Cell Death Dis,* 9**,** 397.

OGBECHI, J., RUF, M. T., HALL, B. S., BODMAN-SMITH, K., VOGEL, M., WU, H. L., STAINER, A., ESMON, C. T., AHNSTROM, J., PLUSCHKE, G. & SIMMONDS, R. E. 2015. Mycolactone-Dependent Depletion of Endothelial Cell Thrombomodulin Is Strongly Associated with Fibrin Deposition in Buruli Ulcer Lesions. *PLoS Pathog,* 11**,** e1005011.

ORGANIZATION, W. H. 2004. Provisional Guidance on the Role of Specific Antibiotics in the Management of Mycobacterium Ulcerans Disease (Buruli ulcer). Manual for Health Care Providers. *Geneva, Switzerland: WHO*.

PAATERO, A. O., KELLOSALO, J., DUNYAK, B. M., ALMALITI, J., GESTWICKI, J. E., GERWICK, W. H., TAUNTON, J. & PAAVILAINEN, V. O. 2016. Apratoxin Kills Cells by Direct Blockade of the Sec61 Protein Translocation Channel. *Cell Chem Biol,* 23**,** 561-6.

PADRICK, S. B. & ROSEN, M. K. 2010. Physical mechanisms of signal integration by WASP family proteins. *Annu Rev Biochem,* 79**,** 707-35.

PAHLEVAN, A. A., WRIGHT, D. J., ANDREWS, C., GEORGE, K. M., SMALL, P. L. & FOXWELL, B. M. 1999. The inhibitory action of Mycobacterium ulcerans soluble factor on monocyte/T cell cytokine production and NF-kappa B function. *J Immunol,* 163**,** 3928-35.

PAKOS-ZEBRUCKA, K., KORYGA, I., MNICH, K., LJUJIC, M., SAMALI, A. & GORMAN, A. M. 2016. The integrated stress response. *EMBO Rep,* 17**,** 1374-1395.

PHILLIPS, R., HORSFIELD, C., KUIJPER, S., SARFO, S. F., OBENG-BAAH, J., ETUAFUL, S., NYAMEKYE, B., AWUAH, P., NYARKO, K. M., OSEI-SARPONG, F., LUCAS, S., KOLK, A. H. & WANSBROUGH-JONES, M. 2006. Cytokine response to antigen stimulation of whole blood from patients with Mycobacterium ulcerans disease compared to that from patients with tuberculosis. *Clin Vaccine Immunol,* 13**,** 253-7.

PHILLIPS, R., SARFO, F. S., GUENIN-MACE, L., DECALF, J., WANSBROUGH-JONES, M., ALBERT, M. L. & DEMANGEL, C. 2009. Immunosuppressive Signature of Cutaneous Mycobacterium ulcerans Infection in the Peripheral Blood of Patients with Buruli Ulcer Disease. *J Infect Dis*.

PHILLIPS, R. O., SARFO, F. S., LANDIER, J., OLDENBURG, R., FRIMPONG, M., WANSBROUGH-JONES, M., ABASS, K., THOMPSON, W., FORSON, M., FONTANET, A., NIANG, F. & DEMANGEL, C. 2014. Combined inflammatory and metabolic defects reflected by reduced serum protein levels in patients with Buruli ulcer disease. *PLoS Negl Trop Dis,* 8**,** e2786.

PLEMPER, R. K., BOHMLER, S., BORDALLO, J., SOMMER, T. & WOLF, D. H. 1997. Mutant analysis links the translocon and BiP to retrograde protein transport for ER degradation. *Nature,* 388**,** 891-5.

PLOEGH, H. L. 2007. A lipid-based model for the creation of an escape hatch from the endoplasmic reticulum. *Nature,* 448**,** 435-8.

PREVOT, G., BOURREAU, E., PASCALIS, H., PRADINAUD, R., TANGHE, A., HUYGEN, K. & LAUNOIS, P. 2004. Differential production of systemic and intralesional gamma interferon and interleukin-10 in nodular and ulcerative forms of Buruli disease. *Infect Immun,* 72**,** 958-65.

READ, J. K., HEGGIE, C. M., MEYERS, W. M. & CONNOR, D. H. 1974. Cytotoxic activity of Mycobacterium ulcerans. *Infect Immun,* 9**,** 1114-22.

REITHINGER, J. H., YIM, C., KIM, S., LEE, H. & KIM, H. 2014. Structural and functional profiling of the lateral gate of the Sec61 translocon. *J Biol Chem,* 289**,** 15845-55.

RICE, A. S. C., DWORKIN, R. H., MCCARTHY, T. D., ANAND, P., BOUNTRA, C., MCCLOUD, P. I., HILL, J., CUTTER, G., KITSON, G., DESEM, N., RAFF, M. & GROUP, E. M. A. S. 2014. EMA401, an orally administered highly selective angiotensin II type 2 receptor antagonist, as a novel treatment for postherpetic neuralgia: a randomised, double-blind, placebo-controlled phase 2 clinical trial. *Lancet,* 383**,** 1637-1647.

ROMISCH, K. 2017. A Case for Sec61 Channel Involvement in ERAD. *Trends Biochem Sci,* 42**,** 171-179.

RUBENSTEIN, E. M., KREFT, S. G., GREENBLATT, W., SWANSON, R. & HOCHSTRASSER, M. 2012. Aberrant substrate engagement of the ER translocon triggers degradation by the Hrd1 ubiquitin ligase. *J Cell Biol,* 197**,** 761-73.

RUF, M. T., STEFFEN, C., BOLZ, M., SCHMID, P. & PLUSCHKE, G. 2017. Infiltrating leukocytes surround early Buruli ulcer lesions, but are unable to reach the mycolactone producing mycobacteria. *Virulence,* 8**,** 1918-1926.

RUGGIANO, A., FORESTI, O. & CARVALHO, P. 2014. Quality control: ER-associated degradation: protein quality control and beyond. *J Cell Biol,* 204**,** 869-79.

SADLER, J. E. 1997. Thrombomodulin structure and function. *Thromb Haemost,* 78**,** 392-5.

SAINT-AURET, S., CHANY, A. C., CASAROTTO, V., TRESSE, C., PARMENTIER, L., ABDELKAFI, H. & BLANCHARD, N. 2017. Total Syntheses of Mycolactone A/B and its Analogues for the Exploration of the Biology of Buruli Ulcer. *Chimia (Aarau),* 71**,** 836-840.

SAKYI, S. A., ABOAGYE, S. Y., DARKO OTCHERE, I. & YEBOAH-MANU, D. 2016. Clinical and Laboratory Diagnosis of Buruli Ulcer Disease: A Systematic Review. *Can J Infect Dis Med Microbiol,* 2016**,** 5310718.

SARFO, F. S., LE CHEVALIER, F., AKA, N., PHILLIPS, R. O., AMOAKO, Y., BONECA, I. G., LENORMAND, P., DOSSO, M., WANSBROUGH-JONES, M., VEYRON-CHURLET, R., GUENIN-MACE, L. & DEMANGEL, C. 2011. Mycolactone diffuses into the peripheral blood of buruli ulcer patients - implications for diagnosis and disease monitoring. *PLoS Negl Trop Dis,* 5**,** e1237.

SARFO, F. S., PHILLIPS, R. O., ZHANG, J., ABASS, M. K., ABOTSI, J., AMOAKO, Y. A., ADU-SARKODIE, Y., ROBINSON, C. & WANSBROUGH-JONES, M. H. 2014. Kinetics of mycolactone in human subcutaneous tissue during antibiotic therapy for Mycobacterium ulcerans disease. *BMC Infect Dis,* 14**,** 202.

SCHAUBLE, N., CAVALIE, A., ZIMMERMANN, R. & JUNG, M. 2014. Interaction of Pseudomonas aeruginosa Exotoxin A with the human Sec61 complex suppresses passive calcium efflux from the endoplasmic reticulum. *Channels (Austin),* 8**,** 76-83.

SCHERR, N., GERSBACH, P., DANGY, J. P., BOMIO, C., LI, J., ALTMANN, K. H. & PLUSCHKE, G. 2013. Structure-activity relationship studies on the macrolide exotoxin mycolactone of Mycobacterium ulcerans. *PLoS Negl Trop Dis,* 7**,** e2143.

SCHUBERT, D., KLEIN, M. C., HASSDENTEUFEL, S., CABALLERO-OTEYZA, A., YANG, L., PROIETTI, M., BULASHEVSKA, A., KEMMING, J., KUHN, J., WINZER, S., RUSCH, S., FLIEGAUF, M., SCHAFFER, A. A., PFEFFER, S., GEIGER, R., CAVALIE, A., CAO, H., YANG, F., LI, Y., RIZZI, M., EIBEL, H., KOBBE, R., MARKS, A. L., PEPPERS, B. P., HOSTOFFER, R. W., PUCK, J. M., ZIMMERMANN, R. & GRIMBACHER, B. 2018. Plasma cell deficiency in human subjects with heterozygous mutations in Sec61 translocon alpha 1 subunit (SEC61A1). *J Allergy Clin Immunol,* 141**,** 1427-1438.

SCHUNK, M., THOMPSON, W., KLUTSE, E., NITSCHKE, J., OPARE-ASAMOAH, K., THOMPSON, R., FLEISCHMANN, E., SIEGMUND, V., HERBINGER, K. H., ADJEI, O., FLEISCHER, B., LOSCHER, T. & BRETZEL, G. 2009. Outcome of patients with buruli ulcer after surgical treatment with or without antimycobacterial treatment in Ghana. *Am J Trop Med Hyg,* 81**,** 75-81.

SCOTT, D. C. & SCHEKMAN, R. 2008. Role of Sec61p in the ER-associated degradation of short-lived transmembrane proteins. *J Cell Biol,* 181**,** 1095-105.

SEGURA, E. & AMIGORENA, S. 2015. Cross-Presentation in Mouse and Human Dendritic Cells. *Adv Immunol,* 127**,** 1-31.

SHAO, S., RODRIGO-BRENNI, M. C., KIVLEN, M. H. & HEGDE, R. S. 2017. Mechanistic basis for a molecular triage reaction. *Science,* 355**,** 298-302.

SHURTLEFF, M. J., ITZHAK, D. N., HUSSMANN, J. A., SCHIRLE OAKDALE, N. T., COSTA, E. A., JONIKAS, M., WEIBEZAHN, J., POPOVA, K. D., JAN, C. H., SINITCYN, P., VEMBAR, S. S., HERNANDEZ, H., COX, J., BURLINGAME, A. L., BRODSKY, J., FROST, A., BORNER, G. H. & WEISSMAN, J. S. 2018. The ER membrane protein complex interacts cotranslationally to enable biogenesis of multipass membrane proteins. *Elife,* 7.

SIMMONDS, R. E., LALI, F. V., SMALLIE, T., SMALL, P. L. & FOXWELL, B. M. 2009. Mycolactone inhibits monocyte cytokine production by a posttranscriptional mechanism. *J Immunol,* 182**,** 2194-202.

SINGH, A., MCBRIDE, W. J. H., GOVAN, B. & PEARSON, M. 2018. Potential animal reservoir of'Mycobacterium ulcerans': A systematic review. *Tropical Medicine and Infectious Disease,* 3**,** 1.

SNAPPER, S. B., TAKESHIMA, F., ANTON, I., LIU, C. H., THOMAS, S. M., NGUYEN, D., DUDLEY, D., FRASER, H., PURICH, D., LOPEZ-ILASACA, M., KLEIN, C., DAVIDSON, L., BRONSON, R., MULLIGAN, R. C., SOUTHWICK, F., GEHA, R., GOLDBERG, M. B., ROSEN, F. S., HARTWIG, J. H.

& ALT, F. W. 2001. N-WASP deficiency reveals distinct pathways for cell surface projections and microbial actin-based motility. *Nat Cell Biol,* 3**,** 897-904.

SNYDER, D. S. & SMALL, P. L. 2003. Uptake and cellular actions of mycolactone, a virulence determinant for Mycobacterium ulcerans. *Microb Pathog,* 34**,** 91-101.

SONG, F., FIDANZE, S., BENOWITZX, A. B. & KISHI, Y. 2007. Total synthesis of mycolactones A and B. *Tetrahedron,* 63**,** 5739-5753.

SONG, O. R., KIM, H. B., JOUNY, S., RICARD, I., VANDEPUTTE, A., DEBOOSERE, N., MARION, E., QUEVAL, C. J., LESPORT, P., BOURINET, E., HENRION, D., OH, S. B., LEBON, G., SANDOZ, G., YERAMIAN, E., MARSOLLIER, L. & BRODIN, P. 2017. A Bacterial Toxin with Analgesic Properties: Hyperpolarization of DRG Neurons by Mycolactone. *Toxins (Basel),* 9.

STINEAR, T. P., MVE-OBIANG, A., SMALL, P. L., FRIGUI, W., PRYOR, M. J., BROSCH, R., JENKIN, G. A., JOHNSON, P. D., DAVIES, J. K., LEE, R. E., ADUSUMILLI, S., GARNIER, T., HAYDOCK, S. F., LEADLAY, P. F. & COLE, S. T. 2004. Giant plasmid-encoded polyketide synthases produce the macrolide toxin of Mycobacterium ulcerans. *Proc Natl Acad Sci U S A,* 101**,** 1345-9.

SZEGEZDI, E., LOGUE, S. E., GORMAN, A. M. & SAMALI, A. 2006. Mediators of endoplasmic reticulum stress-induced apoptosis. *EMBO Rep,* 7**,** 880-5.

THRASHER, A. J. & BURNS, S. O. 2010. WASP: a key immunological multitasker. *Nat Rev Immunol,* 10**,** 182-92.

TYEDMERS, J., LERNER, M., WIEDMANN, M., VOLKMER, J. & ZIMMERMANN, R. 2003. Polypeptide-binding proteins mediate completion of co-translational protein translocation into the mammalian endoplasmic reticulum. *EMBO Rep,* 4**,** 505-10.

VAN DER WERF, T. S., STIENSTRA, Y., JOHNSON, R. C., PHILLIPS, R., ADJEI, O., FLEISCHER, B., WANSBROUGH-JONES, M. H., JOHNSON, P. D., PORTAELS, F., VAN DER GRAAF, W. T. & ASIEDU, K. 2005. Mycobacterium ulcerans disease. *Bull World Health Organ,* 83**,** 785-91.

VAN DER WERF, T. S., VAN DER GRAAF, W. T., TAPPERO, J. W. & ASIEDU, K. 1999. Mycobacterium ulcerans infection. *Lancet,* 354**,** 1013-8.

VAN PUYENBROECK, V. & VERMEIRE, K. 2018. Inhibitors of protein translocation across membranes of the secretory pathway: novel antimicrobial and anticancer agents. *Cell Mol Life Sci,* 75**,** 1541-1558.

VILARDI, F., STEPHAN, M., CLANCY, A., JANSHOFF, A. & SCHWAPPACH, B. 2014. WRB and CAML are necessary and sufficient to mediate tail-anchored protein targeting to the ER membrane. *PLoS One,* 9**,** e85033.

VOORHEES, R. M. & HEGDE, R. S. 2016. Structure of the Sec61 channel opened by a signal sequence. *Science,* 351**,** 88-91.

WALLACE, J. R., MANGAS, K. M., PORTER, J. L., MARCSISIN, R., PIDOT, S. J., HOWDEN, B., OMANSEN, T. F., ZENG, W., AXFORD, J. K., JOHNSON, P. D. R. & STINEAR, T. P. 2017. Mycobacterium ulcerans low infectious dose and mechanical transmission support insect bites and puncturing injuries in the spread of Buruli ulcer. *PLoS Negl Trop Dis,* 11**,** e0005553.

WALSH, D. S., PORTAELS, F. & MEYERS, W. M. 2008. Buruli ulcer (Mycobacterium ulcerans infection). *Trans R Soc Trop Med Hyg,* 102**,** 969-78.

WALTER, P. & BLOBEL, G. 1981. Translocation of proteins across the endoplasmic reticulum. II. Signal recognition protein (SRP) mediates the selective binding to microsomal membranes of in-vitro-assembled polysomes synthesizing secretory protein. *J Cell Biol,* 91**,** 551-6.

WANSBROUGH-JONES, M. & PHILLIPS, R. 2006. Buruli ulcer: emerging from obscurity. *Lancet,* 367**,** 1849-58.

WESTENBRINK, B. D., STIENSTRA, Y., HUITEMA, M. G., THOMPSON, W. A., KLUTSE, E. O., AMPADU, E. O., BOEZEN, H. M., LIMBURG, P. C. & VAN DER WERF, T. S. 2005. Cytokine responses to stimulation of whole blood from patients with buruli ulcer disease in Ghana. *Clinical and Diagnostic Laboratory Immunology,* 12**,** 125-129.

WHO 2018a. Fact sheet Buruli ulcer. *http://www.who.int/mediacentre/factsheets/fs199/en/ (accessed June 2018)*.

WHO 2018b. World Health Organization. Country data for Buruli ulcer. *Available from: http://apps.who.int/neglected_diseases/ntddata/buruli/buruli.html.* .

WIERTZ, E. J., TORTORELLA, D., BOGYO, M., YU, J., MOTHES, W., JONES, T. R., RAPOPORT, T. A. & PLOEGH, H. L. 1996. Sec61-mediated transfer of a membrane protein from the endoplasmic reticulum to the proteasome for destruction. *Nature,* 384**,** 432-8.

YAMAMOTO, H., FUJITA, H., KIDA, Y. & SAKAGUCHI, M. 2012. Pleiotropic effects of membrane cholesterol upon translocation of protein across the endoplasmic reticulum membrane. *Biochemistry,* 51**,** 3596-605.

YEBOAH-MANU, D., KPELI, G. S., RUF, M. T., ASAN-AMPAH, K., QUENIN-FOSU, K., OWUSU-MIREKU, E., PAINTSIL, A., LAMPTEY, I., ANKU, B., KWAKYE-MACLEAN, C., NEWMAN, M. & PLUSCHKE, G. 2013. Secondary bacterial infections of buruli ulcer lesions before and after chemotherapy with streptomycin and rifampicin. *PLoS Negl Trop Dis,* 7**,** e2191.

YEBOAH-MANU, D., PEDUZZI, E., MENSAH-QUAINOO, E., ASANTE-POKU, A., OFORI-ADJEI, D., PLUSCHKE, G. & DAUBENBERGER, C. A. 2006. Systemic suppression of interferon-gamma responses in Buruli ulcer patients resolves after surgical excision of the lesions caused by the extracellular pathogen Mycobacterium ulcerans. *J Leukoc Biol,* 79**,** 1150-6.

ZAVATTARO, E., BOCCAFOSCHI, F., BORGOGNA, C., CONCA, A., JOHNSON, R. C., SOPOH, G. E., DOSSOU, A. D., COLOMBO, E., CLEMENTE, C., LEIGHEB, G. & VALENTE, G. 2012. Apoptosis in Buruli ulcer: a clinicopathological study of 45 cases. *Histopathology,* 61**,** 224-36.

ZEHNER, M., MARSCHALL, A. L., BOS, E., SCHLOETEL, J. G., KREER, C., FEHRENSCHILD, D., LIMMER, A., OSSENDORP, F., LANG, T., KOSTER, A. J., DUBEL, S. & BURGDORF, S. 2015. The translocon protein Sec61 mediates antigen transport from endosomes in the cytosol for cross-presentation to CD8(+) T cells. *Immunity,* 42**,** 850-63.

ZINGUE, D., BOUAM, A., TIAN, R. B. D. & DRANCOURT, M. 2018. Buruli Ulcer, a Prototype for Ecosystem-Related Infection, Caused by Mycobacterium ulcerans. *Clin Microbiol Rev,* 31.

Mechanism underpinning the immunosuppressive effects of the mycobacterial macrolide mycolactone

Mycolactone is a diffusible lipid produced by the human pathogen *Mycobacterium ulcerans*, the causative agent of a tropical skin disease called Buruli ulcer. Bacterial production of mycolactone in infected skin causes local tissue necrosis, while inducing immunosuppressive defects at the systemic level. When I started my PhD, the molecular mechanism(s) underpinning these effects were unknown. Over the course of my thesis, I contributed to demonstrate that mycolactone is a novel inhibitor of the Sec61 translocon, a channel regulating the biogenesis of most secreted and membrane proteins in eukaryotic cells. Indeed, a single point mutation in the alpha subunit of Sec61 protected cells from the cytotoxic and immunosuppressive effects of mycolactone. I showed that mycolactone-mediated blockade of the Sec61 translocon efficiently prevents the synthesis of key immune receptors and signaling molecules, impeding the communication between immune cells that is required for the development of anti-mycobacterial immunity. Through a series of large-scale proteomic studies, I demonstrated that mycolactone is a broad-acting inhibitor of Sec61 and identified the Sec61 clients that are primarily downregulated by mycolactone in physiologically-relevant cell types. These analyses also allowed me to describe a unique stress response, encompassing elements of the unfolded protein response and integrated stress response, that is induced upon protein translocation blockade and ultimately causes cell apoptosis. The Sec61 translocon has been proposed to play a role in other cell functions that require the retrograde transport of proteins across membranes, namely Endoplasmic Reticulum-Associated Degradation (ERAD), an essential process in protein quality control, and antigen export to the cytosol during cross-presentation, a pathway essential to the activation of adaptive immunity to intracellular pathogens and cancer. Using mycolactone, I showed that Sec61 blockade does not affect protein export to the cytosol in either of these pathways, arguing against Sec61 operating as a retrotranslocon. Altogether, my work provided a molecular mechanism for the diverse effects of mycolactone in Buruli Ulcer patients, and thus for *M. ulcerans* virulence. Mycolactone representing the most potent Sec61 blocker identified to date, my studies also revealed the key importance of Sec61-mediated protein translocation in the regulation of immune responses and protein homeostasis.

Keywords: Mycolactone, Sec61 translocon, immunosuppression, stress, Buruli ulcer